Targeting nucleic acid receptors to improve filarial vaccination in the *Litomosoides sigmodontis* model

Dissertation

zur

Erlangung des Doktorgrades (Dr. rer. nat.)

der

Mathematisch-Naturwissenschaftlichen Fakultät

der

Rheinischen Friedrich-Wilhelms-Universität Bonn

vorgelegt von

Johanna Friederike Scheunemann

aus

Hagen

Bonn 2021

Angefertigt mit der Genehmigung der Mathematisch-Naturwissenschaftlichen Fakultät der Rheinischen Friedrich-Wilhelms-Universität Bonn

1. Gutachter: Prof. Dr. Achim Hörauf
2. Gutachter: Prof. Dr. Sven Burgdorf

Tag der Promotion: 29.04.2022

Erscheinungsjahr: 2022

Table of Content

Abbreviations

AAM	alternatively-activated macrophages
Ab	antibody
ADCC	antibody-dependent cellular cytotoxicity
APC	antigen presenting cell
APOC	African Programme for Onchocerciasis Control
Att.	attenuated
cGAMP	cyclic guanosine monophosphate–adenosine monophosphate
cGAS	cyclic GMP-AMP synthase
CpG	deoxycytosine-deoxyguanosine
CLR	C-type lectin receptor
DALY	disability adjusted life years
DEC	diethylcarbamazine
ds	double stranded
ELISA	enzyme-linked immunosorbent assay
EV	extracellular vesicle
FcR	Fc receptor
FMO	fluorescence minus one
GPELF	Global Programme to Eliminate Lymphatic Filariasis
GrzB	granzyme B
HIV	human immunodeficiency virus
IFN	interferon
Ig	immunoglobulin
IL	interleukin
IP-10	interferon-gamma induced protein 10
IRF	*interferon regulatory factor*
ILC2	type two innate lymphocytes
ISD	interferon stimulatory DNA
Ls	*Litomosoides sigmodontis*
LsAg	*Litomosoides sigmodontis* adult worm extract
MAVS	*mitochondrial antiviral-signaling protein*
MDA	mass drug administration
MDA5	*melanoma differentiation associated gene 5*
MF	microfilariae
MHC	major histocompatibility complex
miRNA	microRNA
NF-κB	*nuclear factor kappa-light-chain-enhancer of activated B cells*
NLR	nuclear oligomerization domain (NOD)-like receptors
NTD	neglected tropical disease
OCP	Onchocerciasis Control Programme
ODN	oligodeoxynucleotides
p(I:C)	poly(I:C)
PAMP	pathogen-associated molecular pattern
PBMC	peripheral blood mononuclear cells
pDC	plasmacytoid dendritic cell
PEC	peritoneal exudate cells
PRR	pattern recognition receptor

RBC	red blood cell
RIG-I	*retinoic acid inducible gene I*
RLR	RIG-I-like receptor
RLU	relative light unit
Spp	species pluralis
STING	*stimulator of interferon genes*
Tcm	central memory T cell
Tef	effector T cell
TLR	toll-like receptor
TOVA	The Onchocerciasis Vaccine for Africa
trans.	transfected
WHO	World Health Organization
WSP	*Wolbachia* surface protein
WT	wild-type

Summary

Lymphatic filariasis and onchocerciasis (river blindness) are human filarial diseases, which put a high socio-economic burden on endemic countries. 859 million and 218 million people, respectively, live at risk of infection. The elimination of both diseases until 2030 is a goal of the World Health Organization but until now no vaccination for human helminth diseases is available and elimination efforts rely on mass drug administrations (MDA). The development of a vaccine would be a valuable tool to drive elimination. To that end in 2015 „TOVA – The Onchocerciasis Vaccine for Africa initiative was launched. The initiative aims to develop a vaccine candidate that passes a phase I clinical trial until 2025.

So far protective immunity against filariae is not well understood and has been linked with Th2-associated immune responses. However, also Th1-associated responses were linked to protection and the need for a balanced Th1/Th2 immune response in order to successfully clear infection has been suggested. An unexplored field and its contribution to protective immunity is nucleic acid immunity during filarial infections.

In this thesis it was shown, that the nucleic acids derived from the rodent-pathogenic filarial nematode *Litomosoides sigmodontis* induces type I Interferon secretion by human and murine cells. Further, there was an increase of IFN-β production during the course of infection, which correlated with the worm burden. At the same time, there was no impact on larval migration to the pleural cavity in mice deficient for the nucleic acid receptors TLR3, TLR7, TLR9, STING and MDA5. However, the stimulation of TLR3/MDA5/RIG-I by the agonist poly(I:C) and 3pRNA resulted in reduced larval counts in the pleural cavity. This suggests a possible protective role for nucleic acid sensing during filarial infection. Based on this finding the use of poly(I:C) and 3pRNA as adjuvants for filarial vaccination was analyzed. The injection of agonists resulted in enhanced local immune activation. For full immunization, attenuated (att.) L3 larvae were administered in combination with poly(I:C) or 3pRNA for three times every two weeks. Two weeks after the last immunization parasite specific IgG1 and IgG2a/b antibodies were detected in the serum of immunized mice. Further the serum was potent to inhibit L3 larval motility *in vitro*. The motility was significantly reduced when the mice were immunized with a combination of att. L3 larvae and poly(I:C) or 3pRNA. Mice that were immunized with a combination therapy had a significantly reduced adult worm burden, following challenge infection. The addition of transfected poly(I:C) or 3pRNA as adjuvant resulted in adult worm burden reductions of 73% and 57%,

respectively, while the immunization with att. L3 larvae alone only resulted in a reduction of 45%. Additionally, the percentage of microfilariae positive animals was reduced in the groups that were immunized with the combination therapy. This implies an impact of the immunization on embryogenesis and thereby can aid limiting disease transmission.

Overall, the data of this thesis show that type I interferons might contribute to protective immune responses against filariae and the nucleic acid receptor agonists poly(I:C) and 3pRNA were identified as promising adjuvants for the development of an effective filarial vaccine.

Zusammenfassung

Die Wurmerkrankungen lymphatische Filariose und Onchozerkose (Flussblindheit) gehören zu den verbreitetsten vernachlässigten parasitären Infektionen und stellen eine starke sozio-ökonomische Belastung für endemische Länder dar. Zurzeit leben ca. 859 Millionen und 218 Millionen Menschen in Endemiegebieten mit dem Risiko einer Infektion. Die Eliminierung beider Infektionen bis 2030 gehört zu den Zielen der Weltgesundheitsorganisation. Bisher beruht die Kontrolle der Erkrankungen auf regelmäßigen Massenbehandlungen, da kein Impfstoff zur Verfügung steht. Ein Impfstoff wäre ein wertvolles und effektives Mittel, um die Eliminierungsziele zu erreichen. Um die Entwicklung zu beschleunigen, wurde in 2015 die Initiative „TOVA - The Onchocerciasis Vaccine for Africa“ initiiert, die sich zum Ziel gesetzt hat bis 2025 mit klinischen Studien für eine Onchozerkose-Impfstoff zu beginnen.

Das Verständnis von protektiven Immunantworten gegenüber Filarien ist bisher begrenzt. Schutz wird mit einer Th2-dominierenden Immunantwort assoziiert, doch neuere Erkenntnisse legen nahe, dass auch Th1-assozierte Immunantworten zum Schutz des Wirts beitragen. Welche Rolle die Aktivierung von Nukleinsäurerezeptor-abhängigen Signalwegen durch Filarien während einer Infektion spielt ist noch weitestgehend unerforscht.

Ergebnisse dieser These zeigen, dass die Nukleinsäuren der nagetierpathogenen Filarie *Litomosoides sigmodontis* die Sekretion von Typ I Interferonen durch humane und murine Zellen auslöst. Außerdem führte die Infektion mit *L. sigmodontis* zu erhöhter Produktion des Typ I Interferons IFN-β. Dies korrelierte mit der Wurmlast.

Weiterhin war die Larvenmigration zur Pleura in TLR3-, TLR7-, TLR9-, STING- oder MDA5- defizienten Mäusen unverändert. Doch die Aktivierung von TLR3/MDA5/RIG-I durch die Agonisten poly(I:C) und 3pRNA führte zu einer reduzierten Wurmlast in der Pleura. Darauf basierend wurden das Potential von poly(I:C) und 3pRNA als Adjuvanz für eine Filarienvakzine analysiert. Die Injektion zeigte eine jeweils lokal erhöhte Immunaktivierung. Die dreimalige Immunisierung im Abstand von zwei Wochen mit bestrahlten *L. sigmodontis* L3 Larven in Kombination mit poly(I:C) oder 3pRNA induzierte die Produktion von parasitenspezifischen IgG1 und IgG2a/b Antikörpern im Serum. Des Weiteren inhibierte das Serum von Mäusen die mit Adjuvanz immunisiert wurden signifikant die Motilität von L3 Larven *in vitro*. Eine Infektion im Anschluss an eine Immunisierung wurde erfolgreicher geklärt, wenn die Tiere mit einer Kombination von bestrahlten L3 Larven und transfizierten poly(I:C) oder 3pRNA immunisiert

wurden. Durch die Gabe der Adjuvantien transfiziertes poly(I:C) oder 3pRNA wurde die Wurmlast um 73%, beziehungsweise 57% gesenkt, während die Immunisierung ohne zusätzlichen Adjuvant nur zu einer Wurmreduktion von 45% führte. Außerdem war der Anteil an Mikrofilarien-positiven Tieren geringer, wenn die Immunisierung zusätzlich zu den bestrahlten L3 Larven auch poly(I:C) oder 3pRNA beinhaltete. Dies deutet darauf hin, dass die Immunisierung einen Einfluss auf die Embryogenese hat und dazu beitragen kann die Transmission der Infektion zu unterbinden.

Insgesamt zeigen die Daten dieser These, dass Typ I Interferone zu einer protektiven Immunantwort in Filarieninfektionen beitragen können und, dass die Nukleinsäurerezeptor-Agonisten poly(I:C) und 3pRNA eine Impfstrategie für Filarienvakzine, möglicherweise durch das balancieren einer gegen den Parasiten gerichteten gemischten Th1/Th2 Immunantwort, verbessern können.

1. Introduction

In high-income countries, parasitic infections play a minor role in everyday life. But considering the global perspective, the majority of humanity is impacted by parasitic infections (1). Therefore, their control is in the interest of the global community. Infections with human pathogenic helminths do occur at a high prevalence in the tropics and sub-tropics and have a major impact on the endemic countries (2).

Helminths comprise the three groups of trematodes (flukes), cestodes (tapeworms) and nematodes (roundworms) that each harbor a variety of parasites with distinct life cycles (3). The parasites are residing at different locations in their host and hence show very different symptoms and pathology. Helminths have in common, that they are very efficient in modulating their host's immune system and that infections are generally characterized by the dominance of a type 2-associated immune response (4–6).

A subgroup of nematodes are filariae. These are threadlike parasites that cause a variety of filarial diseases and pose a major socio-economic burden on endemic countries, especially in Africa.

1.1 Filarial diseases

Three major human filarial diseases are river blindness, also called onchocerciasis, lymphatic filariasis, and loiasis (2).

Among these, lymphatic filariasis and onchocerciasis show the highest prevalence with 51 million and 21 million infected people, respectively. Both belong to the group of neglected tropical diseases (NTD) and their control is linked to the sustainable development goals of the United Nations (7, 8). Already in 2012 both diseases were targeted for elimination until 2020, as stated in the WHO roadmap and promoted by the London Declaration on NTDs in 2012 (9, 10). But since the 2020 goals were not achieved, detailed plans of action were renewed in the current road map "Ending the neglect to attain the Sustainable Development Goals: a road map for neglected tropical diseases 2021–2030", presented by the World Health Organization. In specific, onchocerciasis is targeted for elimination, by means of interrupted transmission in 31% of endemic countries, and lymphatic filariasis is targeted for elimination as a public health problem in 81% of endemic countries, until 2030 (7).

The diseases do not only stigmatize the affected and put a considerable socio—economic burden on African low-middle income countries. They also undermine the

control of other diseases like tuberculosis and increase the susceptibility to human immunodeficiency virus (HIV) (11–14). Filarial infections go hand in hand with a generally dampened immune response that also hampers the effectivity of well-established vaccinations (15–19).

Currently there is no vaccination for filarial diseases or human-pathogenic helminth infection available and the efforts of the WHO to eliminate the disease are largely based on mass drug administrations (MDA) (20–22). Since currently available drugs used for MDA are not effective in killing adult worms, annual treatment has to continue for several years to prevent disease transmission (21, 23). Lack of infrastructure in wide parts of endemic areas, political tensions, as well as patients' compliance are challenges for efficient MDA coverage. Further, arising resistances to the established drugs bring the urge for new treatment strategies (24, 25). A deeper understanding of parasite-host interactions may open the window to new treatment strategies. The attempt to develop potent prophylactic filarial vaccines has been in the focus of research for many years, but has not yet been successful (22, 26). A vaccination would be a new powerful tool to drive the elimination process, since it would have a long-term effect, requires compliance in a shorter time-frame and would likely be more cost-effective (27).

1.1.1 Lymphatic filariasis

Lymphatic filariasis is caused by *Wuchereria bancrofti, Brugia malayi* and *B. timori*. The parasites are transmitted to the human host via the bite of different vector mosquitoes and are endemic throughout the tropics and subtropics in 50 different counties (28). In 2018 there are around 51 million active infections registered, but a population of estimated 859 million people is living in endemic areas and requires MDA treatment in order to control transmission (28).

Roughly 1/3 of infections result in pathology. These patients develop damage of the lymphatics by a strong multifactorial inflammatory responses to the parasites (29, 30). Among those with pathology, nearly 40% are diagnosed with swelling of extremities, called elephantiasis and roughly 60% develop lymph collection in the scrotum, called hydrocele (29). Both pathologies display a strong physical disability and also influence the mental health of the patients (31, 32). The estimated disability-adjusted life years (DALY) per year are 1.6 million (33) and in 2017 the WHO classified lymphatic filariasis as one of the major causes for long-term disability worldwide (34).

However, in the majority of infections, the filariae are successful in modulating the host's immune response, so that the infection remains sub-clinical. Nevertheless, these people can contribute to the spreading of the disease (35). In 2000 the WHO launched the Global Programme to Eliminate Lymphatic Filariasis (GPELF), with the aim to eliminate the disease as a public health problem (36, 37). The treatment of lymphatic filariasis now relies on a triple therapy with the drugs ivermectin, albendazole and diethylcarbamazine (DEC) in areas that are not co-endemic for onchocerciasis and loiasis (28, 38). In areas that are co-endemic with onchocerciasis only albendazole and ivermectin are administered, while only albendazole is used in areas co-endemic with loiasis, due to the risk of severe side effects in co-infected patients (28). Additionally, the disease monitoring and cleaning of affected legs are implemented especially in rural areas, in order to reduce the progression of lymph edema to later stages and prevent co-infections of the skin (39, 40). Besides MDA and morbidity management, the disease prevention relies on education and the use of mosquito nets and insecticides.

1.1.2 Onchocerciasis

Onchocerciasis is caused by the filariae *Onchocerca volvulus*. The parasite is transmitted via S*imulium* black flies in tropical areas of sub-Saharan Africa, Jemen and the border between Brazil and Venezuela (41). According to the WHO there were an estimate of around 21 million cases in 2017 (41), but a population of 218 million people are living in endemic areas (42).

The pathology manifests as itching, skin lesions, subcutaneous nodules and visual impairment up to complete blindness. Adult worms reside in the subcutaneous nodules (onchocercomata), while microfilariae (MF) reside in the skin, lymphatics and cornea (43). Dying parasites expose endosymbiotic *Wolbachia* bacteria that trigger strong inflammatory immune responses and largely contribute to the development of pathology (43–45). The treatment of onchocerciasis relies on annual or bi-annual MDA using ivermectin (20). Since high numbers of dying MF elicit strong pathology, drugs that are slowly microfilaricidal have to be chosen in order to limit severe side effects. The use of tetracycline antibiotics like doxycycline that target the endosymbiotic *Wolbachia* bacteria and thereby induce sterility of adult worms presents a feasible treatment option. However, doxycycline treatment is contraindicated in pregnant and breast-feeding women, as well as children under the age of eight (46, 47).

Despite several decades of intervention programs, in 2017 an estimate of 14.6 million people developed skin disease and 1.15 million had visual impairment (41). Further consequences of disease are sleep deprivation, a negative impact on performance at school and work and therefore in the long run an increased risk for poverty (48). Already in the 1975 the Onchocerciasis Control Programme (OCP) was founded and vector control in West Africa was coordinated (49). As follow up, in 1995 the African Programme for Onchocerciasis Control (APOC) was launched. The APOC worked towards the goal of onchocerciasis elimination by establishing a community-directed MDA treatment with ivermectin. While onchocerciasis was not eliminated, the efforts made by APOC until 2015 still had a major impact on disease control (50, 51). It appears that the current MDA program on its own is not sufficient to achieve successful elimination of onchocerciasis and loses its efficiency once the prevalence is low (52–55). Therefore, united efforts are made to develop new, especially macrofilaricidal drugs (23, 56–59). Additionally, in 2015 an initiative for an onchocerciasis vaccine was launched, named TOVA – The Onchocerciasis Vaccine for Africa (54). This initiative is a partnership between scientists from Africa, Europe and the USA that aims to pass onchocerciasis vaccine candidates through phase I clinical trials until 2025 by combining their manifold expertise (60).

1.1.3 The life cycle of the filariae *Wuchereria bancrofti*

The life cycles of filariae are complex and involve the parasitic development in two different host species.

As example, the life cycle of the filariae *W. bancofti* is shown in Figure 1.1. An infected mosquito feeds on a human and thereby transmits infective L3 larvae to the human host. In the human host the larvae migrate to their site of adult residence, which in case of *W. bancrofti* is the lymphatic system. There the larvae develop into male and female adults, which can mate and release offspring – MF. MF migrate through the lymphatics and the blood. Through another blood meal by the vector, the MF can be taken up again, develop into L3 larvae and the life cycle continues (61).

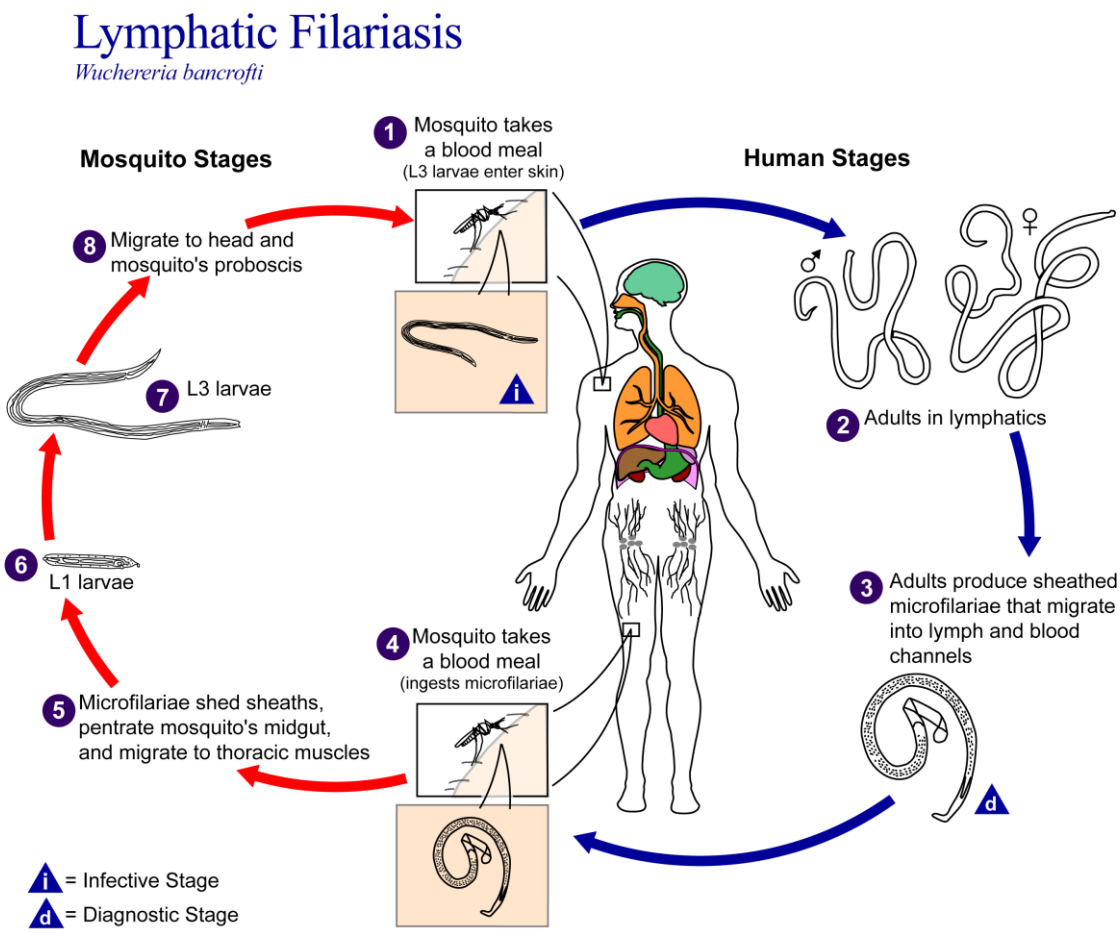

Figure 1.1 I The life cycle of *Wuchereria bancrofti.* During a blood meal infective *W. bancrofti* L3 larvae are transmitted from the mosquito to the human host. Within the human lymphatics, the parasite develops into the adult stage that releases its offspring (microfilariae). The microfilariae migrate to the blood, where they will be taken up during a mosquito's blood meal. In the mosquito the microfilariae develop into infective L3 larvae and the life cycle continues (61) .

1.1.4 The *Litomosoides sigmodontis* laboratory model to study filarial infections

Since human pathogenic filarial nematodes are unable to complete their full life cycle in immunocompetent laboratory rodents, immunological studies greatly rely on the infection of rodents with surrogate filarial nematodes (62, 63). A widely accepted model to study human filariasis is the infection of mice with the rodent filarial nematode *L. sigmodontis* (62, 64–66). The natural host is the cotton rat *Sigmodon hispidus*, and the natural habitat of the parasite is spread throughout South America and south of North America (67). Other rodents that are susceptible to the infection with *L. sigmodontis* include Mongolian gerbils (*Meriones unguiculatus*) (68) and laboratory mouse strains like BALB/c (64).

L. sigmodontis belongs to the family of *Onchocercidae*, that also includes human pathogenic filaria such as *O. volvulus* (3, 69) and an immunological cross-reactivity with *O. volvulus*, *W. bancrofti*, *B. malayi* and *L. loa* has been described (70–72). Immunological studies with *L. sigmodontis* revealed a great resemblance between the murine and human immune responses during filariasis (62, 73). Therefore, substantial advances in immunological understanding and drug development for human filarial diseases have been made with this model and it also builds a base for vaccine development (63, 65, 74, 75).

1.1.4.1 Life cycle of *Litomosoides sigmodontis*

The life cycle of *L. sigmodontis* is similar to the life cycle of human pathogenic filariae (76). During their life cycle, *L. sigmodontis* larvae undergo their first developmental stages in the tropical rat mite *Ornithonyssus bacoti* (Figure 1.2) (67). MF (L1 larvae) are ingested during a blood meal on an infected rodent. In the mite the parasites develop into infective L3 larvae within 12 to 14 days. During feeding, the L3 larvae are then transmitted to the vertebrate host.

In the vertebrate host, for example a susceptible BALB/c (64), the L3 larvae migrate via the skin and lymphatics through the lung into the pleural cavity within 2-6 days (77). Only around 1/5 of the transmitted larvae are successful in their journey to the pleural cavity (77). The L3 larvae develop into L4 larvae from around 8 – 14 days post infection (dpi). At around 30 dpi adult female and male worms have developed and can start mating. Starting at day 50 post infection L1 larvae, also called MF, are released into the blood, so that the full life cycle can continue upon a mite’s blood meal (78).

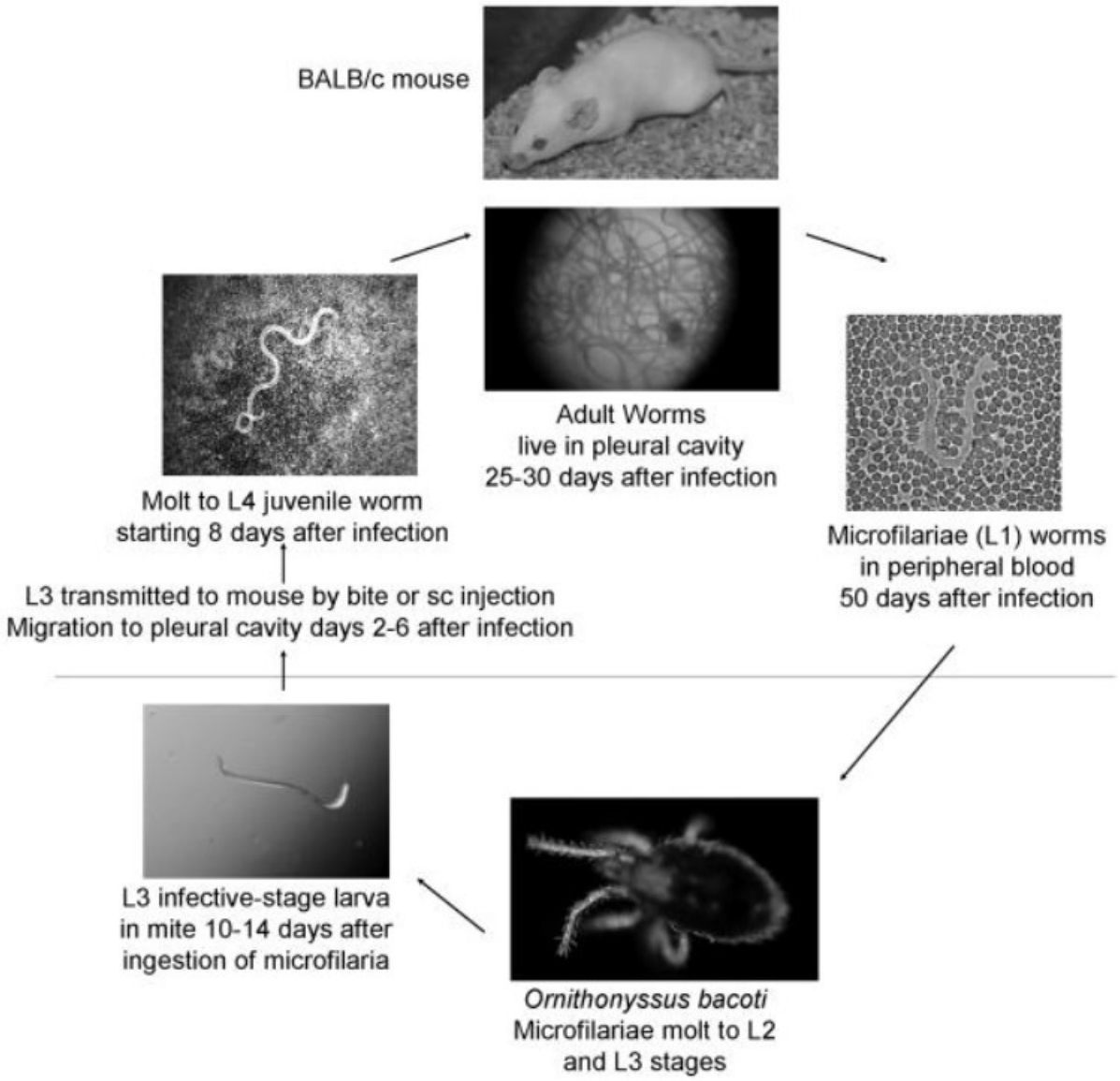

Figure 1.2 I The life cycle of the rodent filarial nematode *Litomosoides sigmodontis* with BALB/c mice as vertebrate host. During a blood meal infective *L. sigmodontis* L3 larvae are transmitted from the intermediate host *Ornithonyssus bacoti* to the vertebrate host. In the vertebrate host the L3 larvae migrate to the pleural cavity within 2 – 6 days. There they first molt into L4 larvae and then into adult worms. Adult female and male worms develop after 25 – 30 days, mate and release microfilariae as their offspring. The microfilariae enter the peripheral blood 50 days post infection, where they can be taken up during a blood meal of the intermediate host. In the intermediate host the larvae develop into infective L3 larvae and the life cycle continues (78).

BALB/c mice are considered as susceptible host. Adult worms survive until around 70 days post infection and in roughly 70% of the infected female mice and 30% of male mice MF can be observed in the blood (64, 79). This reflects human filarial infections and allows to analyze differences in latent (MF negative) and patent (MF positive)

infections (62). Until 70 dpi the adult worm burden remains stable (79). By day 119 after infection the adult worms are mostly cleared (73).

The infection of C57BL/6 mice is considered as semi-susceptible model, since *L. sigmodontis* cannot complete its full life cycle. Already 35-45 days after infection the adult worms are killed in the pleural cavity, so that the release of MF cannot take place (65, 79, 80). Therefore, C57BL/6 mice can be used to study earlier time points during infection and decipher protective immune mechanisms (62).

1.1.5 Immune responses during filarial infection

During human filarial infection the immune response is predominantly Type 2-associated and the parasites release various products that regulate host immunity at several levels (81, 82). Thereby the parasite ensures its survival and at the same time the host is less likely to suffer from self-damage due to intense inflammation (83).

Filariasis patients reveal increased numbers of eosinophils (84), macrophages polarize towards an alternatively-activated state (85) and the cytokine milieu is dominated by IL-4, IL-5, IL-9, IL-10 and IL-13 (82). T helper cells differentiate into Th2 cells, regulatory T cell proliferate, a parasite-antigen-specific T cell hyporesponsiveness develops (82, 86) and B cells produce IgE, IgG4 and IgA antibodies (87–89).

Overall, human immune responses are mimicked by the infection of BALB/c mice with *L. sigmodontis* (63, 65, 80) and the immune responses to *L. sigmodontis* in mice have recently been reviewed (63, 75).

The impact of Immune responses in the skin during natural infection on the long term outcome has not been clarified in detail (75). Mast cells residing in the skin can recognize *Wolbachia* and may impact the migration of *L. sigmodontis* in the skin, since degranulation of granulocytes enhances vascular permeability and facilitate L3 migration (90). Upon infection, neutrophils are recruited to the skin and drive protective immunity against invading L3 larvae (91, 92). The depletion of neutrophils prior to infection results in a significantly elevated adult worm burden (91). While in primary infections eosinophils do not target invading L3 larvae, they are essential for protective immune responses against the adult stage and vaccination efficacy (73, 93, 94). The invading L3 larvae rapidly leave the subcutaneous tissue within a day and start entering the lungs as soon as six hours after natural infection (77, 95). In the lung the invasion by *L. sigmodontis* larvae results in rapid inflammation due to neutrophil recruitment, granuloma formation, hemorrhages and the release of pro-inflammatory cytokines

(77). Lung pathology persists during infection and is later driven by MF (96, 97). Despite the immune responses in the lung, roughly 1/5 of larvae reach the pleural cavity by day 8 after infection (77, 80). Already starting five days after the infection there is an increase of ILC2s limited to the pleural cavity. Therefore, they likely contribute to Type 2-associated immunity (98). During infection, also neutrophils and eosinophils are recruited to the pleural cavity. Over the course of infection, they attach to the parasites and granuloma are formed (99). Pleural eosinophil counts peak eight weeks post infection, correlating with the onset of MF in the peripheral blood (100). Besides granuloma formation, the degranulation of eosinophils plays a crucial role for worm clearance (101). Also, the event of eosinophil ETosis has been shown to target *L. sigmodontis* MF and L3 larvae *in vitro*. Further, the motility inhibition of MF *in vivo* by the entrapment in eosinophil released DNA nets contributes to parasite clearance (102). The lack of eosinophils results in an increased adult worm burden and patency in all animals (73).

The macrophages in the pleural cavity polarize towards an alternatively-activated state during *L. sigmodontis* infection and accumulate in the pleural cavity within two weeks after infection (103). Alternatively-activated macrophages (AAM) express high level of RELMα and can and limit larval induced tissue damage (104). Around the time of molting into adult worms there is an influx of NK and NKT cells into the pleural cavity and the depletion of NK cells results in increased adult worm burden (105).

Next to innate immune responses, mice also mount an adaptive immune response to control the infection with *L. sigmodontis* (106). A key cell for maintaining protective immune responses are T helper cells, which predominantly polarize towards the Th2 type. Their depletion results in reduced numbers of eosinophils, Th2-associated cytokines, parasite-specific and consequently in an increased parasite load (107). Besides an intrinsic Th2 cell hyporesponsiveness, *L. sigmodontis* actively regulates Th2 cells and also regulatory T cell populations expand (108–110). Hyporesponsive Th2 T cells cannot proliferate any longer and do not produce cytokines (108). Regulatory T cells inactivate other T cell populations and regulate immune responses to filariasis via IL-10 (111). Taken together this drives susceptibility to infection (75, 108).

B cells are the most abundant immune cells in the pleural cavity of naïve animals and expand during early *L. sigmodontis* infection (112). During the course of infection, B cells release different antibody isotypes. Especially the release of IgE (107) and IgG1

(113) is associated with *L. sigmodontis* infections. Antibodies can promote pathogen killing by innate immune cells through opsonization (114). The *L. sigmodontis* infection of μMT mice, which lack mature B cells, has no impact on the adult worm burden, but prevents the development of microfilaremia (115).

The cellular immune responses described are largely orchestrated by cytokines. Key cytokines during *L. sigmodontis* infection are IL-4, IL-5 and IL-13 (75). IL-4 for example drives the differentiation of T helper cells into Th2 cells and IL-5 is crucial for eosinophil recruitment and maintenance , while both affect antibody production by B cells (114). Animals that are deficient for IL-5- or the IL-4 receptor and IL-5 develop higher adult worm burden and MF loads (73). IL-4 and IL-13 polarizes macrophages to the alternatively activates state (116). Despite the dominance of Th2- associated cytokines, also interferon (IFN)-γ is relevant for the infection outcome. The deficiency of IFN-γ leads to reduced worm clearance and granuloma formation by impairing neutrophil function (117). Further, a synergetic effect of IFN-γ with IL-5 on worm clearance is described in infection knockout experiments (118).

Overall, the interplay of different immune responses and what accounts as protective immunity during the infection with *L. sigmodontis* is very complex and is continuously understood in more detail.

1.2 Innate pathogen recognition by pattern recognition receptors

The function of cells of the innate immune system is to rapidly and efficiently distinguish self from non-self and thereby quickly clear the body from invading pathogens or toxins, while not damaging cells of the own body. For prompt differentiation, the recognition of self vs. pathogen relies on the detection of larger molecular structures. These pathogen-associated molecular patterns (PAMP) can be sugars or nucleic acids (119). The recognition of nucleic acids is mostly studied in the context of viral infections, but the activation of nucleic acid receptors has also been described for parasites like *Schistosoma* and *Plasmodium* (120, 121).

For different molecular structures, different pattern recognition receptors (PRR) have evolved. Receptors are either found on the cellular surface, in endosomes or freely in the cytosol, dependent on the mechanism of action where the PAMP enters the cell (122). PRR families are the C-type lectin receptors (CLRs), toll-like receptors (TLRs), Retinoic acid - inducible gene - I - like receptors (RLRs) and nuclear oligomerization domain (NOD)-like receptors (NLR). CLRs are found on the cell surface and bind

pathogen-associated carbohydrates. TLRs are found on the cell surface, as well as in the endosome and cover a wide range of PAMPS. RLRs and NLRs reside in the cytosol and recognize nucleic acids and bacterial peptidoglycans, respectively (114). The expression of many PRRs is limited to certain cell populations, which in some cases are different, when comparing human and murine cells (123, 124) and also non-immune cells can express PRRs (125–127).

When it comes to the sensing of nucleic acids, there are different sets of sensors for DNA or RNA. These are either located in the endosome or in the cytosol. Thereby the cells cannot only identify pathogenic DNA or RNA, which is for example differently modified in bacteria, but the cells can also sense whether body own nucleic acids are in the wrong cellular compartment, which indicates damage and danger (122).

The recognition of RNA and DNA involves different sets of receptors, which are described in chapters 1.2.1 and 1.2.2, respectively. The downstream signaling pathways of the different nucleic acid receptors are partially shared and result in the secretion of the Type I interferons (IFN-α and IFN-β) (128).

1.2.1 RNA sensing

During the process of protein biosynthesis host mRNA is exported from the nucleus into the cytoplasm. Therefore, also during healthy biological conditions host RNA is found in the cytosol and recognition of foreign RNA involves the differentiation between structural modifications. Extracellular vesicles (EVs) can deliver information for example in form of RNA to recipient cells and can be taken up by the endosomal pathway (129).

Known endosomal RNA sensors are toll-like receptors TLR3 and TLR7/8 (Figure 1.3). TLR3 recognizes double stranded RNA and can be activated by its agonist naked poly(I:C) (130). TLR7/8 recognizes single stranded RNA and can be activated by the synthetic imidazoquinoline compound Resiquimod (R848) (131, 132). The activation of these receptors can either activate the transcription factors IRF3 (*interferon regulatory factor 3*) - IRF7 and induce the production of Type I IFNs, or result in NF-κB (*nuclear factor kappa-light-chain-enhancer of activated B cells*) dependent production of inflammatory cytokines some of which are linked to inflammasome activation (128).

Cytosolic RNA sensors are members of the RLR family. MDA5 (*melanoma differentiation-associated gene 5*) is known to recognize long double stranded RNA and can be activated by synthetic poly(I:C) that is introduced to the cytosol by

transfection. Dependent on its size, transfected poly(I:C) is also a potent activator of another cytosolic RNA sensor, RIG-I (133). RIG-I recognizes a variety of RNA structures, such as (i) double or single stranded RNA with a 5' tri-phosphate moiety, (ii) short double stranded RNA or (iii) double stranded RNA structures with a blunt end at its 5' (128, 133). A RIG-I-specific agonist is 3pRNA (134).

Upon activation, the sensors MDA5 and RIG-I share their downstream signaling cascade. They interact with the adaptor molecule MAVS (*mitochondrial antiviral-signaling protein*), which leads to the activation of the transcription factors IRF3 - IRF7 and can impact apoptosis or induce the production of type I IFNs (128).

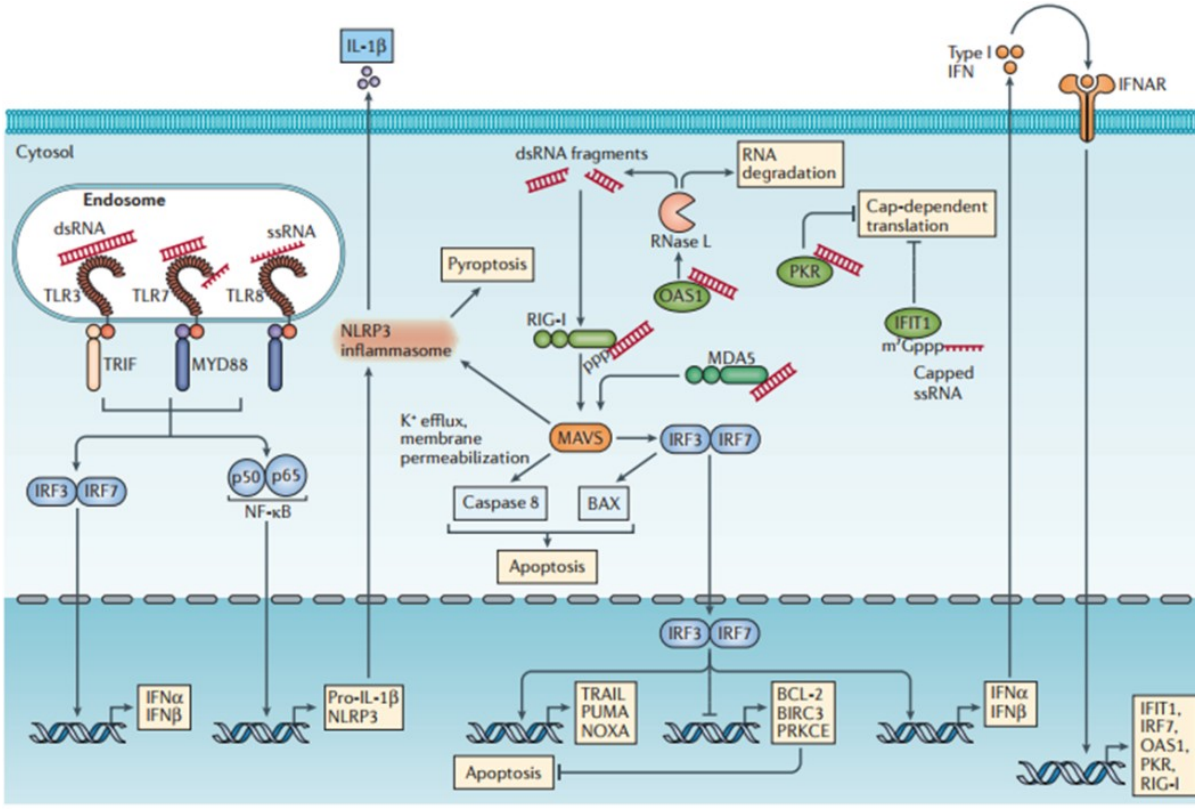

Figure 1.3| RNA sensing. Endosomal RNA recognition is mediated by TLR3 (*toll-like receptor 3*), TLR7 and in humans TLR8, which either results in the production of Type I interferons (IFNα, IFNβ) via the activation of IRF3 (*interferon regulatory factor 3*) - IRF7, or the NF-kB (*nuclear factor kappa-light-chain-enhancer of activated B cells*) dependent production of other pro-inflammatory cytokines and possibly inflammasome activation. Cytosolic recognition involves the receptors RIG-I (*retinoic acid inducible gene I*) or MDA5 (*melanoma differentiation associated gene 5*), which are recruited to the adaptor protein MAVS (*mitochondrial antiviral-signaling protein)* and trigger the downstream cascade of IRF3/7 activation and cytokine production like Type I IFNs (128). The use of this illustration was licensed by Springer nature.

1.2.2 DNA sensing

In eukaryotes the majority of DNA is found in the nucleus. Besides the nucleus, DNA is found inside the mitochondria or membranous compartments. Self-DNA that enters the cytosol is degraded by DNases. The accumulation of DNA is associated with strong IFN signaling and can cause autoimmune diseases (135). Therefore, in the healthy state DNA is not found in the cytosol.

The known endosomal DNA sensor is TLR9 (Figure 1.4). Upon its activation the transcription factors IRF7 or NF-κB are activated and result in the release of type I IFNs or other proinflammatory cytokines and inflammasome activation, respectively (128).

TLR9 recognizes unmethylated deoxycytosine-deoxyguanosine (CpG) DNA (136) and RNA-DNA hybrids (137). Several synthetic oligodeoxynucleotides (ODN) that contain bacteria-like CpG motifs have been developed to target TLR9 and trigger distinct signaling cascades. These agonists are grouped in classes A, B and C (138–140). CpG class A are potent inducers of IFN-α production by plasmacytoid dendritic cells (pDC) (141), but fail to induce NF-κB signaling and B cell activation in the absence of pDCs (140). In contrast to that, CpG class B are potent B cell and NK cell activators but induce low levels of IFN-α (142). The development of CpG class C, provides agonists that cover the action of both of the other classes and are proficient to induce a strong IFN-α response while activating B cells and NK cells, as well (139, 140, 143).

Cytosolic DNA recognition is mediated by several DNA sensors that signal via STING (*stimulator of interferon genes*) and mainly induce an IRF3-dependent type I IFN production (128). An agonist for cytosolic DNA sensors is IFN stimulatory DNA (ISD) derived from the *Listeria monocytogenes* genome (144). STING can directly be activated by the agonist cyclic guanosine monophosphate–adenosine monophosphate (cGAMP), which under biological condition is produced from cytosolic dsDNA by cyclic GMP-AMP synthase (cGAS) (145).

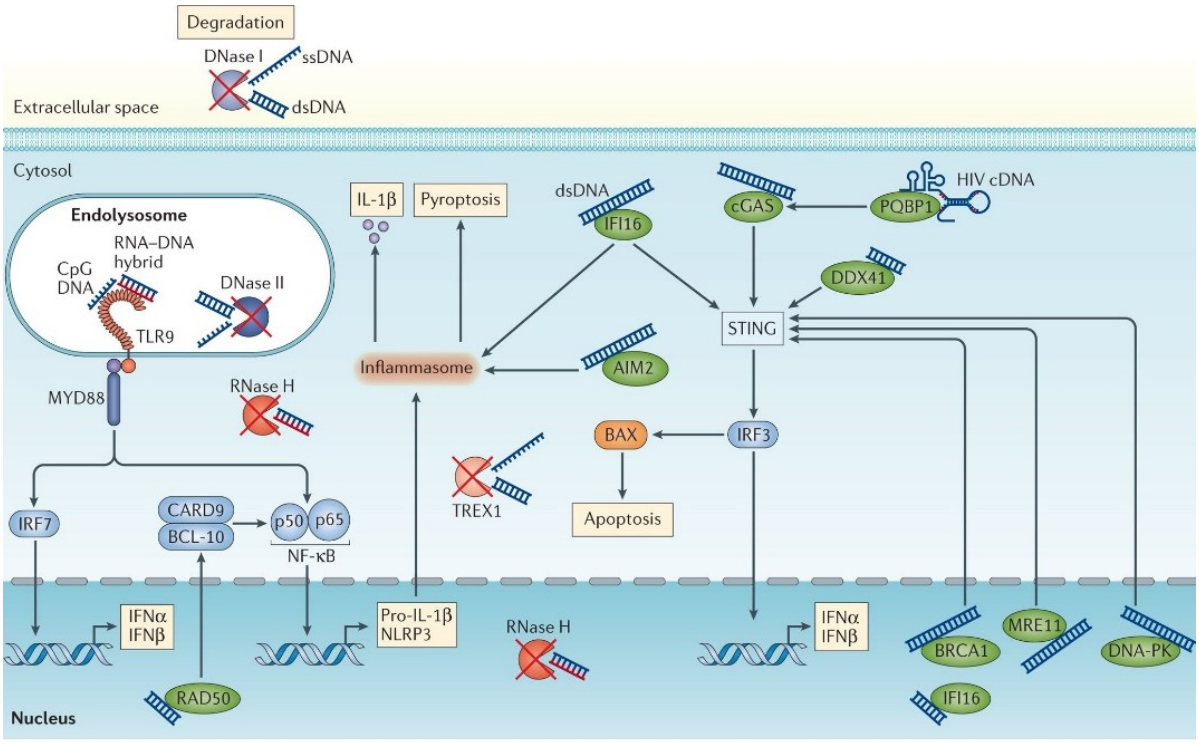

Figure 1.4| DNA sensing. The recognition of DNA in the endosome is mediated by TLR9 (*toll-like receptor 9*), and induces the production of Type I interferons (IFNα, IFNβ) in response to the activation of IRF7 (*interferon regulatory factor 7*) or the production of pro-inflammatory cytokines like IL-1β in consequence of NF-kB (*nuclear factor kappa-light-chain-enhancer of activated B cells)* activation. In the cytosol, DNA is recognized by a range of free cytosolic sensors, which mutually signal via STING (*stimulator of interferon genes*) and induced the production of type I IFNs as result of IRF3 activation (128). The use of this illustration was licensed by Springer nature.

1.2.3 Nucleic acid sensing in helminth infections

The host-pathogen interaction concerning helminths and nucleic acid sensing is not yet well studied but appears to be an important aspect in order to understand regulatory mechanisms and how to overcome these during disease.

One aspect that is discussed in regard to nucleic acids and helminth infection, is the immune modulation via miRNA that is released by the parasite in EVs (146–150).

The immune modulation by helminths also appears to directly affect nucleic acid sensing pathways in the host.

In studies with the filarial nematode *B. malayi*, it was described, that the viable MF downregulated the expression of the RNA sensors TLR3 and TLR7 in monocyte-derived human DCs (151) and monocytes (152), *in vitro*. Further, the monocyte-derived human DCs released significantly less IFN-α in response to activation with the TLR3 agonist poly(I:C) (151). In BALB/c mice that were infected with *B. malayi* L3 larvae, the mRNA expression of TLR9 was significantly decreased in DCs (153). In line

with that, the TLR9 mRNA and protein expression of B cells was significantly reduced in *B. malayi*-infected South Indians. B cells and monocytes from infected individuals also had reduced antigen presentation (CD80, CD86, HLA) upon specific activation of TLR9 by CpG stimulation in comparison to cells from uninfected individuals (154). The TLR9 protein expression of T cells was not reduced due to filarial infection (155). It appears that also the differences in pathology among filariasis patients are linked to nucleic acid sensing. Upon parasitic antigen stimulation the mRNA expression of TLR7 and TLR9 was significantly higher in peripheral blood mononuclear cells from patients with chronic pathology compared to cells from asymptomatic infected people (156). Further, cells from patients with chronic pathology reacted with a stronger Th1- and Th17-associated cytokine response to the stimulation with TLR9 or TLR7 agonists (157).

During *Schistosoma* infection, the RNA sensors TLR3 and TLR7, as well as the DNA sensor cGAS and its adaptor molecule STING, were identified to shape immune responses during infection. The expression of TLR3 on T cells, B cells and NK cells in the lung was significantly increased upon *S. japonicum* infection in C57BL/6 mice (158). TLR3 modulates immune responses by activating NK cells during *S. japonicum* infection in C57BL/6 mice (159) and was also identified as receptor that recognizes dsRNA from *S. mansoni* eggs (120, 160). Further, Vanhoutte and colleagues stated that TLR3 signaling enhanced Th1 immune responses during *S. mansoni* infection in C57BL/6 mice. Thereby TLR3 impacted the Th1/Th2 balance, but did not impact worm and egg burden or liver pathology (160). At the same time, Joshi and colleagues described that the depletion of TLR3 resulted in stronger pulmonary granuloma immunopathology during *S. mansoni* infection in C57BL/6 mice (161). According to Jiang and colleagues, the depletion of TLR7 did not impact worm and egg burden after *S. japonicum* infection (162).

In vitro studies showed that *S. mansoni*-derived DNA is sensed via the cGAS – STING pathway (163). The infection of C57BL/6 STING$^{-/-}$ and C57BL/6 cGAS$^{-/-}$ mice revealed increased worm clearance, but no impact of the C57BL/6 STING$^{-/-}$ on the number of eggs and granuloma (163).

Overall, literature shows that different helminth species manipulate nucleic acid sensing pathways, but can also be recognized by the host immune system via these receptors. This suggests, that the activation of nucleic acid receptors impacts parasite survival and can contribute to protective immunity.

1.3 Vaccination

Prophylactic vaccinations are one of the most powerful tools to prevent the spreading of disease and facilitate broad elimination. First immunization experiments go back far into history before the Christian era and were only brought to Europe by Lady Mary Wortley Montague in the 18th century (164–166). Probably, the most famous example for immunization, and shaping the term vaccination, were experiments by Edward Jenner at the end of the 18th century that paved the way for the eradication of smallpox in 1980 (167, 168).

Since then, the immunological mechanisms behind the observed protection in response to immunization have been analyzed. Researchers identified various strategies to adjust vaccinations for different pathogens, prophylaxis or therapy and increased efficacy and safety.

1.3.1 Principle of vaccination

Broken down, this tool utilizes the capability of the vertebrate immune system to generate long lasting immune memory towards selected pathogen-derived antigens. Thereby upon repeated encounter the immune system efficiently eliminates the invading pathogen before a threatening disease can manifest. In order to generate long lasting protection several players of the immune system have to cooperate. Professional antigen presenting cells, like dendritic cells or macrophages, activate cytotoxic T cells or T helper cells by presenting antigen to the T cell receptor and secreting cytokines. In turn the T cells expand and differentiate into memory and effector cells. While cytotoxic effector T cells can directly kill cells that are infected with an intracellular pathogen, T helper cells can activate other immune cells. Th2 cells for example help to activate B cells. Then the B cells can start to produce antibodies. There the dominant cytokine milieu determines which antibody isotypes are produced. IL-4 for example can induce the production of IgE antibodies, which contributes to allergy. The production of different antibody isotypes and the differentiation into memory cells, largely depends on the activation of conventional B2 B cells by T cells in secondary lymphoid organs like lymph nodes or the spleen (114). In the spleen also neutrophils can provide help to marginal zone B cells and thereby induce antibody production of IgM (169).

In order to achieve this protective effect by an immune system that induces cell- and antibody-mediated responses, different types of vaccinations have been developed.

As strongest vaccines account live attenuated vaccines. Here, the virulence of the living pathogen is weakened, so that the disease is mimicked in a mild form and educates the immune system with the same antigens as the wild type pathogen. Prominent examples for this type of vaccine are measles and mumps vaccine. These provide long-lasting immunity in a high percentage of vaccinated people and elicit strong cellular- and antibody-mediated responses without further assistance needed. Disadvantages of live attenuated vaccines are (i) that the genome of the pathogen has to be controlled, which is more difficult the larger the genome is (for example for bacteria), (ii) the possibility of mutations that bring back stronger pathogenicity and (iii) the vaccine cannot be given to immunocompromised individuals or during pregnancy, due to a risk of severe disease or immune damage (170).

Safer methods of vaccination that mimic the immune stimulation by a pathogen are types of non-live vaccine. These can be (i) inactivated vaccines, where the pathogen is killed prior to injection and cannot replicate (like the influenza vaccine), (ii) subunit vaccines, where pathogen-specific antigens are purified or toxoids are produced by inactivating pathology-inducing exotoxins (for example hepatitis B, diphtheria and tetanus), (iii) conjugate vaccines, where strong immunogenic antigens are linked to a mildly immunogenic antigen (for example the *Haemophilus influenza* type b vaccination) or (iv) recombinant vector vaccines where antigens of the target pathogen are incorporated into an attenuated organism like an adenovirus (114).

In many of these vaccines the antigens on their own lack immunogenicity to induce long-term protection and therefore need to be combined with adjuvants that provide a boost of the immune system (171).

Recent events of the Covid-19 pandemic led to the broad use of newly developed mRNA vaccines in humans. In brief, these vaccines introduce the mRNA of a previously identified potent antigen into the human cells. As a consequence, immunogenic antigens of the pathogen are produced by the host cells and educate the hosts immune system (172). Further, DNA vaccines are being investigated in human clinical trials. In this approach the DNA encoding for an antigen is introduced into cells by using DNA plasmids (173).

Besides prophylactic vaccines, also therapeutic vaccines are used. Here the immune system is not educated prior to an infection, but antigens are administered during infection or disease, like for example cancer, in order to boost the immune system to actively fight the pathogen or malignant cells (174–176).

1.3.2 Vaccine adjuvants

Key features of long-term protection are the generation and maintenance of memory B cells and memory T cells, as well as the persistence of circulating pathogen-specific antibodies. In order to induce these players of immune memory and not simply a single immune response against the presented antigen, the immune response triggered by the vaccine needs to be thoroughly fine-tuned. Multiple players of the immune system have to be involved and need to be skewed in order to produce the desired immune response that is protective for the specific type of pathogen that shall by introduced by the vaccine (171).

Antigens are therefore combined with adjuvants in order to enhance, prolong and shape the elicited immune response (171). Adjuvants can be delivery systems that protect, guide and present the antigens to the desired immune cells and the cellular compartment that harbors the targeted receptor. Further, adjuvants can be immunostimulatory substances themselves that trigger certain receptors and activate their specific downstream signaling cascade (171, 177).

Besides enhancing and shaping the desired immune responses, further advantages of adjuvants are the reduction of antigen or of repeated injections that is needed for successful immunization. Further, adjuvants allow immunization of people with weak immune responses due to age or being immunocompromised (171).

Until now a variety of adjuvants are described, but new adjuvants are continuously evaluated since many are not suitable for clinical use due to side effects (171).

Immunostimulatory adjuvants target different PRRs, and as described before this can result to different actions in different cell types. For example TLR3 activation on dendritic cells leads to IL-12 production and improves antigen presentation, while MDA5 activation mainly induces type I IFN production and the activation of TLR9 boosts antibody production and polarizes towards Th1 immunity (178).

When choosing an adjuvant it has to be considered to select an adjuvant that triggers the desired type of immune response for the targeted pathogen (171).

So far the adjuvants approved by the EMA and FDA are mostly based on formulations containing aluminum (171, 179, 180). Aluminum-salts, known as alum are antigen-adsorbent adjuvants (181). They typically induce a Th2 driven immune response, inflammasome activation (182) and overall rather induce antibody instead of T cell responses (124). For long-term protection against many pathogens the shaping of T cell responses is equally important as antibody production by B cells (124, 182).

In contrast to adsorbent adjuvants, microbial or synthetic adjuvants directly trigger the immune system via PRRs (171). In that regard nucleic acid receptor agonists entered the field of vaccine adjuvants, and have not only been studied as cancer vaccine, but also in the context of viral and parasitic infections (124).

Poly(I:C) as TLR3 agonist was evaluated in clinical phase I-II study for influenza vaccines, where it was well tolerated by the participants (124, 183). In another study it was described as a promising adjuvant for therapeutic vaccination for human immunodeficiency virus (HIV) infection (184).

In murine experiments, 3pRNA was described as potent adjuvant for the induction of strong type I IFN secretion by pDCs and macrophages, and importantly antigen-specific cytotoxic T cell responses (185). A human clinical trial of a RIG-I ligand in tumor therapy was terminated for business reasons (186).

Most advanced is the use of the TLR9 agonist CpG, which has been analyzed in various studies (187, 188) and is used as adjuvant for a hepatitis B vaccination (180). CpG oligonucleotides have also been applied as adjuvant in therapeutic vaccines against parasitic infections (189, 190).

1.3.3 The challenge of helminth vaccinations

Since helminths are specialists in modulating and evading the host's immune system, the development of vaccines remains a challenge. In contrast to viral and bacterial infections, the infection with helminths often results in a non-protective immune response that is not successful in killing the parasite and the infection persists chronically (74). In endemic areas the majority of people are infected at a young age, so by the time a vaccination can be given, the immune system is already modulated by the parasite. This presents a great obstacle, that could be helped by finding a potent macrofilaricidal drug that can be administered prior to vaccination in order to clear the body from the parasite and its immunomodulatory molecules (74). It was reported though, that the infection with helminths can have a long-term shaping effect even after treatment, so that a vaccination still would ideally be administered prior to infection (191, 192).

Hand in hand with their strong immune modulating potential, helminths are more complex than bacteria or viruses and thereby provide a broader range of possible targets, but this of course also makes it more laborious to identify such. To that end the complex interplay of parasite and (innate) immune system has to be studied in

detail, in order to identify mechanisms that are more regulatory or activating (15). There it has to be taken into account, that the parasites undergo several developmental stages in different locations. Therefore, the antigens reactive for a certain parasite stage not necessarily drive protection from other developmental stages and each body location brings its own immunological niche (193). Understanding these interactions is essential to identify potent antigens. In order to overcome immune modulation, it is also advisable to take “hidden-antigens” into account. These are not directly linked to the parasite itself, but are released in order to modulate the immune system. Hence it would be beneficial to neutralize these with the aid of a vaccination and limit the modulatory potential of the parasite. Further, it can be advantageous to focus the vaccination target on the larval stage that is transmitted, so that the infection is cleared before the immunomodulation takes place. Other vaccine approaches could target the stage that drives pathology or target the offspring to stop further transmission.

But even after identifying potential antigens with the help of omics, over the last years it turned out to be troublesome to make the way to a vaccine. Here antigens should be chosen that not only result in antibody- but also T cell responses (193). In cases of hookworm vaccine development, it turned out that the induction of IgE responses led to strong side effects (194), and rather overcoming the T cell hyporesponsiveness, which is associated with chronic infection, is likely to be relevant for vaccine success (111, 124).

A further challenge for the development of helminth vaccines is the diversity of parasites that all have different experimental models, and make it difficult to translate the results from the different models to the human situation despite species homology (74).

In spite of these obstacles there has been great progress over the last decades in developing helminth vaccines and attempts to bring them to the clinic (190).

The major tasks remaining are to (i) identify antigen (maybe even a cocktail of antigens) that induces protective and not modulating immune effects and do not induce pathology themselves, (ii) understand which events contribute to protection and (iii) find new adjuvants that not only support antibody production, but also induce memory effector T cell responses, despite occurring immunomodulation due to previous infection. As a challenge these responses also need to match the suitable protective immune pathways (74, 190).

1.3.4 Current helminth vaccinations

The greatest progress in the development of human helminthic vaccines has been made for *Schistosoma* and hookworm vaccinations.

For schistosomiasis four vaccine candidates are being evaluated in human clinical trials in combination with aluminum-based adjuvants (195). Interestingly, research in animal models with *S. japonicum*, highlighted the beneficial effects of nucleic acid receptor agonists as vaccine adjuvants in the context of parasitic infections. Wang and colleagues observed that the combination of a DNA vaccine with TLR7/8 and TLR9 ligands enhanced the vaccination success. Their immunological analysis revealed a reduction of regulatory T cells, which counteracted immune suppression (196). The use of the TLR9 ligand CpG as adjuvant for a *Schistosoma* vaccine has also been positively evaluated by others (197, 198).

Current human hookworm vaccine studies mainly rely on two recombinant proteins, which have been tested in several clinical studies (199). In most studies, aluminum-based adjuvants were used, but also CpG has been tested in a phase 1 clinical trial for prophylactic hook worm vaccine. A phase 2 study shall be completed by June 2022 (190, 200). So far, the use of CpG as adjuvant led to a significant improvement of humoral responses towards the administered *Necator americanus* antigen (201).

Experiments on filarial vaccination were reviewed by Morris and colleagues (202). Since then, filarial vaccination studies are still performed in several animal models and human serum is used to test for antigen reactivity (203). No clinical trials for vaccines in the context of filariasis were registered at the time of the search (July 2021) (204).

Research on the development on an *O. volvulus* vaccination for Onchocerciasis is performed in several host species. In the bovine model of *O. ochengi* a subunit vaccination is tested, which contains eight recombinant antigens that previously showed protection in other models (205). As adjuvants Freund's complete adjuvant (a water-oil emulsion containing heat-killed *Mycobacterium tuberculosis* (206) or alum was used. This approach did not protect the animals from nodule formation, but 42% of the immunized animals had no MF in the skin.

Most promising recombinant proteins for *O. volvulus* vaccination are *Ov*-103 and *Ov*-RAL-2, which induced host protection up to 64% in mice (207, 208). A further study describes that the protection following immunization with *Ov*-103 and *Ov*-RAL-2 was antibody-dependent (203). The subsequent quantification of antigen-specific antibodies in human serum, revealed that the majority of putatively and concomitantly

immune individuals had increased IgG1 and IgG3 responses. In co-cultures of *O. volvulus* L3 larvae with naïve human neutrophils or monocytes, the supplementation with serum from infected individuals or anti-*Ov*-103 antibodies inhibited larval molting. Interestingly, the serum of putatively and concomitantly immune individuals also had elevated levels of chemokines like interferon-gamma induced protein 10 (IP-10) (203). Most recently the protective effect of *Ov*-103 and *Ov*-RAL-2 formulated with alum was also described for genetically diverse intercross mice challenged with implanted *O. volvulus* L3 larvae in a diffusion chamber (209). This supports the requirement that the immunization will also be successful in a genetically diverse human population.

Vaccine studies targeting the causative agents of lymphatic filariasis have been conducted for several decades, but the progress is rather slow and has recently been reviewed (22). As reviewed by Morris and colleagues, worm homogenates did not result in protection, while the immunization of different animal models with irradiated L3 larvae demonstrated that protection by immunization can be generated (202). The use of radiation attenuated parasites for human vaccines is not suitable. But such studies allow to understand protective immunity and to identify new vaccination strategies. Several antigens that are homologous in *W. bancrofti* and *B. malayi* have been identified by genome analysis and were tested in animal models. The most successful approaches until now have been summarized by Kalyanasundaram and colleagues (22). Similar to the *O. volvulus* vaccine development the *B. malayi* orthologous proteins *Bm*-103 and *Bm*-RAL-2 were tested in an immunization study in gerbils. There a fusion protein of both antigens administered with alum, performed superior to an individual treatment. It resulted in significant worm reduction of 61% and reduced embryogenesis (210). As most successful accounts the *B. malayi* vaccination with a multivalent fusion protein r*Bm*HAXT combined with an alum-based adjuvant. This achieved 88% protection in mice (211) and 57% in rhesus macaques (212).

Overall, progress is being made, but no antigen-adjuvant combination made it yet into human clinical trials for filariasis vaccines.

1.3.5 Experimental filarial vaccination with *Litomosoides sigmodontis*

In order to find successful antigen-adjuvant combinations for filarial vaccinations the work in rodent models remains a favorable approach. Also, the *L. sigmodontis* mouse model, which was introduced in chapter 1.1.4, has been used to study filariasis vaccination. These vaccination experiments largely rely on subcutaneous

immunization with radiation attenuated L3 larvae in BALB/c mice, but also studies with MF were performed.

First studies were published in 1994, describing a reduction in the adult worm burden after triple immunization with irradiated L3 larvae (71). In a follow up study it was stated that the killing during challenge infection after immunization occurred in the early days and targeted L3 larvae, suggesting that the immune response enhanced by the subcutaneous infection occurs in the subcutaneous tissue (213). Immunological studies working in C57BL/6 (214) and BALB/c (94) mice pointed out an essential role of IL-5 for vaccination responses against L3 larvae (214). At the same time it was described that eosinophils degranulate at the site of the subcutaneous challenge infection in IL-5 competent animals (94, 215). In order to assess the impact of antibodies on vaccination success, BALB/c μMT mice that lack mature B cells were immunized and subsequently subcutaneously infected with *L. sigmodontis*. This study revealed that the lack of B cells reduced vaccination efficiency and a lower percentage of eosinophils degranulated (115). They further suggest, that the vaccination effect may depend on a rapid clearance of L3 larvae by antibody-triggered eosinophils in the subcutaneous tissue. Babayan and colleagues described a reduced motility of *L. sigmodontis* L3 larvae in the subcutaneous tissue, six hours after the subcutaneous challenge infection (216). Thereby they support the suggestion that vaccination induces protective mechanisms at an early time point in the subcutaneous tissue. In a follow up study, they report that the vaccine induced immune response was limited to the L3 larval stage (217). Further immunization experiments with irradiated L3 larvae showed, that basophils are essential for protection (218) and the protective effect remains stable after repeated parasite exposure (219). In a different approach irradiated MF in combination with alum were used for immunization (220). Here, embryogenesis was efficiently impaired, resulting in decreased or complete absence of MFs in the peripheral blood. At 70 days, but not at 50 days after infection, mice that were immunized with irradiated MF in alum also showed significantly enhanced clearance of adult worms.

Overall, the immunization with irradiated *L. sigmodontis* life stages was a valuable contribution for the development of vaccination strategies and can be beneficial to identify potent adjuvants for the later use with recombinant vaccine antigens.

1.4 Aim

In brief, the aims of this thesis were to (i) broaden the limited understanding of the innate recognition of filarial nucleic acids and to (ii) utilize nucleic acid sensing for improving a *L. sigmodontis* vaccination.

The host-pathogen interactions during filarial infection are still not understood well enough (74) and especially nucleic acid sensing during filarial infections is one of the least studied areas today. So far, literature dominantly describes a modulating role for filarial nucleic acids. To that end we aimed to clarify whether nucleic acids of filarial nematodes can also induce an inflammatory immune response and lead to type I IFN production, which is mostly associated with viral infections. To further understand host-pathogen interaction during infection we aimed to identify nucleic acid receptors that are important for the *in vivo* recognition of *L. sigmodontis* and might have an impact on disease outcome.

Besides broadening the understanding of parasitic nucleic acid sensing, we aimed to analyze the impact of nucleic acid receptor activation on larval survival and utilize the potential of nucleic acid receptor agonists as adjuvants to improve vaccination efficacy in the model of *L. sigmodontis*. To that end, first the local immune responses that are elicited by radiation attenuated L3 larvae and nucleic acid receptors agonists were analyzed. Then in a second step, nucleic acid receptor agonists were implemented in the experimental immunization setup as a combination therapy. This aimed to clarify whether the immune system is successfully boosted and able to eliminate the parasite. Thereby a new perspective on nucleic acid receptor agonist-based vaccine adjuvants for helminth vaccinations, shall be evaluated.

2. Materials and Methods

2.1 Parasite cultures

2.1.1 *Litomosoides sigmodontis*

Intact adult females were isolated from the pleura of MF-positive infected gerbils (*Meriones unguiculatus*). Worms were washed individually in PBS and pooled prior to nucleic acid isolation. For RNA isolation samples were stored at -20 °C in 700 µL Trizol (QIAGEN, Hilden, Germany), for DNA isolation worms were stored at -20 °C without liquid.

2.1.2 *Plasmodium falciparum*

The *Plasmodium falciparum* 3D7 strain was obtained from the Bernhard Nocht Institute in Hamburg.

Culturing was performed under sterile conditions. RPMI 1640 (+ HEPES, - L-Glutamine) (Life technologies Corporation, Grand Island, NY, USA) was supplemented with 50 mg/L Gentamicin (PAA Laboratories, Cölbe, Germany), 2 mM L-Glutamine (Life technologies Corporation, Grand Island, NY, USA), 50 mg/L Hypoxanthine (Sigma-Aldrich, St. Louis, MO, USA), 3 g/L AlbuMAX^{TM}II (Thermo Fisher Scientific, Waltham, MA, USA) was used as culture medium. The AlbuMAX^{TM}II was dissolved at 37 °C and sterile filtered before adding to the medium. Erythrocytes were obtained from human blood received in citrate tubes from the blood donation service at the University Hospital Bonn, Germany. The tubes were centrifuged at 400x*g* for 5 min at RT. Serum and buffy coat were discarded by aspiration. The erythrocytes were washed twice with RPMI (+ HEPES, - L-Glutamine) (Life technologies Corporation, Grand Island, NY, USA). Finally, the erythrocytes were mixed 1:1 with RPMI (+ HEPES, - L-Glutamine) and stored at 4 °C until usage, maximally for three weeks.

The culture was maintained as previously described (221).

In brief, the parasite culture was maintained in 10 cm ø Petri dishes with 15 mL *P. falciparum* culture medium at a hematocrit of ~10%. The medium was changed daily by aspirating the erythrocyte free top layer. Every second day the parasitemia was determined by counting in a Giemsa-stained blood smear. At a parasitemia higher than 4% the culture was diluted, either by splitting, harvesting, or aspiration of excess

erythrocytes. New erythrocytes were added to restore the hematocrit. For incubation the Petri dishes were placed into a hypoxia incubation chamber filled with a gas mix of 3% oxygen, 5% carbon dioxide, rest nitrogen (Linde plc, Guildford, Surrey, United Kingdom) containing a Petri dish containing distilled water and placed at 37 °C.
The culture was synchronized using the sorbitol-synchronization protocol by Kirsten Moll (221). In brief, the parasite cultures with a parasitemia of >5% with most parasites in ring stage were centrifuged at 600x*g* for 5 min. The supernatant was discarded. The pellet was taken up in 4 mL 5% sorbitol (Sigma-Aldrich, St. Louis, MO, USA) in dH_2O and incubated for 10 min at RT. In between it was mixed 2 - 3 times. The culture was centrifuged at 600x*g* for 5 min and washed three times in malaria culture medium. The culture was diluted to 5% hematocrit and cultured. The procedure was repeated after 48 h.

2.2 RNA isolation

2.2.1 *Litomosoides sigmodontis,* human PBMCs and murine skin

The pelleted pathogens or 3 x 10^7 PBMCs were taken up in 700 µL Trizol (QIAGEN, Hilden, Germany), vigorously vortexed and stored at -20 °C until RNA isolation.
Samples 700 µL Trizol were transferred into a Precellys® 2 mL Soft Tissue Homogenizing Ceramic Beads Tube (Cayman Chemical, Ann Arbor, MI, USA), homogenized in a Precellys® 24 with the program “6000-3x60-120” and transferred back into a new 1.5 mL reaction tube.
The homogenate was incubated at RT for 5 min. 70 µL (1/10^{th} of the total volume) 1-Bromo-3-chloropropane (BCP) (Tokyo Chemical Industry, Tokyo, Japan) was added, vortexed and incubated at RT for 2-3 min. The mixture was centrifuged for 15 min at 12000x*g*, 4 °C. 350 µL of the RNA containing upper aqueous phase was transferred into a 2 mL reaction tube, avoiding contaminations from the undelaying organic phase. The RNA isolation was subjected to the QIAcube (QIAGEN, Hilden, Germany). The animal tissue and cell protocol was followed using the RNeasy® Mini kit (QIAGEN, Hilden, Germany). The 70% ethanol was exchanged with 100% ethanol to increase the binding of smaller RNA fragments to the column. An on-column DNase (QIAGEN, Hilden, Germany) digest was implemented to the protocol. The final elution volume was set to 30 µL.

2.2.2 *Plasmodium falciparum*

The RNA of *P. falciparum* blood culture was isolated using the RiboPure™ RNA Purification kit (Thermo Fisher Scientific, Waltham, MA, USA) and the provided alternate protocol for the isolation of small RNAs was followed.
In short, the erythrocyte pellet was lysed and the RNA was extracted by organic extraction. The aqueous phase was mixed with 100 % ethanol and stepwise applied to a filter cartridge. After a wash step the RNA was eluted and treated with DNase provided in the kit.

2.2.3 Murine splenocytes

Spleens were digested in 0.5 mg/mL collagenase VIII buffer (Sigma-Aldrich, St. Louis, MO, USA) for 20 min on a shaker with 350 rpm at 37 °C. 10 mL MACS buffer were added and a single cell suspension was prepared by passing through a 70 µm metal sieve. The cell suspension was centrifuged at 400x*g* for 5 min at 4 °C. The supernatant was discarded, 7×10^7 cells were taken up in 700 µL Trizol (QIAGEN, Hilden, Germany) and vigorously vortexed. Samples were stored at -20 °C until further processing.
70 µL ($1/10^{th}$ of the total volume) BCP (Tokyo Chemical Industry, Tokyo, Japan) was added, vortexed and incubated at RT for 2-3 min. The mixture was centrifuged for 15 min at 12000x*g*, 4°C. 350 µL of the RNA containing upper aqueous phase was transferred into a 2 mL reaction tube, avoiding contaminations from the undelaying organic phase.
The RNA isolation was subjected to the QIAcube (QIAGEN, Hilden, Germany). The animal tissue and cell protocol was followed using the RNeasy® Mini kit (QIAGEN, Hilden, Germany). The 70% ethanol was exchanged with 100% ethanol to increase the binding of smaller RNA fragments to the column. An on-column DNase (QIAGEN, Hilden, Germany) digest was implemented to the protocol. The final elution volume was set to 30 µL.

2.2.4 RNA quality assessment

To identify possible protein and DNA contaminations, the absorbance of the samples was measured at 230 nm, 260 nm and 280 nm using the 2 µL microplate for the SpectraMax190 plate reader (Molecular Devices LLC, San José, CA, USA) using SoftMax Pro 7 software (Molecular Devices LLC, San José, CA, USA), running the

“Nucleic Acid Quantitation with the SpectraDrop Micro-Volume Plate” program. The Concentration factor was set on 38 for water.

Subsequently the RNA integrity was analyzed using the Experion™ Automated Electrophoresis System (Bio-Rad Laboratories, Hercules, CA, USA). The samples were applied on an RNA StdSens chip (Bio-Rad Laboratories, Hercules, CA, USA). The manufacturer’s protocol was followed. For RNA isolated from *E. coli* the prokaryote total RNA StdSens Assay, for all other samples the eukaryote total RNA StdSens Assay was chosen.

2.3 DNA isolation

2.3.1 *Litomosoides sigmodontis*

The isolation was performed with the QIAamp DNA Mini Kit (QIAGEN, Hilden, Germany) according to the adjusted manufacturer’s protocol, an RNase digest was implemented.

Worms isolated as described in chapter 2.1 were taken up in 180 µL ALT buffer and smashed using a pestle. 40 µL Proteinase K were added and samples were incubated o/n at 56 °C on a shaker with 350 rpm. 400 µg RNase A (Thermo Fisher Scientific, Waltham, MA, USA) were added and incubated at RT for 2 min. 200 µL AL buffer were added, the sample inverted and incubated for 10 min on a shaker with 350 rpm at 70 °C. 200 µL 100% ethanol were added, the solution was applied to the spin column and centrifuged at 6000x*g* for 1 min. The flow through was discarded. 500 µL AW1 buffer were added. The column was centrifuged at 6000x*g* for 1 min. The flow through was discarded. 500 µL AW2 buffer were added. The column was centrifuged at 20,000x*g* for 1 min. The collection tube was renewed. The column was centrifuged at 20,000x*g* for 3 min. The column was transferred to an elution tube, 50 µL AE buffer were added and incubated on the column for 1 min. The column was centrifuged at 6000x*g* for 1 min. Eluted DNA was quantified in 2 µL using a NanoVue (GE Healthcare, Chicago, IL, USA). Samples were stored at -20°C until usage.

2.3.2 *Plasmodium falciparum*

P. falciparum 3D7 was cultured as previously described. At a parasitemia of >5% with mainly trophozoite or schizont stages one Petri dish was harvested. The culture was centrifuged at 400x*g*, 5 min RT and the total volume was reduced to 5 mL. DNA was

isolated using the innuPREP Blood DNA Master Kit (Analytik Jena, Jena, Germany) following an adjusted protocol.

5 mL RBC Lysis Solution A was added to 5 mL *P. falciparum* culture, vortexed and incubated at RT for 15 min. The mix was centrifuged at 5000x*g* for 10 min, RT. The supernatant was discarded carefully. 5 mL RBC Lysis Solution B was added. The mix was vortex, incubated at RT for 2 min and centrifuged at 5000x*g* for 10 min at RT. The supernatant was carefully discarded. The pellet was resuspended in 200 µL dH_2O by vigorous vortexing. The resuspended sample was transferred into a Lysis Tube PLP, vortexed for 5 sec and incubated for 30 min at 70 °C. The lysed sample was mixed with 75 µL Precipitation Buffer and vigorously vortexed. The sample was centrifuged at 16000x*g* for 3 min at RT. The clear supernatant was transferred into a new 1.5 mL reaction tube and incubated for 5 min at RT with 50 µg/mL RNase A (Thermo Fisher Scientific, Waltham, MA, USA). Then the sample was mixed with 500 µL 70% ethanol. The sample was applied onto the spin filter column and centrifuged at 10000x*g* for 2 min, RT. The column was washed with 750 µL washing solution MS, centrifuged at 10000x*g* for 1 min. It was placed onto a new collection tube and centrifuged at 16000x*g* for 2 min. For elution the column was placed into a 1.5 mL reaction tube, 300 µL elution buffer were added, incubated at RT for 3 min and centrifuged at 6000x*g* for 1 min at RT. DNA concentration was measured in 2 µL using a NanoVue (GE Healthcare, Chicago, IL, USA). Samples were stored at -20 °C until usage.

2.3.3 Human PBMCs and murine spleen

The isolation was performed with the QIAamp DNA Mini Kit (QIAGEN, Hilden, Germany) according to the manufacturer's protocol, an RNase digest was implemented. In brief, 15 mg of minced spleen or 5×10^6 human PBMCs were incubated with 400 µg RNase A (Thermo Fisher Scientific, Waltham, MA, USA) for 30 min at 37 °C. Then 180 µL ALT buffer and 20 µL Proteinase K were added and samples were incubated o/n at 56 °C on a shaker with 350 rpm. 200 µL AL buffer were added, the sample inverted and incubated for 10 min on a shaker with 350 rpm at 70 °C. 200 µL 100% ethanol were added, the solution was applied to the spin column and centrifuged at 6000x*g* for 1 min. The flow through was discarded. 500 µL AW1 buffer were added. The column was centrifuged at 6000x*g* for 1 min. The flow through was discarded. 500 µL AW2 buffer were added. The column was centrifuged at 20,000x*g* for 1 min. The collection tube was renewed. The column was centrifuged at

20,000x*g* for 3 min. The column was transferred to an elution tube, 100 µL AE buffer were added and incubated on the column for 1 min. The column was centrifuged at 6000x*g* for 1 min. This step was repeated twice, resulting in three DNA samples per original isolation sample. Eluted DNA was quantified in 2 µL using a NanoVue (GE Healthcare, Chicago, IL, USA). Samples were stored at -20 °C until usage.

2.4 Cell culture

2.4.1 Human PBMCs

Buffy coats for the isolation of human PBMCs were obtained from the Institute of Experimental Hematology and Transfusion Medicine of the University Hospital Bonn. The donors gave their written informed consent and the ethics committee and the University Hospital Bonn have their approval (167/11).

PBMCs were cultured in Advanced RPMI (Life technologies Corporation, Grand Island, NY, USA), 10% FCS (PAN Biotech, Aidenbach, Germany), 2 mM L-Glutamine (Life technologies Corporation, Grand Island, NY, USA), 1% Penicillin (10,000 units/mL)/ Streptomycin (10 mg/mL) (Life technologies Corporation, Grand Island, NY, USA), and 50 mg/L Gentamicin (PAA Laboratories, Cölbe, Germany).

The blood was diluted 1:1 with PBS and carefully overlaid on 15 mL PANcoll (density 1.077 g/mL) (PAN-Biotech, Aidenbach, Germany) in a 50 mL screw-lid tube at RT. Gradient centrifugation was performed at 200x*g* for 20 min at RT without brake. The white interphase containing the PBMCs was aspirated and transferred into a new 50 mL screw-lid tube. The content was washed twice with PBMC culture medium (200x*g*, 8 min, RT). In case of visible red blood cell (RBC) contamination in the pellet, the pellet was incubated for 10 min with 400 µL 1X RBC lysis buffer and washed again. In the final step the pellet was taken up in 10 mL PBMC culture medium.

2.4.2 L929 cell culture

L929 cells were cultured under sterile conditions in Advanced RPMI medium (Life technologies Corporation, Grand Island, NY, USA) supplemented with 10% FCS (PAN Biotech, Aidenbach, Germany), 1% Penicillin (10,000 units/mL)/ Streptomycin (10 mg/mL) (Life technologies Corporation, Grand Island, NY USA), 2 mM L-Glutamine (Life technologies Corporation, Grand Island, NY USA). At a confluency of 90 - 95% cells were split by removing the medium, washing with warm PBS (Life technologies

Corporation, Grand Island, USA) and trypsinization with 0.5% Trypsin-EDTA (Life technologies Corporation, Grand Island, USA). Cultures were incubated at 37 °C, 5% CO_2. In order to harvest supernatant for supplementing the medium for bone marrow-derived macrophages, 2 x 10^6 cells were plated in a T75 flask with 30 mL medium. The supernatant was harvested, sterile filtered and stored at -20 °C, once the culture reached a confluency of ~95%.

2.4.3 Bone marrow-derived macrophages

Mice were killed with an overdose of isoflurane (Piramal Critical Care Deutschland GmbH, Hallbergmoos, Germany), hind legs were removed and bones isolated from the flesh. The following steps were performed under sterile conditions. Femur and tibia were placed in 70% ethanol for 2 min and then transferred to cold Advanced RPMI medium (Life technologies Corporation, Grand Island, USA) until further processing. Bones were cut open at the ends and flushed with RPMI medium using a 27 x gauge needle (B. Braun Melsungen, Melsung, Germany). Cells were centrifuged at 330x*g* for 8 min at 4°C. The supernatant was discarded and RBC lysis was performed using 10x eBioscience™ RBC-lysis buffer diluted in distilled water to working concentration (Thermo Fisher Scientific Inc., Waltham, MA, USA). Lysis was stopped by adding medium, cells were filtered through a 70 µm sieve (Miltenyi Biotech, Bergisch Gladbach, Germany) and taken up in Advanced RPMI medium (Life technologies Corporation, Grand Island, USA) supplemented with 10% FCS (PAN Biotech, Aidenbach, Germany), 1% Penicillin (10,000 units/mL)/ Streptomycin (10 mg/mL) (Life technologies Corporation, Grand Island, NY, USA), 2mM L-Glutamine (Life technologies Corporation, NY, Grand Island, USA) and 20% L929 culture supernatant. 20 x 10^6 cells in 12 mL were seeded on a 10 cm ø Petri dish and incubated at 37 °C, 5% CO_2. On day 3, the supernatant was discarded, cells were removed from the dish by scraping with 2 mM Ethylenediaminetetraacetic acid (EDTA) (Carl Roth, Karlsruhe, Germany) in PBS, taken up in fresh medium and reseeded on twice the number of plates as before. On day 7, cells were harvested by scraping with 2 mM EDTA (Carl Roth, Karlsruhe, Germany) in PBS and used for stimulation experiments.

2.4.4 Bone marrow-derived plasmacytoid dendritic cells

Cells were isolated from bone marrow and seeded on Petri dishes as described for bone marrow derived macrophages. For culturing Advanced RPMI medium (Life

technologies Corporation, Grand Island, NY, USA) was supplemented with 10% FCS (PAN Biotech, Aidenbach, Germany), 1% Penicillin (10,000 units/mL)/ Streptomycin (10 mg/mL) (Life technologies Corporation, Grand Island, USA), 2 mM L-Glutamine (Life technologies Corporation, Grand Island, NY, USA) 50 µM β-mercaptoethanol (Life technologies Corporation, Grand Island, NY, USA) and 100 ng/ml recombinant Flt3L (PeproTech, Hamburg, Germany) was used for culturing. On day 4, 5 mL of culture medium were centrifuged at 400x*g* for 5 min, RT, the pellet was taken up in fresh medium and re-added to the culture plate. On day 7, cells were harvested by scraping with 2 mM EDTA (Carl Roth, Karlsruhe, Germany) in PBS, washed once with medium (without Flt3L) and used for stimulation experiments.

2.4.5 Bone marrow-derived neutrophils

Cells were isolated from bone marrow as described for bone marrow derived macrophages. After filtering 90 µL MACS buffer (PBS (Life technologies Corporation, Grand Island, NY, USA), 1% FCS (PAN Biotech, Aidenbach, Germany), 2 mM EDTA (Carl Roth, Karlsruhe, Germany) per 1 x 10^7 cells and 10 µL of anti-Ly6G-Biotin microbeads (Ly6G clone REA526) (Miltenyi Biotech, Bergisch Gladbach, Germany) were added and incubated at 4°C for 15 min in the dark. Cells were washed with MACS buffer and centrifuged at 400x*g* for 7 min at 4 °C. The pellet was resuspended in 500 µL MACS buffer and applied to a pre-calibrated MS column. The manufacturer's protocol was followed. Eluted cells were used for cell stimulation experiments.

2.5 *In vitro* stimulation with DNA/RNA via Transfection

2.5.1 Cytosolic stimulation

As described by Coch *et al.* (222) 200 ng nucleic acid was mixed with 25 µL OptiMEM™ and 0.5 µL Lipofectamine 2000® (Thermo Fisher Scientific, Waltham, MA, USA) were mixed with 25 µL OptiMEM™ (Thermo Fisher Scientific, Waltham, MA, USA). Then both mixes were pooled, incubated for 15 min at RT and added to 5 x 10^4 plated cells in a final volume of 200 µL. For the stimulation of human PBMCs 1 µg/mL RNA, RNA or agonist were used, for the stimulation of murine cells 1.5 µg/mL RNA or DNA or 1 µg/mL agonist were used. As agonists served ISD (Invivogen, San Diego, CA, USA), poly(I:C) (Invivogen, San Diego, CA, USA), 3p-hpRNA (Invivogen, San Diego, CA, USA).

2.5.2 Endosomal stimulation

As described by Coch *et al.* (222) 200 ng RNA were mixed with 360 ng poly-L-arginine hydrochloride (molecular weight 5,000-15,000) (Sigma Aldrich, St. Louis, MO, USA) in 15 µL PBS and incubated for 10 min at RT. Then the stimulus was added to 5 x 10^4 plated cells in a final volume of 200 µL. For the stimulation of human PBMCs 1 µg/mL RNA or agonist were used, for the stimulation of murine cells 1.5 µg/mL RNA or DNA or 1 µg/mL agonist were used. As agonists, CpG C ODN2395 (Invivogen, San Diego, CA, USA) or R848 (Invivogen, San Diego, CA, USA) were directly added to the medium without the need of complexing.

2.6 Animals

C57BL/6J wild-type (WT), BALB/c WT, gerbils (*Meriones unguiculatus)* were purchased from Charles River Laboratories (Charles River Labs Wilmington, MA, USA) or Janvier Labs (Le Genest-Saint-Isle, France). Cotton rats (*Sigmodon hispidus*) for maintenance of the *L. sigmodontis* cycle were originally obtained from Charles River and bred at the animal facility of the Institute for Medical Microbiology, Immunology and Parasitology (IMMIP), University Hospital Bonn.

C57BL/6 TLR7$^{-/-}$, C57BL/6 TLR9$^{-/-}$, C57BL/6 MDA5$^{-/-}$ and C57BL/6 STING$^{-/-}$ were kindly provided by Prof. Dr. Gunther Hartmann, Institute of Clinical Chemistry and Clinical Pharmacology.

Breeding pairs of albino C57BL/6 IFN-β Luciferase reporter mice were kindly provided by Prof. Dr. Eike Latz, Institute of Innate Immunity, University Hospital Bonn, and further bred in the animal facility of the IMMIP, University Hospital Bonn.

All animals were housed and monitored in the animal facilities of the IMMIP. Food and water were supplied *ad libitum*. The environment was enriched by providing nestlets. Infected animals were scored weekly as determined by the approved animal protocols.

2.7 Ethics statement concerning animal experiments

The performed animal experiments were approved by the corresponding committee (Landesamt für Natur, Umwelt und Verbraucherschutz, Köln, Germany).

2.8 *Litomosoides sigmodontis* life cycle maintenance

The *L. sigmodontis* life cycle was maintained as previously described (78) in a separated area of the animal facilities of the IMMIP.

In brief, the tropical rat mite *Ornithonyssus bacoti* was bred in litter-filled basins at 28 °C with 80% humidity. Mites were fed three times per week with fresh blood. For life cycle maintenance the mites, as intermediate host, were subjected to cotton rats that were chronically infected with *L. sigmodontis*. Thereby the mites took up parasitic L1 larvae/MF that matured in the mite to L3 larvae. Upon encounter the mites infected the experimental animals. The MF count of cotton rats was determined regularly by microscopic count of MF in 50 µL blood. Rats with a load of >1000 MF/µL were exposed to the mites and used for the maintenance of the life cycle.

2.9 *Litomosoides sigmodontis* infection of mice and gerbils

Animals were infected naturally with *L. sigmodontis* by subjecting them overnight to mites that were infected 10-12 days earlier. For the period of infection animals were kept in metal cages that were placed on mite-harboring bedding, surrounded by water to prevent escape of mites. The next day the metal cages were placed on water for one day. The mite containing bedding was discarded. The animals were placed back in regular cages and the bedding was changed daily for a total of five days in order to eliminate remaining mites. For subcutaneous infection of mice, 40 L3 larvae were transferred with a pipette into a 1 mL syringe before attaching a 24 x gauge needle. After adjusting the injection volume while visually checking that no larvae are lost, the syringes were placed upside down, to allow sinking of the larvae into the needle tip before injection. When turning the syringes with the needle facing down, they were rolled between hands to ensure that no larvae would stick to the plunger. For larval migration experiments the injection was placed into the neck fold. For the analysis of local immune responses, the injection was given into the skin fold of the hind leg.

2.10 L3 larvae isolation and preparation

Gerbils were euthanized with an overdose isoflurane (Piramal Critical Care Deutschland GmbH, Hallbergmoos, Germany) 5 days after infection. The larvae were isolated from the pleural cavity by washing with 25 mL warm Advanced RPMI (Life technologies Corporation, Grand Island, NY, USA) supplemented with 1% Penicillin (10,000 units/mL)/ Streptomycin (10 mg/mL) (Life technologies Corporation, Grand Island, NY, USA) and collected in a 10 cm ø Petri dish. L3 larvae were washed twice by transferring them to Petri dishes with fresh medium.

For the following experiments the number of larvae needed were taken up in the required volume using a pipette, then transferred into a well of a 96 well U-bottom plate and stored at 37 °C until further use. For heat inactivation the plate was incubated at 60 °C for 60 min. Attenuation of larvae by irradiation was performed in the clinic for radiation therapy (Klinik für Strahlentherapie und Radioonkologie) of the University Hospital Bonn using a Varian TrueBeam STx® (Brainlab AG, München, Germany). The radiation source had a photon energy of 10 MeV with a dose rate of 25 Gy/min. Larvae were subjected to 450 Gy given in doses of 100 Gy per fraction. The fractions were applied consecutively without breaks.

2.11 Subcutaneous immunization

To exclude that the substances impact the larvae prior to injection, agonists and larvae were administered in two separate shots. Since the diameter of the syringe used to inject the agonists was smaller than the one of the syringes used to administer attenuated L3 larvae, the agonists were injected first. The two injections were administered directly one after the other into the same spot.

2.11.1 Receptor agonists

Injections were administered subcutaneously using an insulin syringe in a total volume of 50 µL. The dose was 20 µg of substance per animal.

LsAg (*Litomosoides sigmodontis* adult worm extract) (prepared as previously described by Ajendra *et al*. (223), R848 VacciGrade™ (Invivogen, San Diego, CA, USA), CpGC 2395 VacciGrade™ (Invivogen, San Diego, CA, USA), or 2'3'cGAMP VacciGrade™ (Invivogen, San Diego, CA, USA) were administered in 0.9% NaCl (Fresenius Kabi, Bad Homburg vor der Höhe, Germany).

Poly(I:C) VacciGrade™ (Invivogen, San Diego, CA, USA) was administered naked in order to target the endosome by mixing with 0.9% NaCl (Fresenius Kabi, Bad Homburg vor der Höhe, Germany).

3p-hpRNA (Invivogen, San Diego, CA, USA) or synthesized 3pRNA provided by the Hartmann lab (University Hospital Bonn) or poly(I:C) VacciGrade™ (Invivogen, San Diego, CA, USA) were given in transfected form in order to target the cytosol by complexing with *in vivo*-jetPEI® (Polyplus-transfection SA, New York City, NY, USA). The manufacturer's protocol was followed working at an N/P ratio of 8. In brief, nucleic acid was mixed with glucose solution and filled up with nuclease-free water to half of

the final volume. In a second vial *in vivo*-jetPEI® was mixed with glucose solution and filled up with nuclease-free water to half of the final volume. Then both solutions were mixed by vortexing and incubated at RT for 15 min.

2.11.2 Attenuated L3 larvae

25 attenuated L3 larvae were transferred into a 1 mL syringe with a pipette before attaching a 24 x gauge needle. After adjusting the injection volume while visually checking that no larvae were lost, the syringes were placed upside down, to allow sinking of the larvae into the needle tip before injection. When turning the syringes upside down, they were rolled between hands to ensure that no larvae would stick to the plunger.

2.12 Organ preparation

2.12.1 Serum

Blood was collected into 1.5 mL reaction tubes from the cheek of animals and stored at RT until clotted. Clotted samples were centrifuged (6000x*g*, 5 min, RT); the serum was transferred into new vials and stored at -20 °C until analysis.

2.12.2 Pleura

Animals were euthanized by an overdose of isoflurane (Piramal Critical Care Deutschland GmbH, Hallbergmoos, Germany). If not stated otherwise, samples were kept on ice. The pleural cavity was washed with a minimum of 8 mL cold PBS until clear. The first mL was filtered through gauze into a 1.5 mL reaction tube. The tube was centrifuged at 400x*g*, 5 min at 4 °C. The supernatant was frozen for ELISA analysis. The cells were pooled with the remaining wash.

In the meantime, the further wash was filtered through gauze into a 15 mL reaction tube. The gauze holding back the worms was placed in a 6 well plate with PBS for worm count. The 15 mL reaction tube including all pleural cells was centrifuged at 400x*g* for 5 min, 4 °C. The supernatant was discarded, the pellet was dissolved in 1 mL RBC lysis buffer (Thermo Fisher Scientific Inc., Waltham, MA, USA) by vortexing and incubated at RT for 10 min. The reaction was stopped by adding 5 mL MACS buffer. The cell suspension was centrifuged at 400x*g* for 5 min at 4 °C. The supernatant was discarded; the pellet was dissolved in 2 mL PBS for counting. 1 x 10^6 cells were plated for flow cytometric analysis.

2.12.3 Spleen

Animals were euthanized by an overdose of isoflurane (Piramal Critical Care Deutschland GmbH, Hallbergmoos, Germany). If not stated otherwise, samples were kept on ice. Isolated spleens were flushed with 3 mL 0.5 mg/mL collagenase VIII buffer (Sigma-Aldrich, St. Louis, MO, USA) using an insulin syringe, cut into small pieces and incubated at 37 °C for 30 min on a shaker with 350 rpm. 10 mL MACS buffer (PBS, 10% FCS (PAN Biotech, Aidenbach, Germany), 2 mM EDTA (Carl Roth, Karlsruhe, Germany) were added. A single cell suspension was generated by passing the cells through a 70 µm metal strainer with the help of a syringe plunger. The cell suspension was centrifuged at 400x*g* for 5 min at 4 °C. The supernatant was discarded, the pellet was dissolved in 1 mL RBC lysis buffer (Thermo Fisher Scientific Inc., Waltham, MA, USA) by vortexing and incubated at RT for 10 min. The reaction was stopped by adding 5 mL MACS buffer. The cell suspension was centrifuged at 400x*g* for 5 min at 4 °C. The supernatant was discarded, the pellet was dissolved in 5 mL RPMI medium (Life technologies Corporation, Grand Island, NY, USA) supplemented with 10% FCS (PAN Biotech, Aidenbach, Germany), 1% Penicillin (10,000 units/mL)/ Streptomycin (10 mg/mL) (Life technologies Corporation, Grand Island, NY, USA) and 2 mM L-Glutamine (Life technologies Corporation, Grand Island, NY, USA). For flow cytometric analysis 1 x 10^6 cells were plated. For ELISA analysis, 2 x 10^6 cells were plated in 1 mL medium in a 24 well plate. Each sample was plated in triplicates. Cells were stimulated with 2.5 µg/mL ConA (Sigma-Aldrich, St. Louis, MO, USA) or 25 µg/mL LsAg prepared as previously described (223) for 24 h. The supernatant was stored at -20 °C until analysis.

2.12.4 Skin

Animals were euthanized by an overdose of isoflurane (Piramal Critical Care Deutschland GmbH, Hallbergmoos, Germany). The previously marked skin in the injection area was isolated and cut in half. If not stated otherwise, samples were kept on ice. The first half was frozen at -20 °C in 700 µL Trizol (QIAGEN, Hilden, Germany) for RNA isolation. The second half was minced and incubated for 75 min on a shaker with 350 rpm at 37 °C in RPMI medium (Life technologies Corporation, Grand Island, NY, USA) supplemented with 10% FCS (PAN Biotech, Aidenbach, Germany), 1% Penicillin (10,000 units/mL)/ Streptomycin (10 mg/mL) (Life technologies Corporation, Grand Island, NY USA), 2 mM L-Glutamine (Life technologies Corporation, Grand

Island, NY USA), 0.25 mg/mL Liberase TL (Hoffmann-La Roche Ltd., Basel, Switzerland), and 0.5 mg/mL DNase I (Thermo Fisher Scientific, Waltham, MA, USA). The reaction was stopped by adding RPMI medium supplemented with 10 mM EDTA (Carl Roth, Karlsruhe, Germany) and 2% FCS. Single cell suspension was prepared by smashing through a 70 µm cell strainer (Miltenyi Biotech, Bergisch Gladbach, Germany). The suspension was centrifuged at 400x*g* for 5 min at 4 °C. The supernatant was discarded, cells were taken up in 500 µL MACS buffer (PBS, 10% FCS (PAN Biotech, Aidenbach, Germany), 2 mM EDTA (Carl Roth, Karlsruhe, Germany) and 1 x 10^6 cells were plated flow cytometric analysis.

2.13 Cell count

10 µL of cell sample were mixed with 10 mL of CASYton solution and measured with a CASY® Cell Counter (Schärfe System GbmH, Reutlingen, Germany) with a 150 µm capillary. TML values were used for further calculations.

For PBMCs, bone marrow, bone marrow derived cells, skin and pleura the evaluation cursor range was set to 7.5-20.0 µm and the normalization cursor range to 5.5-20.0 µm. For splenocytes the evaluation cursor range was set to 7.5-20.0 µm and the normalization cursor range to 4.5-20.0 µm.

2.14 Microfilariae count

Mice were bled from the facial vein into an EDTA-tube. 50 µL of blood were transferred into 1 mL RBC lysis buffer (Thermo Fisher Scientific Inc., Waltham, MA, USA), vortexed, stored at RT for 10 min and placed at 4 °C until further processing. Samples were centrifuged at 400x*g* for 5 min RT and the supernatant was discarded. The entire pellet was applied onto a microscope slide, covered by a glass slip and all MF were counted under a microscope using 10 x magnification objective.

2.15 Cytospin

A microscope slide, bloating paper and a cytofunnel were assembled on a slide carrier (Hettich, Westfalen, Germany). 20 µL of cell suspension were pipetted into the cytofunnel. The loaded slide carrier was pulsed up to 5*xg* in a centrifuge set with no brake. The cytofunnel was detached and the centrifugation step was repeated. Slides were air dried and stained with Giemsa.

2.16 Giemsa staining

After slides were air-dried, the samples were fixed with methanol. 1mL Giemsa-staining solution (Merck KGaA, Darmstadt, Germany) was diluted in 19 mL buffer at pH 7.2 (Merck KGaA, Darmstadt, Germany). The slides were incubated in the staining solution for 5-10 min (cells) or 15 min (Plasmodia), rinsed with water and air dried.

2.17 Antibody-dependent cellular cytotoxicity assay

The assay was adapted from Veerapathran *et al.* (224). Gerbils were infected with *L. sigmodontis*. 5 days after infection the animals were euthanized by an overdose of isoflurane (Piramal Critical Care Deutschland GmbH, Hallbergmoos, Germany) and L3 larvae were prepared. Peritoneal cells were isolated from naïve BALB/c WT donor mice. Mice were sacrificed by an overdose isoflurane (Piramal Critical Care Deutschland GmbH, Hallbergmoos, Germany) and the peritoneum was washed with 5 mL cold Advanced RPMI medium (Life technologies Corporation, Grand Island, NY, USA) supplemented with 1% Penicillin (10,000 units/mL)/ Streptomycin (10 mg/mL) (Life technologies Corporation, Grand Island, NY, USA), and 2mM L-Glutamine (Life technologies Corporation, Grand Island, NY, USA).

2 x 10^5 peritoneal cells were co-cultured with 10-12 *L. sigmodontis* L3 larvae. The medium was supplemented with 25% pooled serum drawn from immunized animals before infection or FCS (PAN Biotech, Aidenbach, Germany). During the next days the motility of L3 larvae was assessed under the microscope. Score: 4: fast and continuous movement, 3: slower but continuous movement, 2: slower and discontinuous movement, 1: sporadic movement limited to larval ends, 0: no movement.

2.18 *Litomosoides sigmodontis*-specific antibody ELISA

ELISA plates were coated with 20 µg/mL LsAg in PBS o/n at 4 °C. After washing the plates were blocked for 2 h at RT with 1% bovine serum albumin (BSA) (PAA Laboratories, Cölbe, Germany) in PBS. The diluted sera were added and incubated o/n at 4 °C. To allow comparison between plates, a sample with pooled sera was prepared and loaded onto each plate. The next day plates were washed 5 times with ELISA wash buffer. Biotinylated murine IgE, IgG1 or IgG2a/b antibodies (BD Biosciences San Jose, CA, USA) at a dilution of 1:400 in 1% BSA (PAA Laboratories, Cölbe, Germany) in PBS were added and incubated for 2 h at RT on a shaker with 40 rpm. After washing streptavidin-HRP (Thermo Fisher Scientific Inc., Waltham, MA,

USA) was incubated for 30 min at RT on a shaker with 40 rpm. Plates were washed, TMB (Thermo Fisher Scientific Inc., Waltham, MA, USA) was added and reaction was stopped with 2 M H_2SO_4 upon coloration. The plates were read at 450 nm and 570 nm wavelength using a SpectraMax190 (Molecular Devices, San Jose, CA, USA) with Soft Max Pro 7 software (Molecular Devices, San Jose, CA, USA) subtracting the values of the latter from the first.

2.19 Enzyme-link immunosorbent assay (ELISA)

Human cytokines were quantified in 24 h cell culture supernatants.

Human IFN-α was quantified using a human IFN-α (pan specific) ELISA development kit (Mabtech AG, Nacka Strand, Sweden). This kit detects the native and recombinant subtypes 1/13, 2, 4-8, 10, 14, 16-17. The manufacturer's protocol was followed. The plates were read at 405 nm wavelength using a SpectraMax190 (Molecular Devices, San Jose, CA, USA) with Soft Max Pro 7 software (Molecular Devices, San Jose, CA, USA).

Human IP-10 was quantified using a CXCL-10 human matched antibody pair - human IP-10 CytoSet™ kit (Thermo Fisher Scientific, Waltham, MA, USA). The manufacturer's protocol was followed.

Human TNF, IL-10 and IL-1β, as well as, murine IL-5, IL-6, IL-10, IL-13, IL-17A, TNF and IFN-γ were quantified using Invitrogen™ eBioscience™ ELISA Ready-SET-Go!™ (Thermo Fisher Scientific, Waltham, MA, USA). The manufacturer's protocol was followed.

Murine RANTES (CCL5), KC, Eotaxin 1 (CCL11), Granzyme B (GrzB), IP-10 (CXCL10) were quantified using DuoSet ELISA kits (R&D Systems, Minneapolis, MN, USA). The manufacturer's protocol was followed.

For all Streptavidin-horseradish peroxidase based ELISAs 2 M H_2SO_4 served as stopping solution. The plates were read at 450 nm and 570 nm wavelength using a SpectraMax190 (Molecular Devices, San Jose, CA, USA) with Soft Max Pro 7 software (Molecular Devices, San Jose, CA, USA) subtracting the values of the latter from the first.

2.20 Luminescence luciferase assay

For *in vitro* analysis 1 x 10^6 bone marrow-derived neutrophils, 1 x 10^6 bone marrow-derived macrophages, or 0.5 x 10^6 bone marrow-derived plasmacytoid dendritic cells were plated and stimulated for 24 h at 37 °C.

For *in vivo* analysis 2 x 10^6 pleura cells were plated and stimulated with 1 µg/mL poly(I:C) (Invivogen, San Diego, CA, USA) for 4 h at 37 °C.

Plates were centrifuged at 400x*g* for 5 min at 4 °C. The supernatant was harvested and cells were incubated in 50 µL Glo lysis buffer (Promega Corporation, Madison, WI, USA) on a shaker with 40 rpm for 5 min RT. Lysates were transferred to a 96 well F-bottom white plate (Thermo Fisher Scientific Inc., Waltham, MA, USA). 50 µL ONE-Glo™ luciferase assay substrate (Promega Corporation, Madison, WI, USA) was added and cells were incubated for 10 min, RT on a shaker with 40 rpm. Luminescence was measured at an integration time of 1 sec with an Infinite® M-plex (Tecan Trading AG, Männedorf, Switzerland), and i-control™ software (Tecan Trading AG, Männedorf, Switzerland).

2.21 Flow cytometry

For surface staining 1 x 10^6 cells were centrifuged at 400x*g* for 7 min at 4 °C, the supernatant was discarded and cells were resuspended in 50 µL master mix and incubated for 20 min on ice in the dark. The mastermix was prepared from FACS buffer including the antibodies of choice, as well as rat IgG (Sigma-Aldrich, St. Louis, MO, USA) diluted 1:1000. Antibodies and their dilution are listed in Table 2.1. Fluorescence minus one (FMO) controls for each antibody were prepared alongside. Post incubation 100 µL FACS buffer were added and samples were centrifuged at 400x*g* for 5 min at 4 °C. The supernatant was discarded and the washing step was repeated with 150 µL FACS buffer per sample. Subsequently the supernatant was discarded and cells were resuspended in 150 µL MACS buffer (PBS, 10% FCS (PAN Biotech, Aidenbach, Germany), 2 mM EDTA (Carl Roth, Karlsruhe, Germany) and stored at 4 °C until measuring.

For intracellular staining 1 x 10^6 cells were centrifuged at 400x*g* for 7 min at 4 °C, the supernatant was discarded and cells were resuspended in 200 µL Fix/Perm (Thermo Fisher Scientific, Waltham, MA, USA) and incubated for 20 min at RT. Then cells were centrifuged at 400x*g* for 7 min at 4 °C, the supernatant was discarded, cells were taken up in 200 µL Fc-block (1 % Bovine serum albumin fraction V (BSA) (PAA Laboratories,

Cölbe, Germany) in PBS, 1:1000 rat IgG (Sigma-Aldrich, St. Louis, MO, USA) and stored at 4 °C o/n. The next day cells were centrifuged at 400x*g* for 7 min at 4 °C, the supernatant was discarded, 200 µL permeabilization buffer (Thermo Fisher Scientific, Waltham, MA, USA) was added and incubated for 20 min at RT. Cells were centrifuged at 400x*g* for 7 min at 4 °C, the supernatant was discarded, 50 µL mastermix was added and incubated for 45 min at 4 °C. For the mastermix antibodies were diluted in permeabilization buffer. After incubation cells were washed twice with 150 µL permeabilization buffer. Finally, the supernatant was discarded and cells were resuspended in 150 µL MACS buffer (PBS, 10% FCS (PAN Biotech, Aidenbach, Germany), 2 mM EDTA (Carl Roth, Karlsruhe, Germany) and stored at 4°C until measuring. Prior to measuring all samples were filtered through 40 µm cell gauze (Labomedic, Bonn, Germany).

For compensation OneComp eBeads™ (Thermo Fisher Scientific, Waltham, MA, USA) were stained with the specific antibodies of each staining panel at the same dilution used for the mastermix. One drop was mixed with 100 µL FACS buffer and 50 µL were used per stain. Beads were incubated with antibody for 5 min at RT, then 150 µL FACS buffer were added and the sample was measured.

Samples were measured at a CytoFLEX S (Beckman Coulter, Brea, CA, USA). Files were exported as flow cytometry standard file format and analyzed in FlowJo V10.6 (FlowJo LLC, Ashland, OR, USA).

Table 2.1 | Flow cytometry antibodies.

Human	Conjugate	Clone	Dilution	Manufacturer
CD3	BV510	SK7	200	BioLegend, San Diego, CA, USA
CD4	Al700	RPA-T4	200	BioLegend, San Diego, CA, USA
CD8	PECy7	SK1	200	BioLegend, San Diego, CA, USA
CD11c	BV605	3.9	100	BioLegend, San Diego, CA, USA
CD14	Al488	M5E2	200	BioLegend, San Diego, CA, USA
CD16	APC/Cy7	B73.1	100	BioLegend, San Diego, CA, USA
CD19	PerCP-Cy5.5	HIB19	100	BioLegend, San Diego, CA, USA

CD56	Pacific Blue™	5.1H11	100	BioLegend, San Diego, CA, USA
CD80	PE	2D10	200	BioLegend, San Diego, CA, USA
HLA-DR	APC	L243	150	BioLegend, San Diego, CA, USA
Murine	**Conjugate**	**Clone**	**Dilution**	**Manufacturer**
CCR7	BV421	4B12	20	BioLegend, San Diego, CA, USA
CD3	AI700	500A2	100	BioLegend, San Diego, CA, USA
CD3	APC-Cy7	15A2	200	BioLegend, San Diego, CA, USA
CD3	BV510	145-2C11	200	BioLegend, San Diego, CA, USA
CD4	AI700	GK1.5	200	BioLegend, San Diego, CA, USA
CD4	APC-Cy7	GK1.5	200	BioLegend, San Diego, CA, USA
CD4	BV605	RM4-5	200	BioLegend, San Diego, CA, USA
CD5	PerCP-Cy5.5	53-7.3(eBio)	100	Thermo Fisher Scientific, Waltham, MA, USA
CD8a	APC-Cy7	PK136	200	BioLegend, San Diego, CA, USA
CD8a	PerCP-Cy5.5	53-6.7	200	BioLegend, San Diego, CA, USA
CD11a	FITC	M17/4	200	Caltag Laboratories, Carlsbad, CA USA
CD11b	AI700	M1/70	300	BioLegend, San Diego, CA, USA
CD11c	BV605	N418	150	BioLegend, San Diego, CA, USA
CD19	APC	6D5	200	BioLegend, San Diego, CA, USA
CD19	BV510	6D5	100	BioLegend, San Diego, CA, USA
CD23	AI700	B3B4	1000	BioLegend, San Diego, CA, USA
CD25	BV421	PC61	100	BioLegend, San Diego, CA, USA
CD25	PE	3C7	100	BioLegend, San Diego, CA, USA

CD44	FITC	IM7	100	BioLegend, San Diego, CA, USA
CD45	PerCP-Cy5.5	30-F11	100	BioLegend, San Diego, CA, USA
CD45R (B220)	PE-Cy7	RA3-6B2	200	BioLegend, San Diego, CA, USA
CD49.b	PE	DX5	200	BioLegend, San Diego, CA, USA
CD62L	PE-Cy7	MEL-14	200	Thermo Fisher Scientific, Waltham, MA, USA
CD80	BV605	16-10A1	100	BioLegend, San Diego, CA, USA
CD86	Al647	GL-1	100	BioLegend, San Diego, CA, USA
CD86	BV510	GL-1	200	BioLegend, San Diego, CA, USA
CD127 (IL-7R)	BV605	A7R34	100	BioLegend, San Diego, CA, USA
CD317 (PDCA-1)	APC	927	200	BioLegend, San Diego, CA, USA
CTLA-4	PE-Cy7	UC10-4B9	150	BioLegend, San Diego, CA, USA
F4/80	APC	A3-1	200	Bio-Rad Laboratories, Hercules, CA, USA
FOXP3	PE-Cy7	FJK-16s	200	BD Biosciences San Jose, CA, USA
GATA3	Al488	16E10A23	100	BD Biosciences San Jose, CA, USA
GrzB	APC	GB11	200	Thermo Fisher Scientific, Waltham, MA, USA
I-Ab	BV421	M5/114.15.2	200	BioLegend, San Diego, CA, USA
I-Ab	PE-Cy7	AF6-120.1	200	BioLegend, San Diego, CA, USA
Ly6C	APC-Cy7	HK1.4	200	BioLegend, San Diego, CA, USA
Ly6G	BV421	1A8	200	BioLegend, San Diego, CA, USA
PD-1	BV421	29F.1A12	200	BioLegend, San Diego, CA, USA
RELMα	/	/	100	PeproTech, Inc., Rocky Hill, NJ, USA

RORγT	PE	AFKJS-9	100	Thermo Fisher Scientific, Waltham, MA, USA
SiglecF	PE	E50-2440	200	Thermo Fisher Scientific, Waltham, MA, USA
T-bet	APC	4B10	100	BioLegend, San Diego, CA, USA
TCR-β	Al700	H57-597	200	BioLegend, San Diego, CA, USA

2.22 cDNA synthesis

cDNA generation was performed from 1 µg RNA using the Omniscript® Reverse Transcription Kit (QIAGEN, Hilden, Germany) with oligoDT_{12-18} primer (Thermo Fisher Scientific Inc., Waltham, MA, USA) and RNaseOUT™ recombinant ribonuclease inhibitor (Thermo Fisher Scientific Inc., Waltham, MA, USA) in a reaction volume of 20 µL. The samples were incubated at 37 °C for 1 h on a thermocycler. For RT-PCR transcribed cDNA was diluted 1:30.

2.23 RT-PCR

Primer sequences were provided by AG Hartmann, University Hospital Bonn, (TBP, IP-10) and AG Scheu, Düsseldorf (β-actin, IFN-β) and are listed in Table 2.2.

Table 2.2 | Primer sequences.

Target (murine)	Primer sequence
TBP	Forward: CTTCACCAATGACTCCTATGACC
	Reverse: ACAGCCAAGATTCACGGTAGA
IP-10	Forward: GCCGTCATTTTCTGCCTCAT
	Reverse: GCTTCCCTATGGCCCTCATT
β-actin	Left: TGA CAG GAT GCA GAA GGA GA
	Right: seq CGC TCA GGA GGA GCA ATG
IFN-β	Left: CAG GCA ACC TTT AAG CAT CAG
	Right: CCT TTG ACC TTT CAA ATG CAG

The mastermixes for TBP and CXCL-10 (IP-10) were prepared according to Table 2.3 using the 5 x QPCR Mix EvaGreen® (ROX) (Bio & Sell GmbH, Feucht, Germany).

Table 2.3 | Mastermix for RT-PCR analyses of TBP and IP-10.

Mastermix (V_{tot}= 9 µL)	**1x**
H_2O	6.4 µL
Fw primer (10 µM)	0.3 µL
Rv primer (10 µM)	0.3 µL
EvaGreen	2 µL
cDNA (V_{tot} = 10 µL)	1 µL

Samples were run on an Applied Biosystems QuantStudio™ 5 (Thermo Fisher Scientific Inc., Waltham, MA, USA) according to the run profile shown in Table 2.4.

Table 2.4 | Temperature profile for RT-PCR analyses of TBP and IP-10.

Temperature profile	
Hold temperature	95 °C 15 min
Cycle 40x	95 °C 15 s
	60 °C 20 s
	72 °C 20 s
Acquire at 72 °C channel green.	

For the melting curve the temperature was ramped from 54 °C – 95 °C in steps of 0.075 °C/s. On the first step it was hold for 30 sec, for each step after it was hold for 5 sec.

The mastermixes for β-actin and IFN-β were prepared as stated in Table 2.5 using the HotStarTaq® DNA Polymerase kit (QIAGEN, Hilden, Germany) and SYBR™ Green Nucleic Acid Stain 10,000X concentrate in DMSO (Thermo Fisher Scientific Inc., Waltham, MA, USA).

Table 2.5 | Mastermix for RT-PCR analyses of β-actin and IFN-β.

Mastermix (V_{tot}= 18 µL)	**1x**
H_2O	12 µL
10x Buffer	2 µL
MgCl2 (25 mM)	0.4 µL
dNTPs (10 mM)	0.1 µL
Fw primer (5 µM)	1.6 µL
Rv primer (5 µM)	1.6 µL
SYBR green (1:1000)	0.2 µL
Hot start taq (250 U)	0.1 µL
cDNA (V_{tot}= 20 µL)	2 µL

Samples were run on a Rotor-Gene Q (QIAGEN, Hilden, Germany), according to the run profile shown in Table 2.6. Data were analyzed using the Rotor-Gene Q Series Software (QIAGEN, Hilden, Germany) and a relative quantification was calculated by the Δct method.

Table 2.6 | Temperature profile for RT-PCR analyses of β-actin and IFN-β.

Temperature profile	
Hold temperature	95 °C 15 min
Cycle 45x	95 °C 15 s
	60 °C 120 s
	72 °C 20 s
Acquire at 72 °C channel green, auto gain.	

For the melting curve the temperature was ramped from 59 °C – 95 °C in steps of 1 °C. On the first step it was hold for 90 sec, for each step after it was hold for 4 sec. The melt was acquired on the green channel.

2.24 Statistical analysis

Graphs were created and statistical analyses were performed using GraphPad Prism 8.0 (GraphPad Software, La Jolla, CA, USA). If not stated differently, data are shown as median with interquartile range. Data sets comprising more than two groups were analyzed by Kruskal-Wallis with Dunn's post-hoc test. Correlations were tested by

computing nonparametric Spearman correlation. Grouped data sets like the motility score and worm gender ratio were analyzed by 2-way ANOVA with Bonferroni's post-hoc test. Pooled data sets did not pass Spearman's test for heterogenicity.

2.25 Copyright statement

The use of the illustrations in Figure 1.3 and Figure 1.4, taken from the publication by Schlee and Hartmann (128), was approved by nature publishing (license number 5112911238130). The pictograms used to create the figures showing experimental setups were taken from Servier Medical Art by Servier, which is licensed under Creative Commons Attribution 3.0 Unported License.

3. Results

3.1 Responses of human peripheral blood mononuclear cells to *Litomosoides sigmodontis*-derived nucleic acids

The recognition of *L. sigmodontis*-derived nucleic acids by the vertebrate immune system is largely unstudied to date, and was aim of this study.

To gain a first insight, human peripheral blood mononuclear cells (PBMCs) were stimulated with parasite-derived nucleic acids and the early immune response was assessed.

For comparison, nucleic acids derived from *Plasmodium falciparum* were used as a second parasitic nucleic acid source. In contrast to helminthic nucleic acid sensing, the sensing of *P. falciparum*-derived nucleic acids was already elucidated *in vitro* by us and published (121) and *in vivo* studies by others confirmed its relevance (225, 226). As a further control, human nucleic acids were used. Host nucleic acid are not expected to elicit an immune response, provided they are not found in a biologically aberrant cellular compartment (122). Therefore, high concentrations of host DNA in the cytosol is accounted as danger signal since it is related to cell damage and the malfunctioning of cytosolic DNases (227).

3.1.1 Pro-inflammatory response of human PBMCs to *L. sigmodontis*-derived RNA

First, human PBMCs were stimulated with RNA that was either directed to the cytosol or the endosome of the cells. The cytosol was targeted by delivering the RNA in a liposome that fuses with the cellular membrane and releases its content to the cytosol (228). Endosomal uptake of RNA was facilitated by complexing with a cell-penetrating peptide (222, 229). The immune responses were assessed by evaluating cytokine secretion and activation of cell populations 24 h after stimulation.

The release of IFN-α, IP-10, TNF, IL-1β and IL-10 in response to RNA stimulation is shown in Figure 3.1. IFN-α is a measure for the production of type I IFNs after activation of the transcription factors IRF3/7, which are typically released after the recognition of nucleic acids (230). IP-10 is released by monocytes after the stimulation with mainly IFN-γ, but also IFN-α and TNF (231). Therefore, it is a direct measure of monocyte activation. At the same time it serves as an indirect measure of IFN-γ responses and

hence of T cell and NK cell activation, since these cell types are the major known IFN-γ producers (232). The secretion of TNF is often associated with the activation of the transcription factor NF-kB, but it has been discussed that TNF transcription also depends on IRF signaling (233). The release of IL-1β allows to draw conclusions regarding inflammasome activation (128). IL-10 was chosen as a marker for regulatory, anti-inflammatory immune responses (234).

The cytosolic stimulation of PBMCs with the RIG-I and MDA5 agonist poly(I:C) resulted in the secretion of all measured cytokines, while unstimulated cells did not secrete any of the measured cytokines (Figure 3.1 A – E). The cytosolic stimulation with *L. sigmodontis*-derived RNA induced significant IFN-α production compared to unstimulated cells ($p<0.001$) as well as compared to cells stimulated with human-derived RNA ($p=0.001$). Therefore, the IFN-α response was not induced by the transfection reagent itself (Figure 3.1 A). Further, there was significant IP-10 secretion in response to *L. sigmodontis*-derived RNA in the cytosol compared to stimulation with human-derived RNA ($p=0.02$) (Figure 3.1B). TNF (Figure 3.1 C) and IL-1β (Figure 3.1 D) secretion were significantly increased compared to unstimulated cells, but not compared to the human-derived RNA stimulus. Therefore, the transfection reagent might be the inducer of TNF and IL-1β. Lastly, there was no IL-10 response to cytosolic stimulation with *L. sigmodontis*-derived RNA (Figure 3.1 E). The cytosolic stimulation with *P. falciparum*-derived RNA revealed a similar pattern, as seen for the stimulation with *L. sigmodontis*-derived RNA. As a difference, there was an IL-10 response to *P. falciparum*-derived RNA, as well as to human-derived RNA (Figure 3.1 E).

The endosomal stimulation of PBMCs with the TLR7/8 agonist R848 resulted in the secretion of all quantified cytokines, while the stimulation with human-derived RNA did not and resembled the unstimulated control group (Figure 3.1 F – J). The endosomal stimulation with *L. sigmodontis*-derived RNA induced significant IFN-α ($p=0.0006$) and IP-10 ($p=0.001$) secretion by human PBMCs from most donors (Figure 3.1 F + G). Further there was a significant release of TNF ($p=0.005$), IL-1β ($p=0.02$) and IL-10 ($p=0.04$) in response to *L. sigmodontis*-derived RNA by all human PBMC donors (Figure 3.1 H – J). The endosomal stimulation with *P. falciparum*-derived RNA revealed a similar pattern, as seen for the stimulation with *L. sigmodontis*-derived RNA.

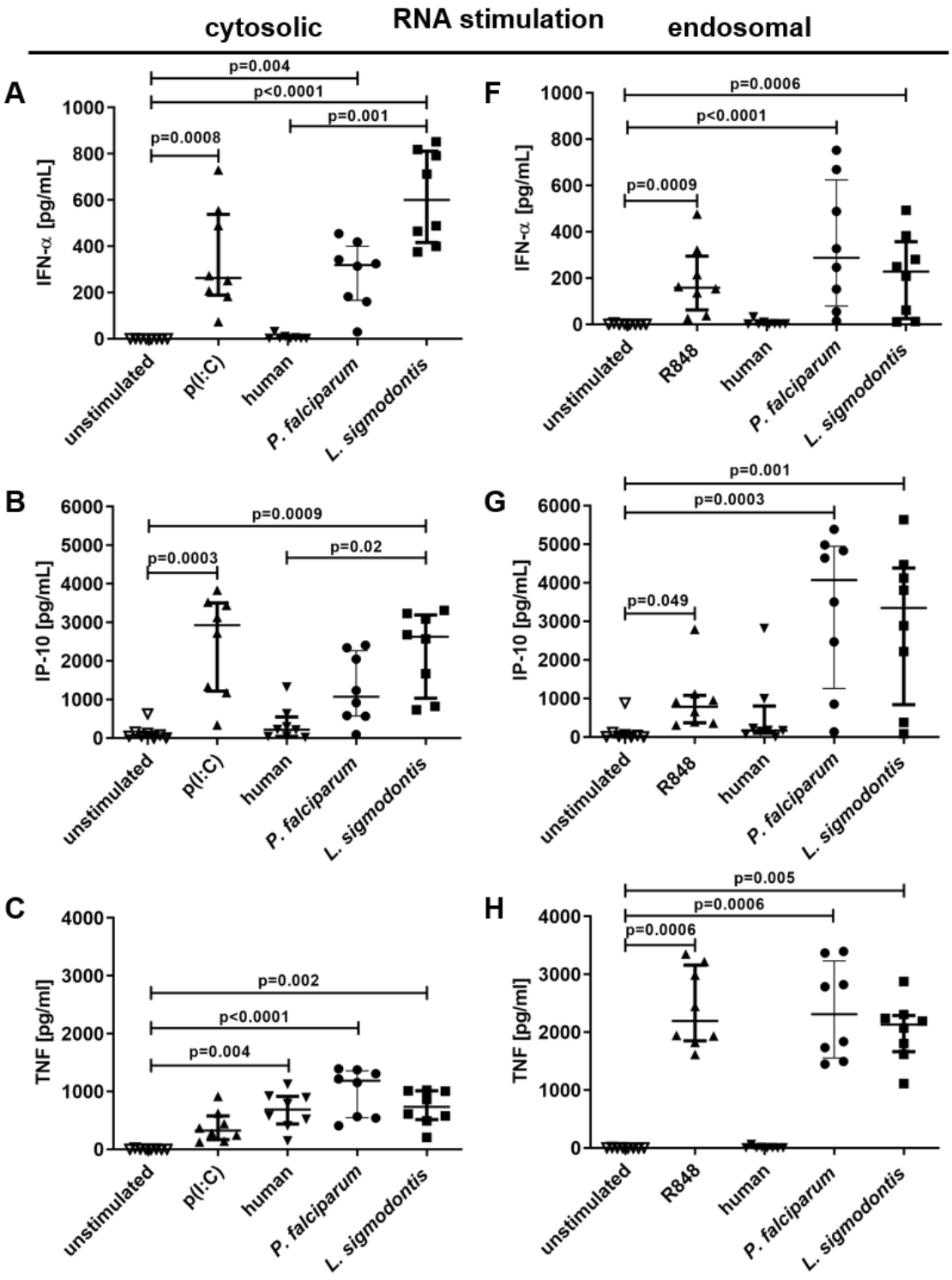

Continued on next page.

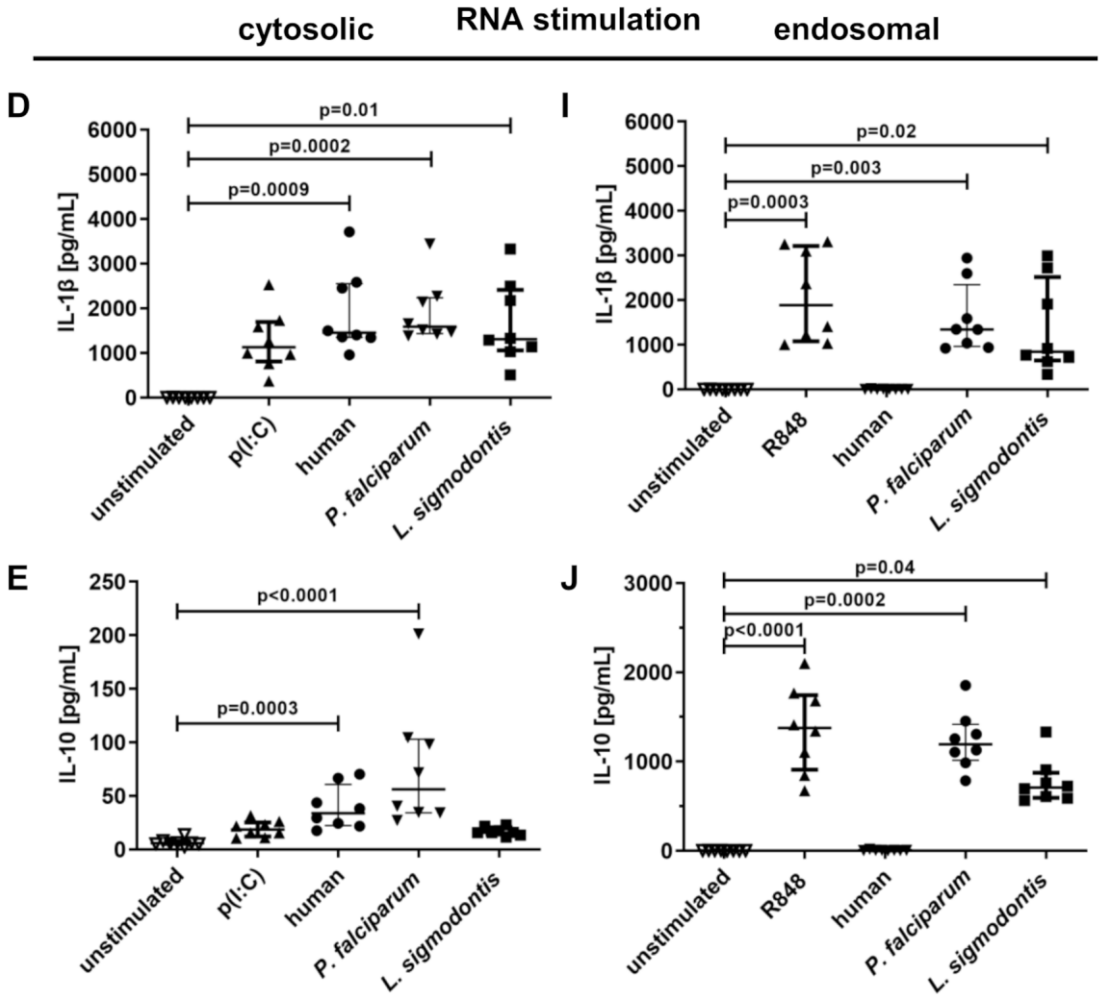

Figure 3.1 | Cytokine response by human PBMCs 24h after stimulation with RNA. **(A-J)** Human PBMCs were stimulated with 1µg/mL total RNA (*Litomosoides sigmodontis*, *Plasmodium falciparum* or human PBMC) or agonist (poly(I:C) or R848) for 24h. **(A-E)** The RNA or p(I:C) was delivered to the cytosol by complexing with Lipofectamine 2000®. **(F-J)** The RNA was delivered to the endosome by complexing with poly-L-Arginine. R848 was added naked. **(A+F)** IFN-α, **(B+G)** IP-10, **(C+H)** TNF, **(D+I)** IL-1β and **(E+J)** IL-10 were quantified by ELISA. **(A-J)** Error bars show median with IQR. Data were statistically analyzed by Kruskal-Wallis with Dunn's post-test. n=8, data pooled from two individual experiments. p(I:C): poly(I:C).

When comparing cytosolic with endosomal *L. sigmodontis*-derived RNA stimulation, the cytosolic stimulation resulted in higher concentrations of IFN-α (Figure 3.1 A + F), while endosomal stimulation resulted in higher concentrations of TNF (Figure 3.1 C + H) and IL-10 (Figure 3.1 E + J).

In order to confirm whether the observed cytokine production was dependent on the recognition of RNA, cells were stimulated with RNA samples that were previously

degraded with RNase. Selectively, the IFN-α response after cytosolic stimulation and the TNF response after endosomal stimulation were quantified by ELISA (Figure 3.2).

In all cases, the stimulation with intact RNA replicated the previous findings displayed in Figure 3.1 A and Figure 3.1 H, while the stimulation with degraded RNA failed to induce cytokine release. Since the agonist R848 is no RNA structure (235), no RNase treatment was applied.

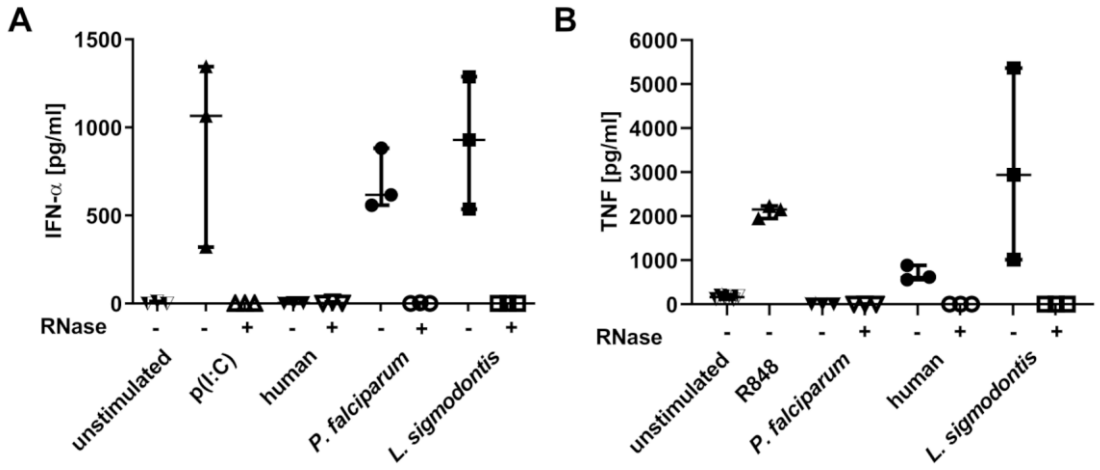

Figure 3.2 | RNA-dependent cytokine secretion. (A+B) Human PBMCs were stimulated with 1µg/mL intact or RNase A-degraded RNA derived from *Litomosoides sigmodontis*, *Plasmodium falciparum* and human PBMCs or agonist (poly(I:C) or R848) for 24h. **(A)** The RNA or p(I:C) were delivered to the cytosol by complexing with Lipofectamine 2000® and IFN-α was quantified by ELISA. **(B)** The RNA was delivered to the endosome by complexing with poly-L-Arginine, R848 was added naked and TNF was quantified by ELISA. Data are shown as median with IQR. n=3. p(I:C): poly(I:C).

Besides analyzing cytokine responses to the stimulation with parasitic RNA, the cellular composition and activation of human PBMCs was analyzed by flow cytometry. Major cell populations were identified by the gating strategy presented in Figure 3.3.

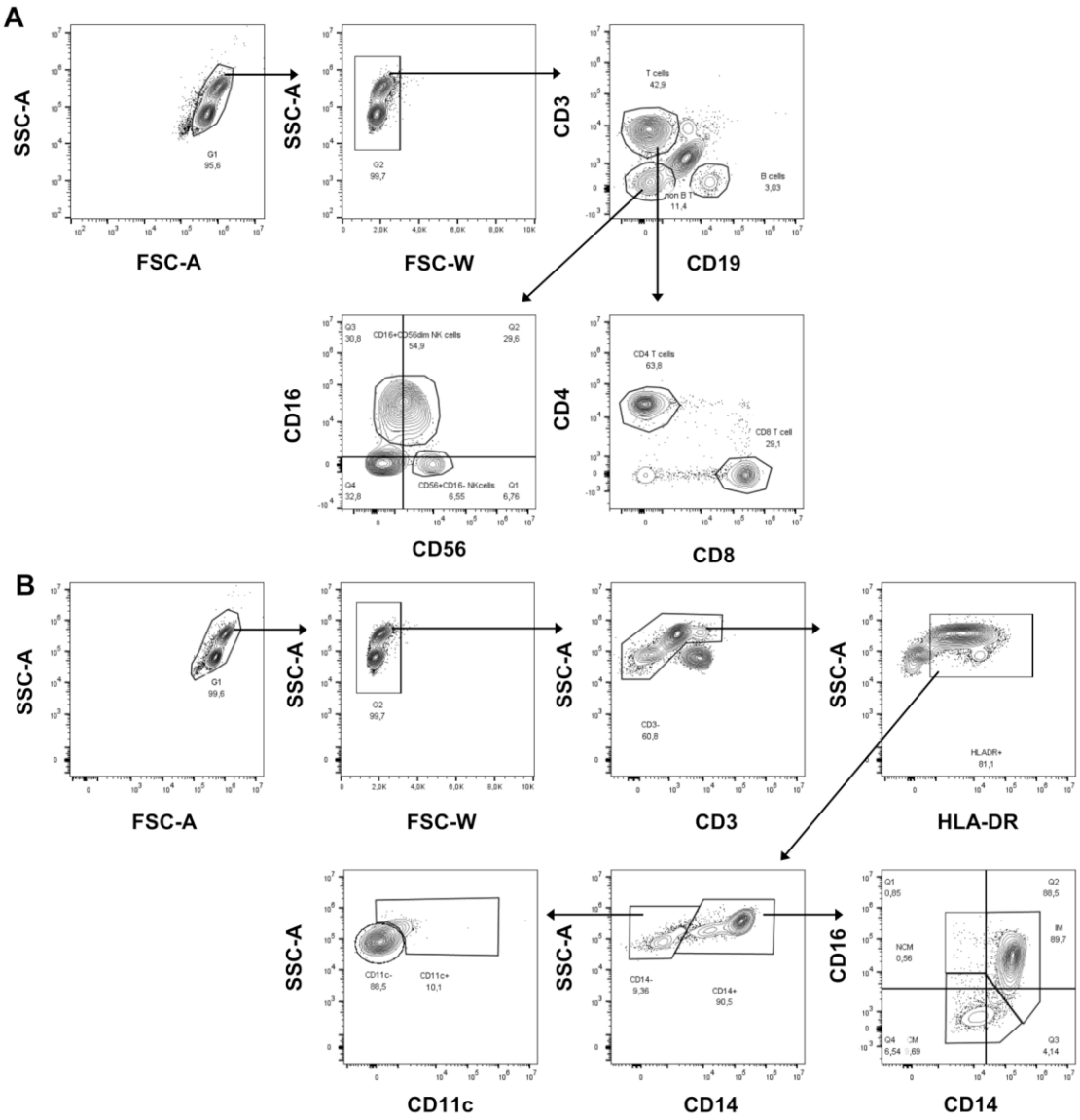

Figure 3.3 | Gating strategy for analysis of human PBMCs by flow cytometry. (A) Staining to identify T cell subsets by the expression of CD3, CD4 and CD8, B cells by the expression of CD19 and NK cell subsets by the expression of CD16 and CD56. **(B)** Staining to identify monocytes and dendritic cell. $CD3^+$ T cells were excluded, the major histocompatibility complex class 2 (HLA-DR) expressing cells were identified as dendritic cells by CD11c expression and monocytes by CD14 expression. Monocyte subsets were analyzed by CD14 and CD16 co-expression.

3.1.1.1 Flow cytometric analysis of human PBMCs after cytosolic RNA stimulation

Since there is a great range of cell frequencies among humans (236), there were no significant changes in the major human PBMC cell populations (T cells, B cells, NK cells, dendritic cells, monocytes) 24 h after cytosolic stimulation and trends ($p<0.1$) were indicated (Figure 3.4).

The frequencies of $CD4^+$ T cells and $CD8^+$ T cells increased by trend (Figure 3.4 A + B) and frequency of monocytes decreased by trend (Figure 3.4 G) upon stimulation with *L. sigmodontis*- and *P. falciparum*-derived RNA. Further, the stimulation resulted in a change of monocyte subsets (Figure 3.4 H). In all stimulated samples there was an increase of the proportion of $CD14^{dim}CD16^-$ monocytes and $CD14^{dim}CD16^+$ monocytes while the proportion of $CD14^+CD16^+$ monocytes was reduced. Since this was observed for all stimulation conditions including the human control, it is likely to be influenced by the transfection reagent

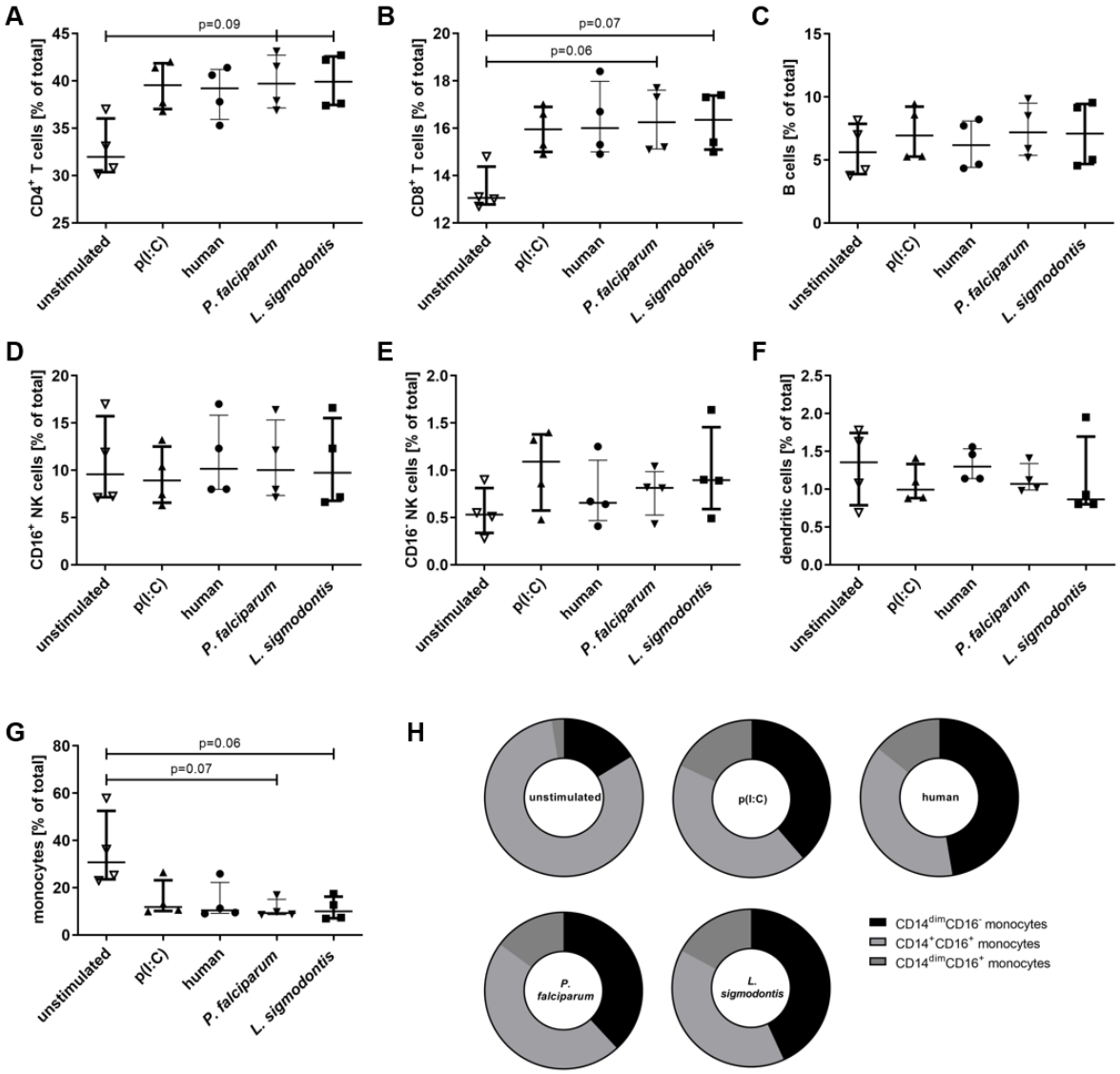

Continued on next page.

Figure 3.4 | Cell composition of human PBMCs after cytosolic RNA stimulation.
(A-H) Human PBMCs were stimulated in the cytosol with 1µg/mL total RNA (*Litomosoides sigmodontis*, *Plasmodium falciparum* or human PBMCs) or agonist (poly(I:C)) by complexing with Lipofectamine 2000® and analyzed by flow cytometry 24h after stimulation. Frequency of **(A)** $CD4^+$ T cells ($CD3^+CD19^-$ $CD4^+CD8^-$), **(B)** $CD8^+$ T cells ($CD3^+CD19^-CD4^-CD8^+$), **(C)** B cells ($CD3^-CD19^+$), **(D)** $CD16^+$ NK cells ($CD3^-CD19^-CD16^+CD56^{dim}$), **(E)** $CD16^-$ NK cells ($CD3^-$ $CD19^-CD16^-CD56^+$), **(F)** dendritic cells ($CD3^-$HLA-$DR^+CD14^-CD11c^+$) and **(G)** monocytes ($CD3^-$HLA-DR^+CD14^+). **(H)** Monocyte subpopulations gated as $CD3^-$ HLA-$DR^+CD14^{dim}CD16^-$monocytes, $CD3^-$HLA-$DR^+CD14^+CD16^+$monocytes and $CD3^-$HLA-$DR^+CD14^{dim}CD16^+$ monocytes shown as average of 4 donors. **(A-G)** Error bars show median with IQR. Data were statistically analyzed by Kruskal-Wallis with Dunn's post-test. n=4, data representative for two individual experiments. p(I:C): poly(I:C).

Next to relatively quantifying cellular populations, their activation was analyzed by measuring the expression of HLA-DR and CD80 by flow cytometry. HLA-DR, a major histocompatibility complex (MHC) class II molecule, is needed for antigen presentation to the adaptive immune system by interacting with the T cell receptor (114). CD80 is involved in co-stimulation and can be found on activated T cells (114).

There was no impact on the expression of CD80 on $CD4^+$ T cells and $CD8^+$ T cells (Figure 3.5 A + B) or HLA-DR expression on B cells and dendritic cells (Figure 3.5 C + D). The expression of HLA-DR on monocytes was analyzed for each subset. Cytosolic stimulation with *L. sigmodontis*-derived RNA resulted in significant upregulation of HLA-DR on $CD14^{dim}CD16^-$ monocytes (p=0.04) and $CD14^+CD16^+$ monocytes (p=0.02) compared to the unstimulated control (Figure 3.5 E + F). The upregulation on $CD14^+CD16^+$ monocytes was also significant compared to the stimulation with human-derived RNA (p=0.03). On $CD14^{dim}CD16^+$ monocytes the HLA-DR expression was reduced upon stimulation. This was significant for *P. falciparum*-derived RNA (p=0.02) compared to the unstimulated control (Figure 3.5 G).

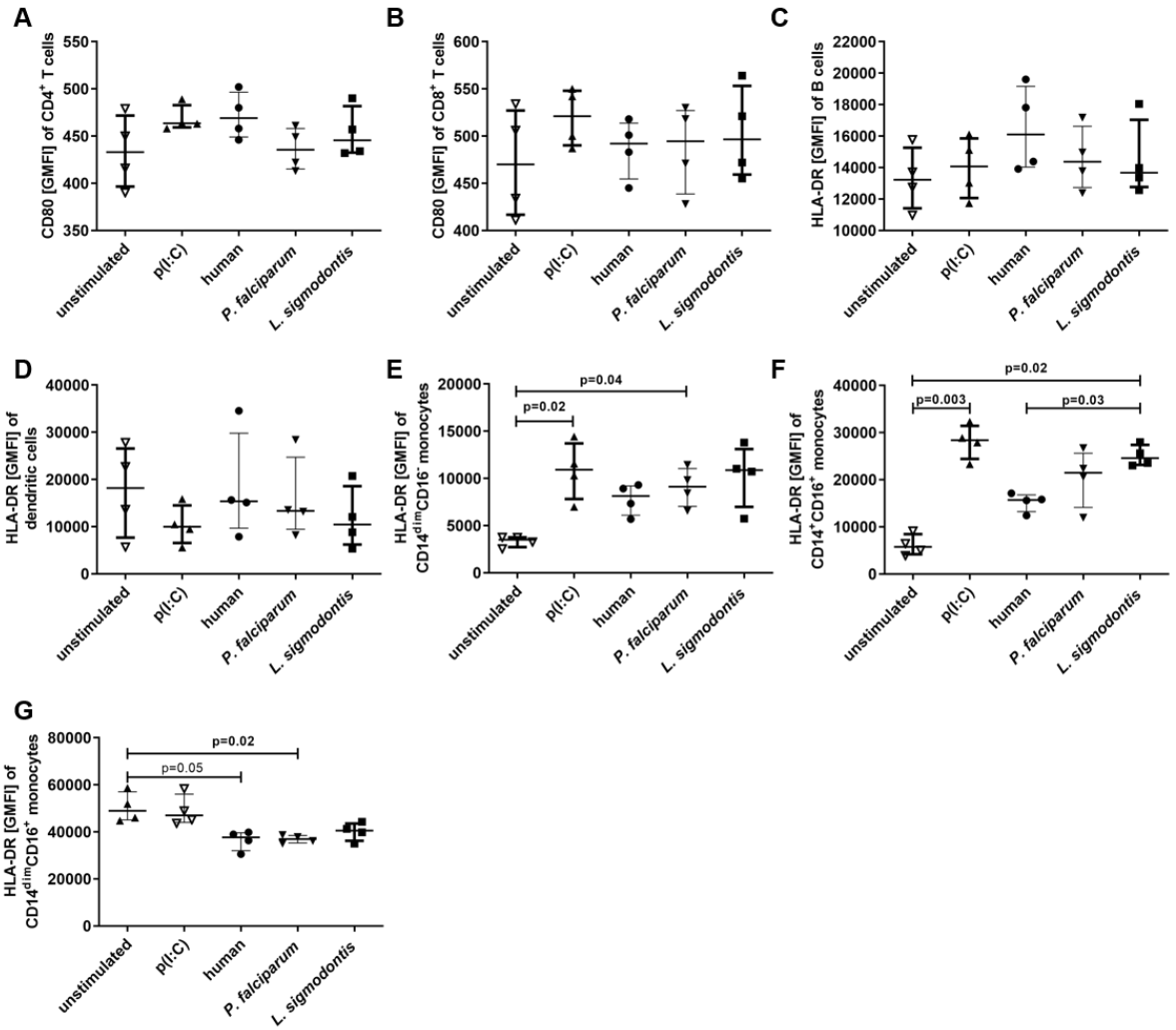

Figure 3.5 | Cell activation after cytosolic RNA stimulation of human PBMCs.
(A-G) Human PBMCs were stimulated in the cytosol with 1µg/mL total RNA (*Litomosoides sigmodontis*, *Plasmodium falciparum* or human PBMCs) or agonist (poly(I:C)) by complexing with Lipofectamine 2000® and analyzed by flow cytometry 24h after stimulation. Expression of CD80 on **(A)** $CD4^+$ T cells ($CD3^+CD19^-$ $CD4^+CD8^-$) and **(B)** $CD8^+$ T cells ($CD3^+CD19^-$ $CD4^-CD8^+$). Expression of HLA-DR on **(C)** B cells ($CD3^-CD19^+$), **(D)** dendritic cells ($CD3^-$ $HLA\text{-}DR^+CD14^-CD11c^+$), **(E)** $CD14^{dim}CD16^-$ monocytes ($CD3^-HLA\text{-}DR^+CD14^{dim}CD16^-$), **(F)** $CD14^+CD16^+$monocytes ($CD3^-HLA\text{-}DR^+CD14^+CD16^+$) and **(G)** $CD14^{dim}CD16^+$ monocytes ($CD3^-HLA\text{-}DR^+CD14^{dim}CD16^+$). Error bars show median with IQR. Data were statistically analyzed by Kruskal-Wallis with Dunn's post-test. n=4, data representative for two individual experiments.
p(I:C): poly(I:C),

3.1.1.2 Flow cytometric analysis of human PBMCs after endosomal RNA stimulation

The endosomal stimulation with RNA resulted in no significant differences in the frequency of $CD4^+$ T cells, $CD8^+$ T cells, B cells and NK cells (Figure 3.6 A – E). After endosomal stimulation with *L. sigmodontis*-derived RNA the frequency of dendritic cells was significantly reduced (p=0.04) compared to unstimulated controls. The stimulation with *P. falciparum*-derived RNA resulted in a significant reduction of the monocyte frequency (p=0.04) compared to unstimulated controls. Overall, there were no further statistical trends, but the changes in cell frequency in response to *L. sigmodontis*-derived RNA and *P. falciparum*-derived RNA followed a similar pattern.

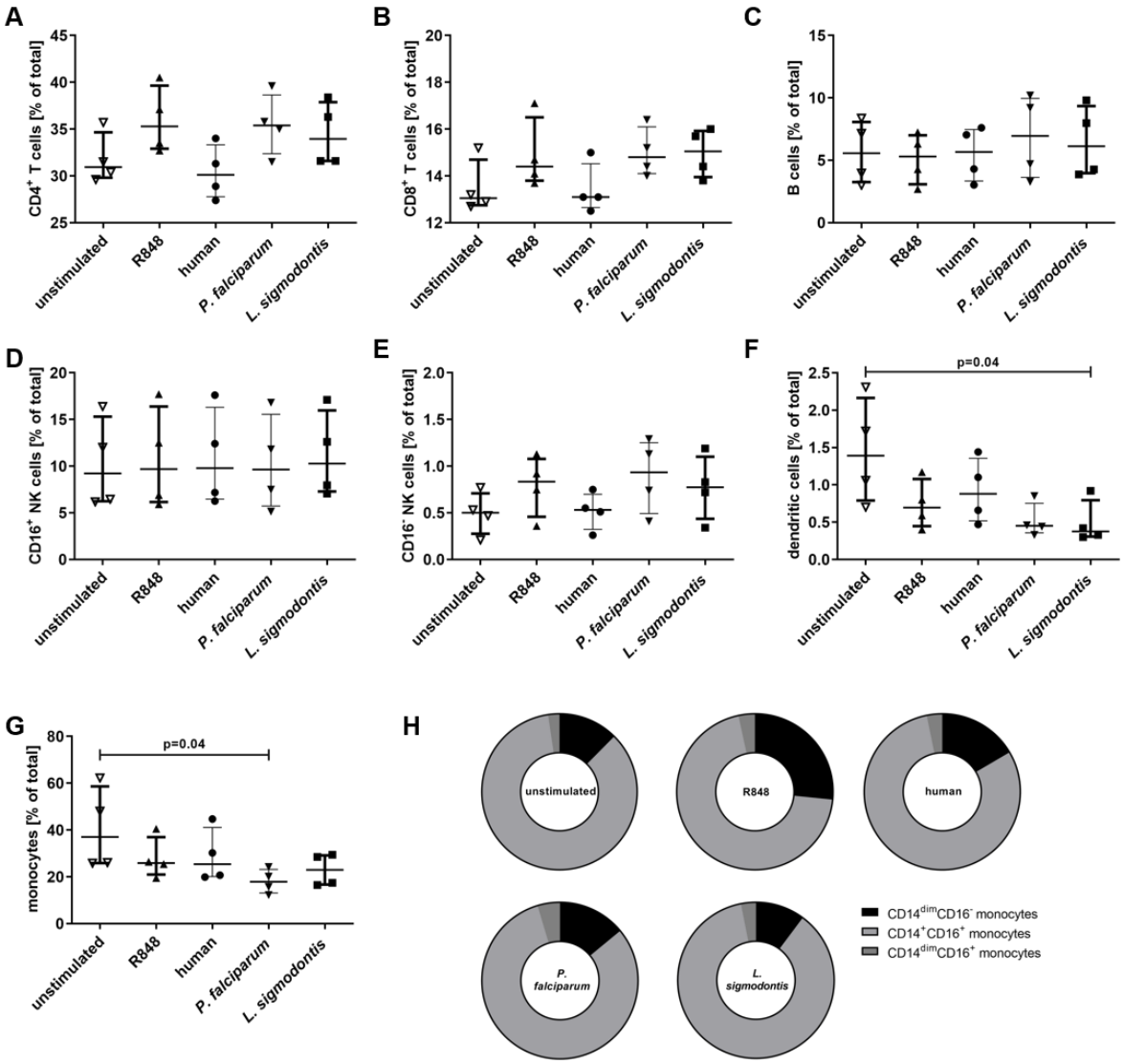

Continued on next page.

Figure 3.6 | Cell composition of human PBMCs after endosomal RNA stimulation.
(A-H) Human PBMCs were stimulated in the cytosol with 1µg/mL total RNA (*Litomosoides sigmodontis*, *Plasmodium falciparum* or human PBMCs) by complexing with poly-L-Arginine or agonist R848 and analyzed by flow cytometry 24h after stimulation. Frequency of **(A)** $CD4^+$ T cells ($CD3^+CD19^-CD4^+CD8^-$), **(B)** $CD8^+$ T cells ($CD3^+CD19^-CD4^-CD8^+$), **(C)** B cells ($CD3^-CD19^+$), **(D)** $CD16^+$ NK cells ($CD3^-CD19^-CD16^+CD56^{dim}$), **(E)** $CD16^-$ NK cells ($CD3^-CD19^-CD16^-CD56^+$), **(F)** dendritic cells ($CD3^-$HLA-DR $CD14^-CD11c^+$) and **(G)** monocytes ($CD3^-$HLA-DR^+CD14^+). **(H)** Monocyte subpopulations gated as $CD14^{dim}CD16^-$ monocytes ($CD3^-$HLA-$DR^+CD14^{dim}CD16^-$), $CD14^+CD16^+$ monocytes ($CD3^-$HLA-$DR^+CD14^+CD16^+$) and $CD14^{dim}CD16^+$ monocytes ($CD3^-$HLA-$DR^+CD14^{dim}CD16^+$) shown as average of 4 donors. Error bars show median with IQR. Data were statistically analyzed by Kruskal-Wallis with Dunn's post-test. n=4, data representative for two individual experiments.

The endosomal stimulation with any of the stimuli had no significant impact on the CD80 expression on $CD4^+$ T cells, $CD8^+$ T cells and the HLAD-DR expression on B cells, dendritic cells and $CD14^+CD16^+$ monocytes (Figure 3.7 A – D + F). The HLA-DR expression on $CD14^{dim}CD16^-$ monocytes was significantly upregulated after stimulation with *L. sigmodontis*-derived RNA (Figure 3.7 E). The HLA-DR expression was not significant in response to the stimulation with *P. falciparum*-derived RNA. The HLA-DR expression on $CD14^{dim}CD16^+$ monocytes was significantly downregulated after stimulation with *P. falciparum*-derived RNA (Figure 3.7 G). This was not significant in response to the stimulation with *L. sigmodontis*-derived RNA.

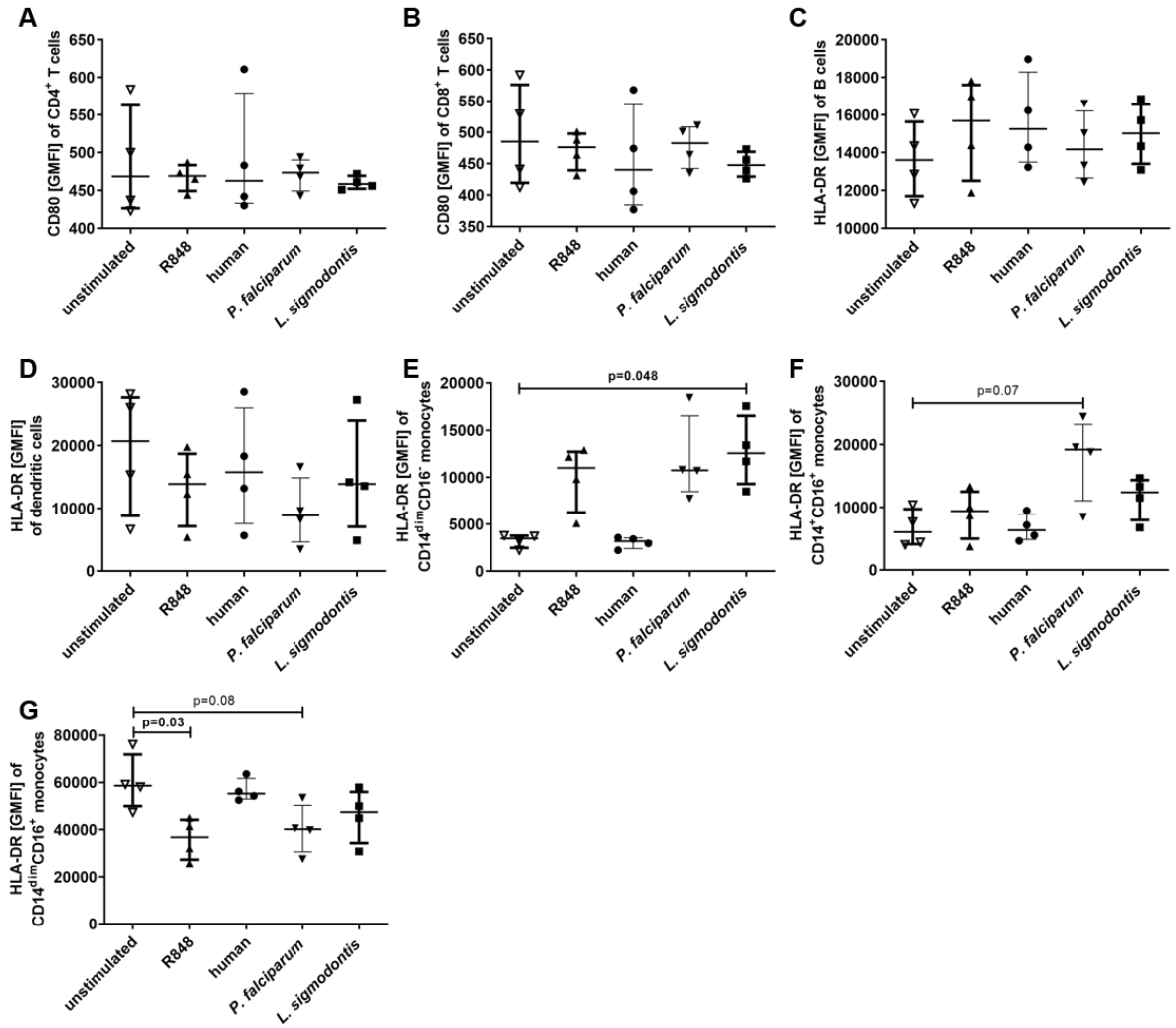

Figure 3.7 | Cell activation of human PBMCs after endosomal RNA stimulation.
(A-G) Human PBMCs were stimulated in the cytosol with 1µg/mL total RNA (*Litomosoides sigmodontis*, *Plasmodium falciparum* or human PBMCs) or agonist (poly(I:C)) by complexing with Lipofectamine 2000® and analyzed by flow cytometry 24h after stimulation. Expression of CD80 on **(A)** $CD4^+$ T cells ($CD3^+CD19^-$ $CD4^+CD8^-$) and **(B)** $CD8^+$ T cells ($CD3^+CD19^-$ $CD4^-CD8^+$). Expression of HLA-DR on **(C)** B cells ($CD3^-CD19^+$), **(D)** dendritic cells ($CD3^-$ $HLA\text{-}DR^+CD14^-CD11c^+$), **(E)** $CD14^{dim}CD16^-$ monocytes ($CD3^-HLA\text{-}DR^+CD14^{dim}CD16^-$), **(F)** $CD14^+CD16^+$ monocytes ($CD3^-HLA\text{-}DR^+CD14^+CD16^+$) and **(G)** $CD14^{dim}CD16^+$ monocytes ($CD3^-HLA\text{-}DR^+CD14^{dim}CD16^+$). Error bars show median with IQR. Data were statistically analyzed by Kruskal-Wallis with Dunn's post-test. n=4, data representative for two individual experiments.
p(I:C): poly(I:C),

Overall, the cytosolic and endosomal stimulation with *L sigmodontis*-derived RNA resulted in a type I interferon responses. Further, there was an activation of human monocytes in form of MHC class II upregulation.

3.1.2 Pro-inflammatory response of human PBMCs to *L. sigmodontis*-derived DNA

After observing cytokine secretion and cell activation in response to *L. sigmodontis*-derived RNA, human PBMCs were then stimulated with DNA that was either directed to the cytosol or the endosome. The immune responses were assessed by evaluating cytokine secretion and activation of cell populations 24 h after applying the stimulus.

The release of IFN-α, IP-10, TNF, IL-1β and IL-10 in response to RNA stimulation is shown in Figure 3.8.

The cytosolic stimulation of PBMCs with the agonist interferon stimulatory DNA (ISD), resulted in the secretion of all accessed cytokines, apart from IL-10 (Figure 3.8 A – E). Since human DNA in the cytosol accounts as danger signal, also the cytosolic stimulation with human-derived DNA resulted in secretion of all assessed cytokines.

Endosomal stimulation with TLR9 agonist CpGC resulted in the secretion of IFN-α and IP-10 (Figure 3.8 F + G). There was no TNF, IL-1β and IL-10 release in response to the agonist or any DNA stimulus (Figure 3.8 H – J). The endosomal stimulation with *L. sigmodontis*-derived DNA induced significant release of IFN-α ($p=0.0006$) and IP-10 ($p=0.004$) (Figure 3.8 F + G). In contrast, the endosomal stimulation with *P. falciparum*-derived DNA failed to induce IFN-α and IP-10 release (Figure 3.8 F + G).

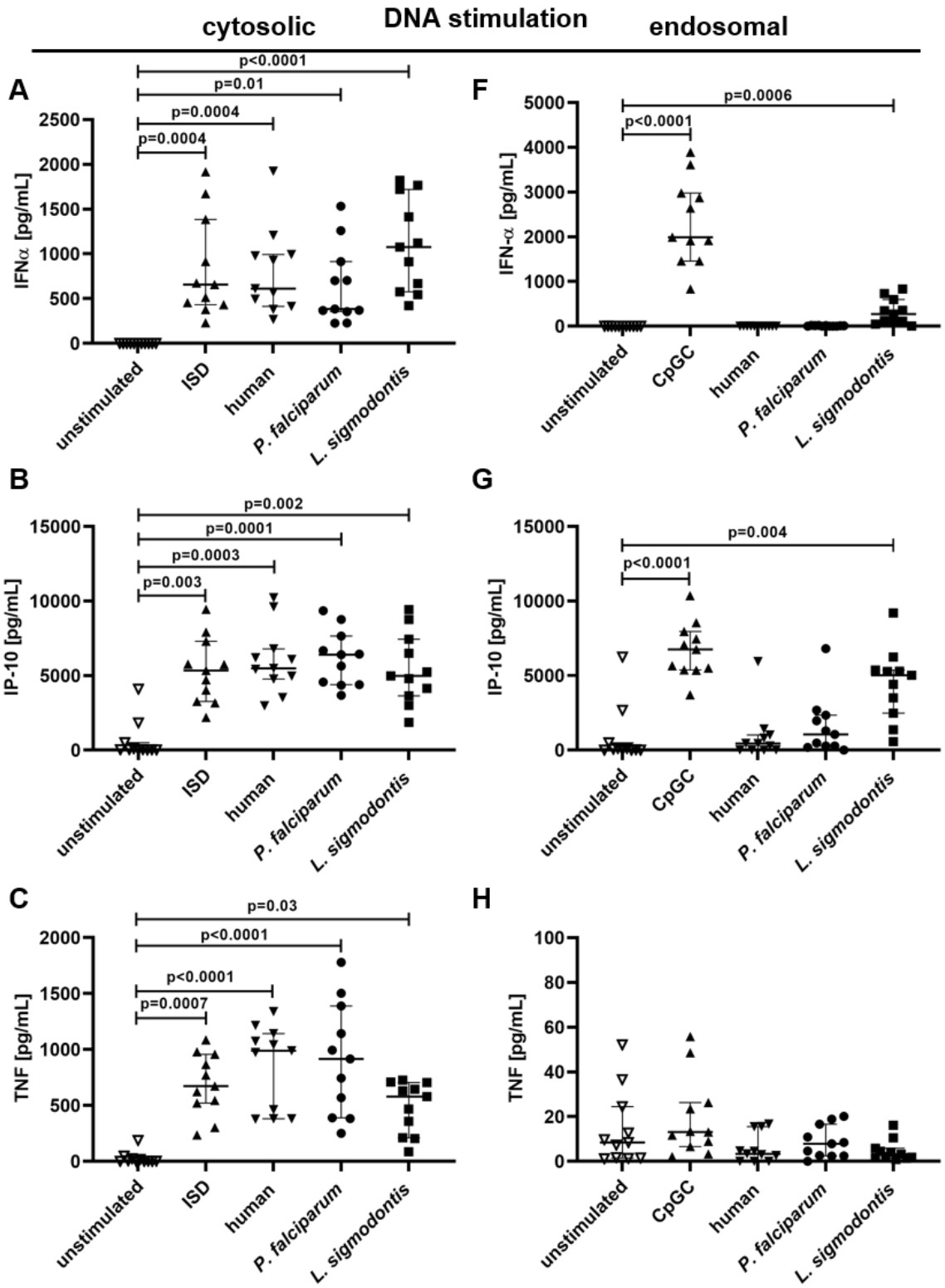

Continued on next page.

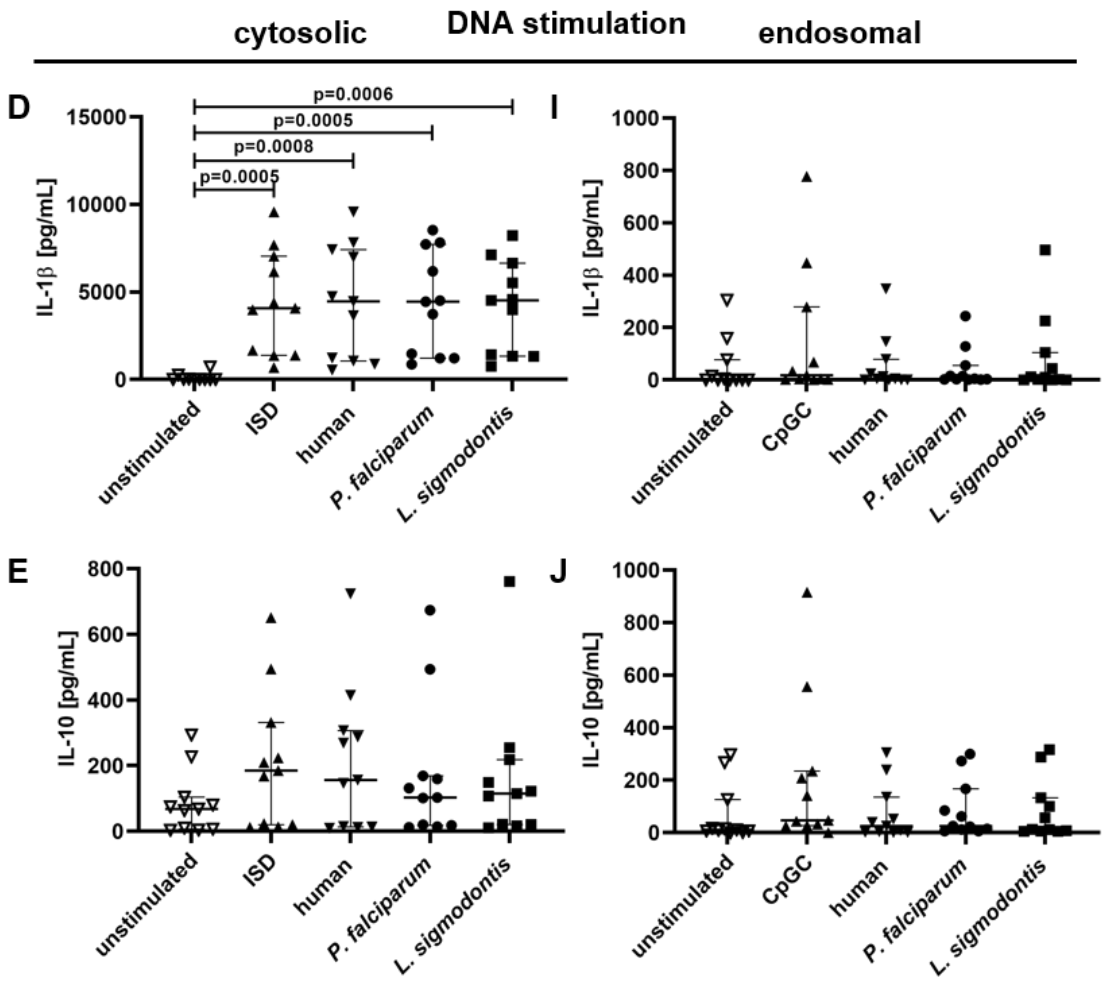

Figure 3.8 | Cytokine response by human PBMCs 24h after stimulation with DNA. **(A-J)** Human PBMCs were stimulated with 1µg/mL total DNA (*Litomosoides sigmodontis*, *Plasmodium falciparum* or human PBMCs) or agonist (ISD or CpGC). **(A-E)** The DNA or ISD were delivered to the cytosol by complexing with Lipofectamine 2000®. **(F-J)** The DNA was delivered to the endosome by complexing with poly-L-Arginine. CpGC was directly added to the cells. **(A+F)** IFN-α, **(B+G)** IP-10, **(C+H)** TNF, **(D+I)** IL-1β and **(E+J)** IL-10 were quantified by ELISA 24h after stimulation. **(A-J)** Error bars show median with IQR. Data were statistically analyzed by Kruskal-Wallis with Dunn's post-test. n=7-11, data pooled from three individual experiments.

3.1.2.1 Flow cytometric analysis of human PBMCs after cytosolic DNA stimulation

For flow cytometric analysis the cells were gated as shown in Figure 3.3.

There was no significant impact on the frequencies of $CD4^+$ T cells, $CD8^+$ T cells, B cells, $CD16^+$ NK cells, and $CD16^-$ NK cells (Figure 3.9 A – E). Upon cytosolic DNA stimulation there was an increase in dendritic cell frequency, which was significant after the stimulation with *L. sigmodontis*-derived DNA (p=0.008) (Figure 3.9 F). The overall monocyte frequency was not affected by any stimulation (Figure 3.9 G), but monocyte subset frequencies changed. Upon stimulation, there was an increase in $CD14^{dim}CD16^-$ monocytes frequency together with a reduction of $CD14^+CD16^+$ monocyte frequency (Figure 3.9 H).

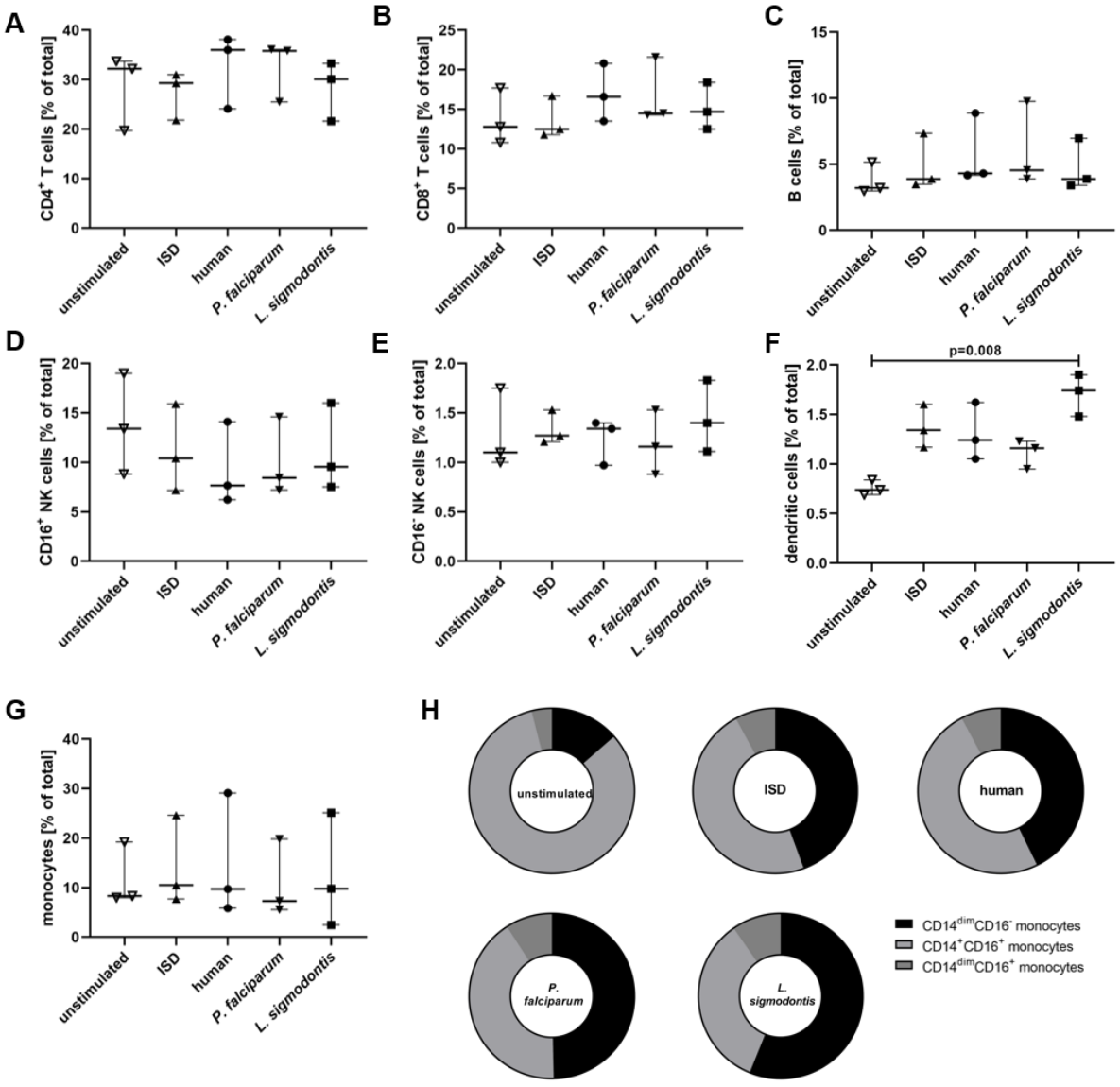

Continued on next page.

Figure 3.9 | Cell composition of human PBMCs after cytosolic DNA stimulation.
(A-H) Human PBMCs were stimulated in the cytosol with 1µg/mL total DNA (*Litomosoides sigmodontis*, *Plasmodium falciparum* or human PBMCs) or agonist (ISD) by complexing with Lipofectamine 2000® and analyzed by flow cytometry 24h after stimulation. Frequency of **(A)** $CD4^+$ T cells ($CD3^+CD19^-CD4^+CD8^-$), **(B)** $CD8^+$ T cells ($CD3^+CD19^-CD4^-CD8^+$), **(C)** B cells ($CD3^-CD19^+$), **(D)** $CD16^+$ NK cells ($CD3^-CD19^-CD16^+CD56^{dim}$), **(E)** $CD16^-$ NK cells ($CD3^-CD19^-CD16^-CD56^+$), **(F)** dendritic cells ($CD3^-$HLA-$DR^+CD14^-CD11c^+$) and **(G)** monocytes ($CD3^-$HLA-DR^+CD14^+). **(H)** Monocyte subpopulations gated as $CD14^{dim}CD16^-$ monocytes ($CD3^-$HLA-$DR^+CD14^{dim}CD16^-$), $CD14^+CD16^+$ monocytes ($CD3^-$HLA-$DR^+CD14^+CD16^+$) and $CD14^{dim}CD16^+$ monocytes ($CD3^-$HLA-$DR^+CD14^{dim}CD16^+$) shown as average of 4 donors. Error bars show median with IQR. Data were statistically analyzed by Kruskal-Wallis with Dunn's post-test. n=3, data representative for two individual experiments. p(I:C): poly(I:C).

The stimulation with parasitic DNA had no impact on CD80 expression on $CD4^+$ T cells and $CD8^+$ T cells or HLA-DR expression on dendritic cells (Figure 3.10 A – B + D). There was a great range of HLA-DR expression on B cells, $CD14^{dim}CD16^-$ monocytes and $CD14^{dim}CD16^+$ monocytes among donors and no trend or significance between groups (Figure 3.10 C + E + G). The expression of HLA-DR on $CD14^+CD16^+$ monocytes was upregulated by trend (p=0.09) in response to *L. sigmodontis*-derived DNA (Figure 3.10 F).

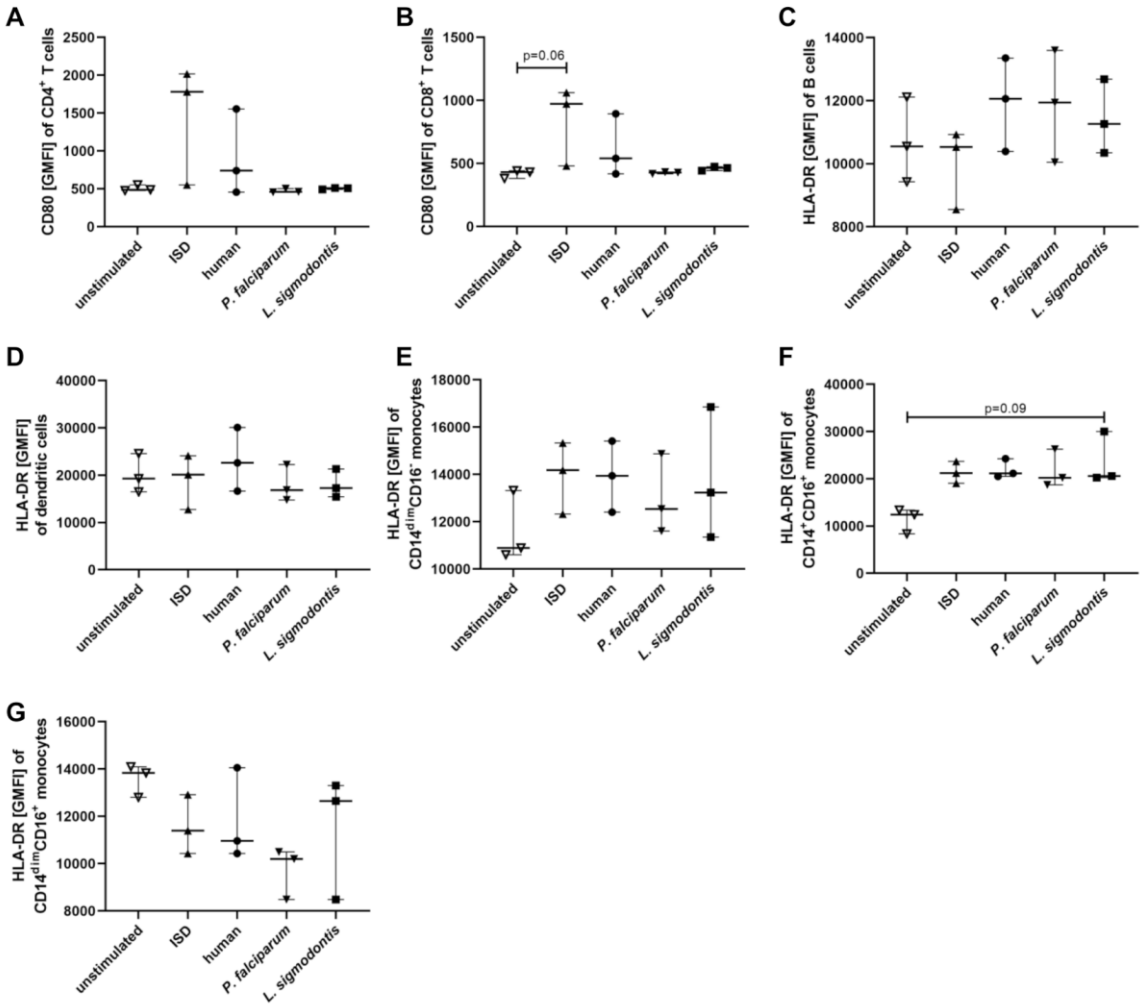

Figure 3.10 | Cell activation of human PBMCs after cytosolic DNA stimulation.
(A-G) Human PBMCs were stimulated in the cytosol with 1µg/mL total DNA (*Litomosoides sigmodontis*, *Plasmodium falciparum* or human PBMCs) or agonist (ISD) by complexing with Lipofectamine 2000® and analyzed by flow cytometry 24h after stimulation. Expression of CD80 on **(A)** $CD4^+$ T cells ($CD3^+CD19^-$ $CD4^+CD8^-$) and **(B)** $CD8^+$ T cells ($CD3^+CD19^-$ $CD4^-CD8^+$). Expression of HLA-DR on **(C)** B cells ($CD3^-CD19^+$), **(D)** dendritic cells ($CD3^-$ $HLA\text{-}DR^+CD14^-CD11c^+$), **(E)** $CD14^{dim}CD16^-$ monocytes ($CD3^-HLA\text{-}DR^+CD14^{dim}CD16^-$), **(F)** $CD14^+CD16^+$ monocytes ($CD3^-HLA\text{-}DR^+CD14^+CD16^+$) and **(G)** $CD14^{dim}CD16^+$ monocytes ($CD3^-HLA\text{-}DR^+CD14^{dim}CD16^+$).
Error bars show median with IQR. Data were statistically analyzed by Kruskal-Wallis with Dunn's post-test. n=3, data representative for two individual experiments. p(I:C): poly(I:C),

3.1.2.2 Flow cytometric analysis of human PBMCs after endosomal DNA stimulation

The endosomal stimulation with DNA had no significant impact on the frequencies of $CD4^+$ T cells, $CD8^+$ T cells, B cells, $CD16^+$ NK cells, and $CD16^-$ NK cells (Figure 3.11 A – E). Despite a lack of statistical significance due to low sample size, the frequencies of dendritic cells only appeared to increase upon CpGC stimulation (Figure 3.11 F). Monocyte frequencies appeared to increase after the stimulation with CpGC and

L. sigmodontis-derived DNA (Figure 3.11 G). Only CpGC had an impact on monocytic subset frequencies shown by an increase in $CD14^{dim}CD16^-$ monocyte frequency together with a reduction of $CD14^+CD16^+$ monocyte frequency, due to a loss of CD16 expression (Figure 3.11 H).

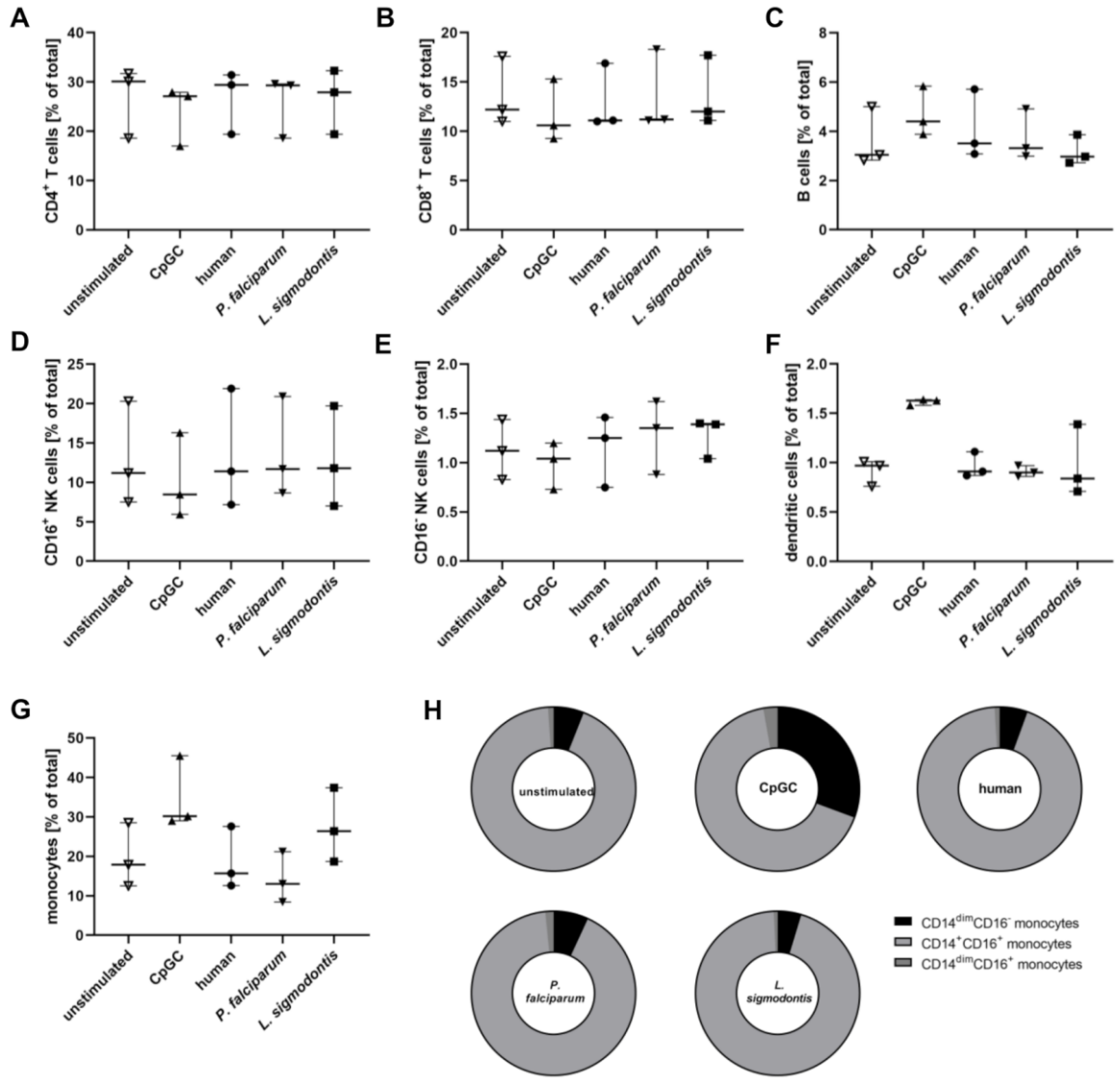

Figure 3.11 | Cell composition after endosomal DNA stimulation of human PBMCs. **(A-H)** Human PBMCs were stimulated in the cytosol with 1µg/mL total DNA (*Litomosoides sigmodontis*, *Plasmodium falciparum* or human PBMCs) by complexing with poly-L-Arginine or agonist CpGC and analyzed by flow cytometry 24h after stimulation. Frequency of **(A)** $CD4^+$ T cells ($CD3^+CD19^-CD4^+CD8^-$), **(B)** $CD8^+$ T cells ($CD3^+CD19^-CD4^-CD8^+$), **(C)** B cells ($CD3^-CD19^+$), **(D)** $CD16^+$ NK cells ($CD3^-CD19^-CD16^+CD56^{dim}$), **(E)** $CD16^-$ NK cells ($CD3^-CD19^-CD16^-CD56^+$), **(F)** dendritic cells ($CD3^-$HLA-$DR^+CD14^-CD11c^+$) and **(G)** monocytes ($CD3^-$HLA-DR^+CD14^+). **(H)** Monocyte subpopulations gated as $CD14^{dim}CD16^-$ monocytes ($CD3^-$HLA-$DR^+CD14^{dim}CD16^-$), $CD14^+CD16^+$ monocytes ($CD3^-$HLA-$DR^+CD14^+CD16^+$) and $CD14^{dim}CD16^+$ monocytes ($CD3^-$HLA-$DR^+CD14^{dim}CD16^+$) shown as average of 4 donors. Error bars show median with IQR. Data were statistically analyzed by Kruskal-Wallis with Dunn's post-test. n=3, data representative for two individual experiments.

The endosomal stimulation failed to induce significant upregulation of CD80 on $CD4^+$ T cells and $CD8^+$ T cells (Figure 3.12 A + B) or HLAD-DR on B cells, dendritic cells and monocyte subsets (Figure 3.12 C – G). However, the HLAD-DR expression seems to be upregulated on B cells and $CD14^+CD16^+$ monocytes (Figure 3.12 C + F).

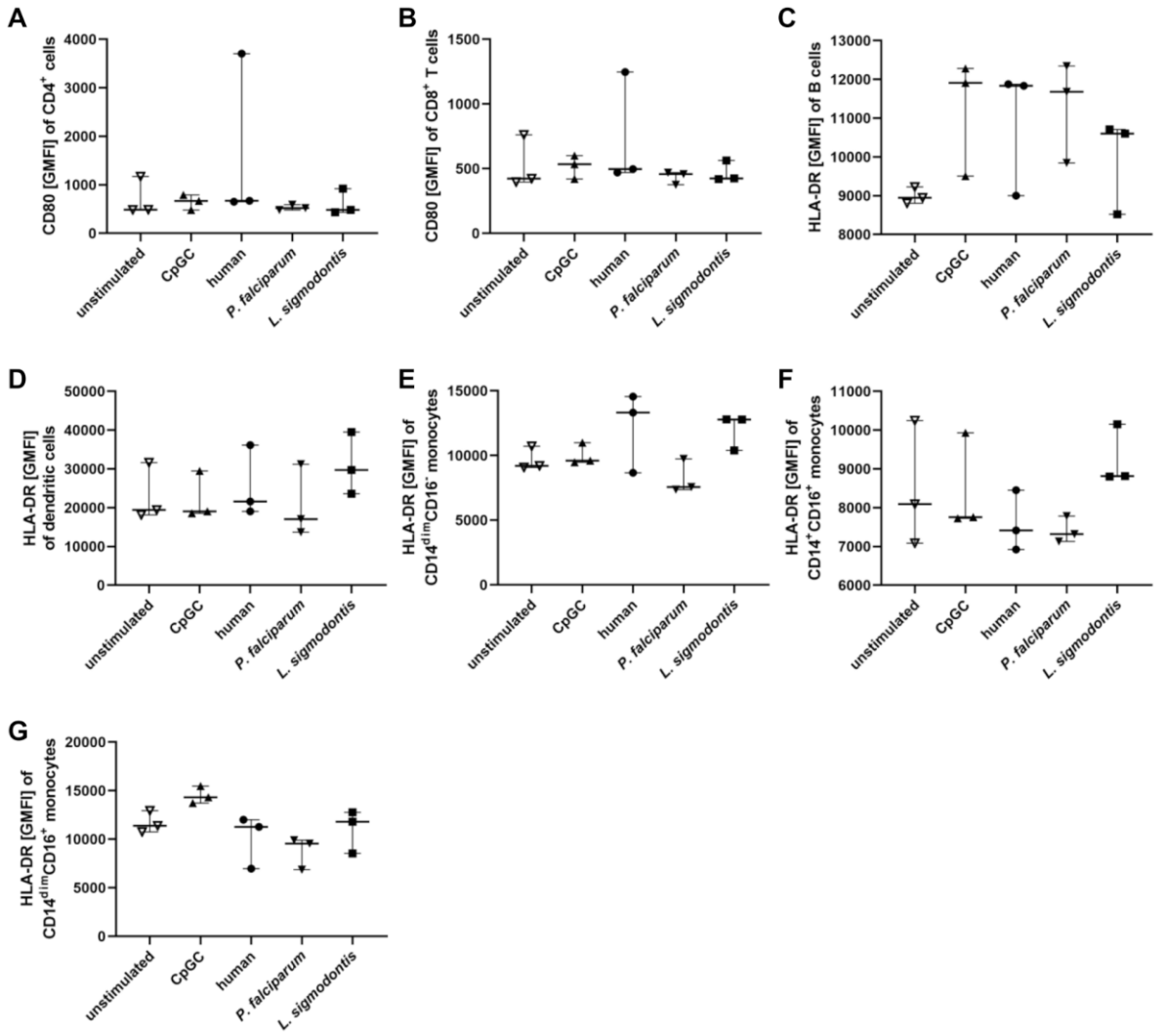

Figure 3.12 | Cell activation of human PBMCs after endosomal DNA stimulation.
(A-G) Human PBMCs were stimulated in the cytosol with 1µg/mL total DNA (*Litomosoides sigmodontis*, *Plasmodium falciparum* or human PBMCs) by complexing with poly-L-Arginine or agonist CpGC and analyzed by flow cytometry 24h after stimulation. Expression of CD80 on **(A)** $CD4^+$ T cells ($CD3^+CD19^-CD4^+CD8^-$) and **(B)** $CD8^+$ T cells ($CD3^+CD19^-CD4^-CD8^+$). Expression of HLA-DR on **(C)** B cells ($CD3^-CD19^+$), **(D)** dendritic cells ($CD3^-$HLA-$DR^+CD14^-CD11c^+$), **(E)** $CD14^{dim}CD16^-$ monocytes ($CD3^-$HLA-$DR^+CD14^{dim}CD16^-$), **(F)** $CD14^+CD16^+$ monocytes ($CD3^-$HLA-$DR^+CD14^+CD16^+$) and **(G)** $CD14^{dim}CD16^+$ monocytes ($CD3^-$HLA-$DR^+CD14^{dim}CD16^+$). Error bars show median with IQR. Data were statistically analyzed by Kruskal-Wallis with Dunn's post-test. n=3, data representative for two individual experiments. p(I:C): poly(I:C),

Overall, the cytosolic and endosomal stimulation with *L sigmodontis*-derived DNA resulted in type I interferon responses. This was different for *P. falciparum*-derived DNA, which induced IFN-α only after cytosolic, but not endosomal stimulation. Further there was an activation of human monocytes in form of MHC class II upregulation upon cytosolic and endosomal stimulation with *L sigmodontis*-derived DNA.

3.2 Type I IFN response by murine cells to *Litomosoides sigmodontis*

3.2.1 IFN-β production by bone marrow-derived cells in response to *Litomosoides sigmodontis* RNA

Since the stimulation of human cells revealed that nucleic acids, especially RNA, from *L. sigmodontis* induced type I IFN secretion, it was investigated whether RNA stimulation induced type I IFN production in murine cells, as well.

To that end macrophages (BMDM) and plasmacytoid DCs (BMpDC) were generated and neutrophils (BMDN) were isolated from the bone marrow of albino C57BL/6 IFN-β Luc reporter mice. Macrophages were chosen since they are professional antigen presenting cells and an important cytokine source during T cell differentiation (237). pDCs are known to be strong type I IFN producers (238) and neutrophils are an important cell type during early infection with *L. sigmodontis*.

C57BL/6 IFN-β Luc reporter mice express the enzyme luciferase under the promotor for IFN-β. Therefore, the production of IFN-β in response to RNA can be assessed by measuring luminescence generated by the reaction of luciferase with its substrate, and is stated as relative light units (RLU). Homozygous and heterozygous animals were used and are indicated in the figures per color code.

Bone marrow-derived cells were characterized by flow cytometry and Giemsa-stained cytospins (Figure 3.13).

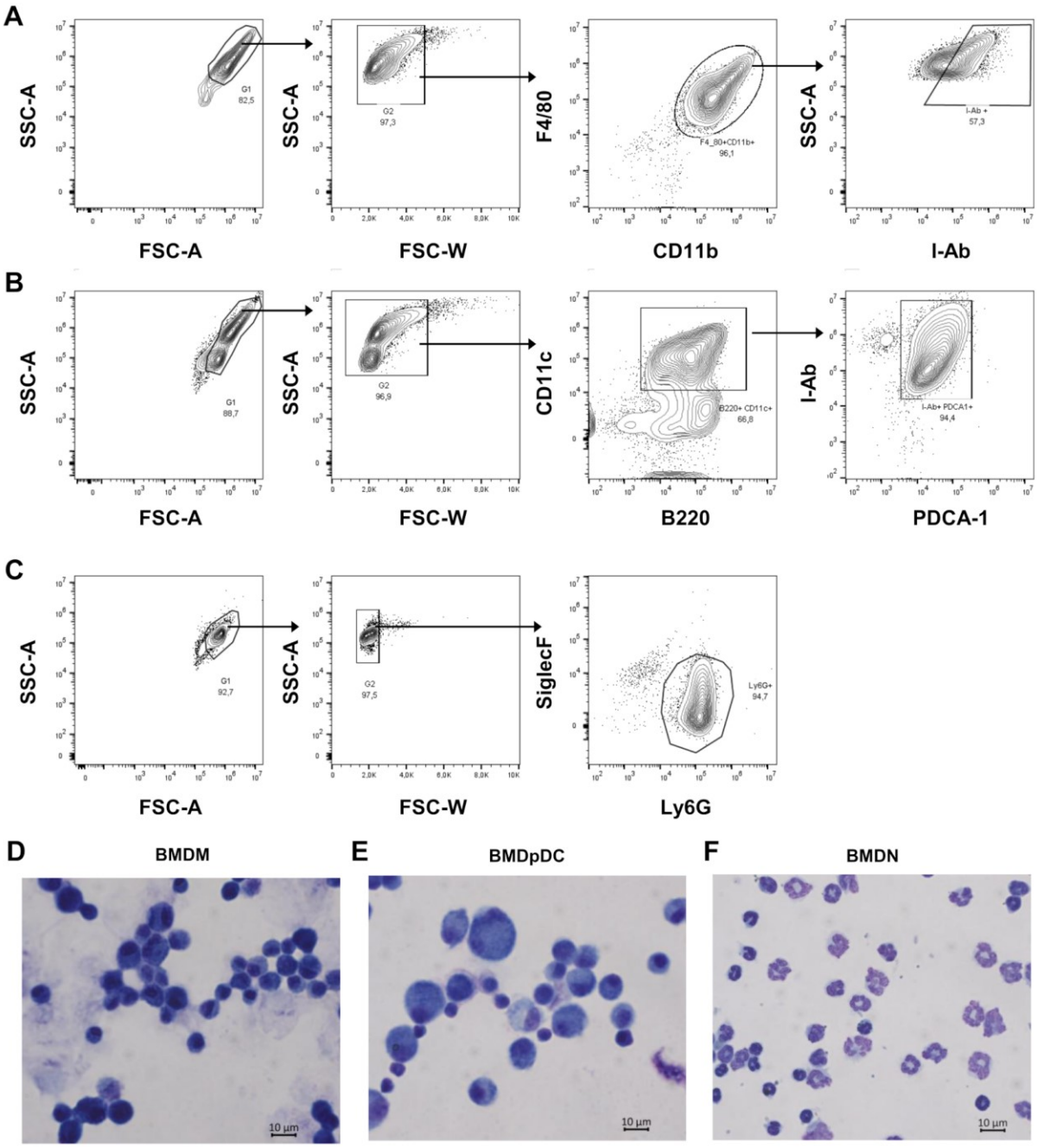

Figure 3.13 | Purity assessment of bone marrow-derived cells. (A-C) Bone marrow-derived cells from albino C57BL/6 IFN-β luciferase reporter mice were analyzed by flow cytometry. Gating of **(A)** bone marrow-derived macrophages (BMDM), **(B)** bone marrow-derived plasmacytoid dendritic cells (BMDMpDC) and **(C)** bone marrow-derived neutrophils (BMDN). **(D-F)** Visualization by microscopy in Giemsa-stained cytospins of **(D)** BMDMs, **(E)** BMDpDCs and **(F)** BMDNs. Bars: 20µm. **(A-F)** Representative for three individual experiments.
BMDM: bone marrow-derived macrophages, BMDN: bone marrow-derived neutrophils, BMDpDC: bone marrow-derived plasmacytoid dendritic cells.

BMDMs were $CD11b^+F4/80^+$ at a purity of ~96% and ~60% of these cells were MHC class II (I-Ab) positive (Figure 3.13 A). Based on microscopy, the cells were 10-20 µm in size (Figure 3.13 D). ~70% of the BMpDCs were $B220^+CD11c^+$ and expressed the pDC marker PDCA-1 (Figure 3.13 B). The cells varied in size with a single round nucleus (Figure 3.13 E). BMDNs were gated as $Ly6G^+SiglecF^-$, had a purity of ~95% (Figure 3.13 C) and appeared with the neutrophil-associated nuclear shape (Figure 3.13 F).

Luminescence activity in the different cell types, as measure for IFN-β production, in response to *in vitro* stimuli is shown in Figure 3.14. As control RNA, cells were stimulated with murine RNA, since it is not expected to induce an immune response.

BMDMs responded with a significantly increased IFN-β production to *L. sigmodontis*-derived RNA delivered to the cytosol (p=0.03). A similar response was observed after stimulation with naked poly(I:C), which targets TLR3 and is known to induce IFN-β production (Figure 3.14 A). In order to account for possible effects of the transfection reagent on IFN-β production *L. sigmodontis*-derived RNA was compared to murine RNA. This revealed a significantly increased IFN-β production (p=0.02) in response to *L. sigmodontis*-derived RNA. In contrast, BMDMs did not respond with IFN-β production to the endosomal stimulation with *L. sigmodontis*-derived RNA and murine RNA, and only weakly to cytosolic stimulation with murine RNA.
A similar pattern was observed after the stimulation of BMpDCs (Figure 3.14 B). Cytosolic stimulation with *L. sigmodontis*-derived RNA led to a significant increase in RLU (p=0.02) compared to unstimulated cells. Comparing cytosolic *L. sigmodontis*-derived RNA with murine RNA, revealed a significantly increased IFN-β production (p=0.009) in response to *L. sigmodontis*-derived RNA as well. The endosomal stimulation with *L. sigmodontis*-derived RNA did not affect IFN-β production.
The stimulation of BMDN led to low RLUs for all conditions including naked poly(I:C) (Figure 3.14 C). Therefore, cells were also stimulated with transfected poly(I:C) as a positive control, which targets the cytosolic sensors RIG-I and MDA5. The stimulation with transfected poly(I:C) and cytosolic stimulation with murine RNA resulted in an increase in IFN-β. In contrast, there was a significant IFN-β response to cytosolic stimulation with *L. sigmodontis*-derived RNA (p=0.001). Comparing cytosolic *L. sigmodontis*-derived RNA with murine RNA, also revealed a significantly increased IFN-β production (p=0.02) in response to parasitic RNA.

Of note, the *in vitro* stimulation with 50 viable or heat inactivated *L. sigmodontis* L3 larvae did not induce IFN-β in BMDMs and BMpDCs (not shown).

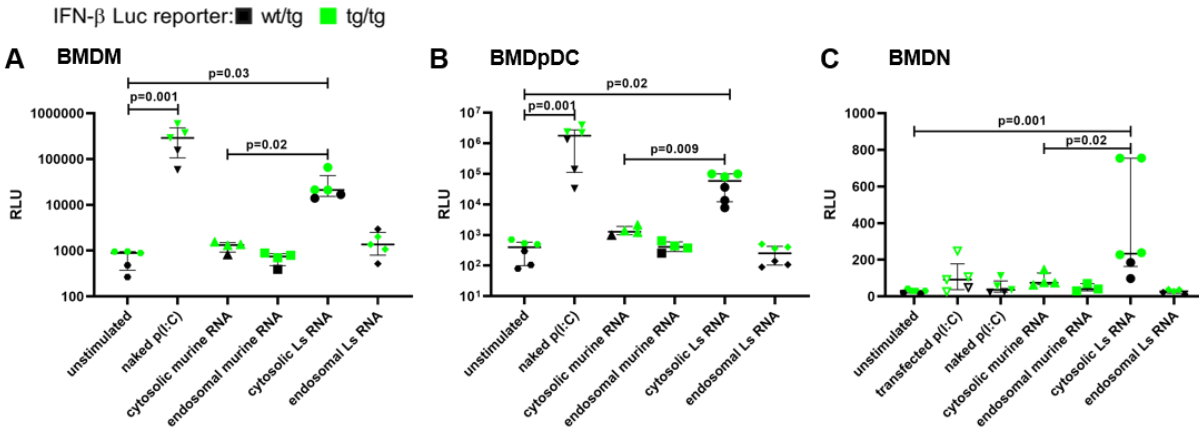

Figure 3.14 | *In vitro* INF-β production in response to cytosolic stimulation with *L. sigmodontis*-derived RNA. **(A)** Macrophages (BMDM – F4/80$^+$CD11b$^+$), **(B)** pDCs (BMpDC – B220$^+$CD11c$^+$PDCA-1$^+$) and **(C)** neutrophils (BMDN – SiglecF$^-$Ly6G$^+$) were isolated from bone marrow of albino C57BL/6 IFN-β luciferase reporter mice. **(A-C)** Cells were stimulated with 1µg/mL *L. sigmodontis* (Ls) RNA, 1µg/mL murine splenocyte RNA (cytosolic delivery with Lipofectamine 2000, endosomal delivery with poly-L-Arginine) or 1µg/mL naked poly(I:C). After 24h stimulated luciferase activity was measured as relative light units (RLU). Data are shown as median with IQR, statistical analysis Kruskal-Wallis with Dunn's post-hoc test. Cytosolic Ls RNA and murine RNA were additionally analyzed with Mann-Whitney U test. **(A+B)** Data on murine RNA pooled from 2 individual experiments, other stimuli from 3 individual experiments. **(C)** Data on murine RNA pooled from 2 individual experiments, data on transfected poly(I:C) were pooled from 3 individual experiments, other stimuli from 4 individual experiments.
BMDM: bone marrow-derived macrophages, BMDN: bone marrow-derived neutrophils, BMDpDC: bone marrow-derived plasmacytoid dendritic cells, p(I:C): poly(I:C), RLU: relative light unit.

3.2.2 *In vivo* IFN-β response to *Litomosoides sigmodontis* infection

After observing an *in vitro* response to *L. sigmodontis*-derived nucleic acids, we were interested, whether there is an *in vivo* response towards the parasite that can be linked to nucleic acid recognition.

To that end albino C57BL/6 IFN-β luciferase reporter mice were naturally infected with *L. sigmodontis*, pleural cells were isolated at different time points after the infection and analyzed regarding their IFN-β production (Figure 3.15).

Time points of choice were 5-days post infection (dpi) - when the majority of L3 larvae reached the pleural cavity, 12 dpi - when the L3 larvae molt into L4 larvae, and 30 dpi

-after the molt into adult worms but before worm elimination has started in C57BL/6 mice (63, 77, 78).

As positive control, isolated pleural cells were stimulated with naked poly(I:C), which is a known agonist of TLR3 and results in downstream IFN-β production (128).

In order to compare the relative IFN-β response of different time points, the fold change of RLU in comparison to the average RLU of naïve control animals was calculated. Homozygous and heterozygous animals were used and are indicated in the figures per color code (black for heterozygous, green for homozygous).

At all time points after the infection with *L. sigmodontis* there was a significant increase in IFN-β production in pleura cells (Figure 3.15 A). The fold change increased over the duration of infection. The same was observed in cells isolated from the infected animals at the different time points following *in vitro* stimulation with poly(I:C). At 5 and 12 dpi, there was a higher fold change in the cells from animals that were homozygous for the transgene than cells from heterozygous animals, while this was not observed for cells isolated 30 dpi. The stimulation of cells from homozygous animals isolated 12 dpi with poly(I:C), did not further increase IFN-β production.
Besides differences in the genetic background, also the worm burden in the individual animals may impact the IFN-β response. Therefore, the RLU fold change was correlated to the worm burden recovered from the pleural cavity. On 5 dpi, there was no correlation between worm burden and fold change in RLU (Figure 3.15 B). At the later time points there was a significant, positive correlation, which was strong (R^2=0.75) on day 12 after infection (Figure 3.15 C) and moderate (R^2=0.66) on day 30 after infection (Figure 3.15 D).

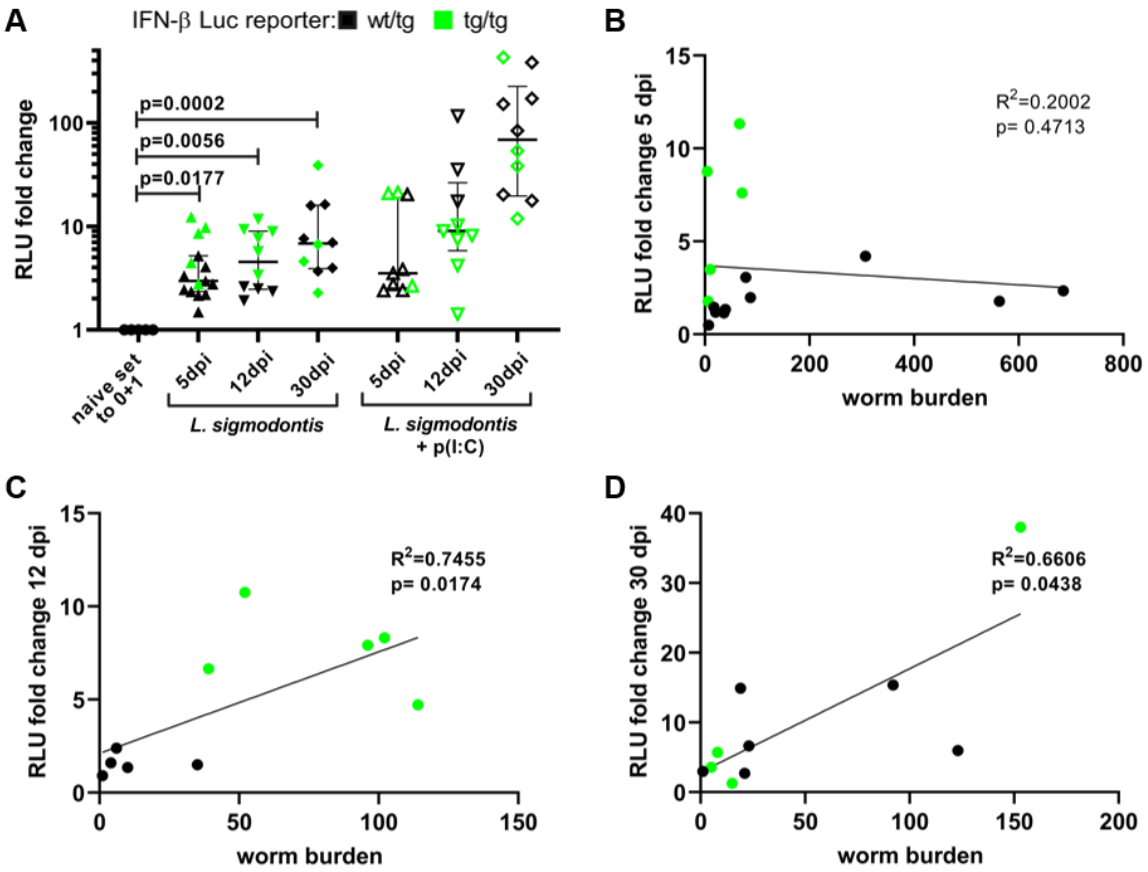

Figure 3.15 | IFN-β production in pleura cells positively correlates with *L. sigmodontis* worm burden and infection duration. (A-D) Pleura cells were isolated from naïve and *L. sigmodontis*-infected albino C57BL/6 IFN-β luciferase reporter animals on 5, 12 and 30 dpi and IFN-β production was measured. IFN-β production calculated as fold change based on the average RLU of naïve control animals **(A)** 5, 12 and 30 dpi with or without additional p(I:C) stimulation. Correlation of RLU fold change and worm burden per animal on **(B)** 5 dpi, **(C)** 12 dpi and **(D)** 30 dpi. **(A)** Error bars show median with IQR. Data were statistically analyzed using Kruskal-Wallis with Dunn's post-hoc test. **(B-D)** The calculated RLU fold change of each animal was plotted against the worm burden in the pleural cavity. Spearman correlation was computed and the linear regression line is shown. **(A-D)** Data from 5 dpi are pooled from 3 and data from 12 dpi and 30 dpi are pooled from 2 individual experiments, after failing Spearman's rank correlation test for heteroscedasticity. dpi: days post infection, p(I:C): poly(I:C), RLU: relative light unit.

3.3 Natural *Litomosoides sigmodontis* infection in nucleic acid receptor-deficient mice

The activation of nucleic acids receptors is known to result in type I IFN responses. Since the analysis of IFN-β reporter mice revealed an *in vivo* release of IFN-β in response to *L. sigmodontis* infection, it was of interest whether the lack of nucleic acid sensors has an impact on infection.

We hypothesized that the lack of nucleic acids receptors hampers larval recognition and elimination by the immune system upon infection. Therefore, a higher number of larvae would reach the pleural cavity in knockout animals.

In order to test this hypothesis MDA5$^{-/-}$ (C57BL/6), TLR7$^{-/-}$ (C57BL/6), TLR9$^{-/-}$ (C57BL/6) and STING$^{-/-}$ (C57BL/6) mice were naturally infected with *L. sigmodontis* and the worm count in the pleural cavity was determined 14 dpi (Figure 3.16). Since the knockout of RIG-I results in retarded animals that do not survive for more than 3 weeks after birth (239), RIG-I$^{-/-}$ animals were not included in this experiment. On day 14 post infection there was no significant difference in the worm burden between the different genotypes.

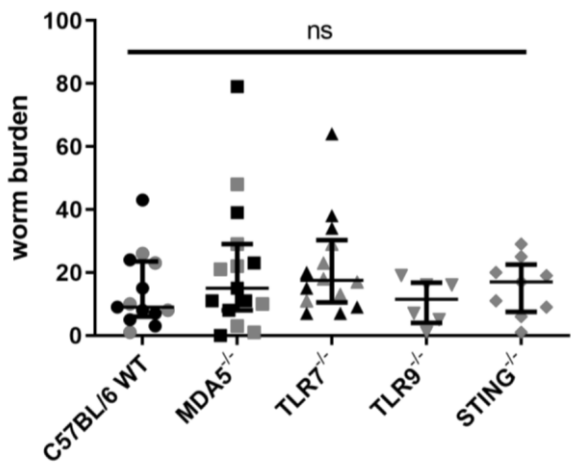

Figure 3.16| Nucleic acids receptor knockout animals have an unchanged *L. sigmodontis* worm burden.
L. sigmodontis larvae isolated from the pleura cavity of mice 14 days after infection and quantified. Error bars show median with IQR. Data were statistically analyzed using Kruskal-Wallis with Dunn's post-hoc test. Data for C57BL/6 WT, MDA5$^{-/-}$, and TLR7$^{-/-}$ mice are pooled from 2 individual experiments presented in black and grey. n=6-15.

Regarding immunological analysis, in two individual experiments the level of IL-5, IL-6, IL-10 and IFN-γ in the pleural cavity of all animals were under the detection limit of the ELISA (not shown).

Pleural cell populations were analyzed by flow cytometry and gated as shown in Figure 3.17.

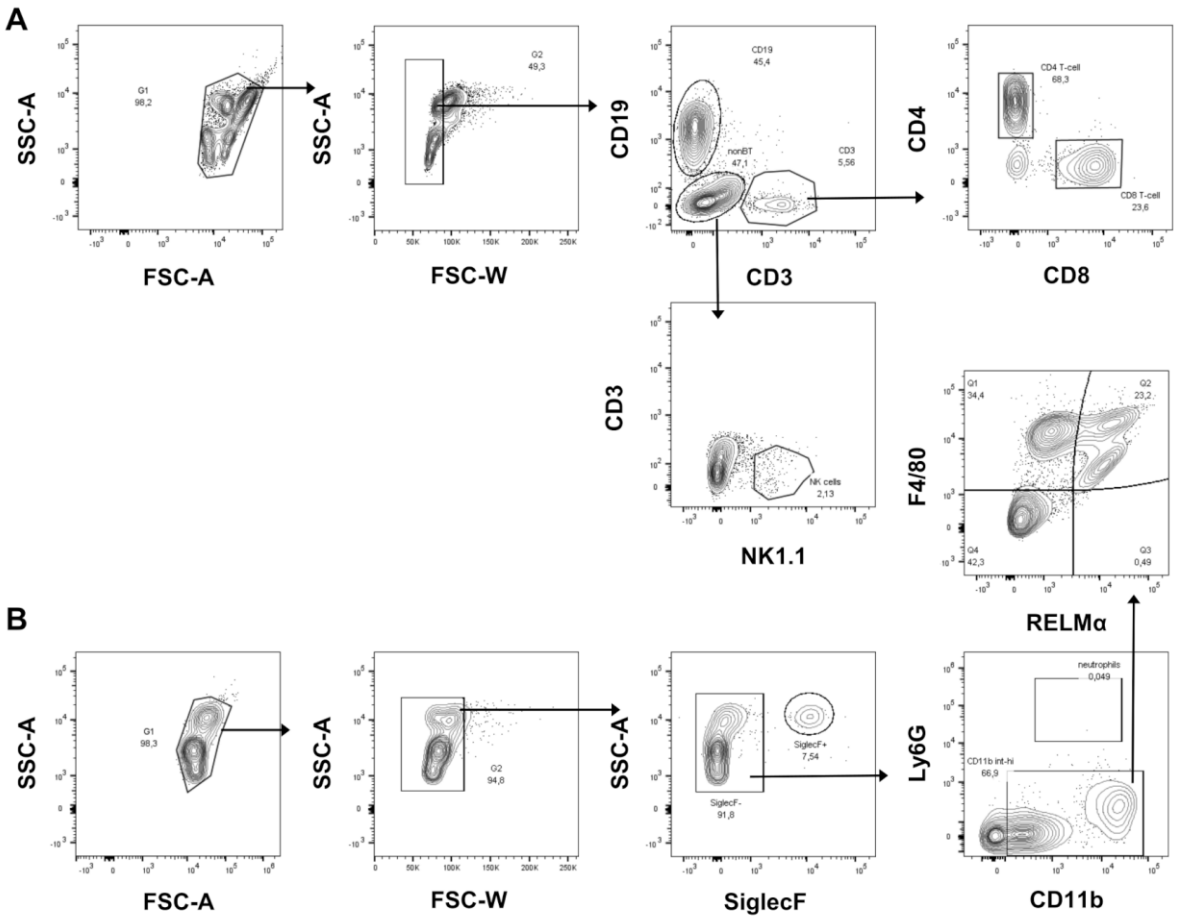

Figure 3.17| Gating strategy for analysis of murine pleura cells by flow cytometry.

Overall, there was no significant difference in the cell composition between naïve wild-type (WT) and naïve MDA5$^{-/-}$ mice (Figure 3.18). The total number of cells in the pleural cavity was similar in all infected animals (Figure 3.18 A). Since pooled flow cytometry data from two experiments cluster into two groups, a color code was used. Upon *L. sigmodontis* infection there were no genotype-dependent significant differences in the counts of CD4$^+$ T cells, CD8$^+$ T cells, B cells, NK cells, F4/80$^+$RELMα$^-$ cells, alternatively activated macrophages (AAM) (F4/80$^+$RELMα$^+$), neutrophils and eosinophils (Figure 3.18 B – I).

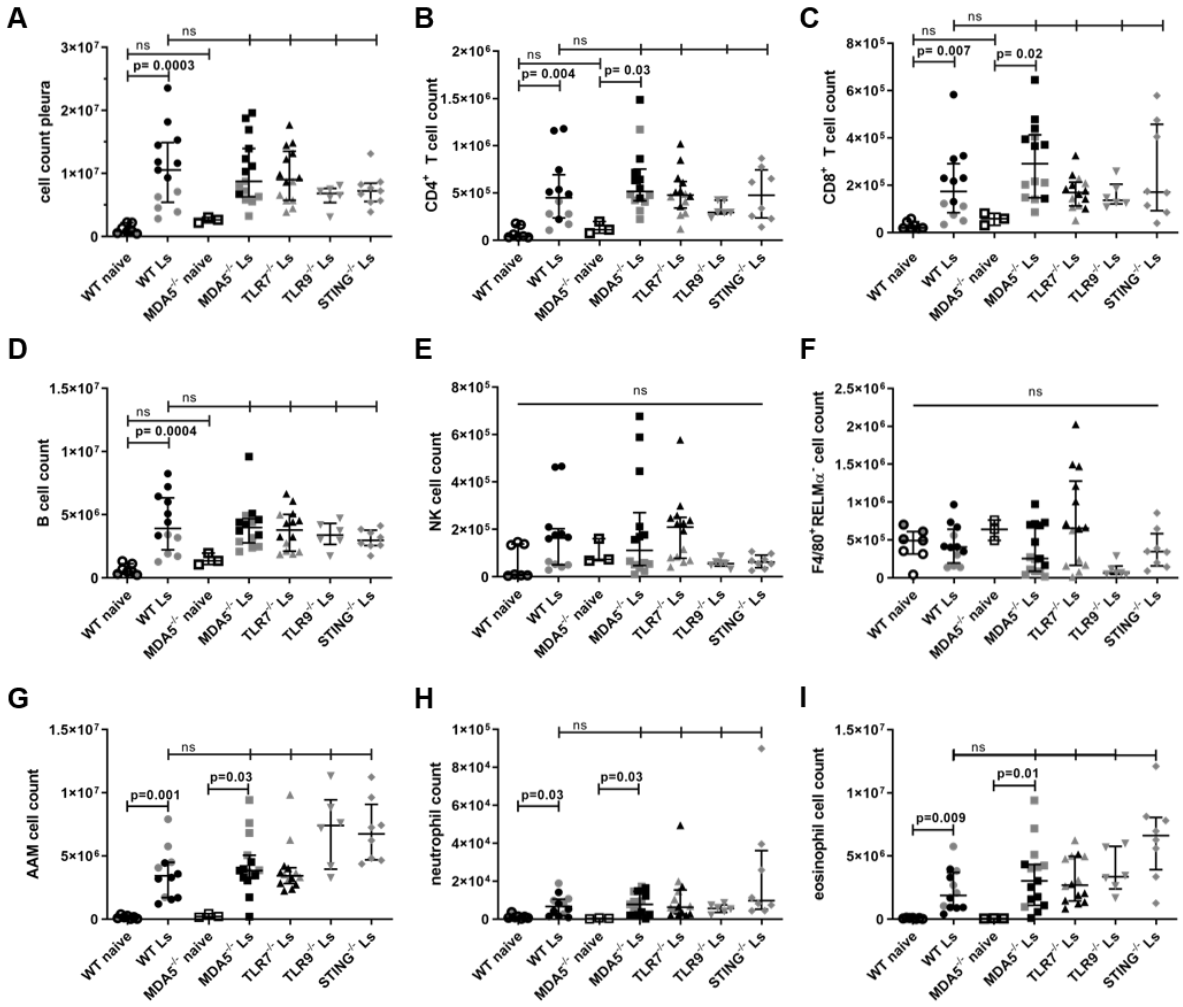

Figure 3.18| Cellular composition in the pleural cavity 14 days after *L. sigmodontis* infection. Wild-type (WT), MDA5$^{-/-}$, TLR7$^{-/-}$, TLR9$^{-/-}$ and STING$^{-/-}$ mice were naturally infected with *L. sigmodontis*, pleura cells were isolated 14 days after the infection **(A-I)** and analyzed by flow cytometry **(B-I)**. **(A)** Total pleura cell count. Total cell counts of **(B)** CD4$^+$ T cells (CD19$^-$ CD3$^+$CD4$^+$CD8$^-$), **(C)** CD8+ T cells (CD19$^-$CD3$^+$CD4$^-$CD8$^+$), **(D)** B cells (CD19$^+$CD3$^-$), **(E)** NK cells (CD19$^-$CD3$^-$NK1.1$^+$), **(F)** F4/80$^+$RELMα$^-$ macrophages (SiglecF$^-$Ly6G$^-$ CD11b$^+$F4/80$^+$RELMα$^-$), **(G)** alternatively activated macrophages (AAM) (SiglecF$^-$Ly6G$^-$ CD11b$^+$F4/80+RELMα$^+$), **(H)** neutrophils (SiglecF$^-$Ly6G$^+$CD11b$^+$) and **(I)** eosinophils (SiglecF$^+$). **(A-I)** Error bars show median with IQR. Data were statistically analyzed using Kruskal-Wallis with Dunn's post-hoc test. Data on TLR9$^{-/-}$ and STING$^{-/-}$ were statistically analyzed in comparison to WT data from the same experiment, not to the pooled WT data. Data for C57BL/6 WT, MDA5$^{-/-}$, and TLR7$^{-/-}$ mice are pooled from 2 individual experiments. Data of one experiment are presented in black, from the other in grey. N=3-15. Ls: *L. sigmodontis.*

Next to analyzing pleural cell populations, the activation status of the immune cells was assessed. Upon *L. sigmodontis* infection the CD4$^+$ T cells and CD8$^+$ T cells of all mice showed reduced CTLA-4 expression, independent of the genotype (Figure 3.19 A + B). The CD80 expression of B cells was not significantly altered (Figure 3.19 C). The

CTLA-4expression of NK cells was significantly increased in *L. sigmodontis*-infected WT mice and *L. sigmodontis* infected TLR9$^{-/-}$ mice compared to naïve WT mice (Figure 23.19 D). F4/80^{+}RELMα^{-} cells significantly increased their expression of I-Ab upon infection with *L. sigmodontis* in TLR7$^{-/-}$ mice and STING$^{-/-}$ mice compared to naïve WT mice (Figure 3.19 E). In STING$^{-/-}$ mice the increase in I-Ab expression was also significant compared to *L. sigmodontis*-infected WT mice (Figure 3.19 E). The expression of I-Ab on AAMs was significantly upregulated in infected STING$^{-/-}$ mice compared to infected WT mice (Figure 3.19 F). The expression of I-Ab on neutrophils was significantly increased in all *L. sigmodontis*-infected knock out animals, but not infected WT animals, compared to naïve WT animals (Figure 3.19 G). At the same time the expression on eosinophils was downregulated upon *L. sigmodontis* infection (Figure 3.19 H). This was significant in infected WT and infected TLR7$^{-/-}$ mice compared to naïve WT mice.

Overall, the infection with *L. sigmodontis* affected the activation status of T cells, NK cells macrophages and eosinophils. However, there was a minor impact of the single MDA5, TLR3, TLR7, TLR9 or STING deficiency on the activation of pleural cells 14 days after *L. sigmodontis* infection.

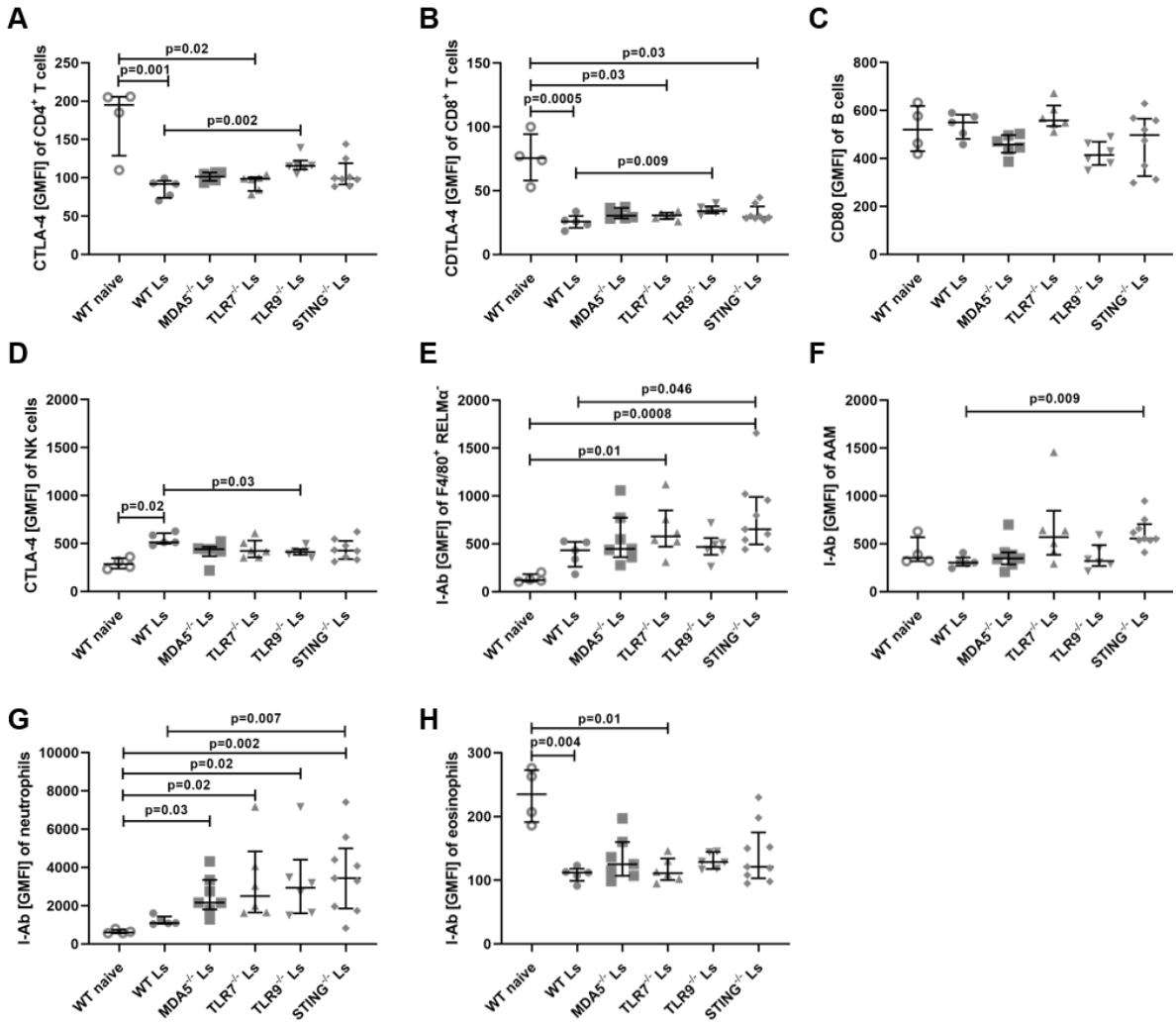

Figure 3.19| Cellular composition in the pleural cavity 14 days after *L. sigmodontis* infection. Wild-type (WT), MDA5$^{-/-}$, TLR7$^{-/-}$, TLR9$^{-/-}$ and STING$^{-/-}$ mice were naturally infected with *L. sigmodontis* (Ls), pleura cells were isolated 14 days after the infection and analyzed by flow cytometry **(A-H)**. CTLA-4 expression of **(A)** CD4$^+$ T cells (CD19$^-$ CD3$^+$CD4$^+$CD8$^-$) and **(B)** CD8$^+$ T cells (CD19$^-$CD3$^+$CD4$^-$CD8$^+$). **(C)** CD80 expression of B cells (CD19$^+$CD3$^-$). **(D)** CTLA-4 expression of NK cells (CD19$^-$CD3$^-$NK1.1$^+$). I-Ab expression of **(E)** F4/80$^+$RELMα$^-$ macrophages (SiglecF$^-$Ly6G$^-$CD11b$^+$F4/80$^+$RELMα$^-$), **(F)** alternatively activated macrophages (AAM) (SiglecF$^-$Ly6G$^-$CD11b$^+$F4/80$^+$RELMα$^+$), **(G)** neutrophils (SiglecF$^-$Ly6G$^+$CD11b$^+$) and **(H)** eosinophils (SiglecF$^+$). **(A-H)** Error bars show median with IQR. Data were statistically analyzed using Kruskal-Wallis with Dunn's post-hoc test. Except for the analysis of NK cells, the data on WT naïve, WT Ls, MDA5$^{-/-}$ Ls and TLR7$^{-/-}$ Ls are representative for 2 individual experiments. n=3-9. Ls: *L. sigmodontis*

In order to assess peripheral responses to the *L. sigmodontis* infection, splenocytes were restimulated with *L. sigmodontis* antigen (LsAg) in an *in vitro* culture and IL-5 was quantified by ELISA (Figure 3.20). Unstimulated splenocytes of all animals did not

release IL-5. Stimulation with concanavalin A (ConA) induced IL-5 release by cells from all animals, but the cytokine release was stronger for cells isolated from infected animals compared to cells from naïve animals. The restimulation with LsAg did not induce IL-5 release by cells from naïve animals, while cells of all infected animals responded with comparable IL-5 release independent of the genetic background.

Overall, we did not observe an influence of a single nucleic acid receptor knockout on the early phase of *L. sigmodontis* infection.

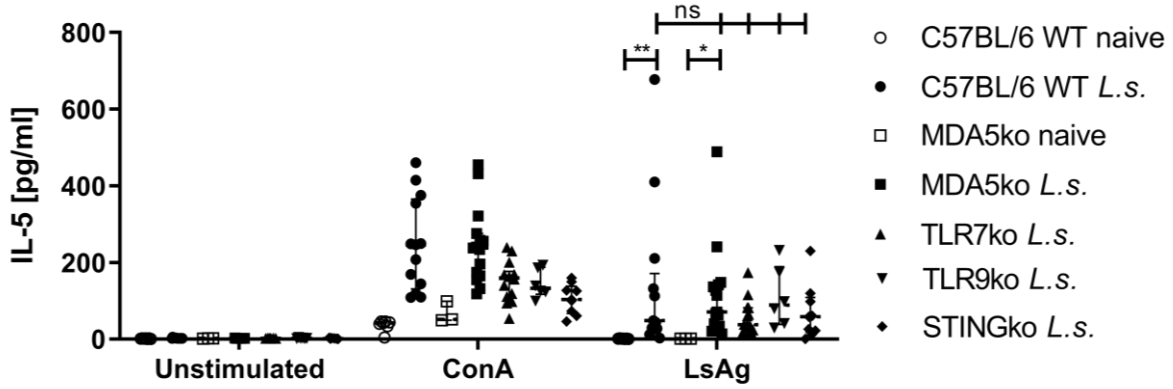

Figure 3.20| Splenic IL-5 production in restimulated splenocytes isolated 14 days after *L. sigmodontis* infection. Splenocytes were isolated from wild-type (WT), MDA5$^{-/-}$, TLR7$^{-/-}$, TLR9$^{-/-}$ and STING$^{-/-}$ mice 14 days after the natural infection with *L. sigmodontis*. Cells were stimulated with 2.5µg/mL ConA or 25µg/mL *L. sigmodontis* antigen (LsAg) and cultured for 72h. IL-5 was quantified in the supernatant by ELISA. Error bars show median with IQR. LsAg data were statistically analyzed using Kruskal-Wallis with Dunn's post-hoc test. Data for C57BL/6 WT, MDA5$^{-/-}$, and TLR7$^{-/-}$ mice are pooled from 2 individual experiments. Data of one experiment are presented in black, from the other in grey. n=3-15, *p=0.02, **p=0.001. ConA: Concanavalin A, *L.s.*: *L. sigmodontis*, LsAg: *L. sigmodontis* antigen.

3.4 Enhanced local immune response after subcutaneous injection of nucleic acid receptor agonists

After observing no impact on the larval migration and survival in mice deficient for a single nucleic acid receptor (Figure 3.16), we were interested whether the activation of these pathways would impact larval survival. There was only little *in vivo* IFN-β detected in the pleural cavity in the presence of L3 larvae on day five after infection, but increased levels occured during later stages of infection (Figure 3.15 A). Therefore, we hypothesized that the early activation of nucleic acid receptors and subsequent type I IFN production might improve vaccination efficacy in the *L. sigmodontis* model by combining irradiation attenuated L3 larvae with nucleic acid receptor agonists.

3.4.1 Screening for most promising agonists

Prior to vaccination experiments the impact of nucleic acid receptor agonists on the local milieu after subcutaneous injection was analyzed in form of a pre-screening to identify the most promising agonists.

To that end BALB/c mice were subcutaneously injected with *L. sigmodontis* L3 larvae, LsAg or various nucleic acid receptor agonists (Figure 3.21). Four hours after injection the local responses in the skin and systemic responses in the blood were analyzed. Agonists that target endosomal as well as cytosolic RNA and DNA sensors were chosen. Naked poly(I:C) dominantly targets the endosomal RNA receptor TLR3, but can also trigger the cytosolic RNA sensors RIG-I and MDA5. 3pRNA is a specific RIG-I ligand. R848 targets the endosomal RNA sensors TLR7/8. CpGC ODN2395 targets the endosomal DNA sensor TLR9 and 2'3'cGAMP activates the adaptor molecule STING, which is involved in cytosolic DNA recognition.

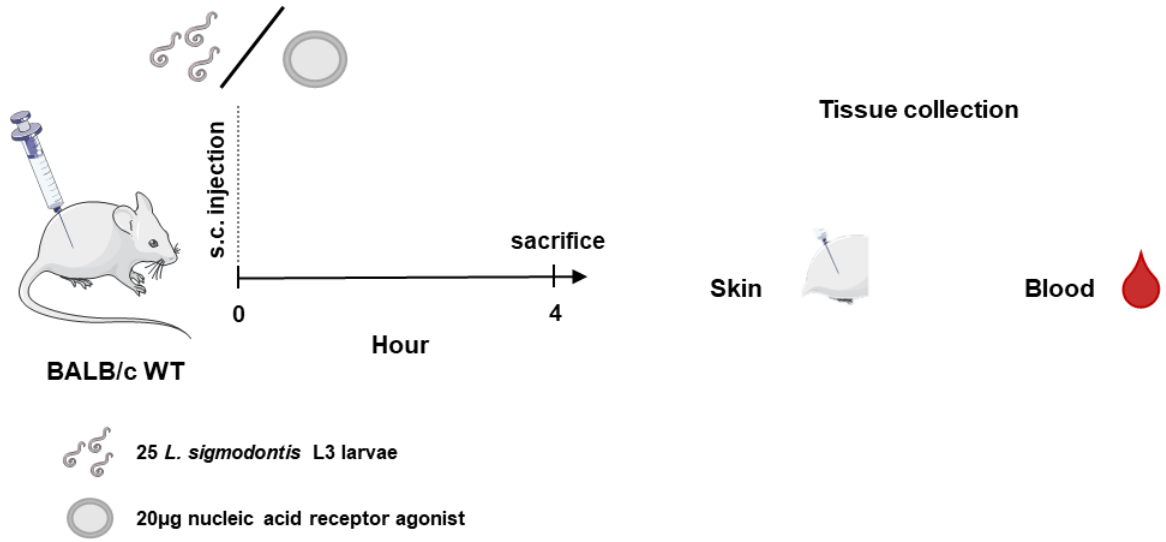

Figure 3.21| Experimental setup of the screening for potential immunization adjuvants.

Local immune responses in the skin were analyzed by flow cytometry. Cells were gated as shown in Figure 3.22 and the expression of MHC class II (I-Ab) and co-stimulatory CD86 was assessed as marker for cell activation.

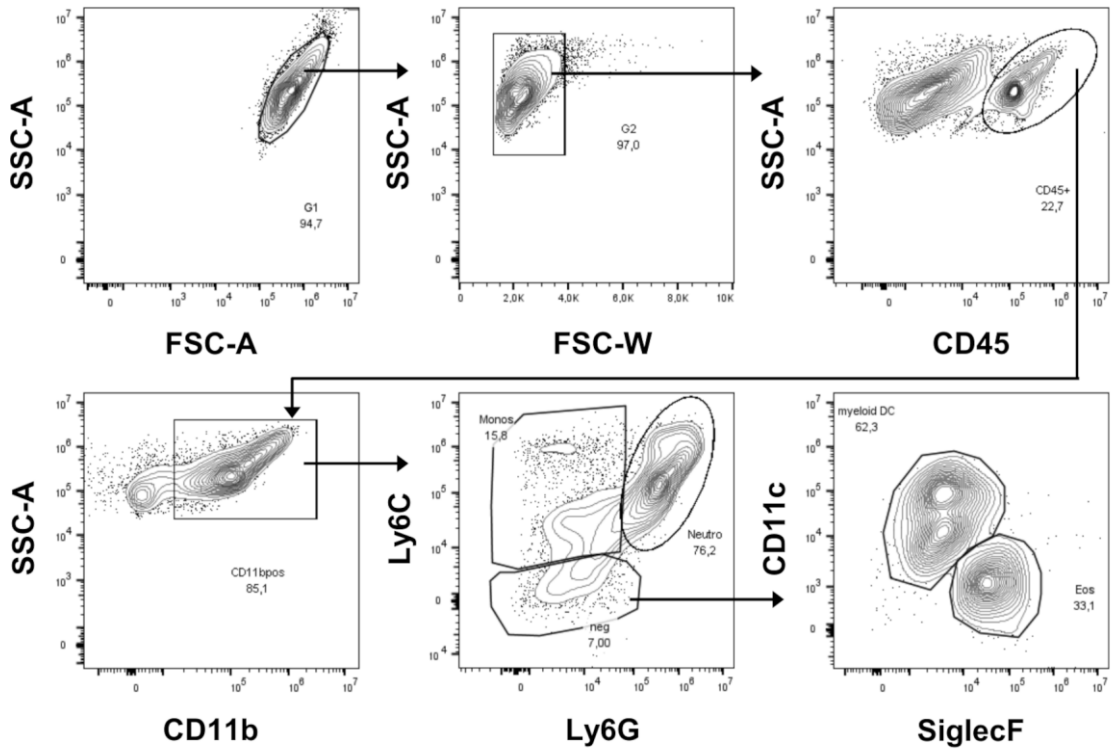

Figure 3.22| Gating strategy for flow cytometric analysis of the skin. Leukocytes were identified by the expression of CD45. Among the leukocytes, myeloid cells were gated as CD11b$^+$. Myeloid subsets were gated by expression of Ly6C on monocytes, Ly6G on neutrophils, CD11c on dendritic cells and SiglecF on eosinophils. Fluorescence minus one (FMO) controls were applied for gating.

The injection of LsAg and *L. sigmodontis* L3 larvae had no impact on the frequency of CD11b$^+$ cells or their expression of I-Ab and CD86 (Figure 3.23 A – C). In response to the injection of any agonist there was a wide range within each group. Upon injection of the TLR7/8 agonist R848 and the TLR9 agonist CpGC ODN2395 the frequency of CD11b$^+$ cells roughly doubled and increased even further after injection of the TLR3 agonist naked poly(I:C) and the RIG-I agonist 3pRNA (Figure 3.23 A). Only the injection of the STING agonist 2'3'cGAMP induced a significant increase in the frequency of CD11b$^+$ cells compared to the control group (p=0.01) and the injection of *L. sigmodontis* L3 larvae (p=0.02). Likely due to the limited sample size, no significant impact on the expression of I-Ab and CD86 by any agonist was observed (Figure 3.23 B + C). After the injection of 3pRNA the expression of I-Ab and CD86 was lower than in the control group.

Next, the frequency and activation of different myeloid cells among the CD11b$^+$ cell population was analyzed. LsAg and *L. sigmodontis* L3 larvae had a minor impact on

monocyte and neutrophil frequencies (Figure 3.23 D + G). In contrast, the injection of most agonists induced a reduction on monocyte frequencies accompanied by an increased frequency of neutrophils. This effect was strongest after the injection of 3pRNA and was significant compared to the injection with L3 larvae (monocytes: p=0.004, neutrophils: p=0.006). There was no significant impact on the expression of I-Ab and CD86 on monocytes and neutrophils (Figure 3.23 E – F + H – I). The overall pattern is similar to the expression on all $CD11b^+$ cells (Figure 3.23 B + C).

The impact of any injection on the frequency of DCs and eosinophils was not significant and varied strongly within each group (Figure 3.23 J + M). Regarding the activation of DCs there was no significant impact on I-Ab expression (Figure 3.23 K). But compared to the injection with L3 larvae, there was a significant increase of CD86 expression after the injection of 3pRNA (p=0.02) or 2'3'cGAMP (p=0.003) (Figure 3.23 L). The expression of I-Ab on eosinophils appeared higher after the injection of agonists, but this was only significant after the injection of 2'3'cGAMP compared to the control group (p=0.002) (Figure 3.23 N). The expression of CD86 on eosinophils was not significantly altered, but was highest after the injection of 2'3'cGAMP (Figure 3.23 O). The overall pattern of CD86 on eosinophils was similar to the expression on all $CD11b^+$ cells (Figure 3.23 C).

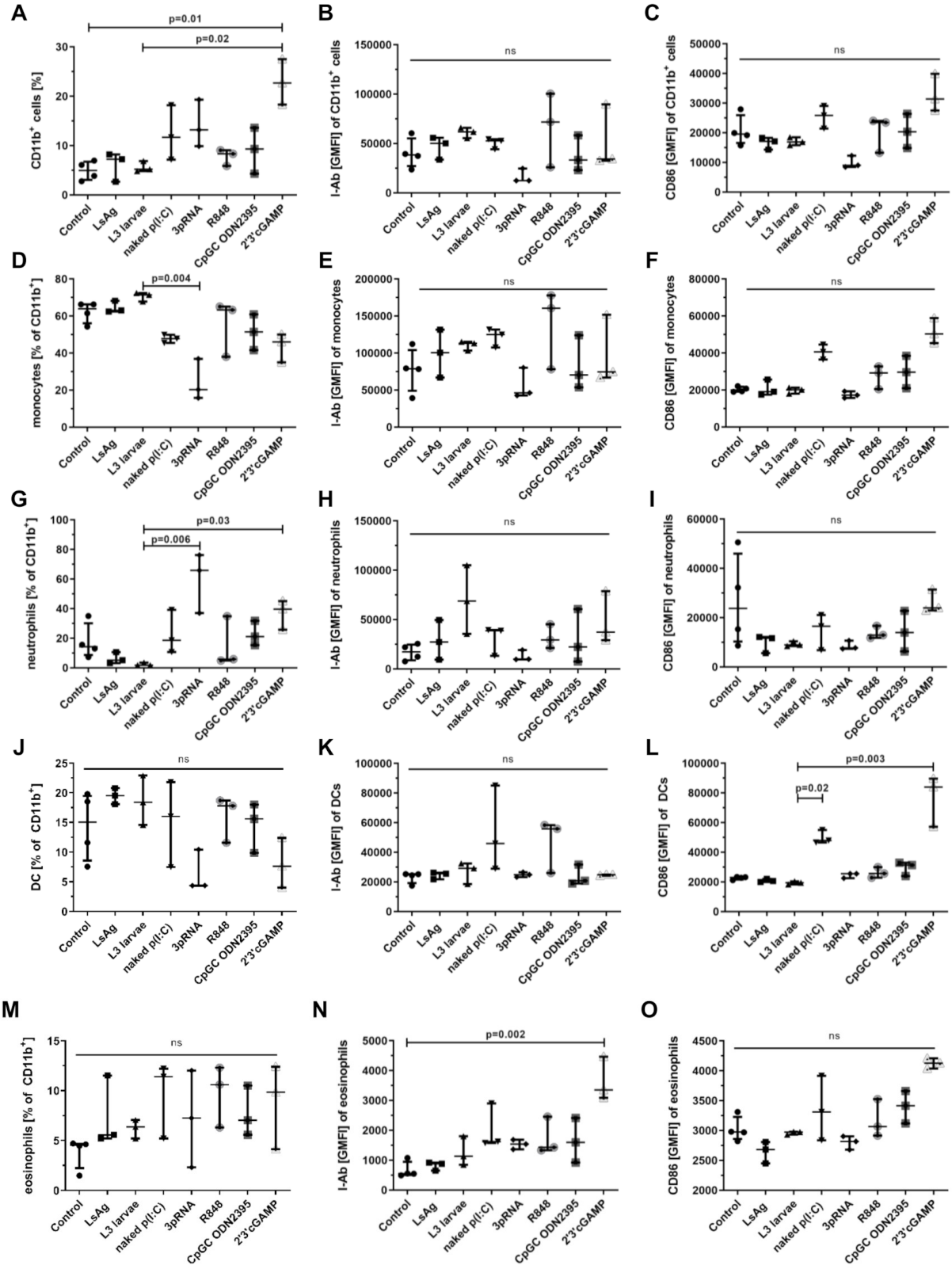

Figure 3.23| Cell composition and activation of murine skin cells in response to different stimuli.

Continued on next page.

(A-O) Mice were injected with 25 *L. sigmodontis* L3 larvae or 20µg of LsAg, naked poly(I:C) (p(I:C)), 3pRNA, R848, CpGC ODN2395 or 2'3'cGAMP. 3pRNA was complexed with *in vivo*-jetPEI®. Skin cells were isolated after 4h and analyzed by flow cytometry. Frequency of **(A)** $CD11b^+$ cells ($CD45^+CD11b^+$) of all leukocytes, **(D)** monocytes ($CD45^+CD11b^+Ly6C^+Ly6G^-$) of $CD11b^+$ cells, **(G)** neutrophils ($CD45^+CD11b^+Ly6G^+$) of $CD11b^+$ cells, **(J)** dendritic cells (DC) ($CD45^+CD11b^+Ly6C^-Ly6G^-CD11c^+SiglecF^-$) of $CD11b^+$ cells and **(M)** eosinophils ($CD45^+CD11b^+Ly6C^-Ly6G^-CD11c^-SiglecF^+$) of $CD11b^+$ cells. Expression of I-Ab on **(B)** $CD11b^+$ cells, **(E)** monocytes, **(H)** neutrophils, **(K)** DCs and **(N)** eosinophils. Expression of CD86 on **(C)** $CD11b^+$ cells, **(F)** monocytes, **(I)** neutrophils, **(L)** DCs and **(O)** eosinophils. Error bars show median with IQR. Data were statistically analyzed by Kruskal-Wallis with Dunn's post-test. n=3.
p(I:C): poly (I:C)

Besides the analysis of cell frequencies in the skin and their expression of molecules needed for antigen presentation, their inflammatory response was analyzed by RT-PCR (Figure 3.24 A + B). On the one hand, IFN-β as a typical marker for nucleic acid pathway activation was assessed (Figure 3.24 A). The injection of LsAg, L3 larvae, TLR7/8 agonist R848 and the TLR9 agonist CpGC ODN2395 did not impact the expression of IFN-β. An increased expression of IFN-β was observed after injection of naked poly(I:C) ($p=0.17$), RIG-I ligand 3pRNA ($p=0.03$) and the STING ligand 2'3'cGAMP ($p=0.03$). Next the IFN-γ induced chemokine IP-10 was assessed, which attracts DCs, macrophages, NK cells and T cells and is associated with inflammation (240) (Figure 3.24 B). The injection of LsAg and L3 larvae did not impact the expression of IP-10. The injection of 3pRNA, R848 and CpGC ODN2395 resulted in increased IP-10 expression, but the increase was not significant. The IP-10 expression in skin cells was significantly upregulated after injection of naked poly(I:C) ($p=0.02$) and 2'3'cGAMP ($p=0.02$).
Systemic immune responses to the local agonist injection were assessed by IP-10 quantification in the serum by ELISA (Figure 3.24 C). The injection of LsAg, L3 larvae, 3pRNA and CpGC ODN2395 did not induce a systemic IP-10 response, while the injection of naked poly(I:C), R848 and 2'3'cGAMP increased IP-10 systemically.

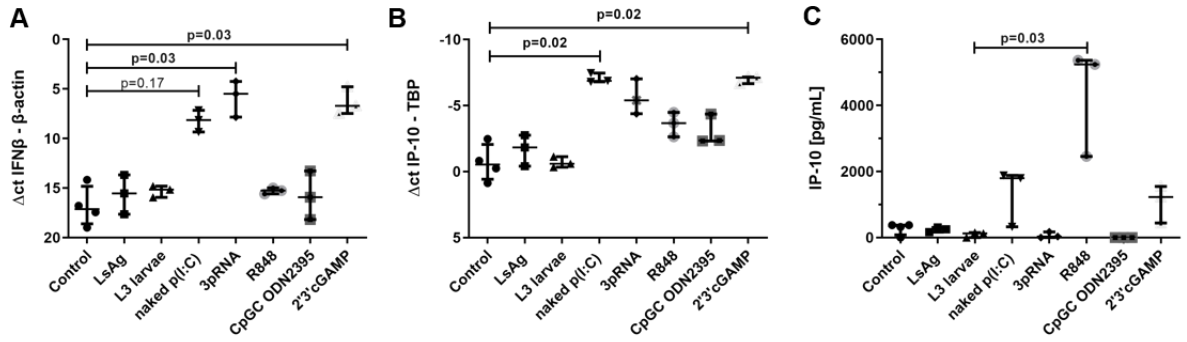

Figure 3.24| Local and systemic cytokine and chemokine response to different stimuli. **(A-C)** Mice were injected with 25 *L. sigmodontis* L3 larvae or 20µg of LsAg, naked poly(I:C) (p(I:C), 3pRNA, R848, CpGC ODN2395 or 2'3'cGAMP. 3pRNA was complexed with *in vivo*-jetPEI®. **(A+B)** Skin cells were isolated after 4h and analyzed by RT-PCR. Δct values of **(A)** IFN-β expression based on β-actin level and **(B)** IP-10 expression based on TBP level in the corresponding sample. **(C)** Serum concentration of IP-10 was quantified by ELISA. Error bars show median with IQR. Data were statistically analyzed by Kruskal-Wallis with Dunn's post-test. n=3. p(I:C): poly(I:C)

The relative responses to the injection of agonists that were presented in Figures 3.23 and Figure 3.24 are summarized in Table 3.1 in order to narrow down further analysis to the use of two agonists. Due to little effects, LsAg and CpGC ODN2395 were eliminated from further analysis. R848 was excluded due to a strong systemic but mild local response. 2'3'cGAMP was eliminated despite promising local effects due to the development of splenomegaly in a long-term experiment (not shown). Concluding poly(I:C) and 3pRNA were chosen for more detailed analysis (Table 3.1).

Table 3.1| Summary of local and systemic immune responses to potential adjuvants.

Injection	Target	Leukocyte recruitment	CD86 expression	Local IFN-β response	Local IP-10 response	Systemic IP-10 response
LsAg		/	/	(+)	(+)	/
L3 larvae		/	/	(+)	/	/
Naked Poly(I:C)	TLR3	++	+	++	+++	+
3pRNA	RIG-I	++	/	+++	++	/
R848	TRL7/8	(+)	+	+	+	+++
CpGC ODN 2395	TLR9	(+)	+	(+)	+	/
2'3'cGAMP	STING	+++	++	+++	+++	+

3.4.2 Local and systemic immune responses in skin 4h after single immunization injection

After a pre-screening, poly(I:C) and 3pRNA were chosen for a more detailed analysis. The injection mode of poly(I:C) was adjusted. Instead of using naked poly(I:C), the agonist was transfected in order to target cytosolic RNA receptors. As depicted in Figure 3.25, WT BALB/c mice received a subcutaneous injection of attenuated L3 larvae in combination with the chosen nucleic acid receptor agonists. Four hours post injection systemic responses in the blood and local responses in the skin were analyzed.

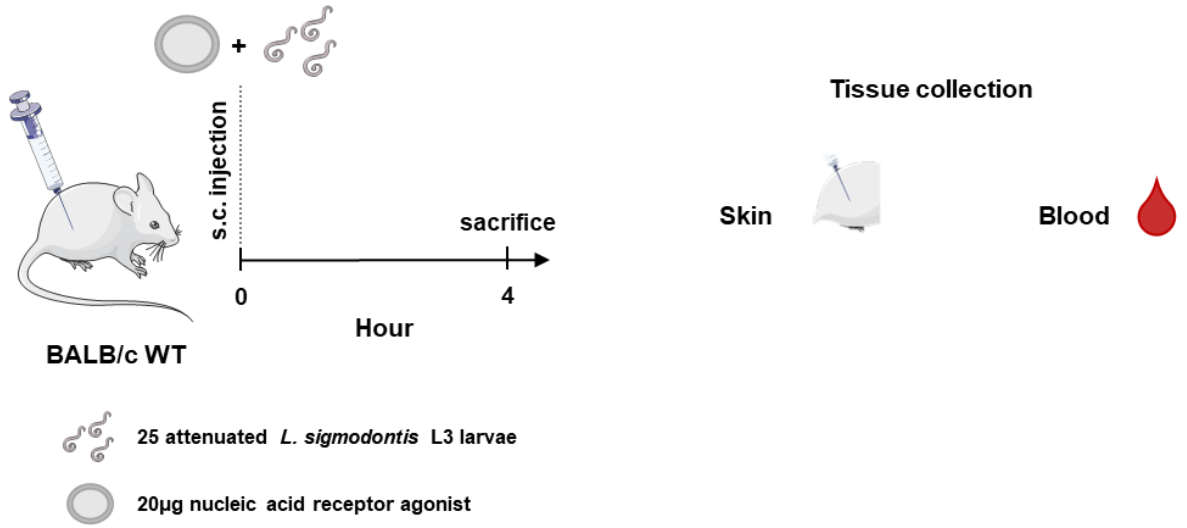

Figure 3.25| Experimental setup for studying local immune responses to immunization with transfected poly(I:C) and 3pRNA in combination with attenuated L3 larvae.

The local cell populations in the skin were analyzed by flow cytometry (Figure 3.26). The cells were gated according to Figure 3.22.

Four hours after the injection the median frequency of $CD11b^+$ cells in the skin was lowest in control animals (Figure 3.26 A). Upon injection of att. L3 larvae alone, a wide range of $CD11b^+$ cell frequencies was detected, but the median was higher for the att. L3 larvae group compared to the median of the control group. The combination of att. L3 larvae and the agonists trans. poly(I:C) or 3pRNA resulted both in a higher median $CD11b^+$ cell frequencies compared to the control group or the injection of att. L3 larvae alone. Due to a high variance among the individual animals, the increases were not significant. The expression of I-Ab and CD86 on $CD11b^+$ cells was significantly decreased after the injection of att. L3 larvae and trans. poly(I:C) or att. L3 larvae and

3pRNA compared to the expression in control animals (Figure 3.26 B + C). The I-Ab expression was also significantly decreased upon agonist administration in comparison to the treatment with att. L3 larvae alone (Figure 3.26 B). In case of CD86 only the addition of trans. poly(I:C) resulted in significantly reduced expression compared to the injection of att. L3 larvae alone. Among the $CD11b^+$ cells there was a significant reduction in monocytes and DC frequencies upon injection of either agonist and att. L3 larvae compared to the control group and the treatment with att. L3 larvae alone (Figure 3.26 D + G). The eosinophil frequency remained stable upon the injection of att. L3, while the injection of agonist lead to a reduction in the eosinophil frequency (Figure 3.26 J). This reduction in eosinophil frequency was only significant when comparing the injection of att. L3 larvae alone or in combination with trans. poly(I:C). The decrease of those cell populations was accompanied by a significant increase in neutrophil frequency upon injection of trans. poly(I:C) or 3pRNA (Figure 3.26 M). The increase was significant in comparison to control animals, as well as to the injection of att. L3 larvae alone. The expression of I-Ab was significantly decreased on all cell types after the injection of att. L3 larvae in combination with either agonist compared to control animals (Figure 3.26 E + H + K +N). The same applies for the comparison to the treatment with att. L3 larvae alone, with the exception that on neutrophils this reduction was only significant after the use of trans. poly(I:C) as agonist (Figure 3.26 N). The expression of CD86 was significantly decreased on monocytes, eosinophils and neutrophils (Figure 3.26 F + L + O). On DCs the CD86 expression was significantly increased after the injection of att. L3 larvae and poly(I:C) when compared to control animals (Figure 3.26 I).

Overall, the frequency of neutrophils increased in response to the injection of att. L3 larvae in combination with trans. poly(I:C) or 3pRNA and the expression of I-Ab and CD86 measured as GMFI was significantly reduced in most cases in response to agonist injection.

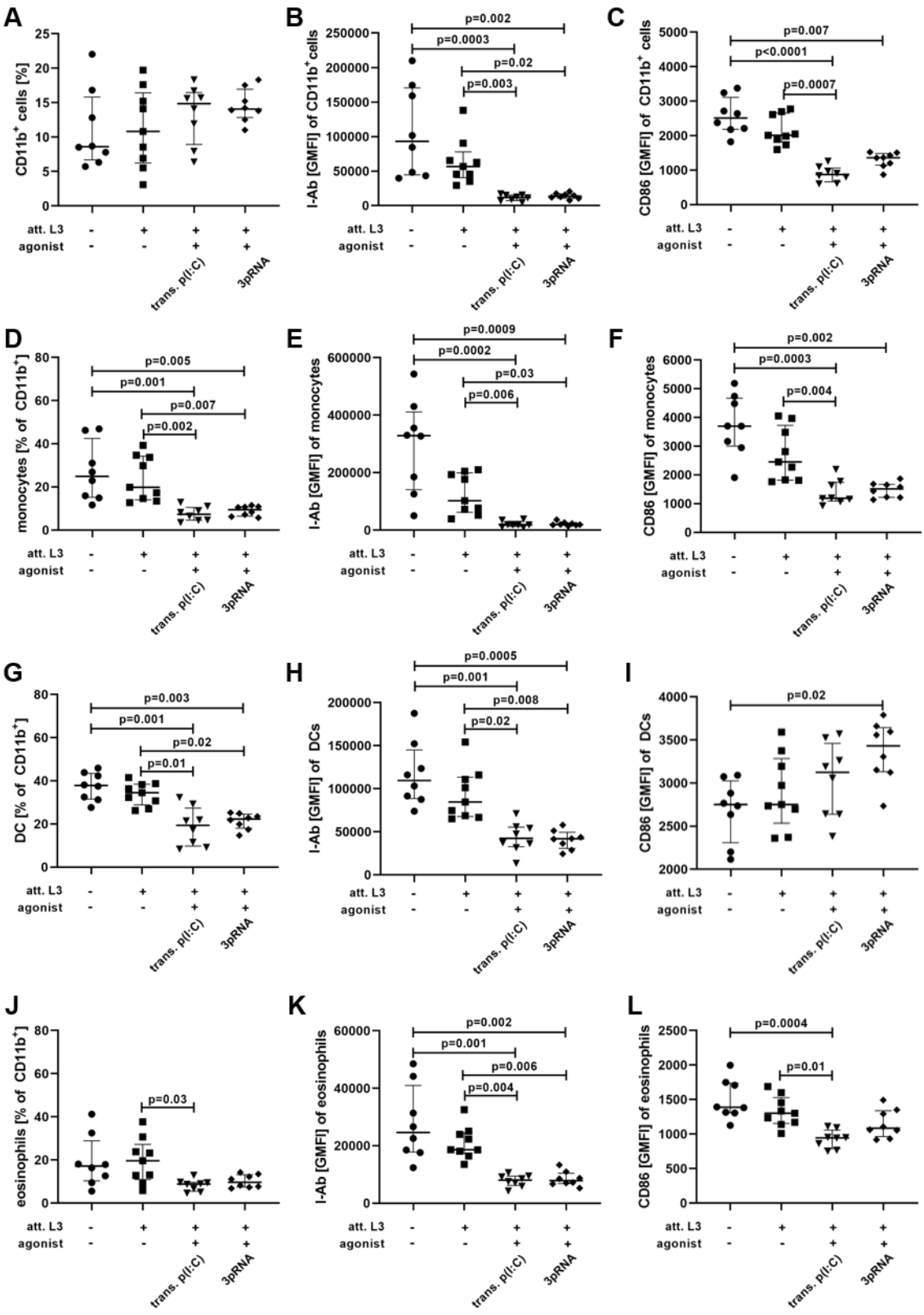

Continued on next page.

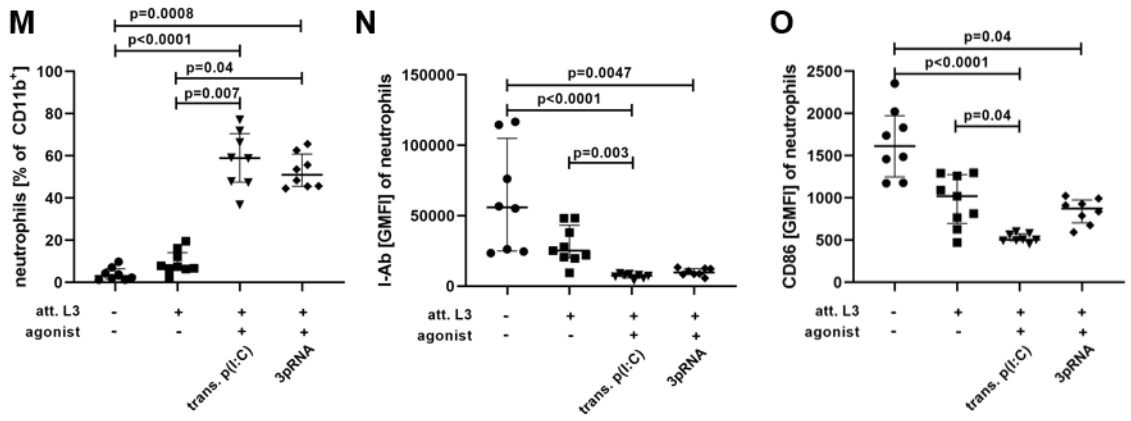

Figure 3.26| Cell composition and activation of murine skin cells in response to immunization injections. **(A-O)** Mice were injected subcutaneously with 25 irradiation attenuated (att.) *L. sigmodontis* L3 larvae with or without 20µg of agonist. 3pRNA and poly(I:C) (p(I:C)) were complexed with *in vivo*-jetPEI®. Skin cells were isolated after 4h and analyzed by flow cytometry. Frequency of **(A)** $CD11b^+$ cells ($CD45^+CD11b^+$) of all leukocytes, **(D)** monocytes ($CD45^+CD11b^+Ly6C^+Ly6G^-$) of $CD11b^+$ cells, **(G)** dendritic cells (DC) ($CD45^+CD11b^+Ly6C^-Ly6G^-CD11c^+SiglecF^-$) of $CD11b^+$ cells **(J)** eosinophils ($CD45^+CD11b^+Ly6C^-Ly6G^-CD11c^-SiglecF^+$) of $CD11b^+$ cells and **(M)** neutrophils ($CD45^+CD11b^+Ly6G^+$) of $CD11b^+$ cells. Expression of I-Ab on **(B)** $CD11b^+$ cells, **(E)** monocytes, **(H)** DCs **(K)** eosinophils and **(N)** neutrophils. Expression of CD86 on **(C)** $CD11b^+$ cells, **(F)** monocytes, **(I)** DCs, **(L)** eosinophils and **(O)** neutrophils. Error bars show median with IQR. Data were statistically analyzed by Kruskal-Wallis with Dunn's post-test. n=8
att.: attenuated, p(I:C): poly(I:C), trans.: transfected.

Next to analyzing the cell populations at the site of injection, cytokine responses were evaluated. The expression of IFN-β and IP-10 in skin cells of the injection site were relatively quantified by RT-PCR (Figure 3.27 A + B). The injection of att. L3 larvae alone did not upregulate the expression of IFN-β compared to the control group that received 0.9% NaCl. There was a significant increase in expression of IFN-β as response to the injection of trans. poly(I:C) (p=0.03) as well as 3pRNA (p=0.001) (Figure 3.27 A). In case of 3pRNA this was also significant compared to the injection with att. L3 larvae alone (p=0.008). A similar pattern was observed for IP-10, where the expression was significantly upregulated as a response to 3pRNA compared to the control group (p=0.0004) and att. L3 larvae alone (p=0.02) (Figure 3.27 B). The systemic immune response to the injection was assessed by quantifying circulating IP-10 in the serum. There was no significant release of IP-10 in response to any immunization injection (Figure 3.27 C).

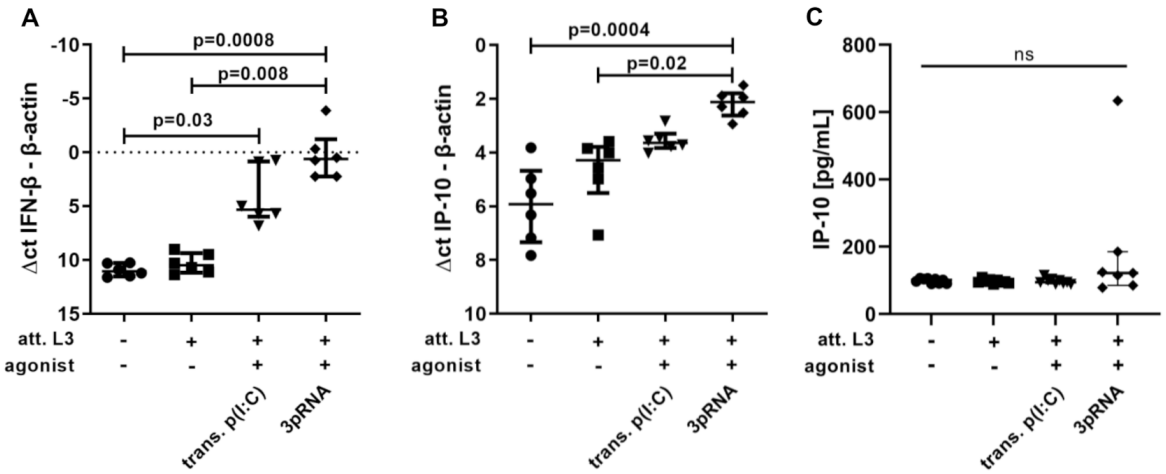

Figure 3.27| Local and systemic cytokine and chemokine response to different stimuli. **(A-C)** Mice were injected with 20µg of agonist. Poly(I:C) (p(I:C)) and 3pRNA were complexed with *in vivo*-jetPEI®. **(A+B)** Skin cells were isolated after 4h and analyzed by RT-PCR. Δct values of **(A)** IFN-β expression based on β-actin level and **(B)** IP-10 expression based on β-actin level in the corresponding sample. **(C)** Serum concentration of IP-10 were quantified by ELISA. Error bars show median with IQR. Data were statistically analyzed by Kruskal-Wallis with Dunn's post-test. (A-B) n=5-6, representative for 3 experiments. **(C)** n=7-9, data pooled from two individual experiments. p(I:C): poly(I:C), trans.: transfected

3.5 Hampered larval migration after activation of nucleic acid receptors

The analysis after the injection of att. L3 larvae with nucleic acid receptor agonists poly(I:C) and 3pRNA revealed an enhanced local immune activation. Before performing a full vaccination study, we aimed to clarify whether the early activation of nucleic acid receptors with poly(I:C) and 3pRNA also impacts larval migration during infection. We hypothesized that the activation of nucleic acid receptors, which induces the production of type I IFNs, would lead to reduced numbers of L3 larvae reaching the pleural cavity.

To test this hypothesis, BALB/c WT animals were treated according to the experimental setup presented in Figure 3.28. In brief, the mice receive a subcutaneous injection of the agonist half a day prior to the subcutaneous infection with 40 *L. sigmodontis* L3 larvae at the same site. This was followed by an intravenous injection of the same agonist half a day after infection, when larvae are migrating to the pleural cavity.

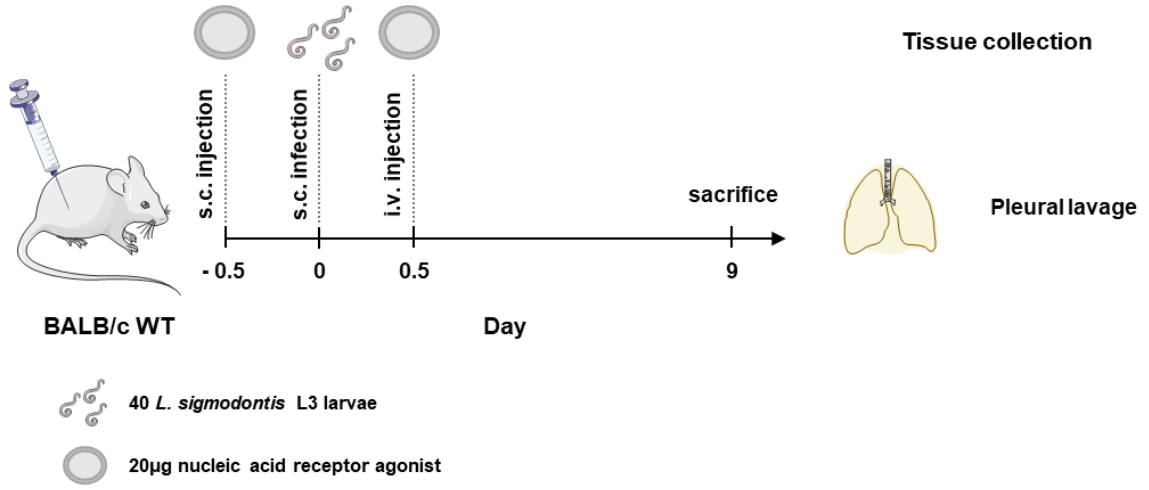

Figure 3.28| Experimental setup of the larval migration study.

The quantification of recovered worms in the pleural cavity from two different experiments is shown in Figure 3.29. To differentiate the data obtained of the two pooled experiments, the data points from the different experiments are color-coded. In control animals, on average 8.4 of the 40 injected larvae were recovered from the pleural cavity nine days after subcutaneous infection. In two out of 15 mice (13.33%) no larvae were recovered. After administration of transfected (trans.) poly(I:C), which mainly targets RIG-I and MDA5, but can also target TLR3, an average of 7.25 larvae was recovered, while four out of 16 animals were worm free (25%). The treatment with 3pRNA resulted in a significant reduction in the worm burden. There the average dropped to four larvae per animal and in seven of 16 animals (43.75%) no larvae were recovered.

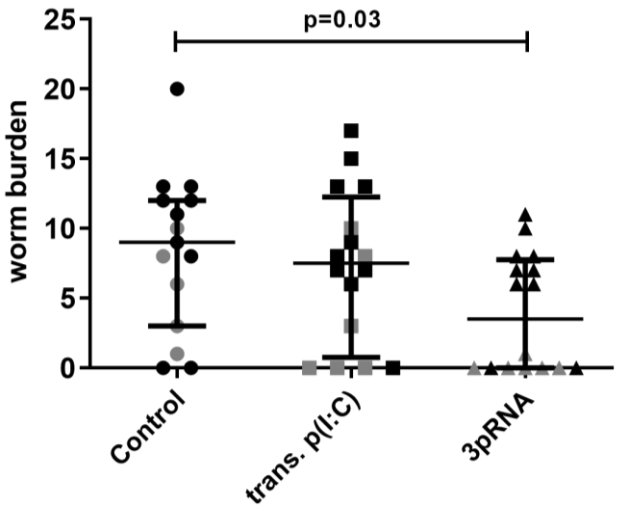

Figure 3.29| Hampered *L. sigmodontis* larval migration to the pleura after nucleic acid receptor activation. Mice were subcutaneously (s.c.) injected with 20µg poly(I:C) or 3pRNA, both complexed with *in vivo*-jetPEI®, prior to the s.c. infection with 40 *L. sigmodontis* L3 larvae and then intravenously injected with the same dose after infection. Nine days after infection, larvae were isolated from the pleural cavity and quantified. Error bars show median with IQR. Data were statistically analyzed using Kruskal-Wallis with Dunn's post-hoc test. n=15-16, data pooled from 2 individual experiments, after failing Spearman's rank correlation test for heteroscedasticity, labelled via color-code.

Next to quantifying *L. sigmodontis* larvae in the pleural cavity, the immune response in the pleural cavity on day nine after infection was assessed via flow cytometry. The gating strategy of cell populations is presented in Figure 3.30.

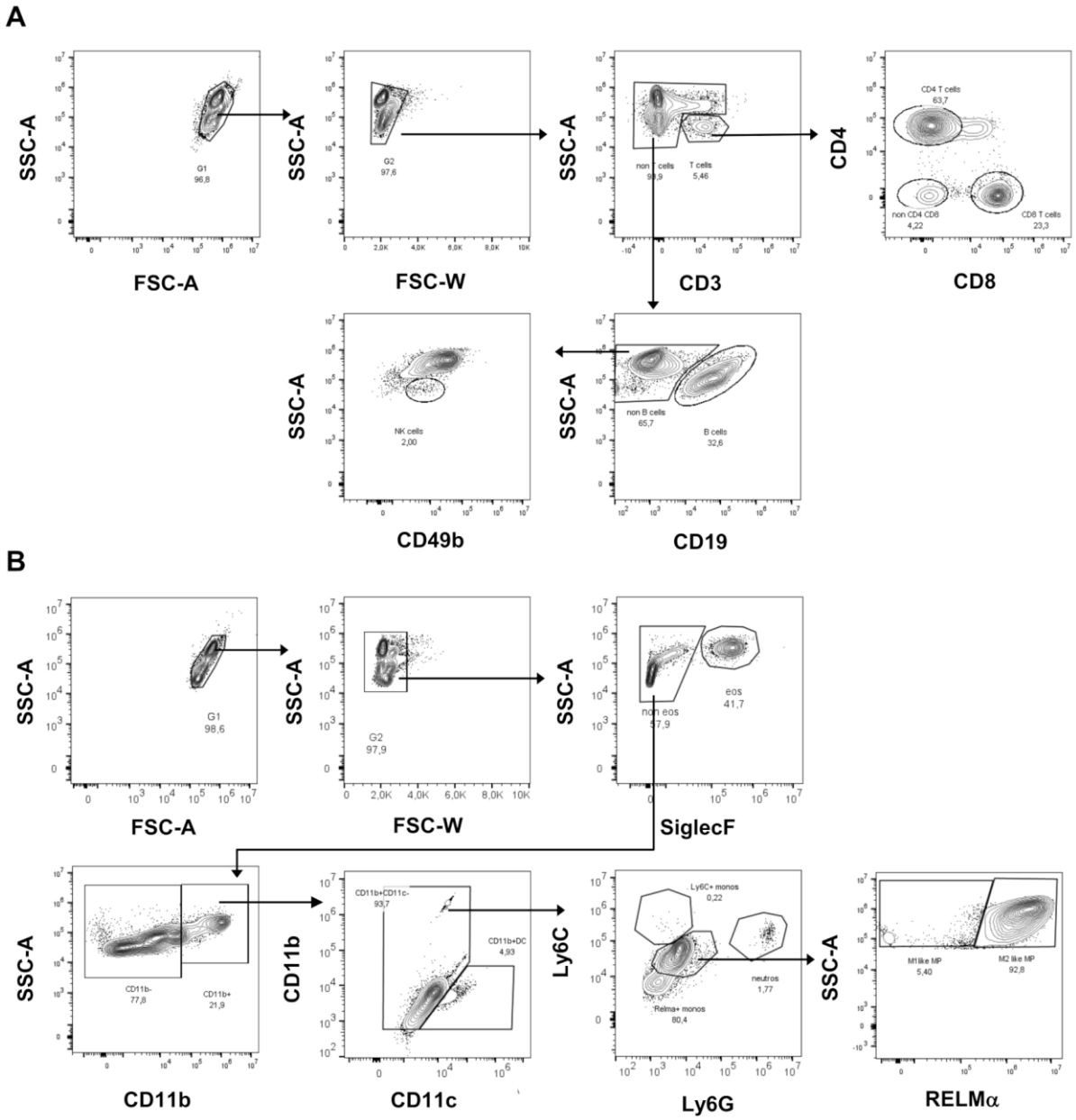

Figure 3.30| Gating strategy for murine BALB/c pleural cells by flow cytometry. (A) Gating to identify T cell subsets by the expression of CD3, CD4 and CD8, B cells by the expression of CD19 and NK cells by the expression of CD49b. **(B)** Gating to identify myeloid cells subsets. Eosinophils were identified by SiglecF expression, CD11b expressing dendritic cells by CD11c expression and neutrophils by Ly6G expression. Further monocyte and macrophage populations were classified by Ly6C and RELMα expression. **(A-B)** Fluorescence minus one (FMO) controls were applied for gating.

The total cell count in the pleura was reduced in animals that were treated with agonist (Figure 3.31 A). This was significant after the treatment with trans. poly(I:C) ($p=0.009$). The overall reduction was due to reductions in several cell populations, including $CD4^+$ T cells, $CD8^+$ T cells, B cells, $CD11b^+$ DCs, M2-like macrophages and eosinophils (Figure 3.31 B – D + F + H + J). Significant reductions were observed for $CD4^+$ T cells, M2-like macrophages and eosinophils after 3pRNA treatment (Figure 3.31 B + H + J) and for $CD11b^+$ DCs and M2-like macrophages after treatment with trans. poly(I:C) (Figure 3.31 F + H). The reduction in M2-like macrophages was accompanied by increased numbers of M1-like macrophages (Figure 3.31 G), which reached statistical significance after 3pRNA treatment. NK cell and neutrophil counts were least affected by the treatments (Figure 3.31 E + I).

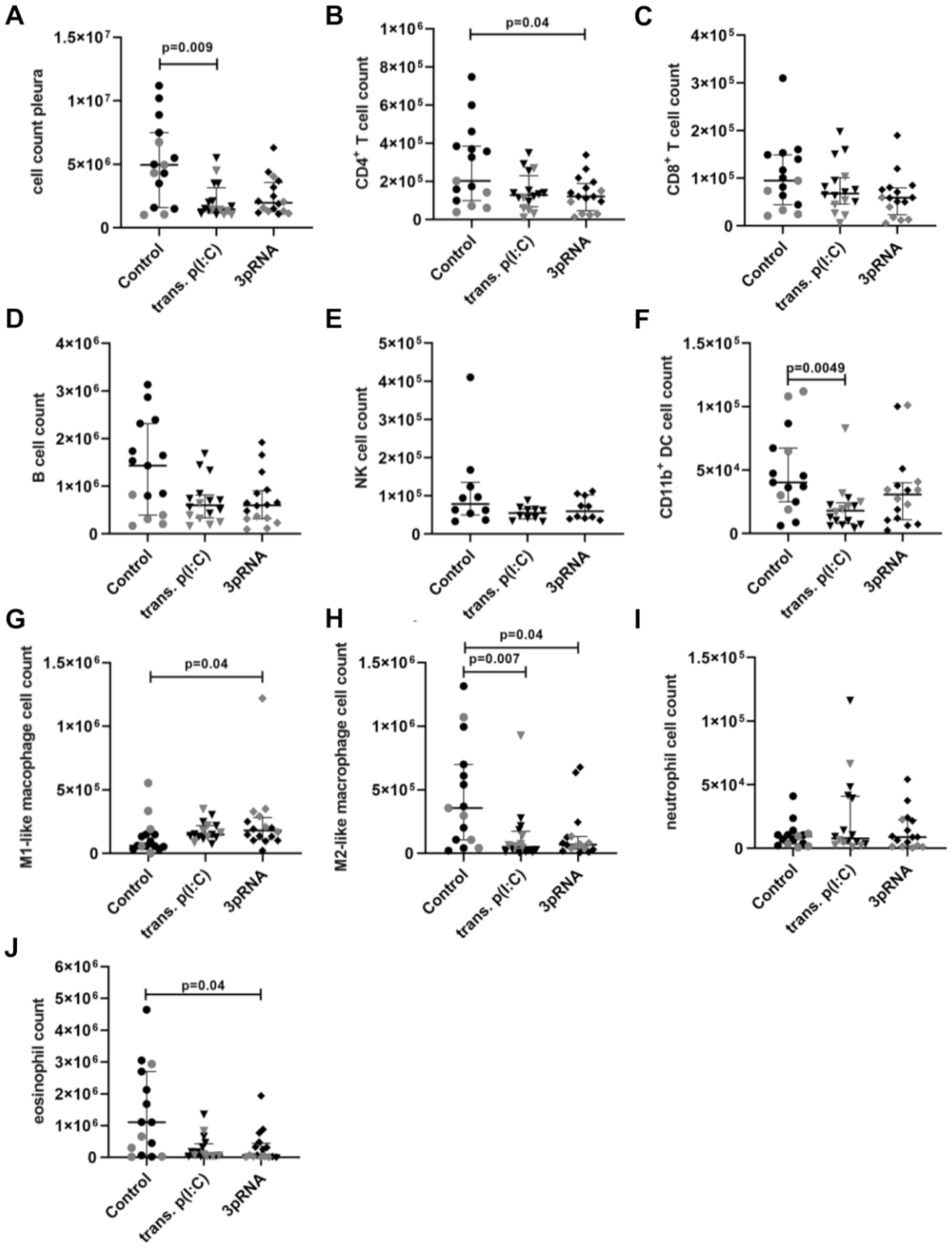

Figure 3.31| Reduced cell counts in the pleural cavity of *L. sigmodontis*-infected mice after nucleic acid receptor activation.

Continued on next page.

(A-O) Mice were subcutaneously (s.c.) injected with 20µg poly(I:C) or 3pRNA, both complexed with *in vivo*-jetPEI®, prior to the s.c. infection with 40 *L. sigmodontis* L3 larvae and then intravenously injected with the same dose after infection. Nine days after infection pleural cells were quantified **(A)** and analyzed by flow cytometry **(B-I)**. **(A)** Pleural cell count of **(B)** $CD4^+$ T cells ($CD3^+CD4^+$), **(C)** $CD8^+$ T cells ($CD3^+CD8^+$), **(D)** B cells ($CD3^-CD19^+$), **(E)** NK cells ($CD3^-CD19^+CD49b^+$), **(F)** $CD11b^+$ dendritic cells (DCs) ($SiglecF^-CD11b^+CD11c^+$), **(G)** M1-like macrophages ($SiglecF^-CD11b^+CD11c^-Ly6G^-Ly6C^{int}RELM\alpha^-$), **(H)** M2-like macrophages ($SiglecF^-CD11b^+CD11c^-Ly6G^-Ly6C^{int}RELM\alpha^+$), **(I)** neutrophils ($SiglecF^-CD11b^+CD11c^-Ly6C^{int}$ $Ly6G^+$) and **(J)** eosinophils ($SiglecF^+$). Error bars show median with IQR. Data were statistically analyzed using Kruskal-Wallis with Dunn's post-hoc test. n=10-16. Except for graph (E), data were pooled from two individual experiments and labelled via color-code.

Besides quantification of cell populations in the pleural cavity, the cells were analyzed regarding their activation status by flow cytometry (Figure 3.31). Data from the experiment depicted in Figure 3.29 and Figure 3.31 which are labelled in black are shown as representative for the activation status, as data did not qualify for pooling.

The I-Ab expression of B cells and I-Ab and CD86 expression of $CD11b^+$ DCs was not significantly affected by the agonist injection (Figure 3.32 A – C). M1-like macrophages showed significantly decreased expression of I-Ab after 3pRNA treatment, but CD86 expression was not altered by any treatment (Figure 3.32 D + E). In contrast the I-Ab expression of M2-like macrophages was not affected by either agonist, but the expression of CD86 was significantly reduced after trans. poly(I:C) or 3pRNA treatment (Figure 3.32 F + G). There was a significant upregulation of I-Ab and CD86 on neutrophils in response trans. poly(I:C) and 3pRNA (Figure 3.32 H + I). The I-Ab of eosinophils was not affected (Figure 3.25 J), but the treatment with trans. poly(I:C) led to a significant upregulation of CD86 on eosinophils (Figure 3.32 J).

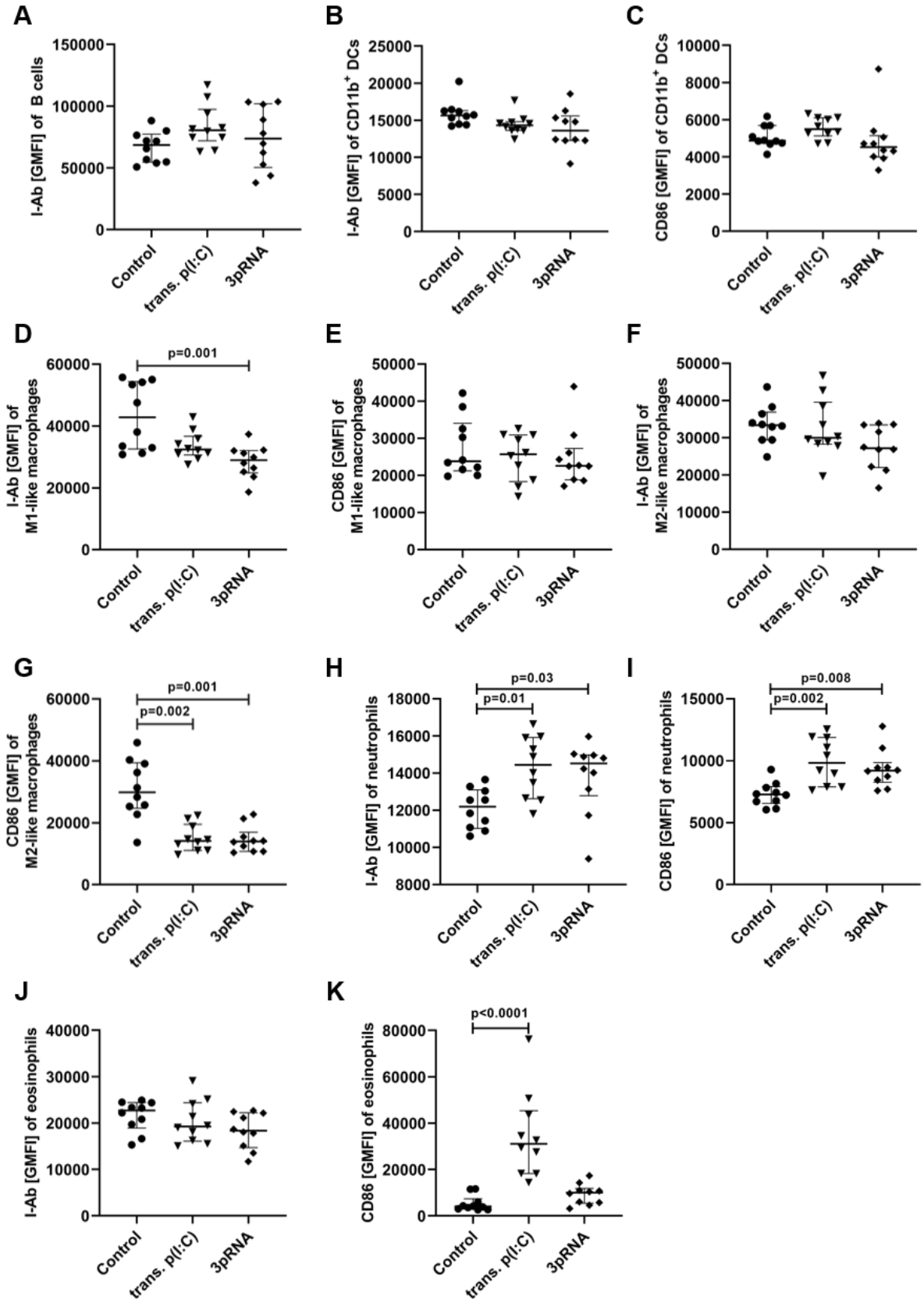

Figure 3.32| Cell activation in the pleural cavity of *L. sigmodontis*-infected mice after nucleic acid receptor activation.

Continued on next page.

(A-K) Mice were subcutaneously (s.c.) injected with 20µg poly(I:C) or 3pRNA, both complexed with *in vivo*-jetPEI®, prior to the s.c. infection with 40 *L. sigmodontis* L3 larvae and then intravenously injected with the same dose after infection. Nine days after infection pleural cells were analyzed by flow cytometry. **(A)** I-Ab expression of B cells ($CD3^-CD19^+$). **(B)** I-Ab and **(C)** CD86 expression of $CD11b^+$ dendritic cells (DCs) ($SiglecF^-CD11b^+CD11c^+$), **(D)** I-Ab and **(E)** CD86 of M1-like macrophages ($SiglecF^-CD11b^+CD11c^-Ly6G^-Ly6C^{int}RELM\alpha^-$), **(F)** I-Ab and **(G)** CD86 of M2-like macrophages ($SiglecF^-CD11b^+CD11c^-Ly6G^-Ly6C^{int}RELM\alpha^+$), **(H)** I-Ab and **(I)** CD86 expression of neutrophils ($SiglecF^-CD11b^+CD11c^-Ly6C^{int}$ $Ly6G^+$), **(J)** I-Ab and **(K)** CD86 expression of eosinophils ($SiglecF^+$). Error bars show median with IQR. Data were statistically analyzed using Kruskal-Wallis with Dunn's post-hoc test. n=8, except trans. p(I:C) data in (D – G) representative for two individual experiments.
GMFI: geometric mean fluorescence intensity; trans.: transfected

Overall, the *L. sigmodontis* L3 larval count in the pleural cavity was reduced after the activation of nucleic acid receptors. The reduction in worm burden was accompanied by reduced cell counts in the pleural cavity as well as a downregulation of M2-like macrophages and an increased activation of neutrophils.

3.6 Improved worm clearance after combination vaccination of nucleic acid receptor agonists and irradiated *L. sigmodontis* L3 larvae

After characterization of the immunostimulatory potential of nucleic acid receptor agonists after subcutaneous injection and confirming that the treatment with poly(I:C) or 3pRNA enhanced worm clearance, the combination therapy was applied to the vaccination setup.

The overall experimental setup is depicted in Figure 3.33. In brief, mice received three injections every fortnight of a combination therapy including att. L3 larvae and nucleic acid receptor agonists during the immunization phase. Two weeks after the last vaccination, blood was drawn and mice were naturally infected with *L. sigmodontis*. Once MF were released to the peripheral blood, further blood samples for MF counts were drawn until *ex vivo* analysis.

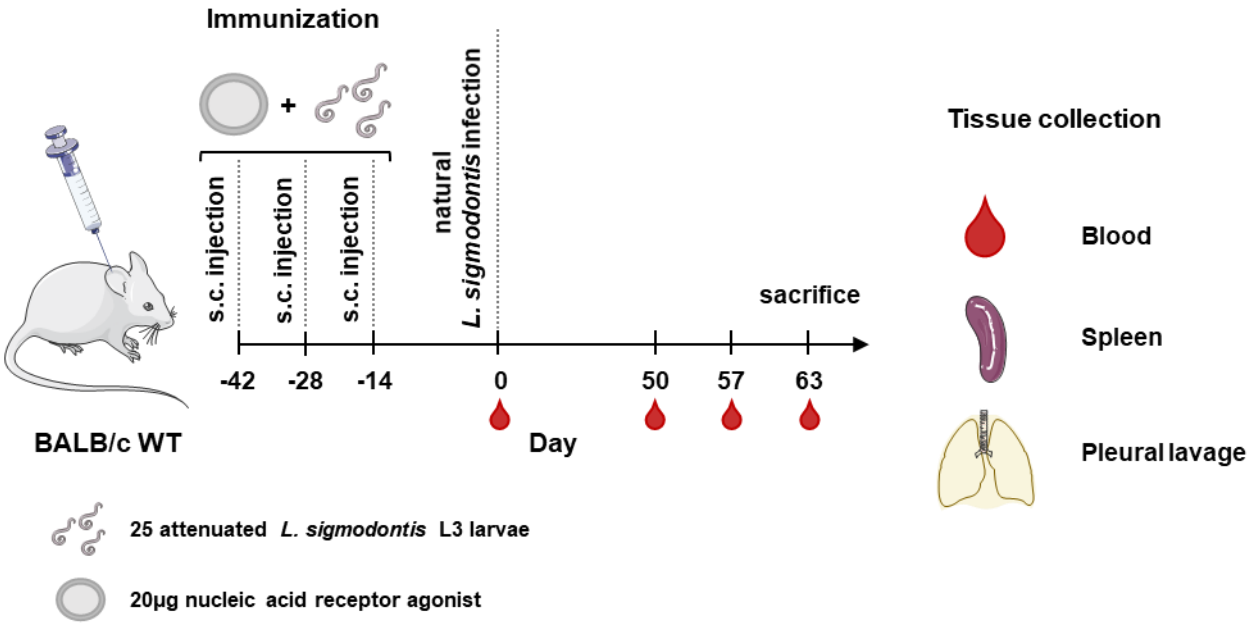

Figure 3.33| Experimental setup of the vaccination study.

3.6.1 Antibody generation

As a measure of immunization success, parasite-specific antibody production was measured in the serum of mice. It was isolated from the blood drawn on day zero, after the immunization, but prior to infection with *L. sigmodontis*. Antibodies were only relatively quantified, allowing a comparison between groups for each individual antibody isotype.

In the serum of all animals that were not immunized with att. L3 larvae, no parasite specific IgE, IgG1 and IgG2a/b antibodies were detectable (Figure 3.34). In unimmunized animals or animals that only received trans. poly(I:C) or 3pRNA, no IgE, IgG1 and IgG2a/b were detected. Further, there was no IgE response to the immunization with att. L3 + naked poly(I:C) (Figure 3.34 A). The immunization with att. L3 alone or in combination with trans. poly(I:C) or 3pRNA resulted in a significant IgE response (Figure 3.34 A). IgG1 antibody levels were significantly increased in all animals that received att. L3 larvae, independent of the addition of an agonist, compared to the untreated control. IgG1 antibody levels further increased in groups that received the agonists and att. L3 larvae compared to att. L3 larvae alone, which was however not statistically significant (Figure 3.34 B). IgG2a/b antibody levels were only significantly increased compared to the control, when mice were immunized with a combination of att. L3 larvae and agonist. In the direct comparison to the

immunization with att. L3 larvae, IgG2a/b levels were significantly increased after combination treatment with trans. poly(I:C) (p=0.007) (Figure 3.34 C).

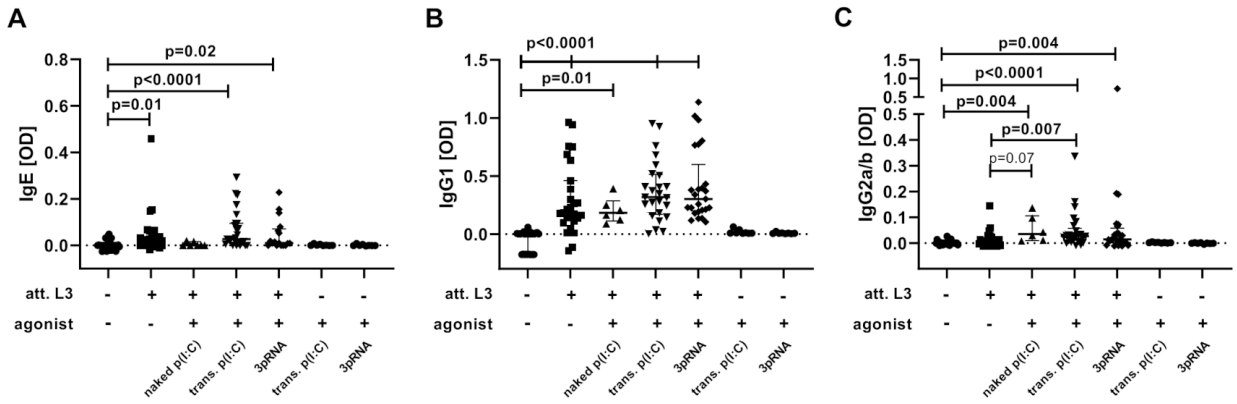

Figure 3.34| Relative quantification of *Litomosoides sigmodontis*-specific Ig-subtypes induced by immunization. Mice were immunized three times every fortnight by subcutaneous injection of attenuated (att.) *L. sigmodontis* L3 larvae in combination with 20µg of different agonists. Transfected (trans.) poly(I:C) (p(I:C)) and 3pRNA were complexed with *in vivo*-jetPEI®. Two weeks after the last injection, blood was drawn and relative level of parasite-specific **(A)** IgE, **(B)** IgG1 and **(C)** IgG2a/b antibodies were measured by ELISA. Error bars show median with IQR. Data were statistically analyzed by Kruskal-Wallis with Dunn's post-test. n=8-28. Data from untreated and groups receiving att. L3 larvae with or without agonist were pooled from 3 individual experiments, only data from att. L3 with naked p(I:C) are from one experiment. Data from groups that only received agonist are from one experiment.
att.: attenuated, p(I:C): poly(I:C), trans.: transfected.

3.6.2 Antibody-dependent cellular cytotoxicity assay

After detecting parasite-specific antibodies in the serum of immunized mice, a functional antibody dependent cellular cytotoxicity (ADCC) assay assessing larval motility was performed. To that end peritoneal exudate cells (PEC) from naïve BALB/c mice were co-cultured with *L. sigmodontis* L3 larvae and the culture medium was supplemented with the serum of immunized mice (Figure 3.35).

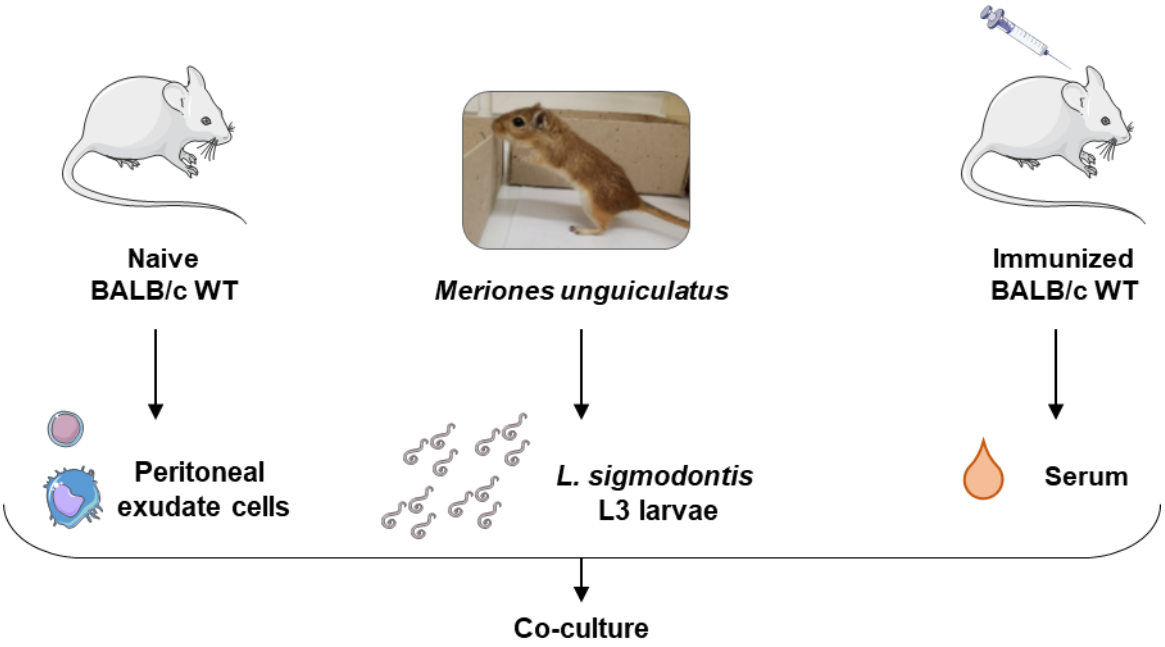

Figure 3.35| Experimental setup of the antibody-dependent cellular cytotoxicity assay.

The composition of peritoneal cells isolated from naïve mice was assessed by flow cytometry. The gating strategy is depicted in Figure 3.36 A. Around 25% of the peritoneal exudate cells were identified as CD19^{+} B cells, but may include mast cells. Roughly 8% of the cells were CD11b^{hi}F4/80^{hi} macrophages, around 10% of the cells were neutrophils (CD11b$^{low\text{-}int}$F4/80$^{neg\text{-}int}$Ly6G^{+}) and nearly 4% of the cells were other myeloid cells (CD11b$^{low\text{-}int}$F4/80$^{neg\text{-}int}$). The remaining cells were CD19^{neg}CD11b^{neg} (Figure 3.36 B).

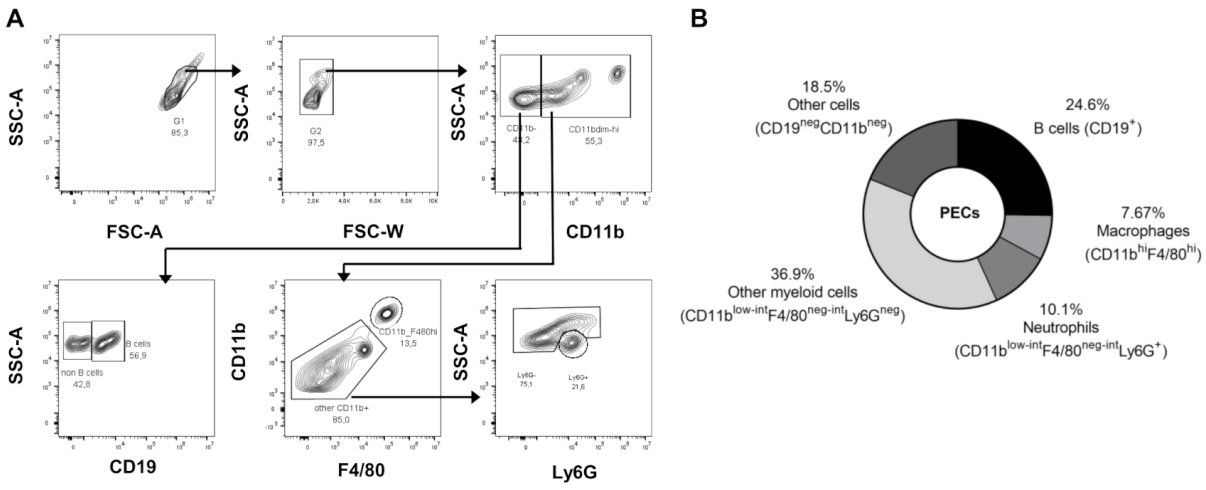

Figure 3.36| Cellular composition of peritoneal exudate cells. Isolated peritoneal exudate cells (PECs) were characterized by flow cytometry. **(A)** Gating strategy. **(B)** Percental distribution of identified cells. Data are representative for three individual experiments.

The motility score of the *L. sigmodontis* L3 larvae was evaluated at the start of the co-culture and the following three days. A score of 4 represents fast and continuous movement of the entire larvae, which is slower at a score of 3. At a score of 2 the movement is slow and discontinuous. Sporadic movement at the larval ends is scored as 1 and lack of movement is scored as 0. At the start of the co-culture all larvae were fully motile. Larvae that were cultured alone, with cells, or medium that was supplemented with cell culture fetal calf serum (FCS) did not reduce their motility over the entire co-culture (Figure 3.37). In cultures where the medium was supplemented with serum from control animals, that were not immunized, larval motility was reduced gradually reaching the lowest score of 1.3 on day three (orange data set). The supplementation with serum from animals that were immunized with attenuated L3 larvae alone (pink data set), resulted in a significant reduction in the score at day one and three compared to the serum control group. On day three, a score of 0.8 was reached as the lowest motility score. For the statistical analysis of the combination therapies using att. L3 larvae and an agonist, the groups were compared to the group of att. L3 larvae serum. The green data set represents the larval motility when the medium was supplemented with serum from animals that were immunized with a combination of att. L3 larvae and naked poly(I:C). After one day the motility score dropped to 0.9, which was significantly lower than the control with att. L3 larvae serum. On the second day that score stabilized at 1 similar to the att. L3 control group. On the third day, the larval motility recovered to a score of 2. Therefore, the larval motility was higher than in the control. The turquoise data set represents the larval motility of cultures that were supplemented with serum from animals that were immunized with a combination of att. L3 larvae and trans. poly(I:C). After one day of co-culture, the motility significantly dropped to a score of 2. On the following days, the motility was further significantly reduced reaching the lowest score of 0.4 on day three. The blue data set represents the larval motility of cultures that were supplemented with serum from animals that were immunized with a combination of att. L3 larvae and 3pRNA. After one day of co-culture, the motility dropped significantly to a score of 1.8. On the second day the motility decreased to a score of 1.4 and remained stable on day three. Therefore, on day two and three the motility was similar to the control group that was supplemented with serum from unimmunized animals. In conclusion, the implementation of poly(I:C) or 3pRNA in the immunization protocol induced a significant larval motility reduction after one day of culture. Over the three-day culturing

period the combination immunization with trans. poly(I:C) led to a significant reduction in larval motility compared to the immunization with att. L3 larvae alone.

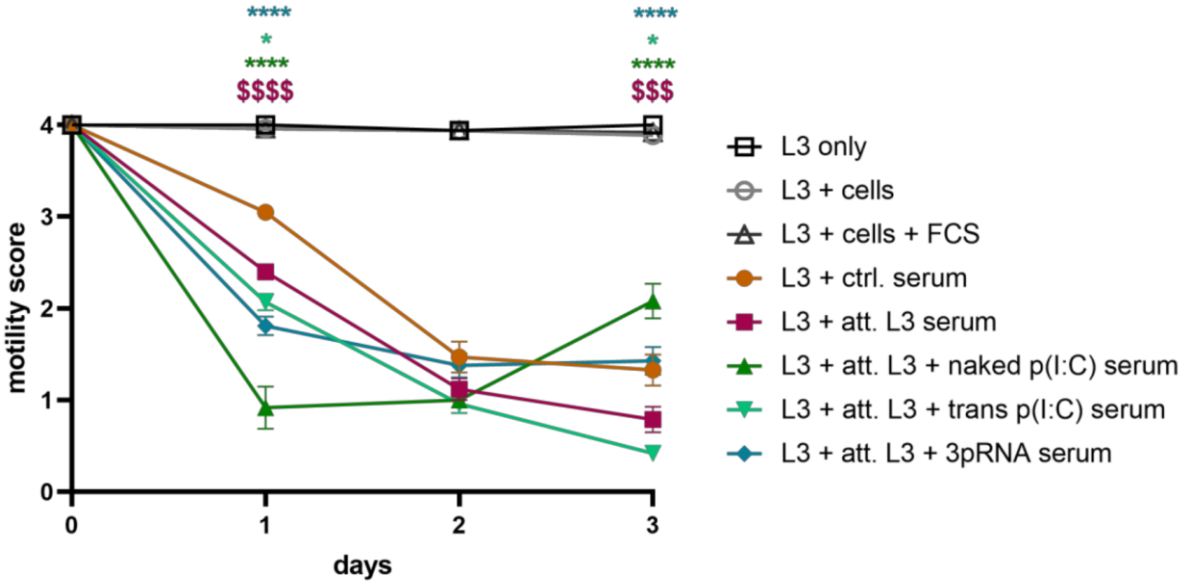

Figure 3.37| Reduced *L. sigmodontis* L3 larval motility after co-culture with serum from vaccinated animals. Mice were immunized three times every fortnight by subcutaneous injection of attenuated (att.) *L. sigmodontis* L3 larvae in combination with 20µg of different agonists. Transfected (trans.) poly(I:C) (p(I:C)) and 3pRNA were complexed with *in vivo*-jetPEI®. Two weeks after the last injection, blood was drawn and serum was used as cell culture supplement. Naïve peritoneal exudate cells were co-cultured with *L. sigmodontis* L3 larvae. The motility of individual larvae was scored for three days. The score was defined as followed: 4: fast and continuous movement, 3: slower but continuous movement, 2: slower and discontinuous movement, 1: sporadic movement limited to the ends, 0: no movement. Data shown as mean ± SEM from. Data were statistically analyzed by a 2way ANOVA with Bonferroni's multiple comparison test. $$$$ $p<0.0001$ comparison of L3 + att. L3 serum to L3 + ctrl. serum. * $p<0.05$, *** $p<0.0001$: comparison of groups including agonist treatment to L3 + att. L3 serum. Data from L3 + cells + FCS pooled from two independent experiments. Data from L3 + att. L3 + naked p(I:C) serum from one experiment. Other data pooled from three individual experiments. For L3 + att. L3 + naked p(I:C) serum n=12 larvae. For other groups n=49 - 72 larvae.
att.: attenuated, p(I:C): poly(I:C), trans.: transfected.

3.6.3 Antibody time course

Besides relatively quantifying the parasite-specific antibody production in response to the immunization (Figure 3.33), parasite-specific IgE, IgG1 and IgG2a/b antibodies in the serum of immunized mice receiving att. L3 larvae and agonists were measured during the course of a subsequent infection (Figure 3.38). The relative IgE level was lowest in unimmunized animals and remained stable over the time course of infection from 37 – 63 dpi (Figure 3.38 A). The same was observed for animals that were

previously immunized with att. L3 larvae + 3pRNA. In the serum of animals that were immunized with att. L3 + naked poly(I:C) or att. L3 + trans. poly(I:C) the IgE level were higher, but remained stable over time. IgE level in the serum from animals that were immunized with att. L3 alone was higher than in the control group and then further increased between 57 – 63dpi. The IgG1 level was lowest in the control group on day 37, then rapidly increased until day 50 and remained at the highest level of all groups from day 50 to 63 (Figure 3.38 B). The IgG1 level was similar in all immunized groups and remained stable at all time point with a slight increase over time. The IgG2a/b level remained lowest in the serum of unimmunized (control) animals during the time course of infection (Figure 3.38 C). In animals that were immunized with att. L3 larvae alone the IgG2a/b level rose over the time course of infection. Animals that received a combination-immunization with any agonist had higher serum IgG2a/b level at day 37 after the infection than animals that did not receive the agonist. These levels remained relatively stable until day 63 after the infection. When comparing the agonists, the serum IgG1a/b level was the lowest after 3pRNA treatment and highest in response to naked poly(I:C) treatment.

Overall, animals that received immunization had higher parasite-specific antibody responses in the serum at day 37 after infection and during the course of infection, only IgG1 level was higher in unimmunized animals.

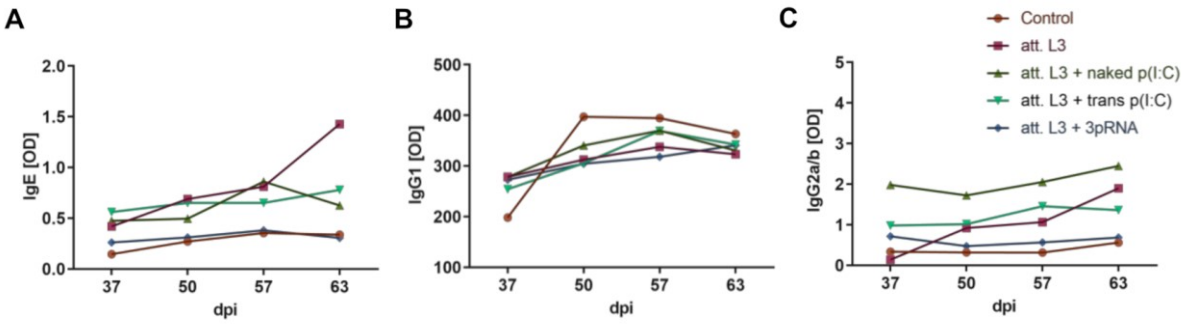

Figure 3.38| *L. sigmodontis*-specific Ig-subtype levels over the time course of infection. Mice were immunized three times every fortnight by subcutaneous injection of attenuated (att.) *L. sigmodontis* L3 larvae in combination with 20µg of different agonists. Transfected (trans.) poly(I:C) (p(I:C)) and 3pRNA were complexed with *in vivo*-jetPEI®. Two weeks after the last injection the animals were naturally infected with *L. sigmodontis*. Blood was drawn on days 37, 50, 57 and 63 after the infection. Serum level of parasite-specific **(A)** IgE, **(B)** IgG1, **(C)** IgG2a/b was relatively quantified by ELISA. Data show median from one experiment.
att.: attenuated, trans.: transfected, (p(I:C): poly(I:C).

3.6.4 Worm burden in the pleural cavity 63 days after infection

As readout for the vaccination success, the number of adult worms surviving in the pleural cavity were quantified 63 days after the infection (Figure 3.39).

Control animals had a median of 22 worms in their pleural cavity. Animals that were immunized with att. L3 larvae had a median of 12 worms in the pleural cavity resulting in a non-significant reduction of 45% (Figure 3.39 and Table 3.2). The immunization with a combination of att. L3 larvae and naked poly(I:C) had a reduced impact on the worm burden and achieved a reduction of 39%. The worm burden was significantly reduced after the treatment with trans. poly(I:C) (p=0.0002), when compared to the unimmunized group. The worm burden was reduced by 73% to a median worm count in the pleural cavity of 6. The adult worm burden was reduced by trend (p=0.06) due to the addition of trans. poly(I:C) to the immunization in comparison to animals that were immunized with att. L3 larvae alone. The combination therapy with att. L3 larvae and 3pRNA resulted in a significant reduction of adult worm burden compared to unimmunized animals (p=0.0008). The median worm count was reduced by 57% from 22 to 9.5 worms in the pleural cavity.

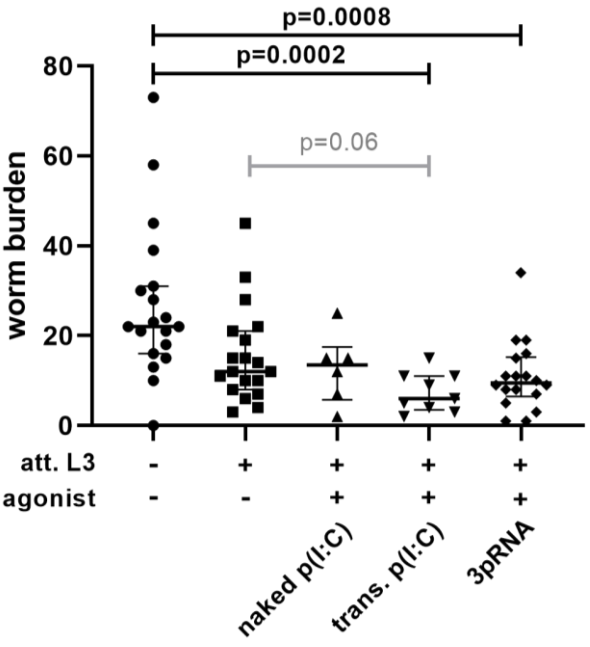

Figure 3.39| Significantly reduced adult worm burden 63 days after infection with *L. sigmodontis* in animals that received combination vaccination. Mice were immunized three times every fortnight by subcutaneous injection of attenuated (att.) *L. sigmodontis* L3 larvae in combination with 20µg naked poly(I:C) (p(I:C)), transfected (trans.) p(I:C) or 3pRNA. Trans. p(I:C) and 3pRNA were complexed with *in vivo*-jetPEI®. Two weeks after the last injection the mice were naturally infected with *L. sigmodontis*. 63 days after infection adult *L. sigmodontis* worms were isolated from the pleural cavity and quantified. Error bars show median with IQR. Data were statistically analyzed by Kruskal-Wallis with Dunn's post-test. n=6-20. Pooled data from 2 individual experiments for naked and trans. p(I:C) data from one experiment.
att.: attenuated, p(I:C): poly(I:C), trans.: transfected.

Administering trans. poly(I:C) or 3pRNA to the immunization with att. L3 larvae further increased the percent reduction in adult worm burden by 28% and 12%, respectively compared to the immunization with att. L3 larvae alone (Table 3.2).

Table 3.2: Percent reduction in worm burden 63 days after infection with *L. sigmodontis* in immunized animals. Mice were immunized three times every fortnight by subcutaneous injection of attenuated (att.) *L. sigmodontis* L3 larvae in combination with 20µg of naked poly(I:C) (p(I:C)), transfected (trans.) p(I:C) or 3pRNA. Trans. p(I:C) and 3pRNA were complexed with *in vivo*-jetPEI®. 63 days after infection the adult worm burden in the pleural cavity was quantified and the reduction in worm burden was calculated based on the group median. n=6-20. Pooled data from two individual experiments apart from naked p(I:C) experiment from one experiment.
att.: attenuated, p(I:C): poly(I:C), trans.: transfected

Immunization therapy	Percent worm reduction due to immunization	Percent worm reduction changed by agonist
Attenuated L3 larvae	45%	/
Attenuated L3 larvae + naked p(I:C)	39%	- 6%
Attenuated L3 larvae + trans. p(I:C)	73%	+ 28%
Attenuated L3 larvae + 3pRNA	57%	+ 12%

A similar distribution of female (~60%) and male (~40%) worms was recovered from the pleural cavities from animals of all groups (Figure 3.40). In three animals that were immunized with attenuated L3 larvae alone and two animals immunized with a combination therapy with 3pRNA, only female worms were recovered. Further, only male worms were recovered from two animals immunized with a combination therapy with 3pRNA.

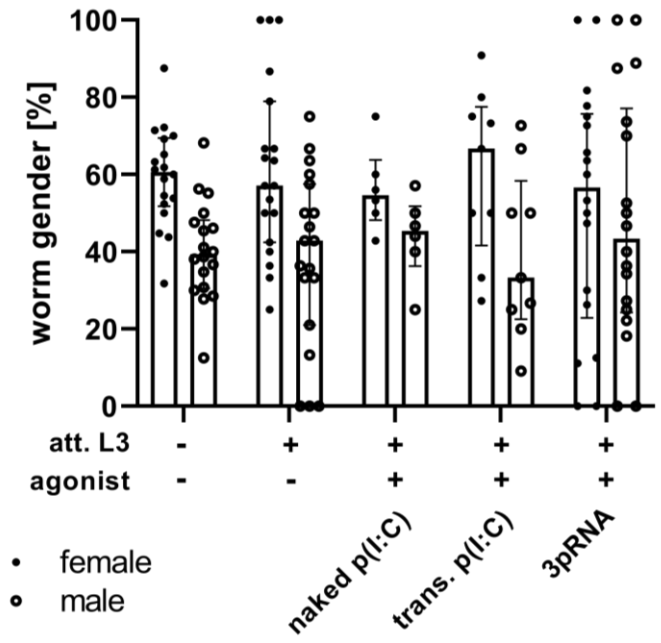

Figure 3.40| Vaccination-induced worm clearance affects both male and female *L. sigmodontis* filariae similarly. Frequency of female and male worms isolated of mice that were immunized three times every fortnight by subcutaneous injection of attenuated (att.) *L. sigmodontis* L3 larvae in combination with 20µg of naked poly(I:C), transfected (trans.) poly(I:C) or 3pRNA. Trans. poly(I:C) (p(I:C)) and 3pRNA were complexed with *in vivo*-jetPEI®. Two weeks after the last injection the mice were naturally infected with *L. sigmodontis*. 63 days after infection adult *L. sigmodontis* worms were isolated from the pleural cavity and females and males were quantified. Error bars show median with IQR. Data were statistically analyzed by 2-way ANOVA with Bonferroni's multiple comparison test. n=6-20. Pooled data from two individual experiments apart from naked poly(I:C) (p(I:C) experiment from one experiment.
att.: attenuated, p(I:C): poly(I:C), trans.: transfected.

3.6.5 Vaccination regimens tested have a minor impact on the occurrence of microfilaremia

In order to analyze the impact of the immunization on the fecundity of the filariae, peripheral MF counts were determined. Starting 50 days post infection, adult *L. sigmodontis* parasites start releasing MF. The MF load in 50µL of peripheral blood is visualized in Figure 3.41, showing the values MF+1 to allow logarithmic scaling. On day 50 after infection, none of the animals had detectable MF in their peripheral blood. On days 57 and 63 after infection, there were no significant differences in the MF counts between the different groups. Overall, there was a wide range of MF numbers in the peripheral blood of MF-positive animals, independent of the immunization prior to infection.

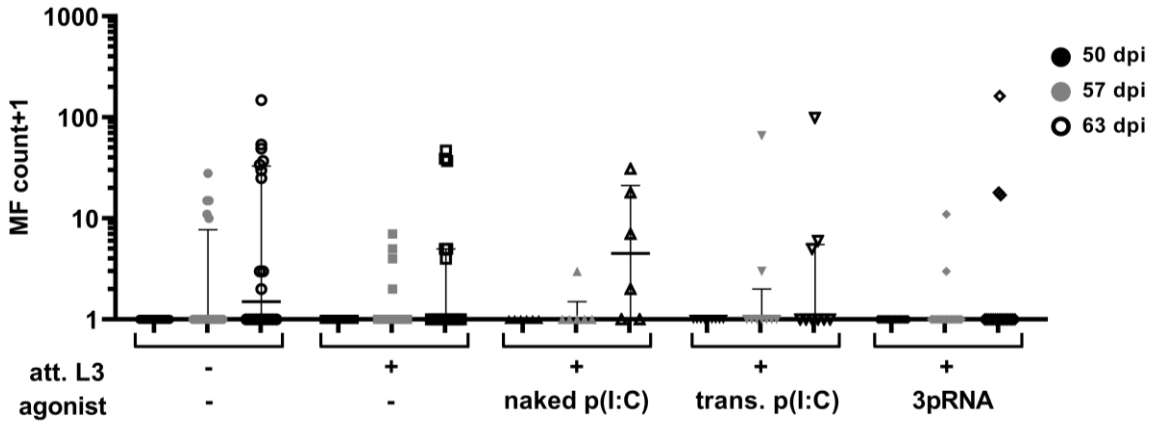

Figure 3.41| Similar microfilariae count in the peripheral blood following challenge infection with *L. sigmodontis* in immunized and unimmunized mice. Mice were immunized three times every fortnight by subcutaneous injection of attenuated (att.) *L. sigmodontis* L3 larvae in combination with 20µg of naked poly(I:C) (p(I:C)), transfected (trans.) p(I:C) or 3pRNA. Trans. p(I:C) and 3pRNA were complexed with *in vivo*-jetPEI®. Two weeks after the last injection, the mice were naturally infected with *L. sigmodontis*. On days 50, 57 and 63 after infection, peripheral blood was drawn and microfilariae (MF) were quantified. Counts were plotted as MF+1 to allow logarithmic scaling. Error bars show median with IQR. Data were statistically analyzed by Kruskal-Wallis with Dunn's post-test. n=6-20. Pooled data from two individual experiments apart from naked p(I:C) experiment from one experiment.
att.: attenuated, p(I:C): poly(I:C), trans.: transfected.

Next to quantifying the MF load in the animals, the percentage of MF-positive animals per group was determined (Table 3.3).

In the unimmunized control group, 25% of animals were MF-positive on day 57 after infection and 50% of animals were positive on day 63 after infection. In animals that were immunized with att. L3 larvae, the percentages were reduced to 22.2% and 33.3%, respectively. The combination of the immunization with att. L3 larvae and naked poly(I:C) reduced the percentage of MF-positive animals on day 57 after infection to 16.7%, but on day 63 the same percentage of animals were MF-positive as in the unimmunized control group. In contrast to that, the addition of trans. poly(I:C) had a minor impact on patency on day 57 after infection, but only 29.4% of animals were MF-positive 63 days after infection. The combination-immunization with att. L3 larvae and 3pRNA resulted in only 11.1% MF-positive animals on day 57 after infection and 16.7% MF-positive animals on day 63 after infection.

Taken together the immunization had no effect on the numbers of MFs in MF-positive animals, but the immunization with att. L3 larvae, especially in combination with trans. poly(I:C) or 3pRNA may reduce the percentage of MF-positive animals.

Table 3.3: Percentage of animals with detectable *L. sigmodontis* MF counts in their peripheral blood. Mice were immunized three times every fortnight by subcutaneous injection of attenuated (att.) *L. sigmodontis* L3 larvae in combination with 20µg of naked poly(I:C) (p(I:C)), transfected (trans.) p(I:C) or 3pRNA. Trans. p(I:C) and 3pRNA were complexed with *in vivo*-jetPEI®. Two weeks after the last injection, the mice were naturally infected with *L. sigmodontis*. On days 50, 57 and 63 after infection, peripheral blood was drawn and microfilariae (MF) were quantified. The percentage of MF-positive animals among all animals in the group was determined. n=6-20. Pooled data from two individual experiments apart from naked p(I:C) experiment from one experiment.
att.: attenuated, p(I:C): poly(I:C), trans.: transfected

	time point					
Group	day 50		day 57		day 63	
	% of MF-positive mice					
control	0/20	→0%	5/20	→25%	10/20	→50%
att. L3	0/18	→0%	4/18	→22.2%	6/18	→33.3%
att. L3 + naked p(I:C)	0/6	→0%	1/6	→16.7%	3/6	→50%
att. L3 + trans. p(I:C)	0/17	→0%	4/17	→23.5%	5/17	→29.4%
att. L3 + 3pRNA	0/18	→0%	2/18	→11.1%	3/18	→16.7%

3.6.6 Local immune milieu in the pleural cavity 63 days after infection

Besides determining the adult worm burden, the total cell count in the pleural cavity was determined (Figure 3.42). No significant changes in the pleural cell count in response to any immunization was observed.

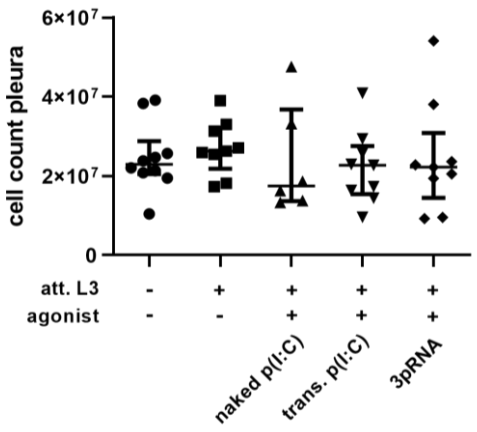

Figure 3.42| No impact of an immunization on total pleural cell count. Mice were immunized three times every fortnight by subcutaneous injection of attenuated (att.) *L. sigmodontis* L3 larvae in combination with 20µg of naked poly(I:C) (p(I:C)), transfected (trans.) p(I:C) or 3pRNA. Trans. p(I:C) and 3pRNA were complexed with *in vivo*-jetPEI®. Two weeks after the last injection, the mice were naturally infected with *L. sigmodontis*. 63 days after infection the total organ cell count was determined. n=6-10. att.: attenuated, p(I:C): poly(I:C), trans.: transfected.

In order to identify changes in cell populations, pleural cells were analyzed by flow cytometry. Cell populations were identified by the gating presented in Figure 3.43.

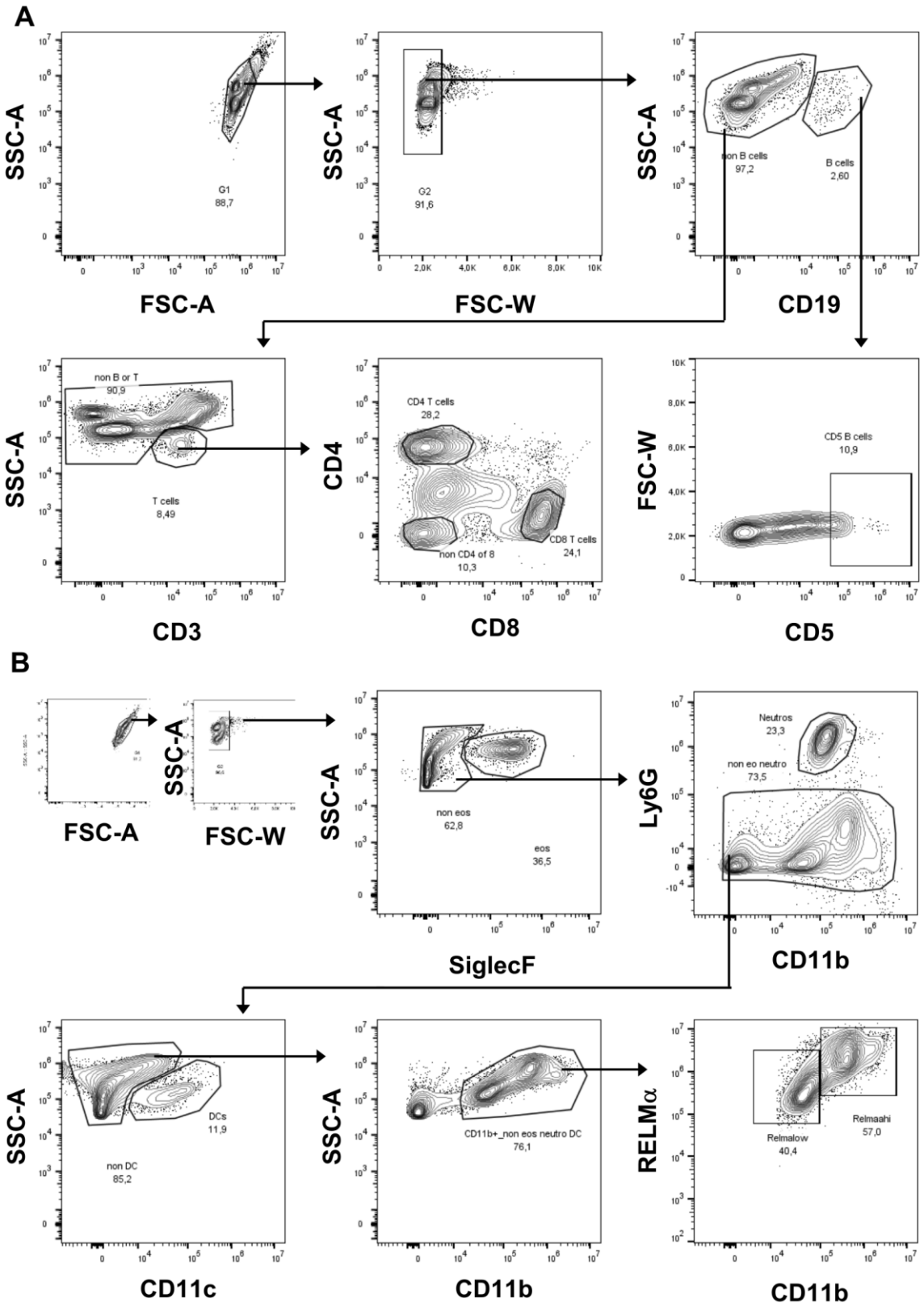

Figure 3.43| Gating strategy for flow cytometric analysis of pleural immune cells. (**A**) Gating to identify B cells by CD19 and CD5 and T cell subsets by the expression of CD3, CD4 and CD8. **(B)** Gating to identify myeloid cell populations by the expression of SiglecF on eosinophils, Ly6G on neutrophils, CD11c on dendritic cells and RELMα in alternatively activated macrophages. **(A-B)** Fluorescence minus one (FMO) controls were applied for gating.

The impact of the immunization on innate cell populations in the pleural cavity is shown in Figure 3.44. There were no significant differences in the cell counts of eosinophils, neutrophils, M2-like macrophages, RELMα^{low} myeloid cells and dendritic cells (Figure 3.44 A + D + G + J + M). The expression of I-Ab by eosinophils was significantly lower in animals that were immunized with the combination of att. L3 larvae and trans. poly(I:C) ($p=0.04$) compared to unimmunized mice, despite a low sample number due to a technical problem when analyzing this immunized group for this staining panel (Figure 3.44 B). Further, there was no significant impact on CD86 expression by eosinophils and the I-Ab and CD86 expression of neutrophils, M2-like macrophages, RELMα^{low} myeloid cells and dendritic cells by any immunization compared to the unimmunized group (Figure 3.44 C, E + F, H + I, K + L, N + O).

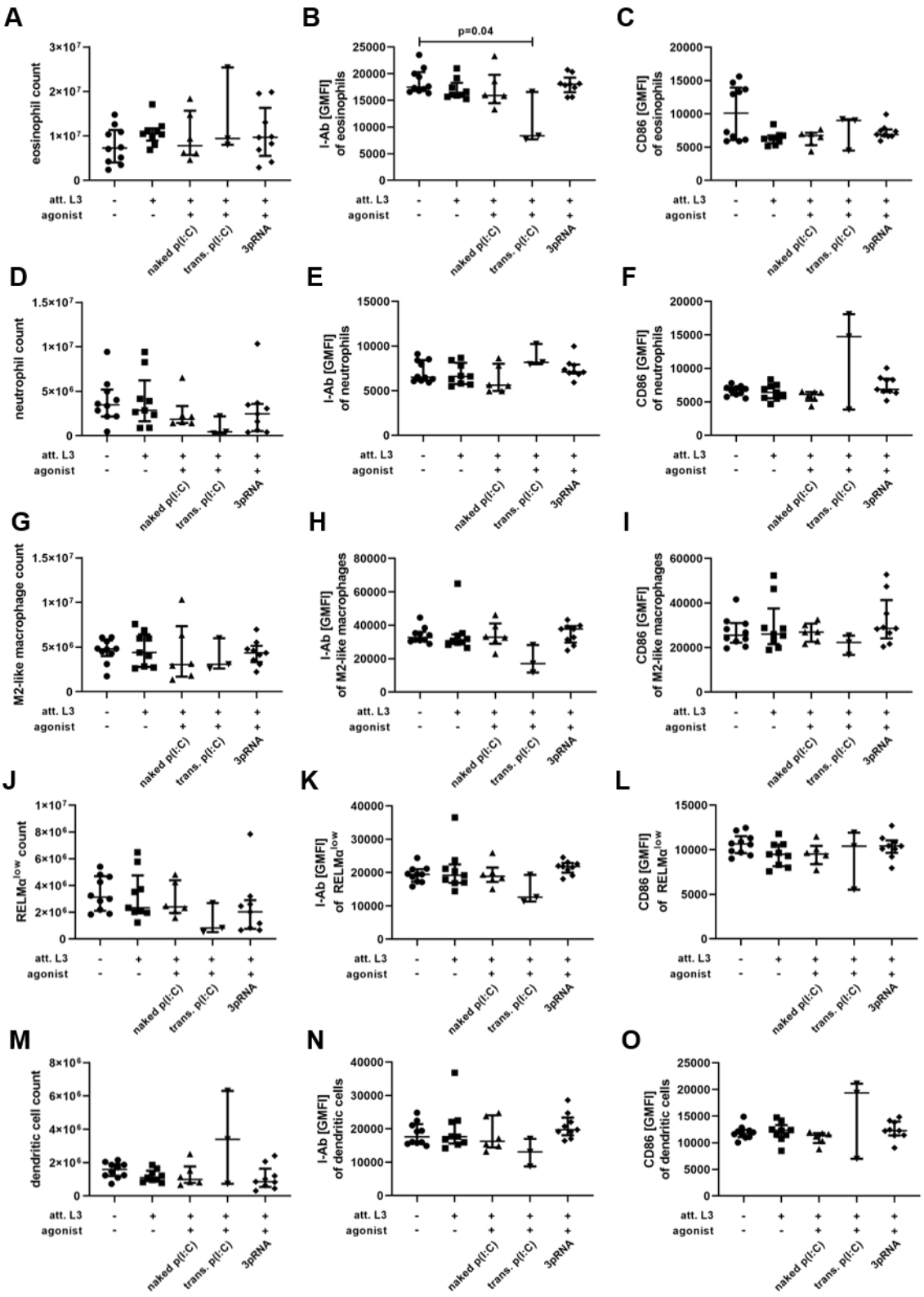

Figure 3.44| Minor impact on innate immune cell populations in the pleura of immunized mice at 63 days after infection with *L. sigmodontis*.

Continued on next page.

(A-O) Mice were immunized three times every fortnight by subcutaneous injection of attenuated (att.) *L. sigmodontis* L3 larvae in combination with 20µg of naked poly(I:C) (p(I:C)), transfected (trans.) p(I:C) or 3pRNA. Trans. p(I:C) and 3pRNA were complexed with *in vivo*-jetPEI®. Two weeks after the last injection, the mice were naturally infected with *L. sigmodontis*. 63 days after infection cell populations were analyzed by flow cytometry. Cell counts of **(A)** eosinophils (SiglecF$^+$), **(D)** neutrophils (SiglecF$^-$Ly6G$^+$CD11b$^+$), **(G)** M2-like macrophages (SiglecF$^-$Ly6G$^-$CD11c$^-$CD11b$^+$RELMα^{high}), **(J)** RELMα^{low} myeloid cells (SiglecF$^-$Ly6G$^-$CD11c$^-$CD11b$^+$ RELMα^{low}) and **(M)** dendritic cells (SiglecF$^-$Ly6G$^-$CD11c$^+$). Expression of I-Ab and CD86 by **(B+C)** eosinophils, **(E+F)** neutrophils, **(H+I)** M2-like macrophages, **(K+L)** RELMα^{low} myeloid cells and **(N+O)** dendritic cells. Data were statistically analyzed by Kruskal-Wallis with Dunn's post-test. n=3-10. att.: attenuated, p(I:C): poly(I:C), trans.: transfected.

The analysis of adaptive immune cells revealed no change in B cell counts in response to any immunization (Figure 3.45 A). The percentage of CD5 expressing B cells among all B cells was reduced after the immunization with a combination of att. L3 larvae and either of the agonists. This was only statistically significant for the combination therapy of att. L3 larvae with trans. poly(I:C) (p=0.02) compared to the unimmunized group (Figure 3.45 B). The expression of I-Ab on B cells was not significantly altered by any immunization (Figure 3.45 C). CD8$^+$ T cell counts were reduced in response to all immunization strategies. This was only significant after the combination immunization with att. L3 larvae and trans. poly(I:C) (p=0.02) or 3pRNA (p=0.002) (Figure 3.45 D). CD4$^+$ T cell counts were non-significantly reduced by any immunization (Figure 3.45 E). Consequently, the CD4$^+$:CD8$^+$ T cell ratio was significantly increased in animals immunized with att. L3 larvae and trans. poly(I:C) (p=0.01) or att. L3 larvae and 3pRNA (p=0.0003), when compared to the unimmunized group (Figure 3.45 F). The increase in the CD4$^+$:CD8$^+$ T cell ratio was also significantly increased after the immunization with att. L3 larvae and 3pRNA (p=0.04) compared to the mice immunized with att. L3 larvae alone. The expression of CD11a on CD8$^+$ T cells was significantly reduced in mice immunized with a combination of att. L3 and trans. poly(I:C) (p=0.03) or 3pRNA (p=0.01) when compared to unimmunized mice (Figure 3.45 G). The expression of CTLA-4, GrzB and PD-1 by CD8$^+$ T cells was not significantly altered by any immunization strategy (Figure 3.45 H-J). Regarding CD4$^+$ T cells, there was a reduced expression of CD11a, which was significant after the immunization with att. L3 larvae and 3pRNA (p=0.01) compared to cells from unimmunized mice (Figure 3.45 K). The reduction of CLTA-4 expression by CD4$^+$ T cells from immunized compared to

unimmunized mice was not significant and the PD-1 expression by CD4⁺ T cells was not altered by any immunization strategy (3.45 L).

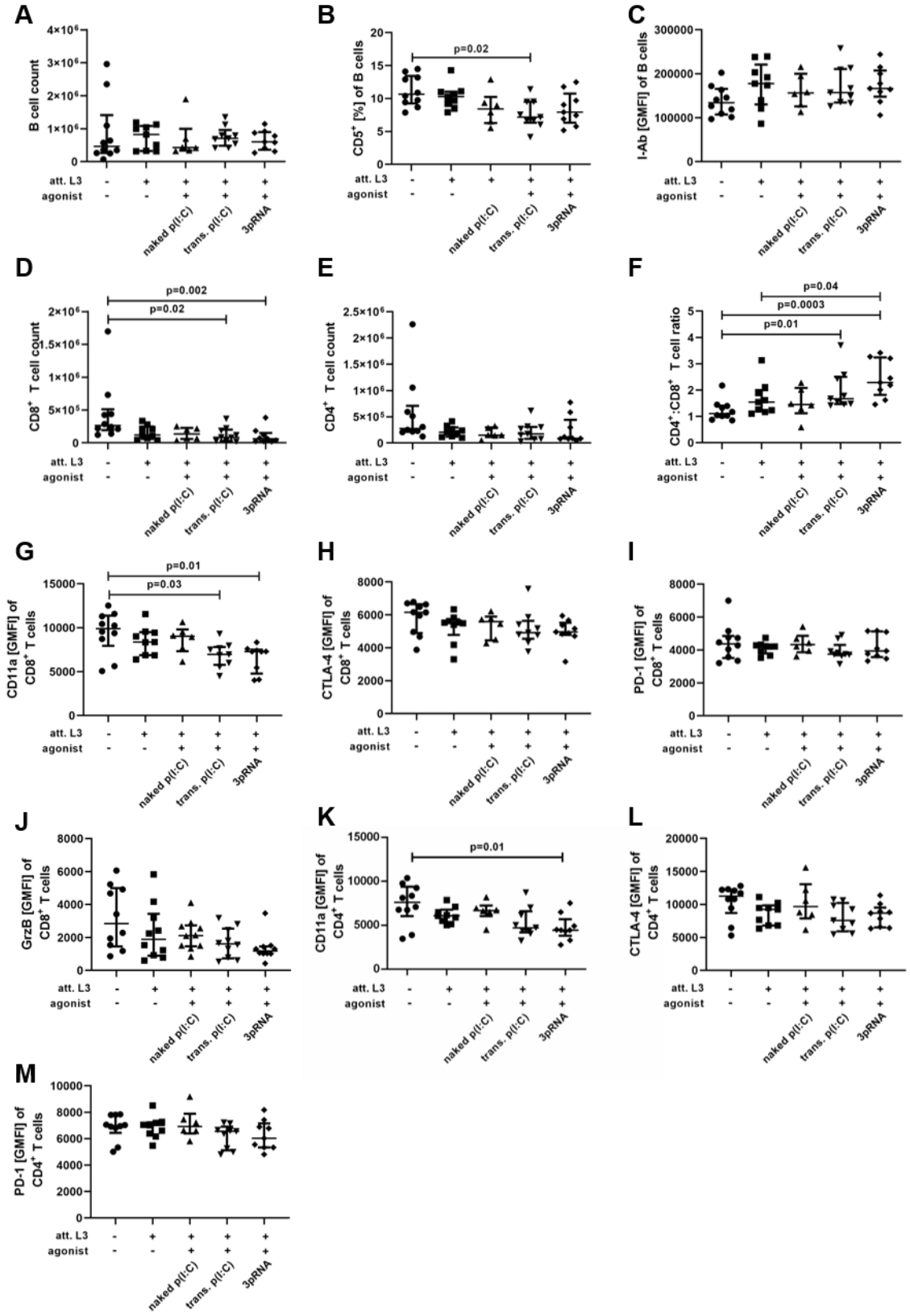

Continued on next page.

Figure 3.45| Impact on adaptive immune cell populations in the pleura of immunized mice at 63 days after infection with *Litomosoides sigmodontis*. (A-M) Mice were immunized three times every fortnight by subcutaneous injection of attenuated (att.) *L. sigmodontis* L3 larvae in combination with 20µg of naked poly(I:C) (p(I:C)), transfected (trans.) p(I:C) or 3pRNA. Trans. p(I:C) and 3pRNA were complexed with *in vivo*-jetPEI®. Two weeks after the last injection, the mice were naturally infected with *L. sigmodontis*. 63 days after infection cell populations were analyzed by flow cytometry. **(A)** Cell count **(B)** percentage of $CD5^+$ and **(C)** I-Ab expression of B cells ($CD19^+$). Cell counts of **(D)** $CD8^+$ T cells ($CD19^-CD3^+CD4^-CD8^+$) and **(E)** $CD4^+$ T cells ($CD19^-CD3^+CD4^+CD8^-$). **(F)** $CD4^+$ T cell to $CD8^+$ T cell ratio based on cell counts. Expression of **(G)** CD11a, **(H)** CTLA-4, **(I)** PD-1 and **(J)** Granzyme B (GrzB) by $CD8^+$ T cells. Expression of **(K)** CD11a, **(L)** CTLA-4 and **(M)** PD-1 by $CD4^+$ T cells. Data were statistically analyzed by Kruskal-Wallis with Dunn's post-test. n=6-10. att.: attenuated, p(I:C): poly(I:C), GrzB: Granzyme B, trans.: transfected.

Overall, no major differences due to any immunization strategy in cell counts and cell activation in the pleural cavity were detected.

In addition to identifying cellular populations, soluble immune mediators were quantified in the pleural cavity by ELISA (Figure 3.46).

There were no significant differences between the groups regarding IL-5, IL-12, IL-10, and TNF concentrations (Figure 3.46 A – D). Most immunized mice had lower levels of GrzB than unimmunized mice, but the reduction was only statistically significant compared to animals that were immunized with a combination therapy of att. L3 larvae and 3pRNA (p=0.002) (Figure 3.46 E). At the same time, IFN-γ concentrations were highest in unimmunized animals and were significantly reduced in animals that were immunized with att. L3 larvae and trans. poly(I:C) (p=0.009) and animals immunized with att. L3 larvae and 3pRNA (p=0.004) (Figure 3.46 F). The concentrations of the chemokines IP-10 (CXCL10), KC (CXCL1) and Eotaxin-1 (CCL11) were similar in all groups (Figure 3.46 G – I). The concentration of the chemokine RANTES (CCL5) was highest in unimmunized animals and significantly reduced after the immunization with a combination therapy with att. L3 larvae and naked poly(I:C) (p=0.001), trans. poly(I:C) (p=0.001) and 3pRNA (p=0.001) (Figure 3.46 J). The relative quantification of parasite-specific IgE and IgG2a/b antibodies revealed no significant differences among the groups (Figure 3.46 K + M). The level of parasite-specific IgG1 antibodies was significantly reduced in animals immunized with att. L3 larvae and 3pRNA compared to unimmunized mice (p=0.01) and compared to animals immunized with att. L3 larvae alone (p=0.03) (Figure 3.46 L).

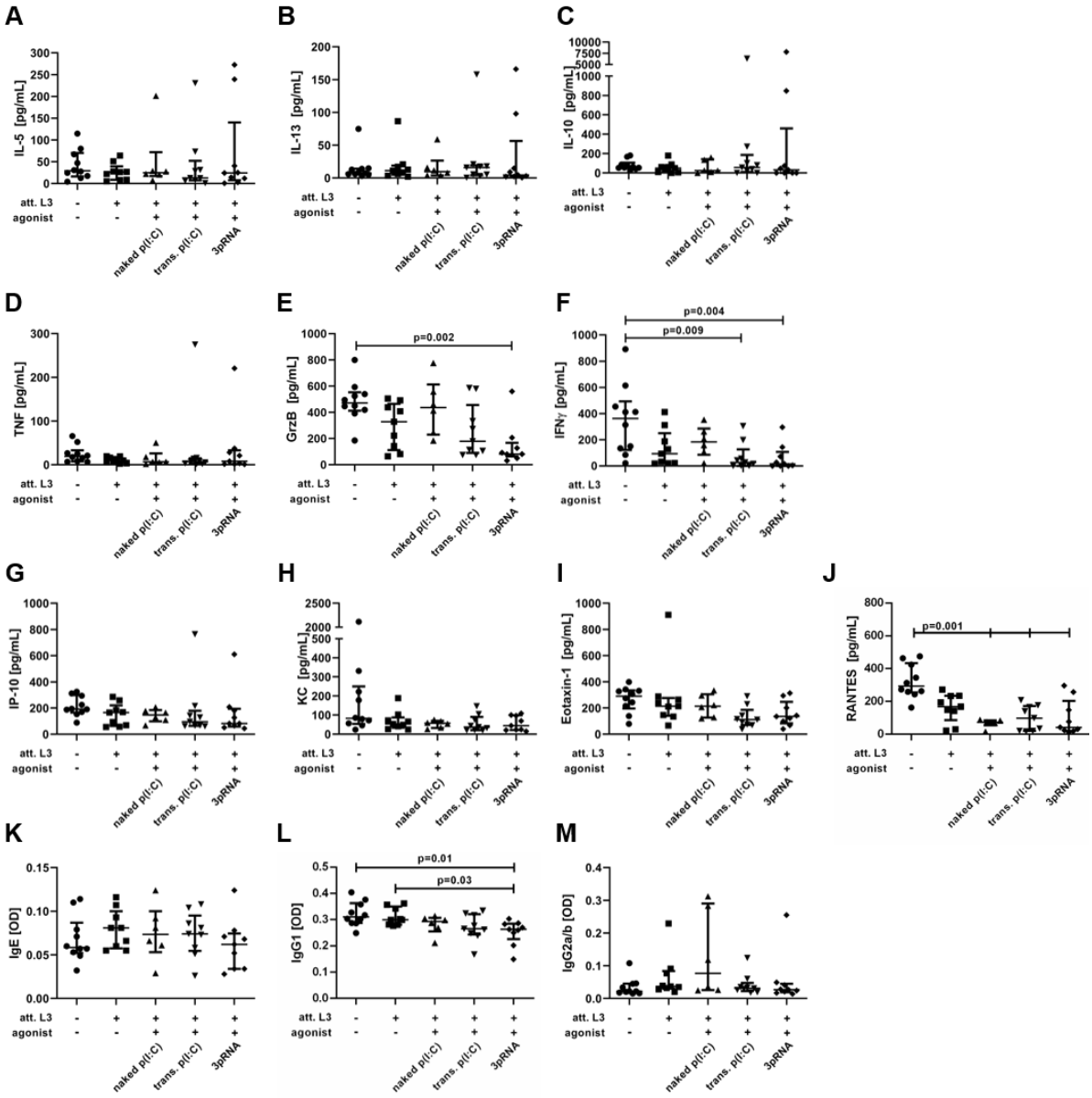

Figure 3.46| Changes in soluble immune mediators in the pleural cavity 63 days after infection with *L. sigmodontis* in previously immunized animals. (A-M) Mice were immunized three times every fortnight by subcutaneous injection of attenuated (att.) *L. sigmodontis* L3 larvae in combination with 20µg of naked poly(I:C) (p(I:C)), transfected (trans.) p(I:C) or 3pRNA. Trans. p(I:C) and 3pRNA were complexed with *in vivo*-jetPEI®. Two weeks after the last injection, the mice were naturally infected with *L. sigmodontis*. 63 days after infection cytokines were quantified in the pleural cavity by ELISA **(A-J)** and parasite-specific antibodies were relatively quantified by ELISA **(K-M)**. Concentration of **(A)** IL-5, **(B)** IL-13, **(C)** IL-10, **(D)** TNF, **(E)** Granzyme B, **(F)** IFN-γ, **(G)** IP-10 (CXCL10), **(H)** KC (CXCL1), **(I)** Eotaxin-1 (CCL-11) and **(J)** RANTES (CCL5). Relative concentration of parasite-specific **(K)** IgE, **(L)** IgG1 and **(M)** IgG2a/b. Error bars show median with IQR. Data were statistically analyzed by Kruskal-Wallis with Dunn's post-test. n=6-10. Representative for two individual experiments apart from naked p(I:C). att.: attenuated, GrzB: Granzyme B, p(I:C): poly(I:C), trans.: transfected.

Table 3.4 summarizes the immunological analysis of the pleura on day 63 after infection with *L. sigmodontis*. Overall, minor changes were detected in the pleural cavity due to any immunization protocol and the detected changes mostly indicate reduced immune reactions.

Table 3.4: Overview of relative immunological changes in the pleural cavity of immunized and *L. sigmodontis*-infected mice. Mice were immunized three times every fortnight by subcutaneous injection of attenuated (att.) *L. sigmodontis* L3 larvae in combination with 20µg of naked poly(I:C) (p(I:C)), transfected (trans.) p(I:C) or 3pRNA. Trans. p(I:C) and 3pRNA were complexed with *in vivo*-jetPEI®. Two weeks after the last injection, mice were naturally infected with *L. sigmodontis*. On day 63 after infection, pleural cells were analyzed via flow cytometry and cytokines and parasite-specific antibodies in the pleural lavage were quantified by ELISA. The original data (n=6-10, ELISA data representative for 2 individual experiments) summarized in this table were statistically analyzed by Kruskal-Wallis with Dunn's post-test. Statistically significant changes are indicated as ↑ ↓. Statistically non-significant changes with a p-value <0.3 are indicated as ↗ ↘.
att.: attenuated, MF: macrophage, p(I:C): poly(I:C), trans.: transfected

Continued on next page.

Celltype	Parameter	Compared to control				Compared to att. L3		
		Att. L3	Att. L3 + naked p(I:C)	Att. L3 + trans. p(I:C)	Att. L3 + 3pRNA	Att. L3 + naked p(I:C)	Att. L3 + trans. p(I:C)	Att. L3 + 3pRNA
eosinophils	Count	↔	↔	↔	↔	↔	↔	↔
	I-Ab	↔	↔	↓	↔	↔	↘	↔
	CD86	↘	↔	↔	↔	↔	↔	↗
neutrophils	Count	↔	↔	↘	↔	↔	↔	↔
	I-Ab	↔	↔	↔	↔	↔	↘	↔
	CD86	↔	↔	↔	↔	↔	↔	↔
M2-like MΦ	Count	↔	↔	↔	↔	↔	↔	↔
	I-Ab	↔	↔	↘	↔	↔	↘	↔
	CD86	↔	↔	↔	↔	↔	↔	↔
RELMα^{low}	Count	↔	↔	↘	↘	↔	↔	↔
	I-Ab	↔	↔	↔	↔	↔	↔	↔
	CD86	↘	↔	↔	↔	↔	↔	↔
DC	Count	↔	↔	↔	↔	↔	↔	↔
	I-Ab	↔	↔	↘	↔	↔	↘	↔
	CD86	↔	↔	↔	↔	↔	↔	↔
B cells	Count	↔	↔	↔	↔	↔	↔	↔
	% CD5^{+}	↔	↘	↓	↘	↘	↘	↘
	I-Ab	↔	↔	↔	↔	↔	↔	↔
CD4:CD8	ratio	↔	↔	↑	↑	↔	↔	↑
CD4 T cells	Count	↔	↔	↔	↔	↔	↔	↔
	CD11a	↔	↔	↘	↓	↔	↔	↘
	CTLA-4	↔	↔	↘	↘	↔	↔	↔
	PD-1	↔	↔	↔	↔	↔	↔	↔
CD8 T cells	Count	↘	↘	↓	↓	↔	↔	↔
	CD11a	↔	↔	↓	↓	↔	↔	↘
	CTLA-4	↔	↔	↔	↔	↔	↔	↔
	PD-1	↔	↔	↔	↔	↔	↔	↔
	GrzB	↔	↔	↔	↘	↔	↔	↔
	IgE	↔	↔	↔	↔	↔	↔	↔
	IgG1	↔	↔	↔	↓	↔	↔	↓
	IL-5	↔	↔	↔	↔	↔	↔	↔
	IL-13	↔	↔	↔	↔	↔	↔	↔
	KC	↔	↔	↔	↔	↔	↔	↔
	Eotaxin-1	↔	↔	↔	↔	↔	↔	↔
	RANTES	↘	↓	↓	↓	↔	↔	↔
	GrzB	↔	↔	↔	↓	↔	↔	↔
	IFN-γ	↔	↔	↓	↓	↔	↔	↔
	IP-10	↔	↔	↔	↔	↔	↔	↔
	TNF	↔	↔	↔	↔	↔	↔	↔
	IgG2a/b	↔	↔	↔	↔	↔	↔	↔

3.6.7 Systemic immune milieu in the spleen 63 days after infection

In addition to analyzing local immune responses in the pleural cavity, systemic responses in the spleen as secondary lymphoid organ were analyzed. To that end the cells were quantified, different populations were analyzed by flow cytometry and the secretion of cytokines and chemokines was quantified by ELISA.

The total splenocyte count was not significantly altered by any immunization strategy (Figure 3.47).

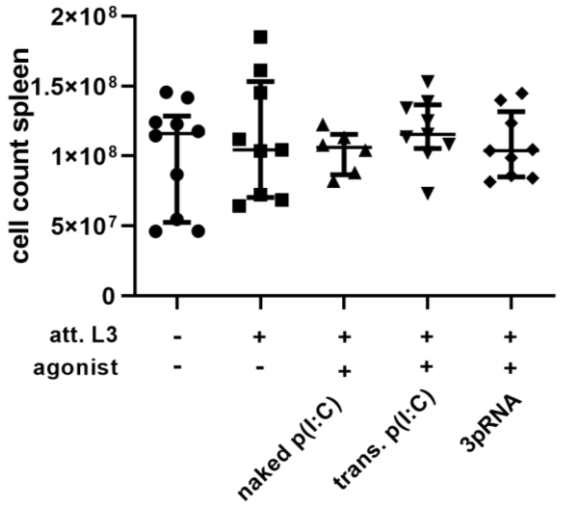

Figure 3.47| No impact of immunization on total splenocyte count. Mice were immunized three times every fortnight by subcutaneous injection of attenuated (att.) *L. sigmodontis* L3 larvae in combination with 20µg of naked poly(I:C) (p(I:C)), transfected (trans.) p(I:C) or 3pRNA. Trans. p(I:C) and 3pRNA were complexed with *in vivo*-jetPEI®. Two weeks after the last injection, the mice were naturally infected with *L. sigmodontis*. 63 days after infection the total organ cell count was determined. n=6-10.
att.: attenuated, p(I:C): poly(I:C), trans.: transfected.

In order to identify changes in spleen cell populations the cells were analyzed by flow cytometry. Innate immune cells like dendritic cells, monocytes, neutrophils and eosinophils were gated as shown in Figure 3.48 A. B cell and T cell populations were identified according to the gating presented for pleural cells in Figure 3.42 A.

The T cell subtypes effector T cells (Tef) and central memory T cells (Tcm) were identified for $CD4^+$ T cells and $CD8^+$ T cells as depicted in Figure 3.48 B. T helper subsets were distinguished based on the intracellular staining of transcription factors as depicted in Figure 3.48 C.

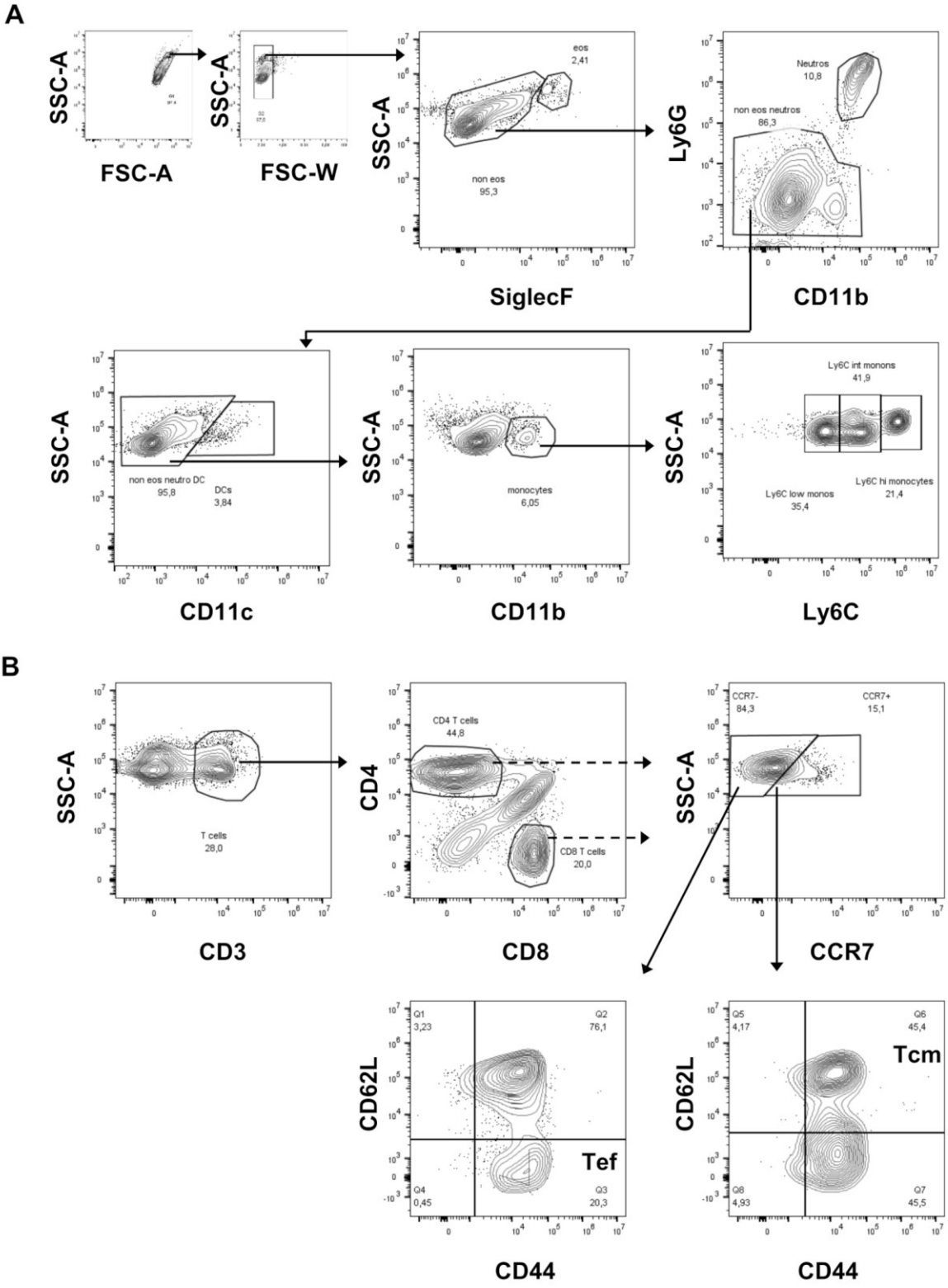

Continued on next page.

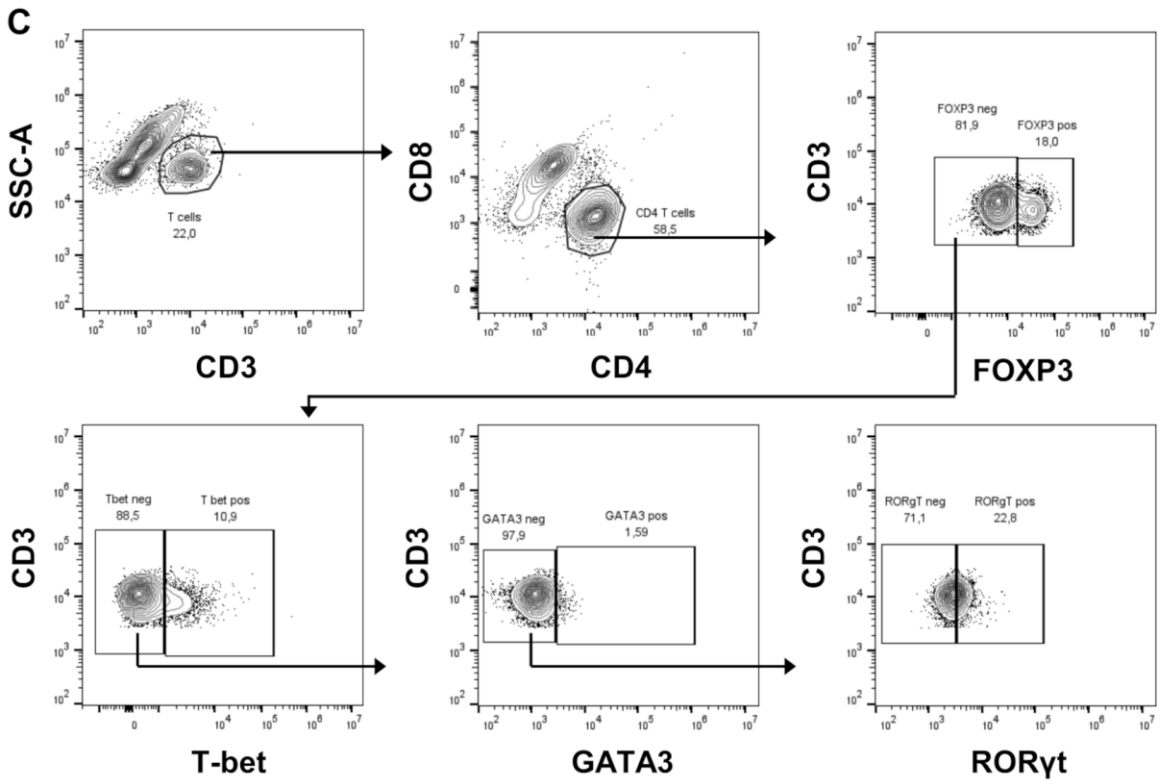

Figure 3.48| Gating strategy for flow cytometric analysis of the spleen. Gating to identify **(A)** myeloid cell populations by the expression of SiglecF on eosinophils, Ly6G on neutrophils, CD11c on dendritic cells and Ly6C on monocytes, **(B)** effector T cells and central memory T cells by the expression of CD3, CD4, CD8, CCR7, CD26L and CD44 and **(C)** T helper subsets by the expression of CD3, CD4 as well as the transcription factors FOXP3, T-bet, GATA3 and RORγt. **(A-C)** Fluorescence minus one (FMO) controls were applied for gating.

There was no significant impact by any immunization on the count of dendritic cells, Ly6C^{hi} monocytes, Ly6C^{int} monocytes, neutrophils and eosinophils (Figure 3.49 A + G + J + M + P). Only the number of Ly6C^{low} monocytes was significantly increased after the combination immunization with att. L3 larvae and 3pRNA (p=0.049) compared to cells from unimmunized animals (Figure 3.49 D). Further, the immunization had no significant impact on the expression of I-Ab and CD86 by dendritic cells, Ly6C^{hi} monocytes, Ly6C^{int} monocytes, Ly6C^{low} monocytes and neutrophils (Figure 3.49 B + C, E + F, H + I, K + L, N + O). The expression of I-Ab by eosinophils was significantly reduced after the combination immunization with att. L3 larvae and 3pRNA (p=0.006) compared to eosinophils from unimmunized mice (Figure 3.49 Q). The CD86 expression on eosinophils was not significantly altered by any immunization (Figure 3.49 R).

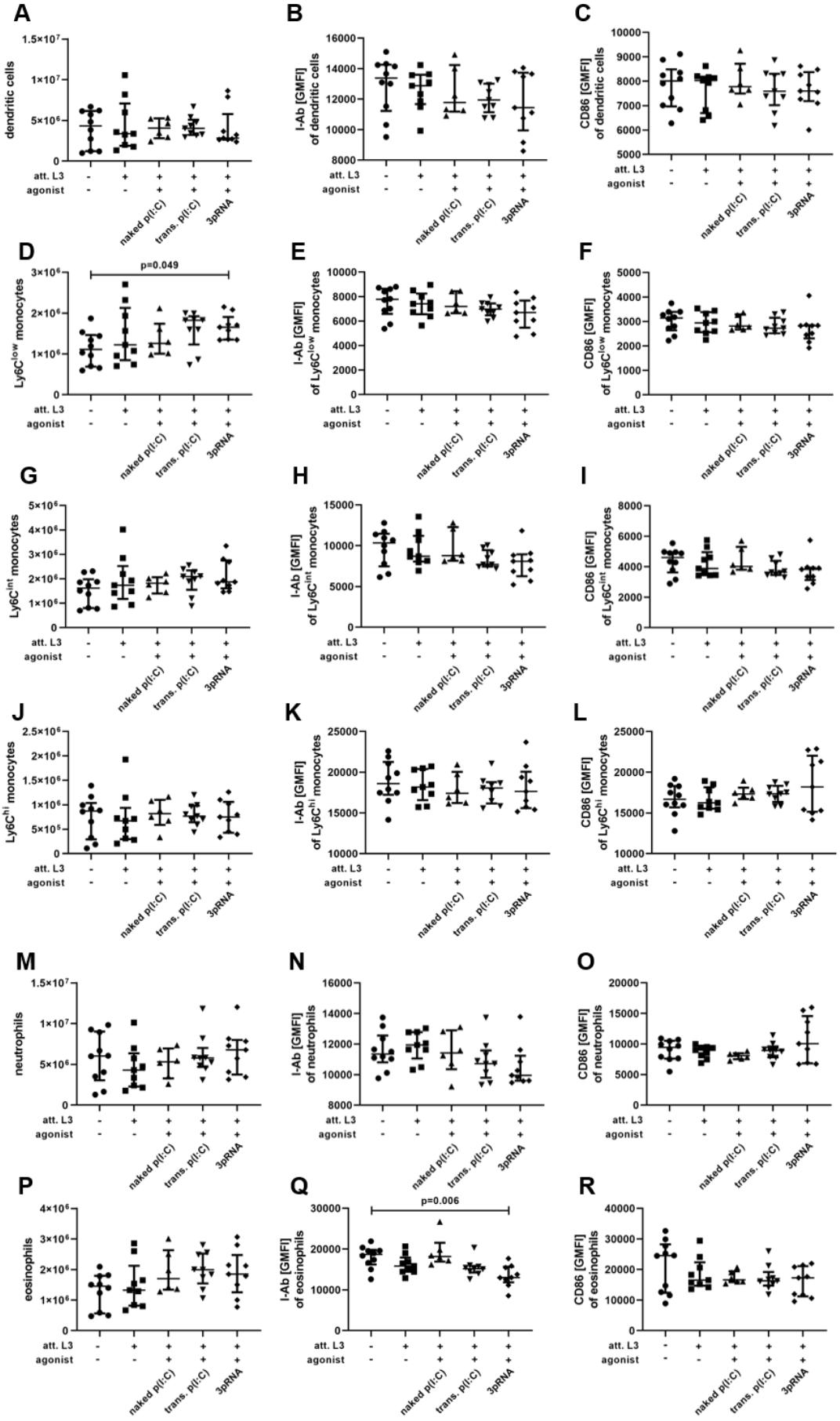

Continued on next page.

Figure 3.49| Minor impact on innate immune cell populations in the spleens of immunized mice at 63 days after infection with *L. sigmodontis*. (A-R) Mice were immunized three times every fortnight by subcutaneous injection of attenuated (att.) *L. sigmodontis* L3 larvae in combination with 20µg of naked poly(I:C) (p(I:C)), transfected (trans.) p(I:C) or 3pRNA. Trans. p(I:C) and 3pRNA were complexed with *in vivo*-jetPEI®. Two weeks after the last injection, the mice were naturally infected with *L. sigmodontis*. 63 days after infection cell populations were analyzed by flow cytometry. Cell counts of **(A)** dendritic cells (SiglecF$^-$Ly6G$^-$CD11c$^+$), **(D)** Ly6C^{hi} monocytes (SiglecF$^-$Ly6G$^-$CD11c$^-$CD11b$^+$Ly6C^{hi}), **(G)** Ly6C^{int} monocytes (SiglecF$^-$Ly6G$^-$CD11c$^-$CD11b$^+$Ly6C^{int}), **(J)** Ly6C^{low} monocytes (SiglecF$^-$Ly6G$^-$CD11c$^-$CD11b$^+$Ly6C^{low}), **(M)** neutrophils (SiglecF$^-$CD11b$^+$Ly6G$^+$) and **(P)** eosinophils (SiglecF$^+$). Expression of I-Ab and CD86 by **(B+C)** dendritic cells, **(E+F)** Ly6C^{hi} monocytes, **(H+I)** Ly6C^{int} monocytes, **(K+L)** Ly6C^{low} monocytes, **(N+O)** neutrophils and **(Q+R)** eosinophils. Data were statistically analyzed by Kruskal-Wallis with Dunn's post-test. n=6-10. att.: attenuated, p(I:C): poly(I:C), trans.: transfected.

The impact of the immunization on adaptive immune cells in the spleen is shown in Figure 3.50. Neither B cell counts nor their expression of I-Ab was significantly altered by any immunization (Figure 3.50 A – B). Also, the counts of CD8$^+$ and CD4$^+$ T cells were not significantly altered by any immunization (Figure 3.50 C + D). But the immunization with att. L3 larvae alone led to a significantly increased CD4$^+$: CD8$^+$ T cell ratio, compared to the combination immunization with att. L3 larvae and trans. poly(I:C) (p=0.02) (Figure 3.50 E). After immunization with att. L3 larvae CD8$^+$ T cells from the spleen had decreased CD11a (p=0.01), CTLA-4, PD-1 (p=0.02) and GrzB expression (Figure 3.50 F - I). The reduced expression of CD11a by CD8$^+$ T cells was also observed after immunization with att. L3 larvae and 3pRNA (p=0.006), but not with either poly(I:C) treatment (Figure 3.50 F). The reduction of CTLA-4 expression appeared less pronounced after any combination immunization compared to the immunization with att. L3 alone, no changes reached statistical significance (Figure 3.50 G). The PD-1 expression of CD8$^+$ T cells after the combination immunization with any agonist was significantly higher than after the immunization with att. L3 larvae alone and resembled the PD-1 expression of cells from unimmunized mice (Figure 3.50 H). The GrzB expression was non-significantly reduced in response to any immunization (Figure 3.50 I). None of the immunization protocols had a significant impact on the frequencies of splenic CD8$^+$ Tcm and Tef (Figure 3.50 J + K). The expression of CD11a by CD4$^+$ T cells was significantly reduced after the immunization with att. L3 larvae alone (p=0.006) or in combination with 3pRNA (p=0.002), when compared to cells from unimmunized animals (Figure 3.50 L). A similar, but non-significant, pattern was observed for the expression of CTLA-4 by CD4$^+$ T cells (Figure

3.50 M). The expression of PD-1 by $CD4^+$ T cells was significantly reduced only after immunization with att. L3 larvae alone compared to cells from unimmunized mice ($p=0.02$) (Figure 3.50 N). The frequency of $CD4^+$ Tcm was not significantly affected by any immunization (Figure 3.50 O). The frequency of $CD4^+$ Tef was significantly increased ($p=0.02$) after immunization with att. L3 larvae alone, when compared to unimmunized mice (Figure 3.50 P). Among the population of $CD4^+$ T cells the frequency of $GATA3^+$ T cells was increased (Figure 3.50 Q), but this was only significant in animals immunized with a combination of att. L3 larvae and naked poly(I:C) ($p=0.02$) compared to unimmunized mice (Figure 3.50 Q). Concomitantly, the frequencies of T-bet^+ Th1 cells, $ROR\gamma t^+$ Th17 cells and $FOXP3^+$ Tregs were reduced (Figure 3.50 R – T). The reduction of Th1 cells was significant after the immunization with att. L3 and 3pRNA compared to unimmunized mice. The reduction of Th17 cells was significant after the immunization with att. L3 and trans. poly(I:C) or 3pRNA compared to unimmunized mice or the immunization with att. L3 larvae alone.

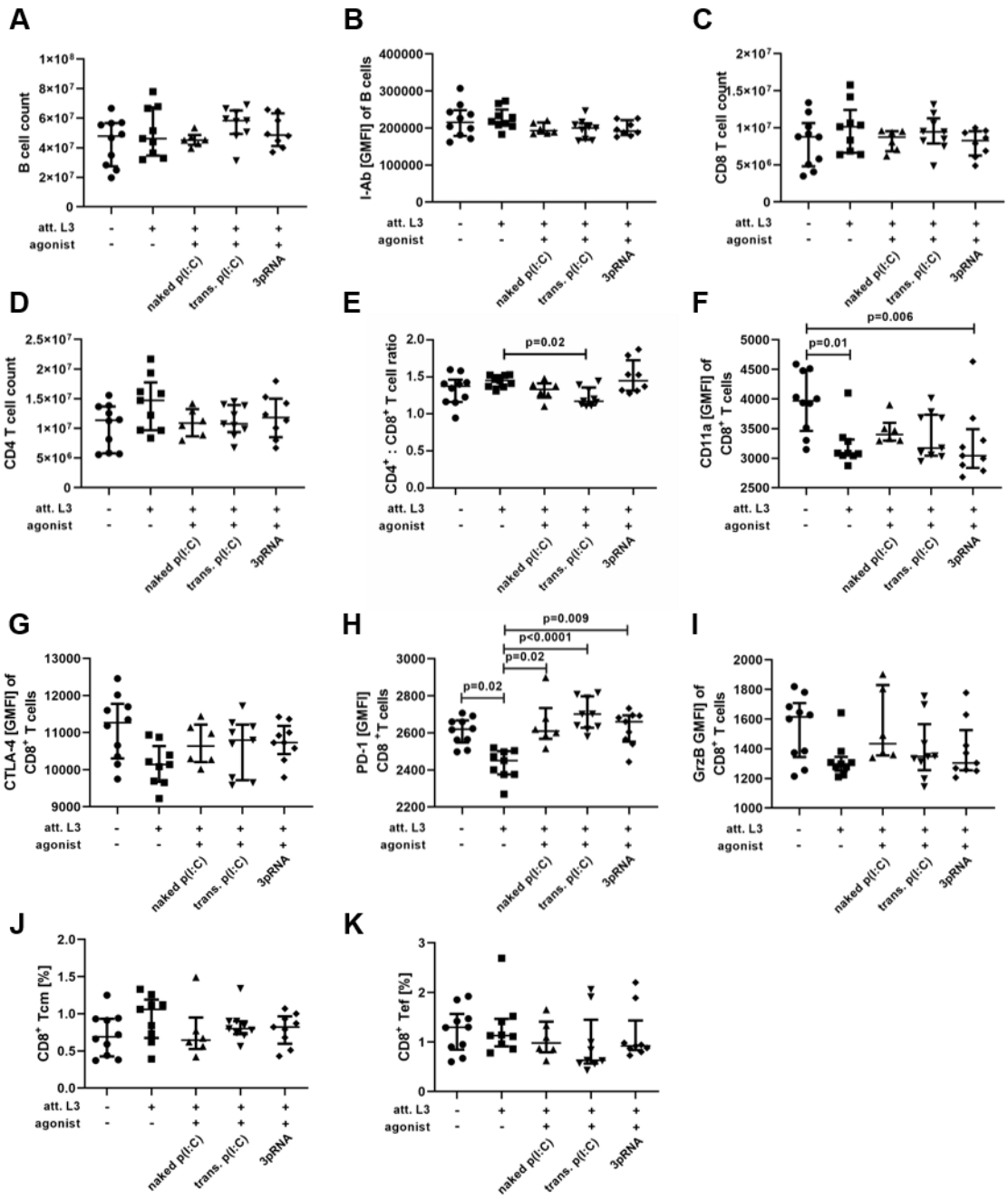

Continued on next page.

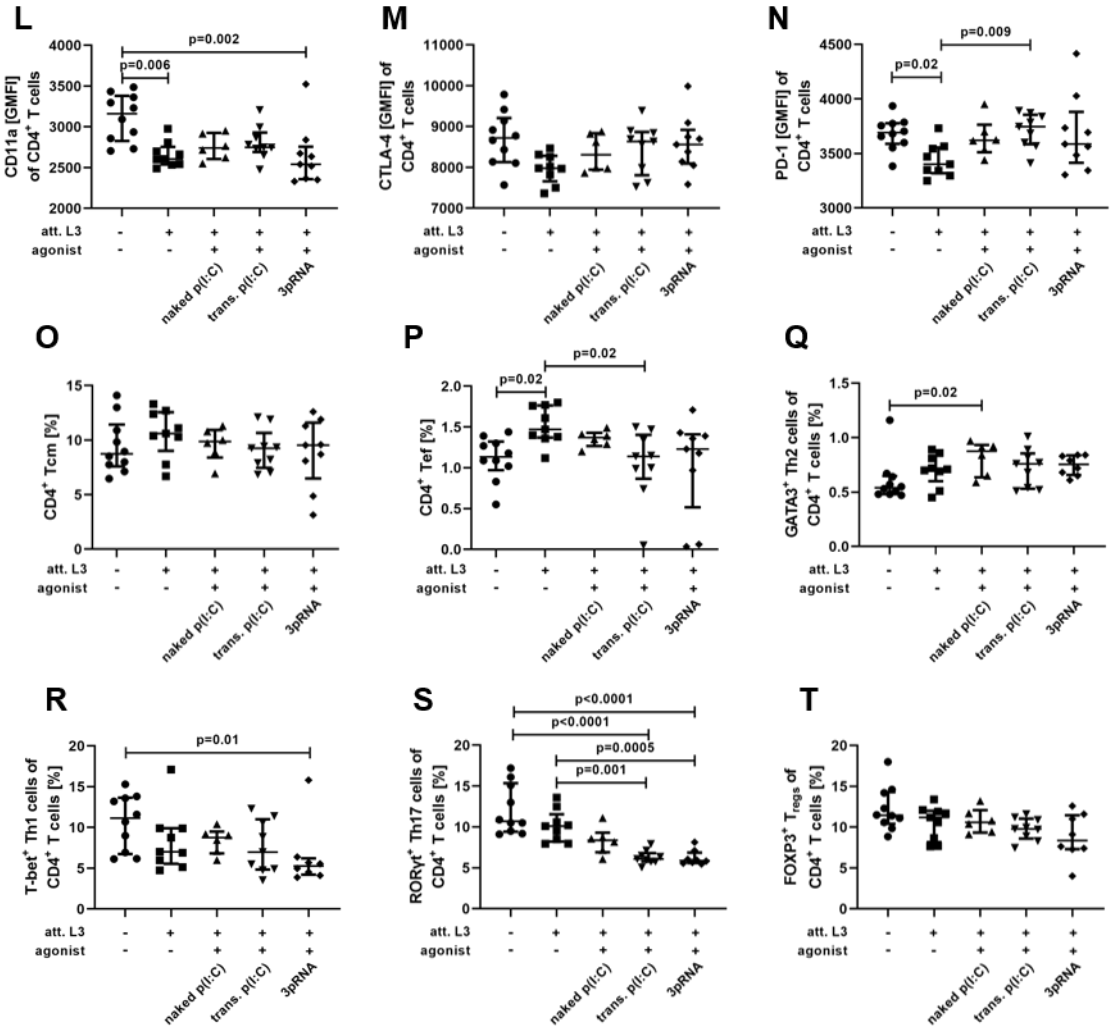

Figure 3.50| Impact on adaptive immune cell populations in the spleens of immunized mice at 63 days after infection with *Litomosoides sigmodontis*. (A-T) Mice were immunized three times every fortnight by subcutaneous injection of attenuated (att.) *L. sigmodontis* L3 larvae in combination with 20µg naked poly(I:C) (p(I:C)), transfected (trans.) p(I:C) or 3pRNA. Trans. p(I:C) and 3pRNA were complexed with *in vivo*-jetPEI®. Two weeks after the last injection, the mice were naturally infected with *L. sigmodontis*. 63 days after infection cell populations were analyzed by flow cytometry. **(A)** Cell count and **(B)** I-Ab expression of B cells ($CD19^+$). Cell counts of **(C)** $CD8^+$ T cells ($CD19^-CD3^+CD4^-CD8^+$) and **(D)** $CD4^+$ T cells ($CD19^-CD3^+CD4^+CD8^-$). **(E)** $CD4^+$ T cell to $CD8^+$ T cell ratio based on cell counts. Expression of **(F)** CD11a, **(G)** CTLA-4, **(H)** PD-1 and **(I)** Granzyme B (GrzB) by $CD8^+$ T cells. Frequency of **(J)** $CD8^+$ central memory T cells (Tcm) ($CD3^+CD8^+CCR7^+CD62L^+CD44^+$) and **(K)** $CD8^+$ effector T cells (Tef) ($CD3^+CD8^+CCR7^-CD62L^-CD44^+$). Expression of **(L)** CD11a, **(M)** CTLA-4 and **(N)** PD-1 by $CD4^+$ T cells. Frequency of **(O)** $CD4^+$ Tcm ($CD3^+CD4^+CCR7^+CD62L^+CD44^+$) and **(P)** $CD4^+$ Tef ($CD3^+CD8^+CCR7^-CD62L^-CD44^+$). Frequency of **(Q)** $GATA3^+$ Th2 cells ($CD3^+CD4^+CD8^-FOXP3^-T\text{-}bet^-GATA3^+$), **(R)** $T\text{-}bet^+$ Th1 cells ($CD3^+CD4^+CD8^-FOXP3^-T\text{-}bet^+$), **(S)** $ROR\gamma t^+$ TH17 cells ($CD3^+CD4^+CD8^-FOXP3^-GATA3^-T\text{-}bet^-ROR\gamma t^+$), and **(T)** $FOXP3^+$ regulatory T cells ($CD3^+CD4^+CD8^-FOXP3^+$), among all $CD4^+$ T cells. Data were statistically analyzed by Kruskal-Wallis with Dunn's post-test. n=6-10. att.: attenuated, GrzB: Granzyme B, p(I:C): poly(I:C), Tcm: central memory T cell, Tef: effector T cell, trans.: transfected.

Further, the cytokine and chemokine secretion by splenocytes isolated from the different immunization groups were quantified by ELISA following *in vitro* culture. Additionally, cells were restimulated with ConA to evaluate general cell responsiveness and with LsAg in order to analyze responsiveness to the infective agent (Figure 3.51). The stimulation with ConA induced the secretion of IL-5, IL-13, IL-10, IFN-γ, IP-10 (CXCL10) and RANTES (CCL5) (Figure 3.51 A – E + G), but not KC (CXCL1) (Figure 3.51 F).

Unstimulated splenocytes from unimmunized control mice did not release IL-5, while splenocytes from all immunized groups did (Figure 3.51 A). The release was significantly increased after immunization with att. L3 larvae alone (p=0.01), in combination with naked poly(I:C) (p=0.003) or trans. poly(I:C) (p=0.0006), but not after the combination therapy of att. L3 larvae and 3pRNA. The restimulation with LsAg induced IL-5 secretion by splenocytes from all groups, however, compared to the unimmunized group, this was significantly higher after immunization with att. L3 larvae and naked poly(I:C) (p=0.02) or trans. poly(I:C) (p=0.007). Unstimulated splenocytes from unimmunized animals secreted low levels of IL-13 (Figure 3.51 B). The IL-13 concentration was higher in all immunized groups. This was statistically significant after the immunization with a combination therapy of att. L3 larvae and naked poly(I:C) (p=0.002) and a combination therapy of att. L3 larvae and trans. poly(I:C) (p=0.009) compared to the control group. The IL-13 secretion in response to LsAg restimulation was comparable among all groups. Overall, regarding IL-10 concentrations there was a great variance within groups (Figure 3.51 C). IL-10 release was lowest in unstimulated cells. Unstimulated cells from animals immunized with att. L3 larvae and naked poly(I:C) released significantly more IL-10 than cells from control animals (p=0.004). The restimulation with LsAg increased IL-10 concentration in all groups compared to the unstimulated controls. Between groups the concentrations in response to LsAg restimulation were significantly increased in samples from mice immunized with att. L3 larvae and naked poly(I:C) (p=0.005) and from mice immunized with att. L3 larvae and trans. poly(I:C) (p=0.02), when compared to samples from mice that were only immunized with att. L3 larvae alone.

Unstimulated splenocytes from unimmunized control mice did not release IFN-γ, while splenocytes from immunized mice did (Figure 3.51 D). The difference was significant after the immunization with a combination therapy of att. L3 larvae and naked poly(I:C) (p=0.0007) and a combination therapy with att. L3 larvae and trans. poly(I:C)

(p<0.0001). Further, the concentration of IFN-γ was significantly higher in samples from mice immunized with att. L3 larvae and trans. poly(I:C) (p=0.047) compared to the immunization with att. L3 larvae alone. The restimulation with LsAg induced IFN-γ release in all groups. Compared to splenocytes from mice immunized with att. L3 larvae alone, the IFN-γ concentrations were significantly higher after the immunization with a combination therapy of att. L3 larvae and naked poly(I:C) (p=0.03) and att. L3 larvae and trans. poly(I:C) (p=0.004).

Unstimulated splenocytes released low levels of the chemokine IP-10 (Figure 3.51 E). Still, the IP-10 concentration was significantly higher in samples from unstimulated splenocytes from mice immunized with a combination of att. L3 larvae and naked poly(I:C) compared to splenocytes from unimmunized control animals (p= 0.008) and from mice immunized with att. L3 larvae alone (p=0.007). The restimulation with LsAg induced IP-10 release by splenocytes from all groups. The concentration was lowest in samples from mice immunized with att. L3 alone or in combination with 3pRNA. The combination immunization with naked poly(I:C) (p=0.004) or trans. poly(I:C) (p=0.048) resulted in a significantly higher IP-10 response by splenocytes to LsAg compared to splenocytes from animals immunized with att. L3 larvae alone.

KC was only released in response to LsAg restimulation (Figure 3.51 F). Concentrations varied greatly among groups and no differences between groups were detected.

Unstimulated splenocytes from all groups released similar level of RANTES (Figure 3.51 G). In all groups RANTES concentrations increased after LsAg restimulation and no significant differences between groups were detected.

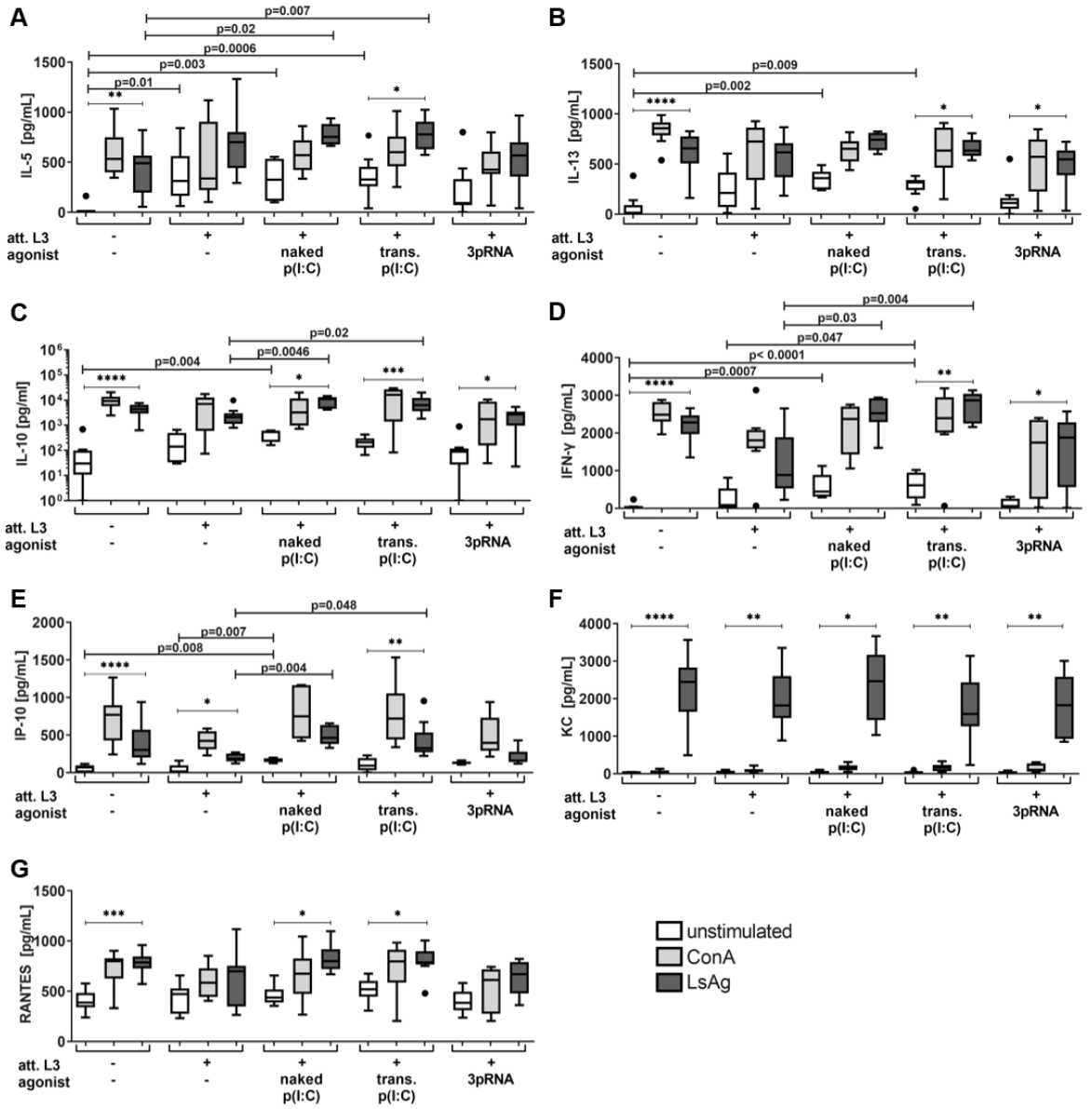

Figure 3.51| Cytokine release by splenocytes 63 days after infection with *Litomosoides sigmodontis* in previously immunized animals in response to LsAg and ConA restimulation (A-G) Mice were immunized three times every fortnight by subcutaneous injection of attenuated (att.) *L. sigmodontis* L3 larvae in combination with 20µg of naked poly(I:C) (p(I:C)), transfected (trans.) p(I:C) or 3pRNA. Trans. p(I:C) and 3pRNA were complexed with *in vivo*-jetPEI®. Two weeks after the last injection, the mice were naturally infected with *L. sigmodontis*. 63 days after infection splenocytes were isolated and restimulated with 25µg/ml LsAg or 2.5µg/mLConA for 72h. Supernatant was used collected and chemokines and cytokines were quantified by ELISA **(A-G)**. Concentration of **(A)** IL-5, **(B)** IL-13, **(C)** IL-10, **(D)** IFN-γ, **(E)** IP-10 (CXCL10), **(F)** KC (CXCL1) and **(G)** RANTES (CCL5). Data plotted as Tukey box and whiskers blot. Data were statistically analyzed by Kruskal-Wallis with Dunn's post-test. *p<0.05, **p<0.01, ***p<0.001, ****p<0.0001. n=6-10. Representative for two individual experiments apart from naked p(I:C).
att.: attenuated, p(I:C): poly(I:C), trans.: transfected.

Overall, only minor changes in splenic cell populations in response to any immunization strategy were detected by flow cytometry, summarized in table 3.5. Most changes were observed regarding the activation status of T cells. However, splenocytes from immunized animals released higher levels of cytokines. For the type 1-associated cytokine IFN-γ and the chemokine IP-10 the concentrations were further enhanced by a combination immunization of att. L3 larvae and agonist.

Table 3.5: Overview of relative immunological changes in the spleen of immunized and *L. sigmodontis*-infected mice. Mice were immunized three times every fortnight by subcutaneous injection of attenuated (att.) *L. sigmodontis* L3 larvae in combination with 20µg of naked poly(I:C) (p(I:C)), transfected (trans.) p(I:C) or 3pRNA. Trans. p(I:C) and 3pRNA were complexed with *in vivo*-jetPEI®. Two weeks after the last injection, mice were naturally infected with *L. sigmodontis*. On day 63 after infection, splenocytes were analyzed via flow cytometry and cytokine secretion by unstimulated splenocytes was quantified in the 72 h supernatant by ELISA. The original data (n=6-10, ELISA data representative for 2 individual experiments) summarized in this table were statistically analyzed by Kruskal-Wallis with Dunn's post-test. Statistically significant changes are indicated as ↑ ↓. Statistically non-significant changes with a p-value <0.3 are indicated as ↗ ↘.
att.: attenuated, mono: monocyte, p(I:C): poly(I:C), trans.: transfected
Continued on next page.

Celltype	Parameter	Compared to control				Compared to att. L3		
		Att. L3	Att. L3 + naked p(I:C)	Att. L3 + trans. p(I:C)	Att. L3 + 3pRNA	Att. L3 + naked p(I:C)	Att. L3 + trans. p(I:C)	Att. L3 + 3pRNA
DC	Count	↔	↔	↔	↔	↔	↔	↔
	I-Ab	↔	↔	↔	↔	↔	↔	↔
	CD86	↔	↔	↔	↔	↔	↔	↔
Ly6C^{low} mono	Count	↔	↔	↗	↑	↔	↔	↔
	I-Ab	↔	↔	↔	↘	↔	↔	↔
	CD86	↔	↔	↔	↔	↔	↔	↔
Ly6C^{int} mono	Count	↔	↔	↗	↗	↔	↔	↔
	I-Ab	↔	↔	↔	↘	↔	↔	↘
	CD86	↔	↔	↔	↔	↔	↔	↔
Ly6C^{hi} mono	Count	↔	↔	↔	↔	↔	↔	↔
	I-Ab	↔	↔	↔	↔	↔	↔	↔
	CD86	↔	↔	↔	↔	↔	↔	↔
neutrophils	Count	↔	↔	↔	↔	↔	↔	↗
	I-Ab	↔	↔	↔	↘	↔	↘	↘
	CD86	↔	↔	↔	↔	↔	↔	↔
eosinophils	Count	↔	↔	↗	↗	↔	↔	↔
	I-Ab	↔	↔	↘	↓	↔	↘	↘
	CD86	↔	↔	↔	↔	↔	↔	↔
B cells	Count	↔	↔	↔	↔	↔	↔	↔
	I-Ab	↔	↔	↔	↔	↔	↔	↔
CD4:CD8	ratio	↔	↔	↔	↔	↘	↓	↔
CD4 T cells	Count	↗	↔	↔	↔	↔	↔	↔
	CD11a	↓	↘	↔	↓	↔	↔	↔
	CTLA-4	↘	↔	↔	↔	↔	↗	↗
	PD-1	↓	↔	↔	↔	↗	↑	↗
	%Tcm	↔	↔	↔	↔	↔	↔	↔
	%Tef	↑	↗	↔	↔	↔	↓	↘
	% Th2	↗	↑	↗	↗	↔	↔	↔
	% Th1	↔	↔	↘	↓	↔	↔	↘
	% Th17	↔	↘	↓	↓	↔	↓	↓
	% Tregs	↔	↔	↘	↘	↔	↔	↘
CD8 T cells	Count	↔	↔	↔	↔	↔	↔	↔
	CD11a	↓	↔	↘	↓	↘	↔	↔
	CTLA-4	↘	↔	↔	↔	↗	↗	↗
	PD-1	↓	↔	↔	↔	↑	↑	↑
	GrzB	↘	↔	↔	↔	↗	↔	↔
	% Tcm	↔	↔	↔	↔	↘	↔	↔
	% Tef	↔	↔	↘	↔	↔	↘	↔
Unstimulated cells								
	IL-5	↑	↑	↑	↗	↔	↔	↔
	IL-13	↗	↑	↑	↗	↔	↔	↔
	IL-10	↗	↑	↗	↗	↔	↔	↔
	IFN-γ	↗	↑	↑	↗	↗	↑	↔
	IP-10	↔	↑	↗	↗	↑	↗	↗
	KC	↔	↔	↔	↔	↔	↔	↔
	RANTES	↔	↔	↔	↔	↔	↔	↔

4. Discussion

The elimination of human filarial diseases like lymphatic filariasis and onchocerciasis is a goal of the WHO and the United Nations. Both diseases pose a high socioeconomic burden on endemic countries, where they affect the lives of 859 million (28) and 218 million people (42), respectively. United efforts were made during the past decades and the recent WHO road map “Ending the neglect to attain the Sustainable Development Goals: a road map for neglected tropical diseases 2021–2030” (7), defines elimination targets until 2030 and the actions required. The goal set regarding lymphatic filariasis is the elimination as public health problem in 81% of the endemic countries. Onchocerciasis is targeted for the interruption of disease transmission in 31% of the endemic countries. Additionally, the “TOVA – The Onchocerciasis Vaccine for Africa” initiative was launched in 2015 (54). This initiative aims to pass an onchocerciasis vaccine candidate through a phase I clinical trial until 2025 (60).

In order to reach these goals, fundamental research for the understanding of host-pathogen interactions, as well as the applied research of vaccine development are driving forces.

A largely unexplored area in filarial biology is the involvement of nucleic acid sensing pathways. In this thesis it was shown that nucleic acids derived from the filaria *L. sigmodontis* induced type I IFN signaling by human and murine cells *in vitro*. Further, the infection with *L. sigmodontis* resulted in a significant type I IFN production *in vivo,* which also might be linked to the recognition of parasitic nucleic acids. However, the hypothesis, that the single knockout of nucleic acid receptors would enhance larval migration to the pleural cavity due to hampered recognition by the immune system was not supported.

At the same time, it was observed that the targeting of nucleic acid receptors enhanced larval killing. Based on that observation, nucleic acid receptor agonists were implemented as novel adjuvants into a *L. sigmodontis* vaccination protocol. Thereby it was shown that the vaccination efficacy was significantly enhanced by targeting cytosolic RNA sensors.

Overall, this thesis delivers valuable insights in the innate immune sensing of the filaria *L. sigmodontis* and supports a new approach for improving helminth vaccinations by using nucleic acid receptor agonists as adjuvants.

4.1 Recognition of *L. sigmodontis*-derived nucleic acids *in vitro*

In the field of analyzing the parasite-host interaction of filariae, the analysis of nucleic acids sensing still presents a broad lack of knowledge. On the contrary, the sensing of *Plasmodium*-derived nucleic acids by certain receptors and the impact on disease progression has already been unraveled in more detail (225, 241–244).

Therefore, when investigating the direct effect of filarial-derived nucleic acids on human cells, also the stimulation with *Plasmodium*-derived nucleic acids was performed for comparison.

Plasmodia are intracellular parasites and the causative agent of malaria, where pathogenesis is linked to an excessive Th1-associated immune dominance (245). Therefore, the organisms pose a strong opposite to extracellular filariae, where the immune response is typically dominated by a Th2-associated immune response (4–6). The differences in cellular location cause the parasites to encounter different branches of the host's immune system *in vivo*. The endosomal stimulation of PBMCs resembles the uptake of extracellular material and the cytosolic stimulation the recognition of intracellular material, which each targets different receptors.

For the analysis of nucleic acid sensing, it has to be considered that *P. falciparum* harbors an apicoplast which is a cyanobacterial remnant (246) and *L. sigmodontis* carries *Wolbachia* bacteria (247). Therefore, the isolated total parasitic nucleic acids probably also include bacterial nucleic acids that contribute to the observed immune response. Since the depletion of the apicoplast or the depletion of *Wolbachia* endosymbiont limits parasite growth and reproduction, it is challenging to isolate bacterial-free nucleic acid samples of either parasite (247, 248).

The differentiation between host and pathogenic RNA and DNA depends on the cellular location, the concentration and modifications that are recognized as non-self-structures (128). Bacterial nucleic acids bear different modifications than eukaryotic nucleic acids, for example a higher percentage of unmethylated CpG DNA motifs, and are immunogenic (227). As other example also RNA with a triple-phosphorylated 5' end were identified as foreign nucleic acid structures (227). Previously it was published by us that after endosomal stimulation *P. falciparum*-derived RNA induced IFN-γ by human PBMC-derived NK cells, while *P. falciparum*-derived DNA did not induced IFN-γ secretion at all (121). Further *P. falciparum*-derived RNA that targeted endosomal receptors induced IFN-α, IL-1β and IL-18 release from human PBMCs, as well as TNF

secretion by the human monocytic cell line THP-1 (121). Regarding the sensing of *L. sigmodontis*-derived nucleic acids no data are published.
In this thesis, a combination of pro-inflammatory cytokines and regulatory IL-10 was measured in order to assess the immune stimulatory potential of the parasite-derived nucleic acids.

RNA stimulation

The *in vitro* experiments showed similar IFN-α, IP-10, TNF and IL-1β responses of human PBMCs to the cytosolic and endosomal stimulation with the RNA of *P. falciparum* or *L. sigmodontis*. The secretion of IFN-α and IL-1β in response to the endosomal delivery of *P. falciparum*-derived RNA was described before (121). The observed cytokine pattern in this thesis indicates that the RNA of both parasites is recognized by receptors in the endosome as well as cytosol and involves the activation of several downstream signaling pathways involving the activation of the transcription factors IRF3/7 but also NF-kB. In conclusion, the RNA isolated from either parasite does induce type I IFNs and also inflammasome signaling. In order to shuttle the parasite-derived nucleic acids into the cytosol, the transfection agent lipofectamine was used. Literature states, that the transfection reagent lipofectamine can induce Type I IFN release (249). However, since there was no IFN-α response to human-derived RNA that was complexed with lipofectamine, it is likely that the IFN-α response was due to the recognition of parasitic RNA. However, there was an unexpected release of TNF and IL-1β in response to cytosolic stimulation with human RNA. Therefore, it is uncertain whether the sensing of parasitic RNA by cytosolic receptors caused the release of TNF and IL-1β. A mixed effect of transfection agent and stimulating RNA appears likely. The cytosolic recognition of viral RNA induced IL-1β secretion in a RIG-I dependent manner (250) and also poly(I:C) as dsRNA was shown to induce inflammasome activation (251).
Further, *P. falciparum*- and human-derived RNA stimulated regulatory IL-10 release after cytosolic stimulation, while *L. sigmodontis*-derived RNA did not. Either the RNA did not trigger this response or the filarial RNA even dampened the IL-10 response, which also might be induced by the transfection reagent lipofectamine.
The *in vivo* relevance will be discussed together with the relevance of DNA signaling at the end of this chapter.

Based on flow cytometric analysis, the release of cytokines 24 hours after cytosolic stimulation with *L. sigmodontis*-derived RNA was accompanied by an increase in T cell and a decrease in monocyte frequencies. Further, there was a shift in the distribution of monocytic subsets. From the collected data it cannot be concluded whether this shift in frequency is based on the proliferation or death of certain cell types. In general human PBMCs comprise T cells, B cells, NK cells, dendritic cells and monocytes and the population proportions vary between donors (236). The $CD4^+$ and $CD8^+$ T cells account for 25-60% and 5-30%, respectively. B cells make up for 5-10% (236). The acquired cell frequencies in this thesis meet these literature values. T cells and B cells belong to the adaptive immune response and in an *in vivo* setting it takes about three to five days from the recognition of antigen by antigen presenting cells, activation of T and B cells and the subsequent proliferation (114). Therefore, a proliferation of T cells within 24h after RNA stimulation is not expected. Since the PBMCs were isolated from donors at the University Hospital in Bonn, it is unlikely that these donors encountered infections with *Plasmodia* or filariae and most likely immune cells were not pre-primed before the stimulus administered in these experiments. However, the stimulation with RNA differs from this setting since no processed peptide antigen is presented by the innate immune system. T cells do express nucleic acid receptors and can directly recognize RNA structure (123). However, nucleic acid sensing by T cells was associated with anti-proliferative and inhibitory effects (123). Therefore, the increase in T cell frequency after cytosolic stimulation is more likely due to a T cell death as response to the lack of stimulation in the unstimulated sample or the death of other cell types upon RNA stimulation. The other significant change in cell populations upon cytosolic stimulation was the reduced frequency of monocytes. Human monocytes are identified by the expression of the LPS receptor, also known as CD14, and subsets are defined by the co-expression of low affinity IgG receptor III (FcγRIII), also known as CD16. In literature the subsets are often classified as classical monocytes ($CD14^+CD16^-$), non-classical monocytes ($CD14^{dim}CD16^+$) and intermediate monocytes ($CD14^+CD16^+$) (252). Based on the flow cytometry data acquired in this thesis, $CD16^-$ classical monocytes had a lower CD14 expression than $CD16^+$ intermediate monocytes. Consequently, the CD14 expression of “classical” monocytes equals the CD14 expression of “non-classical monocytes”. The basis behind this discrepancy from literature is not clear. Therefore, for analysis the monocyte subsets were named by their marker expression and not the terminology used in literature.

Monocytic subsets were affected by cytosolic stimulation with RNA, reflected in a loss of the FcγRIII (CD16). According to literature, $CD14^{+}CD16^{-}$ monocytes have a higher phagocytic capacity than CD16 expressing monocytes which in turn have pro-inflammatory and apoptotic features (253). Possibly the monocytes did not downregulate their CD16 expression but $CD14^{+}CD16^{+}$ monocytes underwent apoptotic cell death in response to the stimulation and thereby contributed to overall reduction of monocyte frequencies. However, there was an upregulation of the MHC II molecule HLA-DR on monocytes in response to cytosolic stimulation with *L. sigmodontis* RNA. This indicates that the filarial RNA stimulus is potent to induce the communication between the innate and adaptive immune response and mount a sophisticated immune response.

Also, the endosomal RNA stimulation of human PBMCs lead to reduced monocyte and DC frequencies. The impact of any stimulation on monocyte subsets, hence on the expression of the LPS receptor (CD14) and FcγRIII (CD16) was minor after the stimulation with parasitic or human RNA. Hence in the experimental setting of endosomal RNA stimulation, the reduction of monocyte frequency cannot be attributed by apoptotic cell death of CD16-expressing monocyte subsets. Further, among the different subsets there was an upregulation of the MHC II molecule HLA-DR in response to *L. sigmodontis*-derived RNA on $CD14^{dim}CD16^{-}$ “classical monocytes”, but a downregulation on $CD14^{dim}CD16^{+}$ “non-classical monocytes”. The determination of the total cell count 24 hours after the stimulation could explain why monocyte and DC frequencies decreased.

All in all, the isolated RNA of *L. sigmodontis* had the potential to activate human monocytes via cytosolic and endosomal RNA receptors and induced the release of Th1-associated cytokines, including the type I IFN IFN-α.

DNA stimulation

After cytosolic DNA stimulation there was an IFN-α, IP-10, TNF, IL-1β and IL-10 response independent of whether the DNA was isolated from *L. sigmodontis*, *P. falciparum* or human cells. Since the accumulation of self-DNA in the cytosol is associated with disease (254), here it cannot by distinguished by the human control to what extend the cytokine release is affected by the transfection reagent lipofectamine. The activation of the inflammasome by cytosolic DNA has been described (255),

therefore it is likely that the release of IL-1β is dependent on the DNA stimulus and is not completely attributed to the transfection reagent.
Striking differences were seen after the endosomal stimulation with parasite-derived DNA. Filarial *L. sigmodontis*-derived DNA, but not *P. falciparum*-derived DNA, induced the secretion of IFN-α and IP-10.
The endosomal stimulation with DNA derived from either parasite did not induce the secretion of TNF, IL-1β and IL-10. This suggests that the endosomal stimulation with *L. sigmodontis*-derived DNA, targeting the receptor TLR9, rather induced interferon signaling, but did not trigger inflammasome activation.
On a cellular level, there was a significant increase in the frequency of DCs in response to the cytosolic stimulation with *L. sigmodontis*-derived DNA. Since the total cell counts were not determined after the stimulation, it cannot be deduced whether the increase is due to DC proliferation or cell death of other subsets. Similar to the cytosolic stimulation with RNA using lipofectamine, there was an impact on monocytes subsets by all DNA-stimuli using lipofectamine. Signs for cell activation on the cellular level were limited to the upregulation of the MHC II molecule HLA-DR on $CD14^{dim}CD16^{+}$ "intermediate monocytes" after cytosolic stimulation with *L. sigmodontis*-derived DNA. For the endosomal stimulation with DNA, no significant cellular impact was identified by flow cytometry. Likely the occurrence of DNA in the endosome is less of a danger signal and results in milder activation than cytosolic DNA.

Overall, it is striking that *L. sigmodontis*-derived RNA and DNA induced the secretion of the type I IFN IFN-α and IP-10 via cytosolic and endosomal receptors. Both cytokines are mostly associated with viral responses, but have also been implicated with bacterial and protozoan infectious diseases (230). The type I IFNs IFN-α and IFN-β shape innate and adaptive immune responses in several aspects. It is a narrow line whether these effects are detrimental or beneficial and the outcome is highly context dependent. In co-infection experiments with *B. malayi* and *M. tuberculosis* it was shown that the pre-exposure to *B. malayi* MF reduced the type I IFN response by macrophages to subsequent *M. tuberculosis* infection (256). This implies that type I IFN signaling might be a pathway that undermines chronic filarial infection and therefore is actively modulated by filariae, in order to ensure their survival in the host.
The protective effects of type I IFN were also described for the infection with extracellular bacteria and appears not to be limited to intracellular pathogens (257).

Interestingly, it has also been shown that type I IFNs are important for the Th2-associated immune responses directed against *S. mansoni*-derived antigen, which are thought to mediate protection (258).
Regarding a possible *in vivo* relevance for the recognition of *L. sigmodontis*-derived RNA, it has to be considered that *L. sigmodontis* prevails extracellularly in its vertebrate host. After parasite death or during molting steps, free RNA and DNA may be available. Else, nucleic acids in secretory vesicles can be taken up by cells of the innate immune system (149). Regarding endosymbiotic *Wolbachia* bacteria it has been shown that bacterial material can trigger the innate immune system. Immune cells sense *Wolbachia* via surface TLRs (43), and *Wolbachia* are necessary for the neutrophil recruitment to the skin during *L. sigmodontis* infection (91). Consequently, bacterial content has to be released either after the death of the parasite or by secretory products. If endosymbiotic material from within the parasite is available it seems likely that also nucleic acid from the nematode itself can encounter the host's immune system.

Taken together, *L. sigmodontis*-derived RNA and DNA were shown to have a pro-inflammatory immunostimulatory potential for human PBMCs. However, to which extent the recognition of *L. sigmodontis*-derived nucleic acids has an *in vivo* relevance has to be further investigated.

4.2 Stimulatory potential of *L. sigmodontis*-derived RNA in murine cells

The *in vivo* work of this thesis with *L. sigmodontis* was performed in a mouse model. Therefore, it was also crucial to confirm the type I IFN release in response to *L. sigmodontis*-derived nucleic acids by murine cells.
The stimulation of pDCs and macrophages resulted in strong IFN-β production. This indicates that these professional APCs are capable to sense *L. sigmodontis*-derived RNA, produce type I IFN and likely communicate the microbial threat to the adaptive immune system. In acute infections, type I IFNs were shown to be important for $CD4^+$ T cell activation and survival and can inhibit regulatory T cell function (259). In chronic infections, type I IFNs induced regulatory DCs that contribute to the exhaustion of $CD4^+$ T cells (259). This highlights again the complexity of type I IFN signaling and the challenge of interpretation. Accordingly, the *in vitro* stimulation mimics an acute infection.

Further, the stimulation of murine bone marrow-derived cells revealed that the RNA of *L. sigmodontis* also induced type I IFN production in neutrophils. Neutrophils are key players for the defense against filarial L3 larvae. During events of neutrophil ETosis (NETosis), where extracellular DNA entraps larvae, or the attachment of neutrophils to larvae in granuloma formation, it appears likely that neutrophils do encounter filarial nucleic acids. Further, the NETs themselves have been shown to induce type I IFN signaling (260). Neutrophils migrate to the site of infection within minutes and are one of the first immune cells at place (114). Therefore, neutrophil-related type I IFN release might support rapid activation of further immune cells.

The stimulation with 10 or 100 vital *L. sigmodontis* L3 larvae did not induce IFN-β production. Possibly in the culture the naïve cells did not target the worm, hence it was not damaged and no sufficient nucleic acid was available to be recognized. Further, the larvae's secretome might have altered the expression of nucleic acid receptors, and thereby limited the production of type I IFNs. The inhibition of innate immune sensing by helminth parasites, by for example the downregulation of nucleic acid sensing TLRs, has been described (81, 261).

Overall, these data show that human and murine cells respond to *L. sigmodontis* derived-RNA with type I IFN production and the *in vivo* investigation of type I IFN responses during *L. sigmodontis* infection is supported.

4.3 *In vivo* type I IFN signaling during *L. sigmodontis* infection

Besides the *in vitro* type I IFN response to *L. sigmodontis*-derived nucleic acids, also the infection with *L. sigmodontis* led to an *in vivo* IFN-β release by pleural cells. This was lowest at five days post infection, when the L3 larvae enter the pleural cavity and increased over time, when parasites prevail in the pleural cavity and molt into L4 larvae. The increase in IFN-β production might be due to differences in the receptor activation of immune cells, the immune cell populations present during the course of infection, or immune modulatory capacities by different developmental parasite stages.

With regard to an increase in IFN-β over time based on the differences in activation status of immune cells, an upregulation of receptors that function upstream of IFN-β production might play a role. These receptors can be nucleic acid receptors (like TLR3), or TLR4 and NOD receptors, which sense bacterial components (114). The stimulation with the TLR3 ligand poly(I:C) resulted in increasing IFN-β levels with the longer onset of infection. This supports a role for increased TLR3 expression or an

influx of TLR3 expressing cell types. Further, the secretion of type I IFNs involves a positive feedback loop that also might support the enhanced secretion (230, 262).
Additionally, the type of immune cells present in the pleural cavity at different time points during *L. sigmodontis* infection might impact the IFN-β production. However, many cell types are able to produce IFN-β, type I IFN responses are highly context dependent, and the cellular source of type I IFN production is influenced by the pathogen, the route of infection and the analyzed tissue (230, 263). Therefore, further investigations would be needed to identify the cellular IFN-β source during *L. sigmodontis* infection, but likely sources are discussed in the following.
During the infection with *L. sigmodontis,* B cells, which are potent IFN-β producers (264), expand in the pleural cavity (112). Thus, they may be a source of the measured *in vivo* IFN-β production. Murine cells were shown to produce type I IFN after the activation of STING, which is involved in cytosolic DNA sensing (123). Further, murine B cells do express low level of TLR3, but were shown to react to direct stimulation (265). Also, macrophage populations increase during the course of *L. sigmodontis* infection in C57BL/6 mice (75). Macrophages express TLR3 and TLR4 and can be potent IFN-β producer (266). However, macrophage populations are polarized towards an alternatively activated state during *L. sigmodontis* infection (75). Alternatively activated macrophages (AAM) are potent producer of IL-4 and IL-13 and part of a Th2-polarized immune response (116). Therefore, their potential to contribute to the IFN-β production during *L. sigmodontis* infection is questionable. Neutrophils and eosinophils are also expanding in the pleural cavity during *L. sigmodontis* infection (75). Both cell types are known to express PRRs like nucleic acid receptors including TLR3, and also the receptors TLR4 (267–269). In this thesis bone marrow-derived neutrophils were shown to produce IFN-β. However, RT-PCR analysis done in our lab revealed only very low expression of IFN-β expression in murine bone marrow-derived eosinophils after stimulation of the cytosolic RNA sensor RIG-I (data not shown).
Nevertheless, during the infection with *L. sigmodontis,* neutrophils (92) and eosinophils (102) release DNA nets that contain granular proteins and can capture and kill the parasite. These processes are known as NETosis and EETosis, respectively. It was shown that the DNA nets released during NETosis enter the cytosol of myeloid cells and induce type I IFN secretion via a cGAS – STING axis (260). Therefore, it is likely that the mechanisms of NETosis and also EETosis contribute to the measured type I IFN release *in vivo*.

The *in vivo* IFN-β response can also be linked to the previously discussed potential role of endosymbiotic *Wolbachia* bacteria or their nucleic acid residues. During the course of infection, the parasites are attacked and damaged by the immune system and *Wolbachia* might be freely accessible (REF). Especially since the reporter animals are on a C57BL/6 background there is a strong immune response, resulting in the killing of worms at around day 40 after infection (80) and makes a *Wolbachia* release from damaged worms at the measured time point 30 days after the infection likely. Contradicting to this speculation is that researchers found that the strongest anti-*Wolbachia* response is linked to the L3 larval stage. However, their analysis is based on immunostimulatory WSP per gram of worm (270) and arguably the total amount of WSP might be increased in the larger adult worms. Interestingly, the activation of TLR3 and TLR4, involves the central adaptor molecule TRIF (261). In the context of *L. sigmodontis* infection it has been shown, that C57BL/6 mice, which lack TRIF, have a higher worm burden and reduced cell counts in the pleural cavity 30 days after the infection (271). This supports the hypothesis that the release of type I IFNs during the infection with *L. sigmodontis* contributes to limiting the infection.

Another pathway that is known to induce type I IFN secretion is the activation of cytosolic NOD receptors, which recognize peptidoglycans, but also viral nucleic acids (272). Also *Wolbachia* have been suggested to activate the receptor NOD2 (91). The depletion of NOD2 during *L. sigmodontis* infection resulted in reduced neutrophil recruitment to the site of infection and increased larval survival (91). Taken together, this implicates that early type I IFN signaling and inflammasome activation might be beneficial for the early clearance of *L. sigmodontis*.

After discussing possibilities of immune responses facilitating the IFN-β responses during the course of infection with *L. sigmodontis*, also the immunomodulatory effects of the parasitic stages have to be considered.

For the filaria *B. pahangi* it has been described that L3 larvae can elicit Th1 and Th2 immune responses (273). But in the context of *B. malayi* it has been shown that antigen presenting cells actively suppress the Th1 response (273, 274). This appeared to be mediated by IL-4 and IL-10 (273–275), which also were shown to dampen IFN-β production by murine peritoneal macrophages (276).

A mechanism that is believed to be involved in immunomodulation by helminths is the release of extracellular vesicles (147). For *B. malayi* it has been shown that all parasitic stages found in the vertebrate host release extracellular vesicles that were internalized

by murine macrophages (277). However, for *L. sigmodontis* minor stage specific differences in the secretome have been identified (278). Overall there was a large overlap between different stages, with the exception that a large number of proteins were only found in the extracellular vesicles released from female worms undergoing embryogenesis (278). In this thesis the latest time point to analyze the *in vivo* IFN-β response to *L. sigmodontis* was 30 days after infection and the parasite just completed the molting process to the adult stage. Consequently, no MF were released yet in the experimental setting in this thesis. However, others showed that live MF from *B. malayi* downregulate the expression of TLR3 and TLR4, which are receptors upstream of type I IFN signaling (230), in human DCs *in vitro* (151), and thereby also the MF stage can impact type I IFN signaling. It would be of interest, whether at a later time point, when reproducing females and released MF are present, the IFN-β secretion in the pleural cavity is decreasing. However, since C57BL/6 mice clear the infection prior to the onset of MF release (80), the infected reporter mice are not a suitable model for this analysis. Further, for the helminths *S. mansoni* and *Fasciola hepatica* it was shown that parasite-derived proteases degraded endosomal TLR3 in macrophages (279). Therefore, it is likely that the modulation of type I IFN-inducing signaling pathways is a common feature of helminths and their diverse developmental stages.

It has to be considered that the kinetics of IFN-β release might be different in BALB/c mice, since these do not start clearing the infection by day 35 after the infection, but the infection prevails chronically (65, 79, 80). It would be of interest to clarify, whether the type I IFN level in BALB/c mice remain lower than in C57BL/6 mice. Overall, it appears that despite the great repertoire of immunomodulatory mechanisms that can limit type I IFN production, an increasing type I IFN response towards *L. sigmodontis* in C57BL/6 mice is mounted. Type I IFNs trigger the transcription of more than 100 genes via different transcription factors (230). As an example, type I IFNs can activate DCs by enhancing their expression of MHC and co-stimulatory CD80 or CD86 (230). Further, they can enhance the migration of DCs to the lymph node and antigen cross-presentation (230). Thereby the communication with the adaptive immune system is enhanced and can result in enhanced T cell proliferation and cytotoxic activity (230). However, as an example, depending on the context, type I IFNs can also inhibit DC activation (230). The downstream effects during the infection with *L. sigmodontis* and how these might affect immunity towards the filariae remain for investigation in future studies.

4.4 Role of nucleic acid receptors for the outcome of *L. sigmodontis* infection

L. sigmodontis-derived nucleic acids, as well as the natural infection induced type I IFNs *in vitro* and *in vivo,* respectively. Arguably, this can influence protective immunity by triggering the type I interferon receptor. The majority of known receptors upstream of type I secretion are linked to the sensing of nucleic acids. Therefore, it is likely that the *in vivo* sensing of *L. sigmodontis* also involves nucleic acid receptors, which are upstream of type I IFN signaling (230).

With regard to other helminth infections, the lack of the adaptor protein STING, which is involved in DNA sensing, resulted in improved resistance to infection with *S. mansoni* (163).

Here we asked the question whether a single nucleic acid receptor can be identified that impacts the course of *L. sigmodontis* infection at an early time point and targets L3 larvae. By infecting nucleic acid receptor knockout mice with *L. sigmodontis*, no impact of the individual receptors MDA5, TLR7, TLR9 or STING on larval survival and migration to the pleural cavity until 12 days after infection was identified. Differences in worm burden are mostly associated with the immune reaction during the migration to the pleural cavity. The analyzed knock strains are available on the semi-resistant C57BL/6 background, which naturally clear *L. sigmodontis* in the pleural cavity shortly after the molting process to the adult stage starting around day 30 after the infection. Therefore, the worm burden was assessed at an earlier time point. In addition, only minor changes in pleural cell populations and their activation were detected. Hence, this thesis revealed that that a single knockout of nucleic acids receptors does not increase susceptibility to *L. sigmodontis* L3 larvae. Redundancy of nucleic acid receptors or an impact on another developmental stage than L3 larvae may be responsible for the lack of increased susceptibility due to the knockout. In reporter animals, the release of IFN-β was low while parasites were in the L3 stage and only increased later during infection. Therefore, the impact of the receptor deficiency might be neglectable during larval migration or L3 larvae might release vesicles that downregulate nucleic acid receptor expression, as the release of miRNA containing exosome-like vesicles has been described for *B. malayi* L3 larvae (148). A downregulation of TLR3 and TLR4 and reduced IFN-α production was described for human DCs after the exposure to *B. malayi* live MF (152). Therefore, a possible effect on larval survival already might be undermined through modulatory mechanisms

induced by the parasite, so that the knockout does not effectively change pathway activation. Possibly, effects of the knockout only become apparent between day 14 and 30 by affecting the larval killing in the pleural cavity.

Whether nucleic acid sensing pathways contribute to protective immunity, are actively modulated by the parasite during infection with *L. sigmodontis* or both can only be speculated. Further research is needed to understand the interplay of filarial-derived nucleic acids with the host's immune system. However, we could show that the early migration of infective *L. sigmodontis* L3 larvae was not altered by the exclusive signaling of the nucleic acid receptors MDA5, TLR7, TLR9 or STING.

4.5 Improving *Litomosoides sigmodontis* vaccination

In order to drive disease elimination, it is not only necessary to identify protective mechanisms, but to also to target these as novel preventive and therapeutic strategies. One way to exploit a possibly sustainable protective effect is by implementing the identified targets into a vaccination strategy. In animal studies, the use of irradiated *L. sigmodontis* larvae was identified as reliable vaccination strategy that nevertheless fails to induce full protection (213, 215, 217, 219).

We hypothesize, that type I IFN signaling might play a protective role during *L. sigmodontis* infection, while the pathways that lead to the observed IFN-β release are not known. Therefore, it is of interest to study protective effects of boosted type I IFN signaling induced by nucleic acid receptor activation. Protective immunity during helminth infection is not yet well understood and so far Th2-associated immune responses have been associated with protection (75). At the same time in a study with *L. sigmodontis* synergistic effects of Th1-associated IFN-γ and Th2-associated IL-5 aided parasite control (118). Also Layland and collages suggest that the clearance of *L. sigmodontis* in C57BL/6 mice not solely depends on Th2-associated immune responses (232) and studies with *B. malayi* suggested that a balanced Th1 – Th2 immune response is beneficial for the outcome of filarial infections (22, 280–282). Previous data in this thesis support a potentially protective effect of Th1-associated type I IFNs. In *S. mansoni*-infected mice the treatment with the type I IFN PEG-interferon-alpha-2a, resulted in a significantly reduced worm burden and inhibited parasite reproduction (283). PEG-interferon-alpha-2a is a conjugate of recombinant IFN-α with polyethylene glycol, which facilitates the retardation of IFN-α in order to prolong bioavailability (284) and is associated with the treatment of hepatitis (285, 286).

All in all, helminths appear to regulate pathways related to type I IFN signaling (151–154) and vice versa, type I IFN and its upstream receptors could be used for a successful therapy (159, 196–198, 283).

For the transition to human treatment, defined antigens have been found for an *O. volvulus* vaccination and further investigations are ongoing (208). The challenge here is to enhance the immune response in order to improve the protection rate by the choice of adjuvants, as antigens on their own often fail to induce immune memory (177). So far, many vaccination studies for lymphatic filariasis used alum as adjuvant (22), which is capable to mount a Th2-associated immune response (287). Side effects that have been described for alum include IgE production and granuloma formation (288). Therefore, in the context of helminth vaccines, the use of alum might add to the problematic side effects induced by high IgE responses towards worm antigens, as observed during the development of a hookworm vaccination (190). At the same time, dependent on the antigen, alum lacks the ability to induce cell-mediated immunity (289). In a study with non-human primates, alum did not perform as well as expected (290) and makes it questionable whether alum is a favorable choice for the development of a vaccination that is efficient for human filarial vaccine. In an ongoing phase 2 clinical study for a hookworm vaccine, alum is combined with CpG (291), which can induce type I IFN secretion via activation of the endosomal DNA receptor TLR9 (136).

Considering the provided data, the use of an agonist that boosts Th1-associated immune responses, including type I IFN release, which shape the long-term immune memory might be a feasible approach for helminth vaccinations. Here we present an analysis of a variety of nucleic acids receptor agonists as filarial vaccine adjuvants.

4.5.1 Local impact of vaccine adjuvants

The injection of sole antigen in form of LsAg and *L. sigmodontis* L3 larvae did not mount a noticeable immune response and supported the predicted need of an adjuvant for improved immunization.

Analysis of local immune responses in a pre-screening of several nucleic acid receptor agonists as adjuvants revealed that the TLR7/8 agonist R848 and the TLR9 agonist CpGC ODN2395 performed inferior regarding general leukocyte recruitment compared to the other agonists tested. Further, R848 showed a strong systemic IP-10 response,

which reflects a diffusion of R848 from the local site of injection into the periphery. Such a diffusion of R848 has been described before (292, 293). Consequently, we deprioritized R848, since systemic chemokine responses may limit selective immune cell recruitment to the site of antigen injection. CpG molecules were already identified as potent vaccine adjuvants with a favorable safety profile and are used for anti-viral vaccination, like hepatitis B (180, 188). CpG also showed promising effects in a *Schistosoma* immunization study in mice (196, 197) and is already used in a clinical studies for a hookworm vaccine (190, 200), where the use of CpG could enhance humoral responses (201). In the mentioned immunization studies, different CpG classes and sequences were used, which may impact the outcome. Our pilot study indicated that CpG was not only inferior to other tested agonists with regard to leukocyte recruitment, but also in respect of the local IFN-β and IP-10 responses. However, since CpG is used in other studies with promising results it might be of interest to directly compare CpG and the chosen agonists poly(I:C) and 3pRNA in the long-term vaccination effect. Thereby conclusions can be drawn on how important leukocyte recruitment and local type I IFN responses are for filarial vaccination success.

The strongest response in all assessed parameters showed the STING agonist 2'3' cGAMP. However, data from out lab revealed the development of splenomegaly after the treatment with 2'3' cGAMP, as undesired side effect. Therefore, the use of a STING agonist as vaccine adjuvant was excluded from further analyses.

Based on leukocyte recruitment and local type I IFN responses poly(I:C) and 3pRNA were chosen for further analysis and their impact on the local immune response in combination with radiation att. *L. sigmodontis* L3 larvae was assessed. Poly(I:C) has been used as in clinical studies for decades and is known to induce strong type I IFN responses (227). However, its mode of action is not well understood (227). 3pRNA was identified as ligand for the cytosolic RNA sensor RIG-I (134) and was successful in inducing type I IFNs and enhancing cross-presentation and $CD8^+$ T cell responses (185). Further, it was recently shown to increase efficacy in a murine tumor vaccination study (294). Since helminths are potent immune modulators, the addition of att. *L. sigmodontis* L3 might alter the overall effect on the local immune milieu mounted by the immunization shot. Therefore, the subcutaneous analysis was performed after the combination of the chosen agonists with att. L3 larvae. In the screening experiment poly(I:C) was delivered to the endosome where it can target TLR3. However, this

agonist is also capable of activating the cytosolic sensors MDA5 and RIG-I. Consequently, stimulation with poly(I:C) most likely not only activates the mainly targeted receptor, but activation of TLR3, MDA5 and RIG-I can contribute to the observed immune response. In order to analyze possible differences in choosing the main target of poly(I:C), poly(I:C) was transfected into the cytosol for the further analysis of local immune responses after subcutaneous injection.

When combining att. L3 larvae with poly(I:C) or 3pRNA, the overall data were similar to the ones gained from the subcutaneous injection of agonists on their own. This indicates that as expected also the att. L3 larvae did not impact cell recruitment and activation. Most striking was an influx of neutrophils to the site of injection. Neutrophils belong to the group of professional APCs (114) and were shown to be important for the control of invading *L. sigmodontis* L3 larvae during primary infection (91, 92). In immunization studies in mice and sheep neutrophils were also identified as immune cells that rapidly transport antigen to lymph nodes and the spleen (295). In the lymph node neutrophils activate the adaptive immune system for example by helping dendritic cells to effectively activate naïve $CD4^+$ T cells or by aiding the production of plasma B cells and enhancing antibody production (296). Also in the spleen, neutrophils can induce antibody production by B cells and induce class switching (296). The production of plasma B cells and antibody production both are directly important for generating immune memory (114).

The influx of neutrophils was accompanied by a reduction in monocyte and DC frequencies. Especially DCs are important for travelling to draining lymph nodes, delivering signals to the adaptive immune system, especially activating naïve T cells, and thereby contributing to the induction of immune memory. Type I IFNs were shown to enhance the migration of DCs to the lymph node (230). Therefore, the type I IFN response induced by poly(I:C) or 3pRNA probably enhanced the delivery of antigen to the lymph node by dendritic cells.

Cell migration dynamics based on total counts after subcutaneous immunization with a CD40 agonist in a squalene-based oil-in-water adjuvant was analyzed by Schetters *et al.* (297). Their chosen time points include a gap between two and 12 hours post infection, so that no clear picture for four hours after injection can be derived. But the authors described a strong neutrophil influx within the first two hours after injection that kept increasing until 12 hours after injection (297), which fits to the influx observed here. At the same time, in their study the numbers of dendritic cells were reduced

between two and 12 hours. As previously discussed, it is likely that in this thesis the dendritic cells migrated to the draining lymph node. Further, the dendritic cells found in the skin after immunization with att. L3 larvae in combination with transfected (trans.) poly(I:C) or 3pRNA reduced their expression of the MHC II molecule I-Ab. It was shown that DCs located in the skin downregulated their MHC II expression in order to travel to the draining lymph node (298). Therefore, the downregulation of MHC II supports the hypothesis that the reduction of DCs is also based on their migration to the draining lymph node. At the same time the DCs upregulated their expression of co-stimulatory CD86 indicating a successful activation of the cells by the combination immunization.
Regarding the counts of Ly6C$^+$ monocytes, Schetters *et al.* describe an increase for the time between two and 12 hours after immunization. Since the data analysis here is based on cell frequencies, conclusions on the actual cell number cannot be drawn. The increase in neutrophils might induce a reduction in monocytes frequency while the overall monocyte numbers still increase as well, just to a smaller extend. In this thesis, the cells were isolated from a skin section that was thickened by the injection, which was not reliably the exact same size between mice. Therefore, no total counts were compared. Generally, monocytes are known to process antigen from invading pathogens in order to present them to the innate immune system (114). Therefore, it is expected that also monocytes travel to the draining lymph node after detecting antigen from att. L3 larvae.
The analysis of draining lymph nodes would provide insight on which cells migrate to the lymph node in order to present antigen recognized from att. *L. sigmodontis* L3 larvae. Analyses at a later time point could reveal whether the stimulus was successful in driving B cell and T cell proliferation. Further, the analysis of proliferating T helper subsets would provide information on how the overall immune response is polarized by the combination of att. L3 larvae, which are associated with a Th2-dominated immune response and an agonist that drives Th1-associated immune responses.

Overall, the results from the subcutaneous analysis four hours after the injection revealed that the nucleic acid receptor agonists poly(I:C) and 3pRNA enhanced the local immune response towards the antigen delivered in form of att. L3 larvae. Whether this effect is successful in generating long-term immune memory and thereby improves the immunization in the *L. sigmodontis* model has to be assessed by analyzing later time points and the outcome of a challenge infection.

4.5.2 Killing of larvae by targeting nucleic acid receptors

Prior to performing full vaccination studies with the chosen nucleic acid receptor agonist trans. poly(I:C) and 3pRNA, we aimed to clarify whether the immune potentiation of nucleic acid immune sensing pathways mediates protective effects that support larval killing without detrimental host damaging effects in the model of *L. sigmodontis*.

The site of infection was primed by injection of the nucleic acid receptor agonist trans. poly(I:C) or 3pRNA. From the experiments, analyzing the subcutaneous tissue four hours after injection, it is known that neutrophils migrated to the site of infection and a strong local type I IFN response was mounted. The infection with *L. sigmodontis* L3 larvae occurred 12 hours later at the same injection site. The pharmacokinetic dynamics of trans. poly(I:C) and 3pRNA transfected with *in vivo*-jetPEI® in mice was not assessed, therefore the remaining effects 12 hours after the injection are speculative. Schetters *et al.* subcutaneously injected a CD40 agonist in a squalene-based oil-in-water adjuvant and monitored immunodynamics in the skin for eight days (297). In their study, there were high numbers of monocytes and neutrophils 12 hours after the injection, but dendritic cells probably have migrated to the draining lymph node. Proliferative effects on T and B cells induced by innate immune cells that migrated to the lymph node will only become apparent after several days (114).
Upon subcutaneous infection at the site of previous subcutaneous injection of agonist, the L3 larvae probably encounter increased numbers of neutrophils that are known to target L3 larvae in primary infection (91, 92). Possibly a substantial number of L3 larvae will thereby be eliminated before entering the pleural cavity via the lymphatics and the lung.
In a setting without previous immune activation *L. sigmodontis* L3 larvae rapidly start migrating via the lymphatics towards the lung (77, 95). According to Kilarski *et al.*, vital and migrating *L. sigmodontis* L3 larvae were found in the skin 18 hours after subcutaneous injection (299). Further, they state that after intradermal injection *L. sigmodontis* L3 larvae reached the draining lymph node in less than 20 minutes (299). In another study, Karadjian *et al.* found that *L. sigmodontis* L3 larvae enter the lungs as soon as two hours until 8 days after subcutaneous injection (77). In conclusion, at the time point 12 hours after the subcutaneous infection with *L. sigmodontis* L3 larvae, when the agonists were injected intravenously, some of the

larvae have already entered the lungs, while the majority is still in the skin and migrated via the lymphatics.
The results regarding the immune activation four hours after immunization revealed minor differences between the injection of poly(I:C) or 3pRNA. As subcutaneous treatment prior to infection and intravenous treatment after the infection, the injection of 3pRNA showed significantly increased worm clearance nine days after the infection. However, there were only minor differences in pleural cell populations and activation, when comparing both treatments. This indicates that the elimination of larvae was mainly based on a mechanism that does not affect pleural cell immunology.
In order to understand the mechanisms that facilitated the larval killing it would be of interest to analyze the effects of subcutaneous treatment prior to the infection and the intravenous treatment after the infection, individually. Further, it would be of interest to analyze whether and how the subcutaneous injection of poly(I:C) or 3pRNA lead to limited motility of L3 larvae upon infection.

Overall, regarding the immune dynamics induced by the treatment with poly(I:C) or 3pRNA and the mechanism underlying the enhanced larval killing, it can only be speculated. However, it was shown that the treatment with the nucleic acid receptors agonists poly(I:C) and 3pRNA enhanced protective immunity in form of larval killing. Therefore, the approach of applying poly(I:C) and 3pRNA for an immunization study was supported by this experiment.

4.5.3 Parasite-specific immune responses after immunization

Successful immunization is based on the generation of long-lived memory cells and antibodies (170, 300).
Due to the dominant Th2-assocated immune response in filarial infections, B cells are driven to a class switch producing IgE and IgG1 antibodies (301). Th1-associated cytokines induce the secretion of IgG2 by plasma B cells, for example IFN-γ induces the production of IgG2a (302). In a bovine model also type I IFN was shown to enhance IgG2, but not IgG1 production (303). In mice, the two subsets of IgG2a and IgG2b antibodies are produced (304).
As expected, the parasite-specific antibody release was induced by the injection of att. L3 larvae, but partially enhanced by the co-administration of the agonists poly(I:C) or 3pRNA. Based on the absorbance values there were only low level of IgE antibodies

and the combination of att. L3 larvae with the agonists poly(I:C) or 3pRNA did not enhance the production of IgE. This is of importance, as high IgE production is associated with mast cell degranulation, allergy and immune damage (114). As experienced during the development of a hookworm vaccine, it is crucial to avoid high level of IgE antibodies in order to prevent severe side effects of the immunization (190). Therefore, it is desirable that the agonists used as vaccine adjuvants did not boost IgE production.

Protective antibody-mediated effects during helminth infections are attributed to IgG1 antibodies (305). A distinct parasite-specific IgG1 response was also measured in this study, which was similar in all groups that received att. L3 larvae for immunization. Since the agonists do not promote Th2-associated immunity, it was not surprising that the IgG1 serum level were not further increased after co-administration of poly(I:C) or 3pRNA. In a *L. sigmodontis* immunization study involving irradiated MF, IgG1 and also IgG2 antibodies were linked to protection (220). In this thesis serum IgG2a/b level were significantly increased after the co-administration of naked or trans. poly(I:C) compared to the immunization with att. L3 larvae alone.

The balanced production of IgG1 and IgG2 subtypes may be a measure for successful immunization after *L. sigmodontis* vaccination. Regarding their function, murine IgG1 antibodies are known to limit inflammation (304), therefore their abundance during filarial infection fits to the overall associated immunomodulation by the parasite. On the contrary, IgG2a antibodies are linked to T helper cell responses (304). Hence, their induction by immunization supports the protective effect of T cell responses. The importance of $CD4^+$ T cells for the clearance of adult worms has been identified by the depletion of $CD4^+$ T Cells in *L. sigmodontis*-infected BALB/c mice (107). Further, murine IgG2b antibodies mediate FcγR-mediated immune responses (304). This can for example include the recognition and subsequent clearance of larvae by eosinophils (301). Therefore, one mechanism how the combination immunization therapy with poly(I:C) or 3pRNA improves vaccination success might be a more balanced IgG1:IgG2a/b antibody response.

An antibody-mediated effector function is antibody-dependent cell-mediated cytotoxicity (ADCC) (114).

The induction of ADCC is dependent on the FcR binding capacity, which differs between different antibody isotypes. In the murine immune system, IgG2a is most

potent to induce ADCC (114). ELISA analysis revealed higher level of IgG2a/b antibodies in the serum of mice immunized with a combination therapy. In line with this finding the larval motility was inhibited strongest when the culture medium was supplemented with serum from the corresponding groups. Further, the larval motility inhibition was accompanied by an attachment of cells. In future experiments in might be of interest to isolate larvae after the co-culture and analyze which types of cells were attached.

In a previous study, parasite-specific IgG1 and IgG3 serum antibodies from humans of endemic areas for *W. bancrofti* that had no symptoms or MF in their peripheral blood induced cell attachment to and death of *B. malayi* L3 larvae in an *in vitro* ADCC assay (306). IgG3 is involved in complement fixation, therefore it might be of interest to measure IgG3 production in response to the immunization with *L. sigmodontis* and analyze the role of complement for the observed larval motility inhibition.
Antibodies activate the classical complement pathway (307). During the classical pathway of complement activation complement protein C1q binds to antibodies bound to antigen and the complement cascade is triggered. This ultimately facilitates the lysis or phagocytosis of the targeted pathogen. The filaria *B. malayi* (308) and other helminths (309) were shown to block C1q and thereby evade the attack of the complement pathway. Therefore, also an enhanced complement activation by the choice of adjuvant for immunization may be beneficial for improving vaccination efficacy. The impact of the chosen nucleic acid receptor agonists poly(I:C) and 3pRNA on complement during in the immunization against *L. sigmodontis* still has to be investigated.

In vivo, probably a combination of all antibody-mediated mechanisms orchestrates the immune response against the pathogen. However, the presence of parasite-specific antibodies in the serum of immunized mice together with an *in vitro* motility inhibition of larvae mediated by serum indicates the generation of functional antibody responses triggered by the applied immunization strategies. This was improved by implementing the use of nucleic acid receptor agonists as adjuvant.

4.5.4 Impact of immunization on long-term disease outcome

Prior to the infection with *L. sigmodontis,* immunization-induced antibody responses were assessed and a successful production of parasite-specific IgG1, but also IgG2a/b and some IgE were measured. As a measure of how the immune response is mounted during the ongoing infection with *L. sigmodontis* and how this is influenced by the previous immunization, parasite-specific antibody levels were assessed during the course of infection. In an immunization study by Le Goff *et al.* (215) it was observed that immunized BALB/c mice had higher IgG2a level than infected control mice, while control mice had higher IgG1 level then immunized mice 60 days after the infection with *L. sigmodontis*. This supports the idea that a successful immunization should increase the IgG2/IgG1 ratio. In this thesis Th2-associated IgE level were higher in immunized animals than control animals following challenge infection. The addition of naked poly(I:C), trans. poly(I:C) or 3pRNA resulted in stable IgE level between days 37 to 63 post infection, while the IgE level kept increasing in animals that were immunized with att. L3 larvae alone. Further, Th2-associated IgG1 level in all immunized groups were lower than in control animals, independent from the chosen agonist as adjuvant. This was accompanied by higher IgG2a/b level in the groups immunized with att. L3 larvae alone or in combination with poly(I:C) over the course of infection compared control animals. Thereby, the immunization supported a more balanced Th1:Th2 immune response over the time course of infection. This was enhanced by the use of poly(I:C) as adjuvant, while the addition of 3pRNA as adjuvant to the immunization had a minor impact on shaping the measured antibody response. In order to see differences in the early response to infection, it would be of interest to additionally analyze antibody levels at earlier time points, for example when L3 larvae enter the pleural cavity or molting into L4 larvae takes place. At the same time, it would be of interest to monitor how long the parasite-specific antibodies are maintained in the mice after the mice have cleared the infection. This would provide evidence on how lasting the protection of the immunization is and how well it could complement the current MDA treatment.

After measuring successful parasite-specific adaptive immune responses in form of antibody generation, a major readout for the success of a filarial vaccination is the reduction in the adult worm burden. The reduction in adult worm burden after the immunization with att. L3 larvae alone was 45% in this study. In previous studies, this immunization strategy resulted in a reduction of adult worm burden of up to 80% (66,

94, 213, 215). Importantly, in these previous studies, the challenge infection occurred via subcutaneous injection of larvae at the site of immunization (94, 213, 215) and not, as done in this thesis, by natural infection. Arguably a natural challenge infection after the immunization mimics the infection via the bite of a vector after an immunization injection more realistically. Further, in previous studies the immunization injections were administered in one-week intervals, while our immunizations were performed in two-week intervals. This implicates that the shorter time between the administered immunizations might also affect the effectiveness. Nevertheless, the comparison between the conventional immunization with att. L3 larvae and a new combination therapy with adjuvant indicated that the worm burden was significantly reduced after a combination of att. L3 larvae and trans. poly(I:C) compared to the immunization with att. L3 alone. This implies that the use of poly(I:C) as adjuvant improves filarial vaccination. The reduction in worm burden after the use of 3pRNA as adjuvant was not statistically significant compared to the reduction achieved with att. L3 larvae alone. Still the reduction was enhanced by additional 12%, so that 3pRNA might be considered for further analysis as adjuvant in filaria vaccination.

In order to limit pathology, as well as transmission of the disease, also the impact of the vaccination on the release of MF is of interest. In female BALB/c mice, as used for this study, only ~70% of the animals develop detectable peripheral blood MF counts following natural infection (79). In this study, a patency of 50% was reached in the control group at day 63 after the infection. In animals immunized with att. L3 larvae alone or in combination with trans. poly(I:C) or 3pRNA, the percentage of patent animals was reduced. Also in another immunization study with irradiated *L. sigmodontis* L3 larvae there was a reduced percentage of MF positive mice after immunization (215). Whether the observed reduction in patency in this thesis was due to a reduction in fecund worms, a delayed MF release, more efficient MF killing or linked to altered embryogenesis is unclear. Transfected poly(I:C) had a greater impact on adult worm reduction (73%) than 3pRNA (57%), while after 3pRNA treatment only 17% of animals were MF positive at 63 days after infection and after trans. pol(I:C) treatment 29% were MF positive. This supports the conclusion that the MF reduction does not solely depend on a reduced number of mating worms. Among MF positive animals, there were no significant differences in the MF counts across the groups. Hence, it appears like the MF stage itself is not targeted more efficiently due to any of

the performed immunizations. To clarify an impact of the immunization on the worms' reproduction, the embryogenesis could be monitored.

In order to understand how the implementation of nucleic acid receptor agonists might support the elimination of parasites and limit the percentage of animals with circulating MF, immunological parameters in the pleura and spleen were assessed.

However, there neither was a difference in total immune cell counts in the pleural cavity 63 days after the infection, nor significant differences in most immune cell populations or measured cytokines. There was a reduction in $CD8^+$ T cell counts and their activation in animals that were immunized with a combination therapy including trans. poly(I:C) or 3pRNA. In this group also the worm burden was significantly reduced. Hence, this might reflect abating cytotoxic T cell responses after enhanced worm killing at an earlier time point. The interpretation of an abating cytotoxic T cell response in mice immunized with a combination of att. L3 larvae and trans. poly(I:C) or 3pRNA was accompanied by reduced levels of GrzB and IFN-γ. Else, in groups with lower worm burden also the secretion of the chemokine RANTES was reduced. This also implies that the immune response in these mice was weakening and less cell recruitment was mediated.

In line with the assumption that the peak of immune response against the parasite was at an earlier time point than 63 days post infection, there were minor changes in splenic cell populations of immunized animals.

Regarding systemic responses, cytokine secretion by splenocytes from immunized mice had a higher baseline secretion of Th2-associated cytokines like IL-5 and IL-13, but also Th1-associated IFN-γ or IP10. Therefore, the use of nucleic acid receptor agonists as adjuvants did not result in a clear change in Th1- or Th2-associated immune dominance.

Previous studies suggested that the vaccine induced elimination of invading parasites after challenge infection occurs early within the subcutaneous tissue (94, 213, 216, 217). In these studies, the challenge infection occurred subcutaneously at the same site of previous subcutaneous immunization. These studies showed that the larvae are limited in their movement, which was mediated by the attachment of cells (216), including eosinophils that attack the larvae (214). Possibly, this involved the mechanism of EETosis, where the larvae are attacked by DNA traps (102). This DNA traps could activate nucleic acid sensing and induce type I IFN secretion, as seen for

NETosis (260). It would be interesting to clarify whether NETosis is performed in the subcutaneous tissue upon primary parasite encounter and whether EETosis occurs in the subcutaneous tissue of immunized mice. Also, independently of a possible mechanism it still has to be investigated, whether the killing of larvae due to the immunization is limited to the subcutaneous tissue after natural challenge infection by analyzing larval survival at earlier time points after the challenge infection.
It was shown that after the immunization with irradiated *B. pahangi* L3 larvae only female larvae survived in the rodent (310). The female irradiated L3 larvae molt into L4 larvae and are then eliminated by the host 15 days after the last immunization injection (215). Therefore, the host is not only encountering the L3 larval stage, but pleural cells could also generate immune memory against L4 larvae. The secretome of irradiated larvae was not assessed, but generally sources of antigen that induce immune memory can also be secretory products. The secretome analysis of *L. sigmodontis* revealed a large overlap between L3, adult male and adult females prior to embryogenesis (278). These aspects allow the speculation that the immunization also induces immune responses that target invading parasites not only in the subcutaneous tissue.

Taken together, the use of poly(I:C) or 3pRNA improved the vaccination efficacy against *L. sigmodontis*. The implementation of the agonists into the immunization strategy with att. L3 larvae reduced the adult worm burden as well as the percentage of MF positive mice after a challenge infection. Further, the immunization was successful in generating parasite-specific antibodies that were functional in limiting the motility of *L. sigmodontis* L3 larvae. Overall, naked or trans. poly(I:C) had a stronger impact on antibody responses, while 3pRNA had a greater impact on $CD8^+$ T cells.

4.6 Conclusions and Outlook

In this thesis, it was shown that *L. sigmodontis*-derived nucleic acids activate monocytes and trigger the release of pro-inflammatory cytokines, including type I IFNs, *in vitro*. More importantly also the infection with *L. sigmodontis* induced increasing *in vivo* IFN-β production by pleural cells over the course of infection. However, the single knock out of the nucleic acid receptors TLR7, TLR9, MDA5 or STING did not influence the larval migration to the pleural cavity. Based on the modulation of nucleic acid sensing pathways by filariae, it was hypothesized that the activation of nucleic acid receptor pathways would enhance larval killing and might contribute to protective immunity. The treatment with the cytosolic RNA sensor agonists poly(I:C) and 3pRNA significantly reduced the adult worm burden and MF positive animals. The immunization with either poly(I:C) or 3pRNA as adjuvant induced functional parasite-specific antibody production and impacted the Th1:Th2 immune balances by further enhancing IgG2a/b antibody production compared to the immunization without agonist, but not IgE or IgG1.

In future studies it would be of interest to analyze whether the immunization-induced immune response is limited to the larval stage or also improves the clearance of later parasite stages. Further, it would be of interest to analyze how the role of complement in parasite clearance is affected by the use of poly(I:C) or 3pRNA as adjuvants.
Since an effective vaccine needs to induce long-lasting immune memory, it also would be of interest to analyze the generation of memory T and B cells, monitor the maintenance of parasite-specific circulating antibodies and perform challenge infections at later time points after the immunization.
In order to further enhance vaccination efficacy, a combination of poly(I:C) or 3pRNA with the TLR9 ligand CpG might be successful. This would combine the activation of cytosolic RNA sensors with the activation of an endosomal DNA sensor and thereby trigger more divers, but Th1-associated downstream signaling cascades. In other studies the combination of two agonists has been shown to increase antigen uptake by and the activation of dendritic cells (311).

For the elimination of onchocerciasis and lymphatic filariasis, the development of an effective vaccine would be a powerful tool. However, until now no fully successful immunization strategy for any human helminth infection has been developed. Based on the hypothesis that type I IFNs, which can be induced by the activation of nucleic

acid receptors, might be protective, the use of nucleic acids receptors agonists as adjuvant for *L. sigmodontis* vaccination was tested. Since a large population is already infected with filaria prior to vaccination, not only a prophylactic, but also the development of a therapeutic vaccine might be a powerful tool. In this setting the enhancement of type I IFNs could be beneficial for worm clearance.

Overall, the work in this thesis delivers valuable insight into the possibly protective role of type I IFNs in filarial infections and how the use of the nucleic acid receptor agonists poly(I:C) or 3pRNA can improve vaccination efficacy, likely by introducing a more balanced Th1/Th2 immune response.

5. References

1. James SL, Abate D, Abate KH, Abay SM, Abbafati C, Abbasi N, Abbastabar H, Abd-Allah F, Abdela J, Abdelalim A, Abdollahpour I, Abdulkader RS, Abebe Z, Abera SF, Abil OZ et al. Global, regional, and national incidence, prevalence, and years lived with disability for 354 diseases and injuries for 195 countries and territories, 1990–2017: a systematic analysis for the Global Burden of Disease Study 2017. The Lancet 2018; 392(10159):1789–858.

2. Hotez PJ, Brindley PJ, Bethony JM, King CH, Pearce EJ, Jacobson J. Helminth infections: the great neglected tropical diseases. J Clin Invest 2008; 118(4):1311–21.

3. Lucius R, Loos-Frank B. Parasitologie: Grundlagen für Biologen, Mediziner und Veterinärmediziner. Heidelberg: Spektrum Akademischer Verl.; 1997. (Spektrum Lehrbuch).

4. MacDonald AS, Araujo MI, Pearce EJ. Immunology of parasitic helminth infections. Infect Immun 2002; 70(2):427–33.

5. Anthony RM, Rutitzky LI, Urban JF, Stadecker MJ, Gause WC. Protective immune mechanisms in helminth infection. Nature Reviews Immunology 2007; 7(12):975–87.

6. Jenkins SJ, Allen JE. Similarity and diversity in macrophage activation by nematodes, trematodes, and cestodes. J Biomed Biotechnol 2010; 2010:262609.

7. WHO. Ending the neglect to attain the Sustainable Development Goals: a road map for neglected tropical diseases 2021–2030. Geneva; 2020.

8. United Nations. Transforming our World_ The 2030 Agenda for Sustainable Development; 2015.

9. WHO. Accelerating work to overcome the global impact of neglected tropical diseases: a roadmap for implementation; 2012.

10. Uniting to Combat NTDs. London Declaration on Neglected Tropical Diseases | Uniting to Combat NTDs; 2021 [cited 2021 Mar 29].

11. Babu S, Bhat SQ, Kumar NP, Jayantasri S, Rukmani S, Kumaran P, Gopi PG, Kolappan C, Kumaraswami V, Nutman TB. Human type 1 and 17 responses in latent tuberculosis are modulated by coincident filarial infection through cytotoxic T lymphocyte antigen-4 and programmed death-1. J Infect Dis 2009; 200(2):288–98.

12. Chatterjee S, Clark CE, Lugli E, Roederer M, Nutman TB. Filarial infection modulates the immune response to Mycobacterium tuberculosis through expansion of CD4+ IL-4 memory T cells. J Immunol 2015; 194(6):2706–14.

13. Kroidl I, Saathoff E, Maganga L, Makunde WH, Hoerauf A, Geldmacher C, Clowes P, Maboko L, Hoelscher M. Effect of Wuchereria bancrofti infection on HIV incidence in southwest Tanzania: a prospective cohort study. The Lancet 2016; 388(10054):1912–20.

14. Mhimbira F, Hella J, Said K, Kamwela L, Sasamalo M, Maroa T, Chiryamkubi M, Mhalu G, Schindler C, Reither K, Knopp S, Utzinger J, Gagneux S, Fenner L et al. Prevalence and clinical relevance of helminth co-infections among tuberculosis patients in urban Tanzania. PLoS Negl Trop Dis 2017; 11(2):e0005342.

15. Maizels RM, McSorley HJ. Regulation of the host immune system by helminth parasites. J Allergy Clin Immunol 2016; 138(3):666–75.

16. Haben I, Hartmann W, Breloer M. Nematode-induced interference with vaccination efficacy targets follicular T helper cell induction and is preserved after termination of infection. PLoS Negl Trop Dis 2014; 8(9):e3170.

17. Hartmann W, Haben I, Fleischer B, Breloer M. Pathogenic nematodes suppress humoral responses to third-party antigens in vivo by IL-10-mediated interference with Th cell function. J Immunol 2011; 187(8):4088–99.

18. Hoerauf A, Santoguina J, Saeftel M, Specht S. Immunomodulation by filarial nematodes. Parasite Immunology 2005; 27(10-11):417–29. Available from: URL: http://dx.doi.org/10.1111/j.1365-3024.2005.00792.x.

19. Kabagenyi J, Natukunda A, Nassuuna J, Sanya RE, Nampijja M, Webb EL, Elliott AM, Nkurunungi G. Urban-rural differences in immune responses to mycobacterial and tetanus vaccine antigens in a tropical setting: A role for helminths? Parasitology international 2020; 78:102132.

20. Lakwo T, Oguttu D, Ukety T, Post R, Bakajika D. Onchocerciasis Elimination: Progress and Challenges. Res Rep Trop Med 2020; 11:81–95.

21. Gyapong JO, Owusu IO, da-Costa Vroom FB, Mensah EO, Gyapong M. Elimination of lymphatic filariasis: current perspectives on mass drug administration. Res Rep Trop Med 2018; 9:25–33.

22. Kalyanasundaram R, Khatri V, Chauhan N. Advances in Vaccine Development for Human Lymphatic Filariasis. Trends Parasitol 2020; 36(2):195–205.

23. Hawryluk NA. Macrofilaricides: An Unmet Medical Need for Filarial Diseases. ACS Infect Dis 2020; 6(4):662–71.

24. Cobo F. Determinants of parasite drug resistance in human lymphatic filariasis. Rev Esp Quimioter 2016; 29(6):288–95.

25. Lustigman S, McCarter JP. Ivermectin resistance in Onchocerca volvulus: toward a genetic basis. PLoS Negl Trop Dis 2007; 1(1):e76.

26. Bergquist R, Lustigman S. Control of Important Helminthic Infections: Elsevier; 2010. (Important Helminth Infections in Southeast Asia: Diversity and Potential for Control and Elimination, Part B). Available from: URL: http://dx.doi.org/10.1016/S0065-308X(10)73010-4.

27. Zawawi A, Else KJ. Soil-Transmitted Helminth Vaccines: Are We Getting Closer? Front Immunol 2020; 11:576748.

28. WHO. Lymphatic filariasis; 2021 [cited 2021 Jun 14]. Available from: URL: https://www.who.int/news-room/fact-sheets/detail/lymphatic-filariasis.

29. Mathew CG, Bettis AA, Chu BK, English M, Ottesen EA, Bradley MH, Turner HC. The Health and Economic Burdens of Lymphatic Filariasis Prior to Mass Drug Administration Programs. Clin Infect Dis 2020; 70(12):2561–7.

30. Babu S, Nutman TB. Immunopathogenesis of lymphatic filarial disease. Semin Immunopathol 2012; 34(6):847–61.

31. Gyapong M, Gyapong J, Weiss M, Tanner M. The burden of hydrocele on men in Northern Ghana. Acta Tropica 2000; 77(3):287–94.

32. Ton TGN, Mackenzie C, Molyneux DH. The burden of mental health in lymphatic filariasis. Infect Dis Poverty 2015; 4:34.

33. Word Health Organization, editor. Diagnostic test for surveillance of lymphatic filariasis: target product profile. Geneva 2021.

34. WHO. Guideline: Alternative Mass Drug Administration Regimens to Eliminate Lymphatic Filariasis. Geneva: World Health Organization; 2017.

35. Alvar J, Alves F, Bucheton B, Burrows L, Büscher P, Carrillo E, Felger I, Hübner MP, Moreno J, Pinazo M-J, Ribeiro I, Sosa-Estani S, Specht S, Tarral A, Wourgaft NS et al. Implications of asymptomatic infection for the natural history of selected parasitic tropical diseases. Semin Immunopathol 2020; 42(3):231–46.

36. Turner HC. Health economic analyses of the Global Programme to Eliminate Lymphatic Filariasis. Int Health 2020; 13(Suppl 1):S71-S74.

37. WHO. Global programme to eliminate lymphatic filariasis: progress report, 2018; 2019.

38. King CL, Suamani J, Sanuku N, Cheng Y-C, Satofan S, Mancuso B, Goss CW, Robinson LJ, Siba PM, Weil GJ, Kazura JW et al. A Trial of a Triple-Drug Treatment for Lymphatic Filariasis. N Engl J Med 2018; 379(19):1801–10.

39. Debrah LB, Mohammed A, Osei-Mensah J, Mubarik Y, Agbenyega O, Ayisi-Boateng NK, Pfarr K, Kuehlwein JM, Klarmann-Schulz U, Hoerauf A, Debrah AY et al. Morbidity management and surveillance of lymphatic filariasis disease and acute dermatolymphangioadenitis attacks using a mobile phone-based tool by community health volunteers in Ghana. PLoS Negl Trop Dis 2020; 14(11):e0008839.

40. Brady M. Seventh meeting of the Global Alliance to Eliminate Lymphatic Filariasis: reaching the vision by scaling up, scaling down, and reaching out. Parasit Vectors 2014; 7:46.

41. WHO. Onchocerciasis (river blindness); 2021 [cited 2021 Jun 15]. Available from: URL: https://www.who.int/news-room/fact-sheets/detail/onchocerciasis.

42. Control of Neglected Tropical Diseases. Elimination of human onchocerciasis: progress report, 2019–2020. World Health Organization 2020 Nov 6 [cited 2021 Jun

22]. Available from: URL: https://www.who.int/publications/i/item/who-wer9545-545-554.

43. Tamarozzi F, Halliday A, Gentil K, Hoerauf A, Pearlman E, Taylor MJ. Onchocerciasis: the role of Wolbachia bacterial endosymbionts in parasite biology, disease pathogenesis, and treatment. Clin Microbiol Rev 2011; 24(3):459–68.

44. Saint André Av, Blackwell NM, Hall LR, Hoerauf A, Brattig NW, Volkmann L, Taylor MJ, Ford L, Hise AG, Lass JH, Diaconu E, Pearlman E et al. The role of endosymbiotic Wolbachia bacteria in the pathogenesis of river blindness. Science 2002; 295(5561):1892–5.

45. Brattig NW. Pathogenesis and host responses in human onchocerciasis: impact of Onchocerca filariae and Wolbachia endobacteria. Microbes and Infection 2004; 6(1):113–28.

46. Gaillard T, Briolant S, Madamet M, Pradines B. The end of a dogma: the safety of doxycycline use in young children for malaria treatment. Malar J 2017; 16(1):148.

47. Hoerauf A. Filariasis: new drugs and new opportunities for lymphatic filariasis and onchocerciasis. Curr Opin Infect Dis 2008; 21(6):673–81.

48. Gebrezgabiher G, Mekonnen Z, Yewhalaw D, Hailu A. Reaching the last mile: main challenges relating to and recommendations to accelerate onchocerciasis elimination in Africa. Infect Dis Poverty 2019; 8(1):60.

49. Boatin B. The Onchocerciasis Control Programme in West Africa (OCP). Ann Trop Med Parasitol 2008; 102 Suppl 1:13–7.

50. Amazigo U. The African Programme for Onchocerciasis Control (APOC). Ann Trop Med Parasitol 2008; 102 Suppl 1:19–22.

51. WHO/APOC. The WHO African Programme for Onchocerciasis ControlFinal Evaluation Report; 2015.

52. Turner HC, Churcher TS, Walker M, Osei-Atweneboana MY, PRICHARD RK, Basáñez M-G. Uncertainty surrounding projections of the long-term impact of ivermectin treatment on human onchocerciasis. PLoS Negl Trop Dis 2013; 7(4):e2169.

53. Kim YE, Remme JHF, Steinmann P, Stolk WA, Roungou J-B, Tediosi F. Control, elimination, and eradication of river blindness: scenarios, timelines, and ivermectin treatment needs in Africa. PLoS Negl Trop Dis 2015; 9(4):e0003664.

54. Hotez PJ, Bottazzi ME, Zhan B, Makepeace BL, Klei TR, Abraham D, Taylor DW, Lustigman S. The Onchocerciasis Vaccine for Africa--TOVA--Initiative. PLoS Negl Trop Dis 2015; 9(1):e0003422.

55. Hamley JID, Milton P, Walker M, Basáñez M-G. Modelling exposure heterogeneity and density dependence in onchocerciasis using a novel individual-based transmission model, EPIONCHO-IBM: Implications for elimination and data needs. PLoS Negl Trop Dis 2019; 13(12):e0007557.

56. Geary TG, Mackenzie CD. Progress and challenges in the discovery of macrofilaricidal drugs. Expert Rev Anti Infect Ther 2011; 9(8):681–95.

57. Kuesel AC. Research for new drugs for elimination of onchocerciasis in Africa. Int J Parasitol Drugs Drug Resist 2016; 6(3):272–86.

58. Johnston KL, Hong WD, Turner JD, O'Neill PM, Ward SA, Taylor MJ. Anti-Wolbachia drugs for filariasis. Trends Parasitol 2021; 37(12):1068–81.

59. Krücken J, Holden-Dye L, Keiser J, PRICHARD RK, Townson S, Makepeace BL, Hübner MP, Hahnel SR, Scandale I, Harder A, Kulke D et al. Development of emodepside as a possible adulticidal treatment for human onchocerciasis-The fruit of a successful industrial-academic collaboration. PLoS Pathog 2021; 17(7):e1009682.

60. Tova; 2021 [cited 2021 Jun 28]. Available from: URL: https://www.riverblindnessvaccinetova.org/.

61. CDC. Lymphatic Filariasis - Biology - Life Cycle of Wuchereria bancrofti; 2021 [cited 2021 Jan 5.424Z]. Available from: URL: https://www.cdc.gov/parasites/lymphaticfilariasis/biology_w_bancrofti.html.

62. Allen JE, Adjei O, Bain O, Hoerauf A, Hoffmann WH, Makepeace BL, Schulz-Key H, Tanya VN, Trees AJ, Wanji S, Taylor DW et al. Of mice, cattle, and humans: the immunology and treatment of river blindness. PLoS Negl Trop Dis 2008; 2(4):e217.

63. Risch F, Ritter M, Hoerauf A, Hübner MP. Human filariasis-contributions of the Litomosoides sigmodontis and Acanthocheilonema viteae animal model. Parasitology research 2021. Available from: URL: https://pubmed.ncbi.nlm.nih.gov/33547508/.

64. Petit G, Diagne M, Maréchal P, Owen D, Taylor D, Bain O. Maturation of the filariaLitomosoides sigmodontisin BALB/c mice; comparative susceptibility of nine other inbred strains. Annales de Parasitologie Humaine et Comparée 1992; 67(5):144–50. Available from: URL: http://dx.doi.org/10.1051/parasite/1992675144.

65. Hoffmann W, Petit G, Schulz-Key H, Taylor D, Bain O, Le Goff L. Litomosoides sigmodontis in Mice: Reappraisal of an Old Model for Filarial Research. Parasitol Today 2000; 16(9):387–9.

66. Maréchal P, Le Goff L, Hoffmann W, Rapp J, Oswald IP, Ombrouck C, Taylor DW, Bain O, Petit G. Immune response to the filaria Litomosoides sigmodontis in susceptible and resistant mice. Parasite Immunology 1997; 19(6):273–9. Available from: URL: http://dx.doi.org/10.1046/j.1365-3024.1997.d01-209.x.

67. Nematoda. In: Cruthers LR, Fourie JJ, Marchiondo AA, editors. Parasiticide Screening: Volume 2: In Vitro and In Vivo Tests with Relevant Parasite Rearing and Host Infection/Infestation Methods. Academic Press; 2020. p. 135–335.

68. Schneider CR, Blair LS, Schardein JL, Boche LK, Thompson PE. Comparison of Early Litomosoides carinii Infections in Cotton Rats and Gerbils. The Journal of Parasitology 1968; 54(6):1099.

69. Fulton A, Babayan SA, Taylor MD. Use of the Litomosoides sigmodontis Infection Model of Filariasis to Study Type 2 Immunity. Methods Mol Biol 2018; 1799:11–26.

70. Marcoullis G, Gräsbeck R. Preliminary identification and characterization of antigen extracts from Onchocerca volvulus. Tropenmed Parasitol 1976; 27(3):314–22.

71. Maréchal P, Petit G, Diagne M, Taylor DW, Bain O. Use of theLitomosoides sigmodontis- Mouse model in development of anOnchocercavaccine. II -L. sigmodontisin the balb/c mouse: vaccination experiments; preliminary immunological studies. Parasite 1994; 1(1S):S31-S32. Available from: URL: http://dx.doi.org/10.1051/parasite/199401s1031.

72. Harnett W, Grainger M, Worms MJ, Parkhouse RM. Evaluation of the potential of excretions-secretions (E-S) of Litomosoides carinii to substitute for human filarial E-S. Parasitology research 1989; 76(1):39–44.

73. Frohberger SJ, Ajendra J, Surendar J, Stamminger W, Ehrens A, Buerfent BC, Gentil K, Hoerauf A, Hübner MP. Susceptibility to L. sigmodontis infection is highest in animals lacking IL-4R/IL-5 compared to single knockouts of IL-4R, IL-5 or eosinophils. Parasit Vectors 2019; 12(1):248.

74. Hewitson JP, Maizels RM. Vaccination against helminth parasite infections. Expert Rev Vaccines 2014; 13(4):473–87.

75. Finlay CM, Allen JE. The immune response of inbred laboratory mice to Litomosoides sigmodontis: A route to discovery in myeloid cell biology. Parasite Immunology 2020; 42(7):e12708.

76. Scott JA, Macdonald EM, Terman B. A Description of the Stages in the Life Cycle of the Filarial Worm Litomosoides carinii. The Journal of Parasitology 1951; 37(5):425.

77. Karadjian G, Fercoq F, Pionnier N, Vallarino-Lhermitte N, Lefoulon E, Nieguitsila A, Specht S, Carlin LM, Martin C. Migratory phase of Litomosoides sigmodontis filarial infective larvae is associated with pathology and transient increase of S100A9 expressing neutrophils in the lung. PLoS Negl Trop Dis 2017; 11(5):e0005596.

78. Hübner MP, Torrero MN, McCall JW, Mitre E. Litomosoides sigmodontis: A simple method to infect mice with L3 larvae obtained from the pleural space of recently infected jirds (Meriones unguiculatus). Experimental Parasitology 2009; 123(1):95–8. Available from: URL: http://www.sciencedirect.com/science/article/pii/S0014489409001453.

79. Graham AL, Taylor MD, Le Goff L, Lamb TJ, Magennis M, Allen JE. Quantitative appraisal of murine filariasis confirms host strain differences but reveals that BALB/c females are more susceptible than males to Litomosoides sigmodontis. Microbes and Infection 2005; 7(4):612–8.

80. Babayan S, Ungeheuer M-N, Martin C, Attout T, Belnoue E, Snounou G, Rénia L, Korenaga M, Bain O. Resistance and susceptibility to filarial infection with

Litomosoides sigmodontis are associated with early differences in parasite development and in localized immune reactions. Infect Immun 2003; 71(12):6820–9.

81. Maizels RM, Smits HH, McSorley HJ. Modulation of Host Immunity by Helminths: The Expanding Repertoire of Parasite Effector Molecules. Immunity 2018; 49(5):801–18.

82. Babu S, Nutman TB. Immunology of lymphatic filariasis. Parasite Immunology 2014; 36(8):338–46.

83. van Riet E, Hartgers FC, Yazdanbakhsh M. Chronic helminth infections induce immunomodulation: consequences and mechanisms. Immunobiology 2007; 212(6):475–90. Available from: URL: https://pubmed.ncbi.nlm.nih.gov/17544832/.

84. Goel TC, Goel A. Eosinophilia in Lymphatic Filariasis. In: Goel TC, Goel A, editors. Lymphatic Filariasis. Singapore: Springer Singapore; 2016. p. 333–8.

85. Babu S, Kumaraswami V, Nutman TB. Alternatively activated and immunoregulatory monocytes in human filarial infections. J Infect Dis 2009; 199(12):1827–37.

86. Wammes LJ, Hamid F, Wiria AE, Wibowo H, Sartono E, Maizels RM, Smits HH, Supali T, Yazdanbakhsh M. Regulatory T cells in human lymphatic filariasis: stronger functional activity in microfilaremics. PLoS Negl Trop Dis 2012; 6(5):e1655.

87. Sahu BR, Mohanty MC, Sahoo PK, Satapathy AK, Ravindran B. Protective immunity in human filariasis: a role for parasite-specific IgA responses. J Infect Dis 2008; 198(3):434–43.

88. King CL, Nutman TB. Regulation of the immune response in lymphatic filariasis and onchocerciasis. Immunol Today 1991; 12(3):A54-A58.

89. Kurniawan A, Yazdanbakhsh M, van Ree R, Aalberse R, Selkirk ME, Partono F, Maizels RM. Differential expression of IgE and IgG4 specific antibody responses in asymptomatic and chronic human filariasis. J Immunol 1993; 150(9):3941–50.

90. Specht S, Frank JK, Alferink J, Dubben B, Layland LE, Denece G, Bain O, Förster I, Kirschning CJ, Martin C, Hoerauf A et al. CCL17 controls mast cells for the defense against filarial larval entry. J Immunol 2011; 186(8):4845–52.

91. Ajendra J, Specht S, Ziewer S, Schiefer A, Pfarr K, Parčina M, Kufer TA, Hoerauf A, Hübner MP. NOD2 dependent neutrophil recruitment is required for early protective immune responses against infectious Litomosoides sigmodontis L3 larvae. Sci Rep 2016; 6:39648.

92. Pionnier N, Brotin E, Karadjian G, Hemon P, Gaudin-Nomé F, Vallarino-Lhermitte N, Nieguitsila A, Fercoq F, Aknin M-L, Marin-Esteban V, Chollet-Martin S, Schlecht-Louf G, Bachelerie F, Martin C et al. Neutropenic Mice Provide Insight into the Role of Skin-Infiltrating Neutrophils in the Host Protective Immunity against Filarial Infective Larvae. PLoS Negl Trop Dis 2016; 10(4):e0004605.

93. Martin C, Le Goff L, Ungeheuer M-N, Vuong PN, Bain O. Drastic reduction of a filarial infection in eosinophilic interleukin-5 transgenic mice. Infect Immun 2000; 68(6):3651–6.

94. Martin C, Al-Qaoud KM, Ungeheuer M-N, Paehle K, Vuong PN, Bain O, Fleischer B, Hoerauf A. IL-5 is essential for vaccine-induced protection and for resolution of primary infection in murine filariasis. Medical Microbiology and Immunology 2000; 189(2):67–74. Available from: URL: http://dx.doi.org/10.1007/PL00008258.

95. Bain O, Wanji S, Vuong PN, Maréchal P, Le Goff L, Petit G. Larval biology of six filariae of the sub-family Onchocercinae in a vertebrate host. Parasite 1994; 1(3):241–54.

96. Ritter M, Tamadaho RS, Feid J, Vogel W, Wiszniewsky K, Perner S, Hoerauf A, Layland LE. IL-4/5 signalling plays an important role during Litomosoides sigmodontis infection, influencing both immune system regulation and tissue pathology in the thoracic cavity. International Journal for Parasitology 2017; 47(14):951–60.

97. Fercoq F, Remion E, Frohberger SJ, Vallarino-Lhermitte N, Hoerauf A, Le Quesne J, Landmann F, Hübner MP, Carlin LM, Martin C. IL-4 receptor dependent expansion of lung CD169+ macrophages in microfilaria-driven inflammation. PLoS Negl Trop Dis 2019; 13(8):e0007691.

98. Boyd A, Killoran K, Mitre E, Nutman TB. Pleural cavity type 2 innate lymphoid cells precede Th2 expansion in murine Litomosoides sigmodontis infection. Experimental Parasitology 2015; 159:118–26.

99. Al-Qaoud KM, Pearlman E, Hartung T, Klukowski J, Fleischer B, Hoerauf A. A new mechanism for IL-5-dependent helminth control: neutrophil accumulation and neutrophil-mediated worm encapsulation in murine filariasis are abolished in the absence of IL-5. International Immunology 2000; 12(6):899–908.

100. Torrero MN, Hübner MP, Larson D, Karasuyama H, Mitre E. Basophils amplify type 2 immune responses, but do not serve a protective role, during chronic infection of mice with the filarial nematode Litomosoides sigmodontis. J Immunol 2010; 185(12):7426–34.

101. Specht S, Saeftel M, Arndt M, Endl E, Dubben B, Lee NA, Lee JJ, Hoerauf A. Lack of eosinophil peroxidase or major basic protein impairs defense against murine filarial infection. Infect Immun 2006; 74(9):5236–43.

102. Ehrens A, Lenz B, Neumann A-L, Giarrizzo S, Reichwald JJ, Frohberger SJ, Stamminger W, Buerfent BC, Fercoq F, Martin C, Kulke D, Hoerauf A, Hübner MP et al. Microfilariae Trigger Eosinophil Extracellular DNA Traps in a Dectin-1-Dependent Manner. Cell Rep 2021; 34(2):108621.

103. Jenkins SJ, Ruckerl D, Cook PC, Jones LH, Finkelman FD, van Rooijen N, MacDonald AS, Allen JE. Local macrophage proliferation, rather than recruitment from the blood, is a signature of TH2 inflammation. Science 2011; 332(6035):1284–8.

104. Gause WC, Wynn TA, Allen JE. Type 2 immunity and wound healing: evolutionary refinement of adaptive immunity by helminths. Nature Reviews Immunology 2013; 13(8):607–14.

105. Korten S, Volkmann L, Saeftel M, Fischer K, Taniguchi M, Fleischer B, Hoerauf A. Expansion of NK cells with reduction of their inhibitory Ly-49A, Ly-49C, and Ly-49G2 receptor-expressing subsets in a murine helminth infection: contribution to parasite control. J Immunol 2002; 168(10):5199–206.

106. Layland LE, Ajendra J, Ritter M, Wiszniewsky A, Hoerauf A, Hübner MP. Development of patent Litomosoides sigmodontis infections in semi-susceptible C57BL/6 mice in the absence of adaptive immune responses. Parasit Vectors 2015; 8:396.

107. Al-Qaoud KM, Taubert A, Zahner H, Fleischer B, Hoerauf A. Infection of BALB/c mice with the filarial nematode Litomosoides sigmodontis: role of CD4+ T cells in controlling larval development. Infect Immun 1997; 65(6):2457–61.

108. van der Werf N, Redpath SA, Azuma M, Yagita H, Taylor MD. Th2 cell-intrinsic hypo-responsiveness determines susceptibility to helminth infection. PLoS Pathog 2013; 9(3):e1003215.

109. Knipper JA, Ivens A, Taylor MD. Helminth-induced Th2 cell dysfunction is distinct from exhaustion and is maintained in the absence of antigen. PLoS Negl Trop Dis 2019; 13(12):e0007908.

110. Taylor MD, van der Werf N, Harris A, Graham AL, Bain O, Allen JE, Maizels RM. Early recruitment of natural CD4+ Foxp3+ Treg cells by infective larvae determines the outcome of filarial infection. European Journal of Immunology 2009; 39(1):192–206.

111. Taylor MD, Le Goff L, Harris A, Malone E, Allen JE, Maizels RM. Removal of regulatory T cell activity reverses hyporesponsiveness and leads to filarial parasite clearance in vivo. J Immunol 2005; 174(8):4924–33.

112. Campbell SM, Knipper JA, Ruckerl D, Finlay CM, Logan N, Minutti CM, Mack M, Jenkins SJ, Taylor MD, Allen JE. Myeloid cell recruitment versus local proliferation differentiates susceptibility from resistance to filarial infection. Elife 2018; 7.

113. Le Goff L, Lamb TJ, Graham AL, Harcus Y, Allen JE. IL-4 is required to prevent filarial nematode development in resistant but not susceptible strains of mice. International Journal for Parasitology 2002; 32(10):1277–84.

114. Owen JA, Punt J, Stranford SA, Jones PP, Kuby J. Kuby immunology. 7th ed. New York: W.H. Freeman; 2013.

115. Martin C, Saeftel M, Vuong PN, Babayan S, Fischer K, Bain O, Hoerauf A. B-Cell Deficiency Suppresses Vaccine-Induced Protection against Murine Filariasis but Does Not Increase the Recovery Rate for Primary Infection. Infect Immun 2001; 69(11):7067–73.

116. van Dyken SJ, Locksley RM. Interleukin-4- and interleukin-13-mediated alternatively activated macrophages: roles in homeostasis and disease. Annu Rev Immunol 2013; 31:317–43.

117. Saeftel M, Volkmann L, Korten S, Brattig N, Al-Qaoud K, Fleischer B, Hoerauf A. Lack of interferon-γ confers impaired neutrophil granulocyte function and imparts prolonged survival of adult filarial worms in murine filariasis. Microbes and Infection 2001; 3(3):203–13. Available from: URL: http://dx.doi.org/10.1016/S1286-4579(01)01372-7.

118. Saeftel M, Arndt M, Specht S, Volkmann L, Hoerauf A. Synergism of gamma interferon and interleukin-5 in the control of murine filariasis. Infect Immun 2003; 71(12):6978–85.

119. Medzhitov R, Janeway CA. Innate immunity: impact on the adaptive immune response. Current Opinion in Immunology 1997; 9(1):4–9.

120. Aksoy E, Zouain CS, Vanhoutte F, Fontaine J, Pavelka N, Thieblemont N, Willems F, Ricciardi-Castagnoli P, Goldman M, Capron M, Ryffel B, Trottein F et al. Double-stranded RNAs from the helminth parasite Schistosoma activate TLR3 in dendritic cells. J Biol Chem 2005; 280(1):277–83.

121. Coch C, Hommertgen B, Zillinger T, Daßler-Plenker J, Putschli B, Nastaly M, Kümmerer BM, Scheunemann JF, Schumak B, Specht S, Schlee M, Barchet W, Hoerauf A, Bartok E, Hartmann G et al. Human TLR8 Senses RNA From Plasmodium falciparum-Infected Red Blood Cells Which Is Uniquely Required for the IFN-γ Response in NK Cells. Front Immunol 2019; 10:371.

122. Mogensen TH. Pathogen recognition and inflammatory signaling in innate immune defenses. Clin Microbiol Rev 2009; 22(2):240-73, Table of Contents.

123. Stögerer T, Stäger S. Innate Immune Sensing by Cells of the Adaptive Immune System. Front Immunol 2020; 11:1081.

124. Junt T, Barchet W. Translating nucleic acid-sensing pathways into therapies. Nat Rev Immunol 2015; 15(9):529–44.

125. Fitzner N, Clauberg S, Essmann F, Liebmann J, Kolb-Bachofen V. Human skin endothelial cells can express all 10 TLR genes and respond to respective ligands. Clin Vaccine Immunol 2008; 15(1):138–46.

126. Price AE, Shamardani K, Lugo KA, Deguine J, Roberts AW, Lee BL, Barton GM. A Map of Toll-like Receptor Expression in the Intestinal Epithelium Reveals Distinct Spatial, Cell Type-Specific, and Temporal Patterns. Immunity 2018; 49(3):560-575.e6.

127. Loo Y-M, Gale M. Immune signaling by RIG-I-like receptors. Immunity 2011; 34(5):680–92.

128. Schlee M, Hartmann G. Discriminating self from non-self in nucleic acid sensing. Nat Rev Immunol 2016; 16(9):566–80.

129. O'Brien K, Breyne K, Ughetto S, Laurent LC, Breakefield XO. RNA delivery by extracellular vesicles in mammalian cells and its applications. Nat Rev Mol Cell Biol 2020; 21(10):585–606.

130. Alexopoulou L, Holt AC, Medzhitov R, Flavell RA. Recognition of double-stranded RNA and activation of NF-kappaB by Toll-like receptor 3. Nature 2001; 413(6857):732–8. Available from: URL: https://pubmed.ncbi.nlm.nih.gov/11607032/.

131. Hemmi H, Kaisho T, Takeuchi O, Sato S, Sanjo H, Hoshino K, Horiuchi T, Tomizawa H, Takeda K, Akira S. Small anti-viral compounds activate immune cells via the TLR7 MyD88-dependent signaling pathway. Nat Immunol 2002; 3(2):196–200.

132. Jurk M, Heil F, Vollmer J, Schetter C, Krieg AM, Wagner H, Lipford G, Bauer S. Human TLR7 or TLR8 independently confer responsiveness to the antiviral compound R-848. Nat Immunol 2002; 3(6):499. Available from: URL: https://www.nature.com/articles/ni0602-499.

133. Kato H, Takeuchi O, Mikamo-Satoh E, Hirai R, Kawai T, Matsushita K, Hiiragi A, Dermody TS, Fujita T, Akira S. Length-dependent recognition of double-stranded ribonucleic acids by retinoic acid-inducible gene-I and melanoma differentiation-associated gene 5. J Exp Med 2008; 205(7):1601–10.

134. Hornung V, Ellegast J, Kim S, Brzózka K, Jung A, Kato H, Poeck H, Akira S, Conzelmann K-K, Schlee M, Endres S, Hartmann G et al. 5'-Triphosphate RNA is the ligand for RIG-I. Science 2006; 314(5801):994–7. Available from: URL: https://pubmed.ncbi.nlm.nih.gov/17038590/.

135. Gao D, Li T, Li X-D, Chen X, Li Q-Z, Wight-Carter M, Chen ZJ. Activation of cyclic GMP-AMP synthase by self-DNA causes autoimmune diseases. Proceedings of the National Academy of Sciences 2015; 112(42):E5699-705.

136. Hemmi H, Takeuchi O, Kawai T, Kaisho T, Sato S, Sanjo H, Matsumoto M, Hoshino K, Wagner H, Takeda K, Akira S et al. A Toll-like receptor recognizes bacterial DNA. Nature 2000; 408(6813):740–5.

137. Rigby RE, Webb LM, Mackenzie KJ, Li Y, Leitch A, Reijns MAM, Lundie RJ, Revuelta A, Davidson DJ, Diebold S, Modis Y, MacDonald AS, Jackson AP et al. RNA:DNA hybrids are a novel molecular pattern sensed by TLR9. EMBO J 2014; 33(6):542–58.

138. Vollmer J, Weeratna R, Payette P, Jurk M, Schetter C, Laucht M, Wader T, Tluk S, Liu M, Davis HL, Krieg AM et al. Characterization of three CpG oligodeoxynucleotide classes with distinct immunostimulatory activities. European Journal of Immunology 2004; 34(1):251–62.

139. Marshall JD, Fearon K, Abbate C, Subramanian S, Yee P, Gregorio J, Coffman RL, van Nest G. Identification of a novel CpG DNA class and motif that optimally stimulate B cell and plasmacytoid dendritic cell functions. J Leukoc Biol 2003; 73(6):781–92.

140. Hartmann G, Battiany J, Poeck H, Wagner M, Kerkmann M, Lubenow N, Rothenfusser S, Endres S. Rational design of new CpG oligonucleotides that combine B cell activation with high IFN-alpha induction in plasmacytoid dendritic cells. European Journal of Immunology 2003; 33(6):1633–41.

141. Krug A, Rothenfusser S, Hornung V, Jahrsdörfer B, Blackwell S, Ballas ZK, Endres S, Krieg AM, Hartmann G. Identification of CpG oligonucleotide sequences with high induction of IFN-α/β in plasmacytoid dendritic cells. European Journal of Immunology 2001; 31(7):2154–63.

142. Kerkmann M, Rothenfusser S, Hornung V, Towarowski A, Wagner M, Sarris A, Giese T, Endres S, Hartmann G. Activation with CpG-A and CpG-B oligonucleotides reveals two distinct regulatory pathways of type I IFN synthesis in human plasmacytoid dendritic cells. J Immunol 2003; 170(9):4465–74.

143. Jurk M, Schulte B, Kritzler A, Noll B, Uhlmann E, Wader T, Schetter C, Krieg AM, Vollmer J. C-Class CpG ODN: sequence requirements and characterization of immunostimulatory activities on mRNA level. Immunobiology 2004; 209(1-2):141–54.

144. Stetson DB, Medzhitov R. Recognition of Cytosolic DNA Activates an IRF3-Dependent Innate Immune Response. Immunity 2006; 24(1):93–103. Available from: URL: https://www.sciencedirect.com/science/article/pii/S1074761305004115.

145. Diner EJ, Burdette DL, Wilson SC, Monroe KM, Kellenberger CA, Hyodo M, Hayakawa Y, Hammond MC, Vance RE. The innate immune DNA sensor cGAS produces a noncanonical cyclic dinucleotide that activates human STING. Cell Rep 2013; 3(5):1355–61.

146. Montaner S, Galiano A, Trelis M, Martin-Jaular L, Del Portillo HA, Bernal D, Marcilla A. The Role of Extracellular Vesicles in Modulating the Host Immune Response during Parasitic Infections. Front Immunol 2014; 5:433.

147. Zakeri A, Hansen EP, Andersen SD, Williams AR, Nejsum P. Immunomodulation by Helminths: Intracellular Pathways and Extracellular Vesicles. Front Immunol 2018; 9.

148. Zamanian M, Fraser LM, Agbedanu PN, Harischandra H, Moorhead AR, Day TA, Bartholomay LC, Kimber MJ. Release of Small RNA-containing Exosome-like Vesicles from the Human Filarial Parasite Brugia malayi. PLoS Negl Trop Dis 2015; 9(9):e0004069.

149. Buck AH, Coakley G, Simbari F, McSorley HJ, Quintana JF, Le Bihan T, Kumar S, Abreu-Goodger C, Lear M, Harcus Y, Ceroni A, Babayan SA, Blaxter M, Ivens A, Maizels RM et al. Exosomes secreted by nematode parasites transfer small RNAs to mammalian cells and modulate innate immunity. Nat Commun 2014; 5:5488.

150. Tritten L, Burkman E, Moorhead A, Satti M, Geary J, Mackenzie C, Geary T. Detection of circulating parasite-derived microRNAs in filarial infections. PLoS Negl Trop Dis 2014; 8(7):e2971.

151. Semnani RT, Venugopal PG, Leifer CA, Mostböck S, Sabzevari H, Nutman TB. Inhibition of TLR3 and TLR4 function and expression in human dendritic cells by helminth parasites. Blood 2008; 112(4):1290–8.

152. Semnani RT, Mahapatra L, Moore V, Sanprasert V, Nutman TB. Functional and phenotypic characteristics of alternative activation induced in human monocytes by interleukin-4 or the parasitic nematode Brugia malayi. Infect Immun 2011; 79(10):3957–65.

153. Sharma A, Sharma P, Vishwakarma AL, Srivastava M. Functional Impairment of Murine Dendritic Cell Subsets following Infection with Infective Larval Stage 3 of Brugia malayi. Infect Immun 2017; 85(1).

154. Babu S, Blauvelt CP, Kumaraswami V, Nutman TB. Diminished expression and function of TLR in lymphatic filariasis: a novel mechanism of immune dysregulation. J Immunol 2005; 175(2):1170–6.

155. Babu S, Blauvelt CP, Kumaraswami V, Nutman TB. Cutting edge: diminished T cell TLR expression and function modulates the immune response in human filarial infection. J Immunol 2006; 176(7):3885–9.

156. Babu S, Bhat SQ, Pavan Kumar N, Lipira AB, Kumar S, Karthik C, Kumaraswami V, Nutman TB. Filarial lymphedema is characterized by antigen-specific Th1 and th17 proinflammatory responses and a lack of regulatory T cells. PLoS Negl Trop Dis 2009; 3(4):e420.

157. Babu S, Anuradha R, Kumar NP, George PJ, Kumaraswami V, Nutman TB. Filarial lymphatic pathology reflects augmented toll-like receptor-mediated, mitogen-activated protein kinase-mediated proinflammatory cytokine production. Infect Immun 2011; 79(11):4600–8.

158. Chen D, Zhao Y, Feng Y, Jin C, Yang Q, Qiu H, Xie H, Xie S, Zhou Y, Huang J. Expression of TLR2, TLR3, TLR4, and TLR7 on pulmonary lymphocytes of Schistosoma japonicum-infected C57BL/6 mice. Innate Immun 2019; 25(4):224–34.

159. Qu J, Li L, Xie H, Zhang X, Yang Q, Qiu H, Feng Y, Jin C, Dong N, Huang J. TLR3 Modulates the Response of NK Cells against Schistosoma japonicum. J Immunol Res 2018; 2018:7519856.

160. Vanhoutte F, Breuilh L, Fontaine J, Zouain CS, Mallevaey T, Vasseur V, Capron M, Goriely S, Faveeuw C, Ryffel B, Trottein F et al. Toll-like receptor (TLR)2 and TLR3 sensing is required for dendritic cell activation, but dispensable to control Schistosoma mansoni infection and pathology. Microbes and Infection 2007; 9(14-15):1606–13.

161. Joshi AD, Schaller MA, Lukacs NW, Kunkel SL, Hogaboam CM. TLR3 modulates immunopathology during a Schistosoma mansoni egg-driven Th2 response in the lung. European Journal of Immunology 2008; 38(12):3436–49.

162. Jiang Y-Y, Xu Y-X, Yuan Z-Y, Shen Y-J, Wu Y, Liu H-P, Hu Y, Cao J-P. Effect of toll-like receptor (TLR) 7 deficiencies on the in vivo immune response against

Schistosoma japonicum. Zhongguo Ji Sheng Chong Xue Yu Ji Sheng Chong Bing Za Zhi 2014; 32(3):172–5.

163. Souza C, Sanches RCO, Assis NRG, Marinho FV, Mambelli FS, Morais SB, Gimenez EGT, Guimarães ES, Castro TBR, Oliveira SC. The role of the adaptor molecule STING during Schistosoma mansoni infection. Sci Rep 2020; 10(1):7901.

164. Tognotti E. The eradication of smallpox, a success story for modern medicine and public health: what lessons for the future? J Infect Dev Ctries 2010; 4(5):264–6.

165. Gregorio E de, Rappuoli R. From empiricism to rational design: a personal perspective of the evolution of vaccine development. Nature Reviews Immunology 2014; 14(7):505–14.

166. Sallusto F, Lanzavecchia A, Araki K, Ahmed R. From vaccines to memory and back. Immunity 2010; 33(4):451–63.

167. Willis NJ. Edward Jenner and the eradication of smallpox. Scott Med J 1997; 42(4):118–21.

168. World Health Assembly 3. Declaration of global eradication of smallpox 1980.

169. Bordon Y. Antibody responses: Neutrophils zone in to help B cells. Nature Reviews Immunology 2012; 12(2):73.

170. Vetter V, Denizer G, Friedland LR, Krishnan J, Shapiro M. Understanding modern-day vaccines: what you need to know. Ann Med 2018; 50(2):110–20.

171. EMEA. Guideline on Adjuvants in vaccines for human use; 2005.

172. Pardi N, Hogan MJ, Porter FW, Weissman D. mRNA vaccines - a new era in vaccinology. Nat Rev Drug Discov 2018; 17(4):261–79.

173. Li L, Petrovsky N. Molecular mechanisms for enhanced DNA vaccine immunogenicity. Expert Rev Vaccines 2016; 15(3):313–29.

174. Sela M, Hilleman MR. Therapeutic vaccines: realities of today and hopes for tomorrow. Proc Natl Acad Sci U S A 2004; 101 Suppl 2:14559.

175. Hancock G, Hellner K, Dorrell L. Therapeutic HPV vaccines. Best Pract Res Clin Obstet Gynaecol 2018; 47:59–72.

176. Gatti-Mays ME, Redman JM, Collins JM, Bilusic M. Cancer vaccines: Enhanced immunogenic modulation through therapeutic combinations. Hum Vaccin Immunother 2017; 13(11):2561–74.

177. Reed SG, Orr MT, Fox CB. Key roles of adjuvants in modern vaccines. Nat Med 2013; 19(12):1597–608.

178. Coffman RL, Sher A, Seder RA. Vaccine adjuvants: putting innate immunity to work. Immunity 2010; 33(4):492–503.

179. CDC. Adjuvants and Vaccines | Vaccine Safety | CDC; 2021 [cited 2021 Jun 15]. Available from: URL: https://www.cdc.gov/vaccinesafety/concerns/adjuvants.html.

180. Wagner R, Hildt E. Zusammensetzung und Wirkmechanismen von Adjuvanzien in zugelassenen viralen Impfstoffen. Bundesgesundheitsbl 2019; 62(4):462–71. Available from: URL: https://link.springer.com/article/10.1007/s00103-019-02921-1#Tab2.

181. Bastola R, Noh G, Keum T, Bashyal S, Seo J-E, Choi J, Oh Y, Cho Y, Lee S. Vaccine adjuvants: smart components to boost the immune system. Arch Pharm Res 2017; 40(11):1238–48.

182. Pulendran B, Ahmed R. Immunological mechanisms of vaccination. Nat Immunol 2011; 12(6):509–17.

183. Overton ET, Goepfert PA, Cunningham P, Carter WA, Horvath J, Young D, Strayer DR. Intranasal seasonal influenza vaccine and a TLR-3 agonist, rintatolimod, induced cross-reactive IgA antibody formation against avian H5N1 and H7N9 influenza HA in humans. Vaccine 2014; 32(42):5490–5.

184. Saxena M, Sabado RL, La Mar M, Mohri H, Salazar AM, Dong H, Da Correa Rosa J, Markowitz M, Bhardwaj N, Miller E. Poly-ICLC, a TLR3 Agonist, Induces Transient Innate Immune Responses in Patients With Treated HIV-Infection: A Randomized Double-Blinded Placebo Controlled Trial. Front Immunol 2019; 10:725.

185. Hochheiser K, Klein M, Gottschalk C, Hoss F, Scheu S, Coch C, Hartmann G, Kurts C. Cutting Edge: The RIG-I Ligand 3pRNA Potently Improves CTL Cross-Priming and Facilitates Antiviral Vaccination. J Immunol 2016; 196(6):2439–43.

186. ClinicalTrials.gov. Study of Intralesional Administration of MK-4621 (RGT100) in Adult Participants With Advanced or Recurrent Tumors (MK-4621-001/RGT100-001) - Full Text View - ClinicalTrials.gov; 2021 [cited 2021 Jun 21]. Available from: URL: https://clinicaltrials.gov/ct2/show/NCT03065023?term=NCT03065023&rank=1.

187. Lipford GB, Bauer M, Blank C, Reiter R, Wagner H, Heeg K. CpG-containing synthetic oligonucleotides promote B and cytotoxic T cell responses to protein antigen: a new class of vaccine adjuvants. European Journal of Immunology 1997; 27(9):2340–4.

188. Bode C, Zhao G, Steinhagen F, Kinjo T, Klinman DM. CpG DNA as a vaccine adjuvant. Expert Rev Vaccines 2011; 10(4):499–511.

189. Zimmermann S, Dalpke A, Heeg K. CpG oligonucleotides as adjuvant in therapeutic vaccines against parasitic infections. Int J Med Microbiol 2008; 298(1-2):39–44.

190. Diemert DJ, Bottazzi ME, Plieskatt J, Hotez PJ, Bethony JM. Lessons along the Critical Path: Developing Vaccines against Human Helminths. Trends Parasitol 2018; 34(9):747–58.

191. Hartmann W, Brunn M-L, Stetter N, Gagliani N, Muscate F, Stanelle-Bertram S, Gabriel G, Breloer M. Helminth Infections Suppress the Efficacy of Vaccination against Seasonal Influenza. Cell Rep 2019; 29(8):2243-2256.e4.

192. Gopinath R, Hanna LE, Kumaraswami V, Pillai SV, Kavitha V, Vijayasekaran V, Rajasekharan A, Nutman TB. Long-term persistence of cellular hyporesponsiveness to filarial antigens after clearance of microfilaremia. The American Journal of Tropical Medicine and Hygiene 1999; 60(5):848–53.

193. Maizels RM, Holland MJ, Falcone FH, Zang XX, Yazdanbakhsh M. Vaccination against helminth parasites--the ultimate challenge for vaccinologists? Immunological Reviews 1999; 171:125–47.

194. Diemert DJ, Pinto AG, Freire J, Jariwala A, Santiago H, Hamilton RG, Periago MV, Loukas A, Tribolet L, Mulvenna J, Correa-Oliveira R, Hotez PJ, Bethony JM et al. Generalized urticaria induced by the Na-ASP-2 hookworm vaccine: implications for the development of vaccines against helminths. J Allergy Clin Immunol 2012; 130(1):169-76.e6.

195. Molehin AJ. Schistosomiasis vaccine development: update on human clinical trials. J Biomed Sci 2020; 27(1):28.

196. Wang X, Dong L, Ni H, Zhou S, Xu Z, Hoellwarth JS, Chen X, Zhang R, Chen Q, Liu F, Wang J, Su C et al. Combined TLR7/8 and TLR9 ligands potentiate the activity of a Schistosoma japonicum DNA vaccine. PLoS Negl Trop Dis 2013; 7(4):e2164.

197. Ricciardi A, Dalton JP, Ndao M. Evaluation of the immune response and protective efficacy of Schistosoma mansoni Cathepsin B in mice using CpG dinucleotides as adjuvant. Vaccine 2015; 33(2):346–53.

198. Teixeira de Melo T, Araujo JM, Campos de Sena I, Carvalho Alves C, Araujo N, Toscano Fonseca C. Evaluation of the protective immune response induced in mice by immunization with Schistosoma mansoni schistosomula tegument (Smteg) in association with CpG-ODN. Microbes and Infection 2013; 15(1):28–36.

199. ClinicalTrials.gov. Search of: vaccine | Hookworm - List Results - ClinicalTrials.gov; 2021 [cited 2021 Jun 22]. Available from: URL: https://clinicaltrials.gov/ct2/results?cond=Hookworm&term=vaccine&cntry=&state=&city=&dist=.

200. ClinicalTrials.gov. Search of: CpG | Hookworm - List Results - ClinicalTrials.gov; 2021 [cited 2021 Jun 21]. Available from: URL: https://www.clinicaltrials.gov/ct2/results?cond=Hookworm&term=CpG&cntry=&state=&city=&dist=.

201. Cordis - European Commission. Final Report Summary - HOOKVAC (Developing and Testing a novel, low-cost, effective HOOKworm VACcine to Control Human Hookworm Infection in endemic countries): Publication Office/CORDIS; 2021 [cited 2021 Jun 22]. Available from: URL: https://cordis.europa.eu/project/id/602843/reporting.

202. Morris CP, Evans H, Larsen SE, Mitre E. A comprehensive, model-based review of vaccine and repeat infection trials for filariasis. Clin Microbiol Rev 2013; 26(3):381–421.

203. George PJ, Hess JA, Jain S, Patton JB, Zhan T, Tricoche N, Zhan B, Bottazzi ME, Hotez PJ, Abraham D, Lustigman S et al. Antibody responses against the vaccine antigens Ov-103 and Ov-RAL-2 are associated with protective immunity to Onchocerca volvulus infection in both mice and humans. PLoS Negl Trop Dis 2019; 13(9):e0007730.

204. ClinicalTrials.gov. Search of: vaccine | Filariasis - List Results - ClinicalTrials.gov; 2021 [cited 2021 Jun 21]. Available from: URL: https://clinicaltrials.gov/ct2/results?cond=Filariasis&term=vaccine&cntry=&state=&city=&dist=.

205. Makepeace BL, Jensen SA, Laney SJ, Nfon CK, Njongmeta LM, Tanya VN, Williams SA, Bianco AE, Trees AJ. Immunisation with a multivalent, subunit vaccine reduces patent infection in a natural bovine model of onchocerciasis during intense field exposure. PLoS Negl Trop Dis 2009; 3(11):e544.

206. Claassen E, Leeuw W de, Greeve P de, Hendriksen C, Boersma W. Freund's complete adjuvant: an effective but disagreeable formula. Research in Immunology 1992; 143(5):478–83.

207. Hess JA, Zhan B, Bonne-Année S, Deckman JM, Bottazzi ME, Hotez PJ, Klei TR, Lustigman S, Abraham D. Vaccines to combat river blindness: expression, selection and formulation of vaccines against infection with Onchocerca volvulus in a mouse model. International Journal for Parasitology 2014; 44(9):637–46.

208. Lustigman S, Makepeace BL, Klei TR, Babayan SA, Hotez P, Abraham D, Bottazzi ME. Onchocerca volvulus: The Road from Basic Biology to a Vaccine. Trends Parasitol 2018; 34(1):64–79.

209. Ryan NM, Hess JA, Villena FP-M de, Leiby BE, Shimada A, Yu L, Yarmahmoodi A, Petrovsky N, Zhan B, Bottazzi ME, Makepeace BL, Lustigman S, Abraham D et al. Onchocerca volvulus bivalent subunit vaccine induces protective immunity in genetically diverse collaborative cross recombinant inbred intercross mice. NPJ Vaccines 2021; 6(1):17.

210. Arumugam S, Wei J, Liu Z, Abraham D, Bell A, Bottazzi ME, Hotez PJ, Zhan B, Lustigman S, Klei TR. Vaccination of Gerbils with Bm-103 and Bm-RAL-2 Concurrently or as a Fusion Protein Confers Consistent and Improved Protection against Brugia malayi Infection. PLoS Negl Trop Dis 2016; 10(4):e0004586.

211. Chauhan N, Khatri V, Banerjee P, Kalyanasundaram R. Evaluating the Vaccine Potential of a Tetravalent Fusion Protein (rBmHAXT) Vaccine Antigen Against Lymphatic Filariasis in a Mouse Model. Front Immunol 2018; 9:1520.

212. Khatri V, Chauhan N, Vishnoi K, Gegerfelt A von, Gittens C, Kalyanasundaram R. Prospects of developing a prophylactic vaccine against human lymphatic filariasis - evaluation of protection in non-human primates. International Journal for Parasitology 2018; 48(9-10):773–83.

213. Le Goff L, Maréchal P, Petit G, Taylor DW, Hoffmann W, Bain O. Early reduction of the challenge recovery rate following immunization with irradiated infective larvae in a filaria mouse system. Trop Med Int Health 1997; 2(12):1170–4.

214. Le Goff L, Loke P, Ali HF, Taylor DW, Allen JE. Interleukin-5 is essential for vaccine-mediated immunity but not innate resistance to a filarial parasite. Infect Immun 2000; 68(5):2513–7.

215. Le Goff L, Martin C, Oswald IP, Vuong PN, Petit G, UNGEHEUER MN, Bain O. Parasitology and immunology of mice vaccinated with irradiated Litomosoides sigmodontis larvae. Parasitology 2000; 120(3):271–80. Available from: URL: http://dx.doi.org/10.1017/S0031182099005533.

216. Babayan SA, Attout T, Vuong PN, Le Goff L, Gantier J-C, Bain O. The subcutaneous movements of filarial infective larvae are impaired in vaccinated hosts in comparison to primary infected hosts. Filaria Journal 2005; 4:3.

217. Babayan SA, Attout T, Harris A, Taylor M, Le Goff L, Vuong P, Renia L, Allen J, Bain O. Vaccination against filarial nematodes with irradiated larvae provides long-term protection against the third larval stage but not against subsequent life cycle stages. International Journal for Parasitology 2006; 36(8):903–14. Available from: URL: http://dx.doi.org/10.1016/j.ijpara.2006.04.013.

218. Torrero MN, Morris CP, Mitre BK, Hübner MP, Fox EM, Karasuyama H, Mitre E. Basophils help establish protective immunity induced by irradiated larval vaccination for filariasis. Vaccine 2013; 31(36):3675–82.

219. Hübner MP, Torrero MN, Mitre E. Type 2 immune-inducing helminth vaccination maintains protective efficacy in the setting of repeated parasite exposures. Vaccine 2010; 28(7):1746–57.

220. Ziewer S, Hübner MP, Dubben B, Hoffmann WH, Bain O, Martin C, Hoerauf A, Specht S. Immunization with L. sigmodontis microfilariae reduces peripheral microfilaraemia after challenge infection by inhibition of filarial embryogenesis. PLoS Negl Trop Dis 2012; 6(3):e1558.

221. Moll K, Ljungström I, Perlmann H, Scherf A, Wahlgren M. Methods in Malaria Research. fifth edition; 2008.

222. Coch C, Lück C, Schwickart A, Putschli B, Renn M, Höller T, Barchet W, Hartmann G, Schlee M. A human in vitro whole blood assay to predict the systemic cytokine response to therapeutic oligonucleotides including siRNA. PLoS One 2013; 8(8):e71057.

223. Ajendra J, Specht S, Neumann A-L, Gondorf F, Schmidt D, Gentil K, Hoffmann WH, Taylor MJ, Hoerauf A, Hübner MP. ST2 deficiency does not impair type 2 immune responses during chronic filarial infection but leads to an increased microfilaremia due to an impaired splenic microfilarial clearance. PLoS One 2014; 9(3):e93072.

224. Veerapathran A, Dakshinamoorthy G, Gnanasekar M, Reddy MVR, Kalyanasundaram R. Evaluation of Wuchereria bancrofti GST as a vaccine candidate for lymphatic filariasis. PLoS Negl Trop Dis 2009; 3(6):e457.

225. Liehl P, Zuzarte-Luís V, Chan J, Zillinger T, Baptista F, Carapau D, Konert M, Hanson KK, Carret C, Lassnig C, Müller M, Kalinke U, Saeed M, Chora AF, Golenbock DT et al. Host-cell sensors for Plasmodium activate innate immunity against liver-stage infection. Nat Med 2014; 20(1):47–53.

226. Gowda DC, Wu X. Parasite Recognition and Signaling Mechanisms in Innate Immune Responses to Malaria. Front. Immunol. 2018; 9:3006.

227. Bartok E, Hartmann G. Immune Sensing Mechanisms that Discriminate Self from Altered Self and Foreign Nucleic Acids. Immunity 2020; 53(1):54–77.

228. How Cationic Lipid Mediated Transfection Works | Thermo Fisher Scientific - DE; 2021 [cited 2021 Dec 9]. Available from: URL: https://www.thermofisher.com/de/de/home/references/gibco-cell-culture-basics/transfection-basics/gene-delivery-technologies/cationic-lipid-mediated-delivery/how-cationic-lipid-mediated-transfection-works.html.

229. Reissmann S. Cell penetration: scope and limitations by the application of cell-penetrating peptides. J Pept Sci 2014; 20(10):760–84.

230. McNab F, Mayer-Barber K, Sher A, Wack A, O'Garra A. Type I interferons in infectious disease. Nature Reviews Immunology 2015; 15(2):87–103.

231. Tokunaga R, Zhang W, Naseem M, Puccini A, Berger MD, Soni S, McSkane M, Baba H, Lenz H-J. CXCL9, CXCL10, CXCL11/CXCR3 axis for immune activation - A target for novel cancer therapy. Cancer Treatment Reviews 2018; 63:40–7.

232. Schoenborn JR, Wilson CB. Regulation of Interferon-γ During Innate and Adaptive Immune Responses. Advances in immunology 2007; 96:41–101. Available from: URL: https://pubmed.ncbi.nlm.nih.gov/17981204/.

233. Falvo JV, Tsytsykova AV, Goldfeld AE. Transcriptional Control of the TNF Gene. In: Kollias G, Sfikakis PP, editors. TNF Pathophysiology. Basel: KARGER; 2010. p. 27–60 (Current Directions in Autoimmunity).

234. Rutz S, Ouyang W. Regulation of Interleukin-10 Expression. In: Ma X, editor. Regulation of Cytokine Gene Expression in Immunity and Diseases. Dordrecht: Springer Netherlands; 2016. p. 89–116 (Advances in Experimental Medicine and Biology; vol. 941).

235. PubChem. Resiquimod; 2021 [cited 2021 Dec 9]. Available from: URL: https://pubchem.ncbi.nlm.nih.gov/compound/Resiquimod.

236. Peripheral Blood | Whole blood | Handbook | Miltenyi Biotec | Deutschland; 2021 [cited 2021 Oct 13]. Available from: URL: https://www.miltenyibiotec.com/DE-en/resources/macs-handbook/human-cells-and-organs/human-cell-sources/blood-human.html.

237. Guerriero JL. Macrophages. In: Biology of T Cells - Part B. Elsevier; 2019. p. 73–93 (International Review of Cell and Molecular Biology).

238. Fitzgerald-Bocarsly P, Dai J, Singh S. Plasmacytoid dendritic cells and type I IFN: 50 years of convergent history. Cytokine & Growth Factor Reviews 2008; 19(1):3–19.

239. Kato H, Sato S, Yoneyama M, Yamamoto M, Uematsu S, Matsui K, Tsujimura T, Takeda K, Fujita T, Takeuchi O, Akira S et al. Cell type-specific involvement of RIG-I in antiviral response. Immunity 2005; 23(1):19–28.

240. Liu M, Guo S, Hibbert JM, Jain V, Singh N, Wilson NO, Stiles JK. CXCL10/IP-10 in infectious diseases pathogenesis and potential therapeutic implications. Cytokine & Growth Factor Reviews 2011; 22(3):121–30.

241. Baccarella A, Fontana MF, Chen EC, Kim CC. Toll-like receptor 7 mediates early innate immune responses to malaria. Infect Immun 2013; 81(12):4431–42.

242. Franklin BS, Ishizaka ST, Lamphier M, Gusovsky F, Hansen H, Rose J, Zheng W, Ataíde MA, Oliveira RB de, Golenbock DT, Gazzinelli RT et al. Therapeutical targeting of nucleic acid-sensing Toll-like receptors prevents experimental cerebral malaria. Proceedings of the National Academy of Sciences 2011; 108(9):3689–94.

243. Kalantari P, DeOliveira RB, Chan J, Corbett Y, Rathinam V, Stutz A, Latz E, Gazzinelli RT, Golenbock DT, Fitzgerald KA. Dual engagement of the NLRP3 and AIM2 inflammasomes by plasmodium-derived hemozoin and DNA during malaria. Cell Rep 2014; 6(1):196–210. Available from: URL: https://pubmed.ncbi.nlm.nih.gov/24388751/.

244. Sharma S, DeOliveira RB, Kalantari P, Parroche P, Goutagny N, Jiang Z, Chan J, Bartholomeu DC, Lauw F, Hall JP, Barber GN, Gazzinelli RT, Fitzgerald KA, Golenbock DT et al. Innate immune recognition of an AT-rich stem-loop DNA motif in the Plasmodium falciparum genome. Immunity 2011; 35(2):194–207.

245. Schofield L, Grau GE. Immunological processes in malaria pathogenesis. Nat Rev Immunol 2005; 5(9):722–35. Available from: URL: https://www.nature.com/articles/nri1686.

246. Foth BJ, McFadden GI. The apicoplast: A plastid in Plasmodium falciparum and other apicomplexan parasites. In: Elsevier; 2003. p. 57–110 (International Review of Cytology).

247. Hoerauf A, Nissen-Pähle K, Schmetz C, Henkle-Dührsen K, Blaxter ML, Büttner DW, Gallin MY, Al-Qaoud KM, Lucius R, Fleischer B. Tetracycline therapy targets intracellular bacteria in the filarial nematode Litomosoides sigmodontis and results in filarial infertility. J Clin Invest 1999; 103(1):11–8.

248. Lim L, McFadden GI. The evolution, metabolism and functions of the apicoplast. Phil. Trans. R. Soc. B 2010; 365(1541):749–63.

249. Guo X, Wang H, Li Y, Leng X, Huang W, Ma Y, Xu T, Qi X. Transfection reagent Lipofectamine triggers type I interferon signaling activation in macrophages.

Immunology & Cell Biology 2019; 97(1):92–6. Available from: URL: https://pubmed.ncbi.nlm.nih.gov/30084169/.

250. Poeck H, Bscheider M, Gross O, Finger K, Roth S, Rebsamen M, Hannesschläger N, Schlee M, Rothenfusser S, Barchet W, Kato H, Akira S, Inoue S, Endres S, Peschel C et al. Recognition of RNA virus by RIG-I results in activation of CARD9 and inflammasome signaling for interleukin 1 beta production. Nat Immunol 2010; 11(1):63–9. Available from: URL: https://pubmed.ncbi.nlm.nih.gov/19915568/.

251. Franchi L, Eigenbrod T, Muñoz-Planillo R, Ozkurede U, Kim Y-G, Arindam C, Gale M, Silverman RH, Colonna M, Akira S, Núñez G et al. Cytosolic double-stranded RNA activates the NLRP3 inflammasome via MAVS-induced membrane permeabilization and K+ efflux. The Journal of Immunology 2014; 193(8):4214–22.

252. Kapellos TS, Bonaguro L, Gemünd I, Reusch N, Saglam A, Hinkley ER, Schultze JL. Human Monocyte Subsets and Phenotypes in Major Chronic Inflammatory Diseases. Front Immunol 2019; 10:2035.

253. Thaler B, Hohensinner PJ, Krychtiuk KA, Matzneller P, Koller L, Brekalo M, Maurer G, Huber K, Zeitlinger M, Jilma B, Wojta J, Speidl WS et al. Differential in vivo activation of monocyte subsets during low-grade inflammation through experimental endotoxemia in humans. Sci Rep 2016; 6:30162. Available from: URL: https://pubmed.ncbi.nlm.nih.gov/27444882/.

254. Paludan SR, Reinert LS, Hornung V. DNA-stimulated cell death: implications for host defence, inflammatory diseases and cancer. Nature Reviews Immunology 2019; 19(3):141–53.

255. Gaidt MM, Ebert TS, Chauhan D, Ramshorn K, Pinci F, Zuber S, O'Duill F, Schmid-Burgk JL, Hoss F, Buhmann R, Wittmann G, Latz E, Subklewe M, Hornung V et al. The DNA Inflammasome in Human Myeloid Cells Is Initiated by a STING-Cell Death Program Upstream of NLRP3. Cell 2017; 171(5):1110-1124.e18.

256. Ma Y, Su X, Lu F. The Roles of Type I Interferon in Co-infections With Parasites and Viruses, Bacteria, or Other Parasites. Front Immunol 2020; 11:1805.

257. Kovarik P, Castiglia V, Ivin M, Ebner F. Type I Interferons in Bacterial Infections: A Balancing Act. Front Immunol 2016; 7:652.

258. Webb LM, Lundie RJ, Borger JG, Brown SL, Connor LM, Cartwright AN, Dougall AM, Wilbers RH, Cook PC, Jackson-Jones LH, Phythian-Adams AT, Johansson C, Davis DM, Dewals BG, Ronchese F et al. Type I interferon is required for T helper (Th) 2 induction by dendritic cells. EMBO J 2017; 36(16):2404–18.

259. Kuka M, Giovanni M de, Iannacone M. The role of type I interferons in CD4+ T cell differentiation. Immunology Letters 2019; 215:19–23.

260. Apel F, Andreeva L, Knackstedt LS, Streeck R, Frese CK, Goosmann C, Hopfner K-P, Zychlinsky A. The cytosolic DNA sensor cGAS recognizes neutrophil extracellular traps. Sci. Signal. 2021; 14(673):eaax7942.

261. Venugopal PG, Nutman TB, Semnani RT. Activation and regulation of Toll-Like Receptors (TLRs) by helminth parasites. Immunologic research 2009; 43(1-3):252–63.

262. Honda K, Takaoka A, Taniguchi T. Type I interferon corrected gene induction by the interferon regulatory factor family of transcription factors. Immunity 2006; 25(3):349–60. Available from: URL: https://www.sciencedirect.com/science/article/pii/S1074761306003943.

263. Ali S, Mann-Nüttel R, Schulze A, Richter L, Alferink J, Scheu S. Sources of Type I Interferons in Infectious Immunity: Plasmacytoid Dendritic Cells Not Always in the Driver's Seat. Front Immunol 2019; 10:778.

264. Akkaya M, Akkaya B, Miozzo P, Rawat M, Pena M, Sheehan PW, Kim AS, Kamenyeva O, Kabat J, Bolland S, Chaturvedi A, Pierce SK et al. B Cells Produce Type 1 IFNs in Response to the TLR9 Agonist CpG-A Conjugated to Cationic Lipids. J Immunol 2017; 199(3):931–40.

265. Marshall-Clarke S, Downes JE, Haga IR, Bowie AG, Borrow P, Pennock JL, Grencis RK, Rothwell P. Polyinosinic acid is a ligand for toll-like receptor 3. Journal of Biological Chemistry 2007; 282(34):24759–66.

266. Sheikh F, Dickensheets H, Gamero AM, Vogel SN, Donnelly RP. An essential role for IFN-β in the induction of IFN-stimulated gene expression by LPS in macrophages. J Leukoc Biol 2014; 96(4):591–600.

267. Gan T, Yang Y, Hu F, Chen X, Zhou J, Li Y, Xu Y, Wang H, Chen Y, Zhang M. TLR3 Regulated Poly I:C-Induced Neutrophil Extracellular Traps and Acute Lung Injury Partly Through p38 MAP Kinase. Front. Microbiol. 2018; 9:3174.

268. Sabroe I, Prince LR, Jones EC, Horsburgh MJ, Foster SJ, Vogel SN, Dower SK, Whyte MKB. Selective roles for Toll-like receptor (TLR)2 and TLR4 in the regulation of neutrophil activation and life span. J Immunol 2003; 170(10):5268–75. Available from: URL: https://pubmed.ncbi.nlm.nih.gov/12734376/.

269. Rosenberg HF, Dyer KD, Foster PS. Eosinophils: changing perspectives in health and disease. Nature Reviews Immunology 2013; 13(1):9–22. Available from: URL: https://pubmed.ncbi.nlm.nih.gov/23154224/.

270. Lamb TJ, Le Goff L, Kurniawan A, Guiliano DB, Fenn K, Blaxter ML, Read AF, Allen JE. Most of the response elicited against Wolbachia surface protein in filarial nematode infection is due to the infective larval stage. J Infect Dis 2004; 189(1):120–7.

271. Wiszniewsky A, Ritter M, Krupp V, Schulz S, Arndts K, Weighardt H, Wanji S, Hoerauf A, Layland LE. The central adaptor molecule TRIF influences L. sigmodontis worm development. Parasitology research 2019; 118(2):539–49.

272. Keestra-Gounder AM, Tsolis RM. NOD1 and NOD2: Beyond Peptidoglycan Sensing. Trends Immunol 2017; 38(10):758–67.

273. Osborne J, Devaney E. Interleukin-10 and antigen-presenting cells actively suppress Th1 cells in BALB/c mice infected with the filarial parasite Brugia pahangi. Infect Immun 1999; 67(4):1599–605.

274. Devaney E, Osborne J. The third-stage larva (L3) of Brugia: its role in immune modulation and protective immunity. Microbes and Infection 2000; 2(11):1363–71. Available from: URL: https://www.sciencedirect.com/science/article/pii/S1286457900012909.

275. MacDonald AS, Maizels RM, Lawrence RA, Dransfield I, Allen JE. Requirement for in vivo production of IL-4, but not IL-10, in the induction of proliferative suppression by filarial parasites. J Immunol 1998; 160(3):1304–12. Available from: URL: https://www.jimmunol.org/content/160/3/1304.short.

276. Varano B, Fantuzzi L, Puddu P, Borghi P, Belardelli F, Gessani S. Inhibition of the constitutive and induced IFN-beta production by IL-4 and IL-10 in murine peritoneal macrophages. Virology 2000; 277(2):270–7. Available from: URL: https://pubmed.ncbi.nlm.nih.gov/11080475/.

277. Harischandra H, Yuan W, Loghry HJ, Zamanian M, Kimber MJ. Profiling extracellular vesicle release by the filarial nematode Brugia malayi reveals sex-specific differences in cargo and a sensitivity to ivermectin. PLoS Negl Trop Dis 2018; 12(4):e0006438.

278. Armstrong SD, Babayan SA, Lhermitte-Vallarino N, Gray N, Xia D, Martin C, Kumar S, Taylor DW, Blaxter ML, Wastling JM, Makepeace BL et al. Comparative analysis of the secretome from a model filarial nematode (Litomosoides sigmodontis) reveals maximal diversity in gravid female parasites. Mol Cell Proteomics 2014; 13(10):2527–44.

279. Donnelly S, O'Neill SM, Stack CM, Robinson MW, Turnbull L, Whitchurch C, Dalton JP. Helminth cysteine proteases inhibit TRIF-dependent activation of macrophages via degradation of TLR3. J Biol Chem 2010; 285(5):3383–92.

280. Dakshinamoorthy G, Samykutty AK, Munirathinam G, Reddy MV, Kalyanasundaram R. Multivalent fusion protein vaccine for lymphatic filariasis. Vaccine 2013; 31(12):1616–22. Available from: URL: https://pubmed.ncbi.nlm.nih.gov/23036503/.

281. Babu S, Ganley LM, Klei TR, Shultz LD, Rajan TV. Role of gamma interferon and interleukin-4 in host defense against the human filarial parasite Brugia malayi. Infect Immun 2000; 68(5):3034–5.

282. Sahoo MK, Sisodia BS, Dixit S, Joseph SK, Gaur RL, Verma SK, Verma AK, Shasany AK, Dowle AA, Murthy PK. Immunization with inflammatory proteome of Brugia malayi adult worm induces a Th1/Th2-immune response and confers protection against the filarial infection. Vaccine 2009; 27(32):4263–71. Available from: URL: http://dx.doi.org/10.1016/j.vaccine.2009.05.015.

283. Draz HM, Mahmoud SS, Ashour E, Shaker YM, Wu CH, Wu GY. Effects of PEG-interferon-alpha-2A on Schistosoma mansoni infection in mice. The Journal of Parasitology 2010; 96(4):703–8. Available from: URL: https://pubmed.ncbi.nlm.nih.gov/20486736/.

284. Park EJ, Choi J, Lee KC, Na DH. Emerging PEGylated non-biologic drugs. Expert Opinion on Emerging Drugs 2019; 24(2):107–19.

285. Fried MW, Hadziyannis SJ. Treatment of chronic hepatitis C infection with peginterferons plus ribavirin. Semin Liver Dis 2004; 24 Suppl 2:47–54.

286. Keating GM. Peginterferon-alpha-2a (40 kD): A review of its use in chronic hepatitis B. Drugs 2009; 69(18):2633–60. Available from: URL: https://pubmed.ncbi.nlm.nih.gov/19943712/.

287. Brewer JM, Conacher M, Satoskar A, Bluethmann H, Alexander J. In interleukin-4-deficient mice, alum not only generates T helper 1 responses equivalent to freund's complete adjuvant, but continues to induce T helper 2 cytokine production. European Journal of Immunology 1996; 26(9):2062–6. Available from: URL: https://pubmed.ncbi.nlm.nih.gov/8814247/.

288. Petrovsky N, Aguilar JC. Vaccine adjuvants: current state and future trends. Immunol Cell Biol 2004; 82(5):488–96.

289. Kool M, Fierens K, Lambrecht BN. Alum adjuvant: some of the tricks of the oldest adjuvant. J Med Microbiol 2012; 61(Pt 7):927–34.

290. Dakshinamoorthy G, Gegerfelt A von, Andersen H, Lewis M, Kalyanasundaram R. Evaluation of a multivalent vaccine against lymphatic filariasis in rhesus macaque model. PLoS One 2014; 9(11):e112982.

291. Efficacy of Na-GST-1/Alhydrogel Hookworm Vaccine Assessed by Controlled Challenge Infection - Full Text View - ClinicalTrials.gov; 2021 [cited 2021 Oct 6]. Available from: URL: https://www.clinicaltrials.gov/ct2/show/NCT03172975?term=CpG&cond=Hookworm&draw=2&rank=3.

292. Lynn GM, Laga R, Darrah PA, Ishizuka AS, Balaci AJ, Dulcey AE, Pechar M, Pola R, Gerner MY, Yamamoto A, Buechler CR, Quinn KM, Smelkinson MG, Vanek O, Cawood R et al. In vivo characterization of the physicochemical properties of polymer-linked TLR agonists that enhance vaccine immunogenicity. Nat Biotechnol 2015; 33(11):1201–10.

293. Angelini C, Varano B, Puddu P, Fiori M, Baldassarre A, Masotti A, Gessani S, Conti L. Direct and Intestinal Epithelial Cell-Mediated Effects of TLR8 Triggering on Human Dendritic Cells, CD14+CD16+ Monocytes and γδ T Lymphocytes. Front Immunol 2017; 8:1813.

294. Heidegger S, Kreppel D, Bscheider M, Stritzke F, Nedelko T, Wintges A, Bek S, Fischer JC, Graalmann T, Kalinke U, Bassermann F, Haas T, Poeck H et al. RIG-I

activating immunostimulatory RNA boosts the efficacy of anticancer vaccines and synergizes with immune checkpoint blockade. EBioMedicine 2019; 41:146–55.

295. Vono M, Lin A, Norrby-Teglund A, Koup RA, Liang F, Loré K. Neutrophils acquire the capacity for antigen presentation to memory CD4+ T cells in vitro and ex vivo. Blood 2017; 129(14):1991–2001.

296. Li Y, Wang W, Yang F, Xu Y, Feng C, Zhao Y. The regulatory roles of neutrophils in adaptive immunity. Cell communication and signaling : CCS 2019; 17(1):147. Available from: URL: https://pubmed.ncbi.nlm.nih.gov/31727175/.

297. Schetters STT, Kruijssen LJW, Crommentuijn MHW, Kalay H, den Haan JMM, van Kooyk Y. Immunological dynamics after subcutaneous immunization with a squalene-based oil-in-water adjuvant. FASEB J 2020:12406–18.

298. Majdoubi A, Lee JS, Balood M, Sabourin A, DeMontigny A, Kishta OA, Moulefera MA, Galbas T, Yun TJ, Talbot S, Ishido S, Cheong C, Thibodeau J et al. Downregulation of MHC Class II by Ubiquitination Is Required for the Migration of CD206+ Dendritic Cells to Skin-Draining Lymph Nodes. The Journal of Immunology 2019; 203(11):2887–98. Available from: URL: https://pubmed.ncbi.nlm.nih.gov/31659013/.

299. Kilarski WW, Martin C, Pisano M, Bain O, Babayan SA, Swartz MA. Inherent biomechanical traits enable infective filariae to disseminate through collecting lymphatic vessels. Nat Commun 2019:2895.

300. Palm A-KE, Henry C. Remembrance of Things Past: Long-Term B Cell Memory After Infection and Vaccination. Front Immunol 2019; 10:1787.

301. Harris N, Gause WC. To B or not to B: B cells and the Th2-type immune response to helminths. Trends Immunol 2011; 32(2):80–8.

302. Snapper CM, Paul WE. Interferon-gamma and B cell stimulatory factor-1 reciprocally regulate Ig isotype production. Science 1987; 236(4804):944–7. Available from: URL: https://pubmed.ncbi.nlm.nih.gov/3107127/.

303. Estes DM, Tuo W, Brown WC, Goin J. Effects of type I/type II interferons and transforming growth factor-beta on B-cell differentiation and proliferation. Definition of costimulation and cytokine requirements for immunoglobulin synthesis and expression. Immunology 1998; 95(4):604–11.

304. Collins AM. IgG subclass co-expression brings harmony to the quartet model of murine IgG function. Immunology & Cell Biology 2016; 94(10):949–54.

305. Babayan SA, Luo H, Gray N, Taylor DW, Allen JE. Deletion of parasite immune modulatory sequences combined with immune activating signals enhances vaccine mediated protection against filarial nematodes. PLoS Negl Trop Dis 2012; 6(12):e1968.

306. Dakshinamoorthy G, Samykutty AK, Munirathinam G, Shinde GB, Nutman T, Reddy MV, Kalyanasundaram R. Biochemical characterization and evaluation of a Brugia malayi small heat shock protein as a vaccine against lymphatic filariasis.

PLOS ONE 2012; 7(4):e34077. Available from: URL: https://journals.plos.org/plosone/article?id=10.1371/journal.pone.0034077#s2.

307. Dunkelberger JR, Song W-C. Complement and its role in innate and adaptive immune responses. Cell Research 2009; 20(1):34–50. Available from: URL: http://dx.doi.org/10.1038/cr.2009.139.

308. Yadav S, Gupta S, Selvaraj C, Doharey PK, Verma A, Singh SK, Saxena JK. In silico and in vitro studies on the protein-protein interactions between Brugia malayi immunomodulatory protein calreticulin and human C1q. PLOS ONE 2014; 9(9):e106413.

309. Shao S, Sun X, Chen Y, Zhan B, Zhu X. Complement Evasion: An Effective Strategy That Parasites Utilize to Survive in the Host. Front. Microbiol. 2019; 10:532.

310. Devaney E, Bancroft A, Egan A. The effect of irradiation on the third stage larvae of Brugia pahangi. Parasite Immunology 1993; 15(7):423–7. Available from: URL: https://pubmed.ncbi.nlm.nih.gov/8414645/.

311. Lu F, Mosley Y-YC, Carmichael B, Brown DD, HogenEsch H. Formulation of aluminum hydroxide adjuvant with TLR agonists poly(I:C) and CpG enhances the magnitude and avidity of the humoral immune response. Vaccine 2019; 37(14):1945–53.

Scientific contributions

Publications in peer-reviewed journals

Published during PhD

Coch C, Hommertgen B, Zillinger T, Daßler-Plenker J, Putschli B, Nastaly M, Kümmerer BM, **Scheunemann JF**, Schumak B, Specht S, Schlee M, Barchet W, Hoerauf A, Bartok E and Hartmann G. Human TLR8 senses RNA from *Plasmodium falciparum*-infected red blood cells which is required for the IFN-γ response in NK cells. Frontiers in Immunology – Microbial Immunology, 2019

Scheunemann JF, Reichwald JJ, Korir PJ, Kuehlwein JM, Jenster L, Hammerschmidt-Kamper C, Lewis MD, Klocke K, Borsche M, Schwendt KE, Soun C, Thiebes S, Limmer A, Engel DR, Mueller A, Hoerauf A, Hübner MP, Schumak B. Eosinophils suppress the migration of T cells into the brain of *Plasmodium berghei*-infected Ifnar1$^{-/-}$ mice and protect them from experimental cerebral malaria. Frontiers in Immunology – Parasite Immunology, 2021

In preparation

Scheunemann JF, Risch F, Reichwald JJ, Lenz B, Garbe S, Frohberger SJ, Koschel M, Hartmann G, Coch C, Hoerauf A, Schumak B, Hübner MP. Nucleic acid receptor ligands improve vaccination efficacy against the filarial nematode *Litomosoides sigmodontis*.

Reichwald JJ, Neumann AL, Risch F, Frohberger SJ, **Scheunemann JF**, Ehrens A, Strutz W, Hoerauf A, Schumak B, Hübner MP. ILC2s control microfilaremia during *Litomosoides sigmodontis* infection.

Conferences

Oral presentation at the 21st Symposium “Infection and Immunity” by the German Society for Immunology (DGfI) in Rothenfels, Germany, 2017 (“Characterization of regulatory immune responses in *Plasmodium berghei* ANKA infected mice”)

Poster presentation at the 5th European Congress of Immunology (ECI) in Amsterdam, Netherlands, 2018 (“RNA derived from *Plasmodium falciparum* and *Litomosoides sigmodontis* is potent to induce a pro-inflammatory immune response in human cells”)

Poster presentation at the 10th Autumn School of the DGfI in Merseburg, Germany, 2018 (“RNA derived from *Plasmodium falciparum* and *Litomosoides sigmodontis* is potent to induce a pro-inflammatory immune response in human cells”)

Poster presentation at the Cluster Science Days of the ImmunoSensation Cluster of Excellence in Bonn, Germany, 2018 (“RNA derived from *Plasmodium falciparum* and *Litomosoides sigmodontis* is potent to induce a pro-inflammatory immune response in human cells”)

Oral presentation at the 23rd Symposium “Infection and Immunity” by the German Society for Immunology (DGfI) in Rothenfels, Germany, 2019 („RNA derived *from P. falciparum* and *L. sigmodontis* is potent to induce a pro-inflammatory immune response in human cells“)

Oral Presentation at the 68th annual meeting of the American Society of Tropical Medicine and Hygiene in National Harbor, vicinity of Washington D.C., USA, 2019 („Improving vaccination efficacy against the filarial nematode *Litomosoides sigmodontis*“)

Oral Presentation at the 29th annual meeting of the German Society for Parasitology (DGP) 2021 in Bonn, („Improving vaccination efficacy against the filarial nematode *Litomosoides sigmodontis*“)

Acknowledgements

First, I thank Prof. Dr. Achim Hörauf, the director of the Institute for Medical Microbiology, Immunology and Parasitology at the University Hospital Bonn, for giving me the opportunity to pursue my Doctoral thesis at this institute.

Second, I thank Prof. Dr. Sven Burgdorf for being by second supervisor, and PD Dr. Gerhild van Echten-Deckert and Prof. Dr. Ian C. Brock for completing my examination committee.

My thanks also go to Dr. Beatrix Schumak, for supervising and supporting my growth during my Master thesis and PhD thesis until her leave from the institute, and having an open ear for me until today. Thank you for teaching me to be critical, while encouraging me to not hide my qualities.

Further I want to thank Prof. Dr. Marc Hübner who already helped supervising my project and then adopted me as a group member. Thank you for your valuable advice, help at any time needed, your trust in me and constant support.

I also want to thank Dr. Christoph Coch, for shaping the project with his valuable knowledge on nucleic acid immunity and Bastian Putschli, Anja Wieland, Marcel Renn, Christian Hagen and Gunther Hartmann for their help with protocols and supplying me with 3pRNA.

I strongly appreciate the help and passion of Dr. Stefan Garbe, who spent several evenings in the radiology department of the University Hospital Bonn for me and only thereby made the vaccination studies possible.

Additionally, I want to thank the Jürgen-Manchot-Foundation for financing my PhD scholarship.

Special thanks go to Frederic Risch, for his terrific support with all animal related tasks and performing all vaccination experiments with me, in an entertaining manner no matter the hour. Further, I especially want to thank Julia Reichwald. We grew together over the years and the PhD time would not have been the same without her. I also want to stress my thankfulness to Dr. Alexandra Ehrens, for her constant support, proofreading of this thesis and close friendship at the IMMIP and beyond.

I thank all colleagues from the IMMIP, who accompanied me during my years at the institute, especially former AG Schumak and AG Hübner, for creating a work environment that I always enjoyed. Over the years more people than I want to list here became very dear to me beyond sharing our workplace and I look forward to stay in touch.

I also want to thank my family and friends for their sympathy and interest in my work during these exciting years and thank you Tilman, for being part of my life.